PROCESSING AND FORMULATION OF CONCENTRATED PROTEIN SOLUTIONS

STRATEGIES FOR THEIR CHARACTERIZATION AND STABILIZATION

zur Erlangung des akademischen Grades eines
DOKTORS DER INGENIEURWISSENSCHAFTEN (Dr.-Ing.)

der Fakultät für Chemieingenieurwesen und Verfahrenstechnik des
Karlsruher Instituts für Technologie (KIT)

genehmigte
DISSERTATION

von
Dipl.-Ing. Katharina Christin Bauer
aus Ludwigsburg

Referent: Prof. Dr. Jürgen Hubbuch
Korreferent: Prof. Dr.-Ing. Michael Türk
Tag der mündlichen Prüfung: 14.12.2016

Acknowledgments

"It's hard to dance with a devil on your back so shake him off."
Florence + The machine

Abstract

Biopharmaceuticals are used for therapy of a wide range of human diseases and conditions, such as diabetes, cancer, hemophilia, myocardial infarction or viral diseases. Requiring high purity, their downstream processing consists of several orthogonal process steps to effectively remove host cell proteins and other contaminants. Due to increasing product concentrations in cell culture and the trend towards highly concentrated formulations, these process units are increasingly confronted to cope with concentrated protein solutions. From an economic point of view, their lower volume enables quicker processing, savings in material and storage space as well as an easier delivery to the patient. However, for downstream processing, concentrated protein solutions represent challenges as they tend to exhibit protein aggregation and high viscosity. On the one hand, protein aggregation could serve as an orthogonal purification step in terms of crystallization or precipitation. On the other hand, undesired protein aggregation and high viscosity may affect the regular operation of process steps, such as filtration or chromatography. Whereas undesired protein aggregation may not only cause product loss but also present the risk of an immune response for the patient, high viscosity complicates pumping as well as a subcutaneous delivery by syringe. Therefore, fundamental knowledge about the aggregation tendency as well as the viscosity of concentrated protein solutions are essential to ensure stable processing and safe formulations. In order to already obtain information on these solution characteristics at an early stage of process development, analytical methods with low sample consumption are of special interest.

From a molecular point of view, the aggregation tendency and viscosity of a protein solution are governed by attractive protein interactions. At high protein concentrations, not only electrostatic interactions, as for dilute solutions, but also additional short-range interactions, such as van der Waals, hydration, hydrophobic, and steric interactions, have an influence. The interplay of these complex protein interactions promotes different aggregation mechanisms. It does not only cause the formation of dense aggregates but also of spacious networks with increased viscosity and enhanced elastic properties. Yet, analytical methods for the determination of these protein interactions as well as the resulting aggregation tendency and viscosity of concentrated protein solutions are rare and not well established. As a result, little is known about the stabilization and the behavior of concentrated protein solutions during the production process.

This work deals with the characterization of protein interactions, protein aggregation, and viscosity of concentrated protein solutions at low sample volume in order to enable strategies for the development of safe processes and stable biopharmaceutical formulations at early process development. To accurately determine rheological properties of concentrated protein solutions, such as the dynamic viscosity η, the impact of different tracer particles on microrheological measurements is investigated. Varying protein interactions and their impact on protein aggregation as well as viscosity are evaluated by analyzing changes in the apparent diffusion coefficient D_{app}. Enabling lower sample consumption and work effort in early process development, the predictability of this parameter from protein surface properties determined *in silico* is examined using quantitative structure-activity relationship (QSAR) modeling. As the impact of hydrophobic protein interactions increases with

increasing protein concentration, protein surface hydrophobicity is investigated through the development of a non-invasive stalagmometric method. To maintain the colloidal stability of concentrated protein formulations, the impact of different additives on the protein aggregation tendency and viscosity is evaluated. Changes in the protein aggregation tendency during the production process are addressed by concentration experiments with different proteins at various solution conditions using tangential flow filtration.

The results of these studies provide strategies to improve characterization and stabilization of concentrated protein solutions. The study on investigating different tracer particles implied that their selection has a strong impact on the microrheological measurement accuracy. Surface modified polystyrene was the only tracer particle that yielded good results for the dynamic viscosity and first measurements of the storage and loss modulus G' and G''. The study indicated that the hydrophobicity of the tracer particle had a greater impact than its electrostatic surface charge. This characteristic was identified to be the crucial surface property for the selection of a suitable tracer particle enabling high measurement accuracy.

As a strategy to characterize the aggregation tendency and viscosity of concentrated protein solutions, the evaluation of changes in the apparent diffusion coefficient D_{app} was shown to be effective. This parameter was able to capture a wide scope of variations in protein interactions depending on protein type, protein concentration, pH, and NaCl concentration. The more the apparent diffusion coefficient deviated from linearity depending on protein concentration, the more probable was the formation of aggregates and high viscosity of the respective samples. Whereas stable samples with relatively low viscosity showed an almost linear dependence, samples prone to aggregation, like precipitation or crystals, deviated. Samples with high viscosity showed an even higher deviation from linearity. This deviation of the apparent diffusion coefficient from concentration-dependent linearity was independent of protein type and solution properties. Thus, this single parameter showed the potential to act as a prognostic tool for the colloidal stability of protein solutions.

The predictability of the apparent diffusion coefficient from protein structure properties determined *in silico* was shown by QSAR modeling. The generated QSAR model for the apparent diffusion coefficient showed a significant correlation with a coefficient of determination $R^2 = 0.9$ and a good predictability for an external test set with $R^2 = 0.91$. The information about the protein structure properties affecting protein interactions present in solution was in agreement with experiment and theory. Furthermore, the model was able to provide a more detailed picture of these properties influencing the acting protein interactions and gave a promising prospect for the modeling of protein phase behavior by *in silico* approaches.

Differences in proteins' hydrophobic character could be resolved with the development of a high resolution stalagmometric method. This method occurred to outclass the widely used spectrophotometric method with bromophenol blue sodium salt as it gave reasonable results without restrictions on pH and protein species. Surface tensions could be derived with a low sample consumption (800 µL) and a high reproducibility (< 0.1 ‰ for water) within a reasonable time (3.5 min per sample). A pH-dependent hydrophobicity ranking was developed, which was found to be in good agreement with literature. For the studied pH

range of 3 to 9, lysozyme from chicken egg white was identified to be the most hydrophilic. α-Lactalbumin at pH 3 exhibited the most pronounced hydrophobic character.

In order to maintain the colloidal stability of concentrated protein solutions while decreasing their dynamic viscosity, the impact of additives on the formation of visible protein aggregates, the dynamic viscosity, and the protein conformation was considered. Influencing protein interactions, this impact was strongly depending on pH. Of all additives investigated, glycine was the only one that maintained protein conformational and colloidal stability while decreasing the dynamic viscosity. Low concentrations of NaCl showed the same effect but increasing concentrations, analogous to ArgHCl, resulted in visible protein aggregation. Those additives proven to stabilize the protein conformation, PEG 300, PEG 1000, and glycerol, increased the dynamic viscosity of the concentrated protein solutions investigated due to their own viscosity.

The concentration of different protein solutions via tangential flow filtration implied that process-related concentration polarization caused product loss due to gel formation on the filtration membrane. Changes in solution conditions influenced these aspects, as stable protein solutions resulted in lower gel formation and higher yields. Contrary to other publications, process-related stresses, like shear, had minor impact on the aggregation tendency of the protein solutions investigated.

In summary, this work describes strategies to characterize protein interactions, protein aggregation, and dynamic viscosity of concentrated protein solutions in order to improve their processing and formulation. The screening of suitable tracer particles for the microrheological measurement enabled the accurate determination of concentrated protein solutions' dynamic viscosity. Changes in the apparent diffusion coefficient were not only shown to characterize protein interactions at high concentrations but also to correlate with concentration-dependent changes in phase behavior and dynamic viscosity. The creation of a QSAR model showed the predictability of this parameter based on protein structure properties and enabled a deeper mechanistic understanding. It gave a promising perspective for the modeling of protein phase behavior by *in silico* approaches. With the development of the stalagmometric method, the impact of hydrophobic protein interactions could be evaluated. For maintaining the colloidal stability of concentrated protein solutions while preserving their processability, glycine was found to be a suitable additive. For the optimization of one of the most common concentration-dependent process steps, tangential flow filtration, the identification of stable solution conditions was shown to be another essential factor to avoid protein aggregation and achieve high protein concentrations.

All of these studies were developed and validated using different model proteins. However, due to low sample consumption and applicability to different proteins, these strategies should be easily transferable to other molecules of interest. Serving as strategies in biopharmaceutical process development, the above mentioned findings will provide valuable information for creating safe formulations and stable processes of concentrated protein solutions.

Kurzfassung

Biopharmazeutika werden zur Behandlung eines weitgefächerten Spektrums an humanen Krankheiten und Störungen, wie Diabetes, Krebs, Hämophilie, Herzinfarkt oder Viruserkrankungen, eingesetzt. Um hohe Reinheiten zu erreichen, besteht deren Aufreinigungsprozess aus verschiedenen orthogonalen Prozessschritten, mit denen effektiv wirtszelleigene Proteine oder andere Verunreinigungen entfernt werden. Diese Prozessschritte müssen, da während der Zellkultur zunehmend höhere Produktkonzentrationen erreicht werden und ein Trend zu hochkonzentrierten Formulierungen besteht, immer häufiger konzentrierte Proteinlösungen bewältigen. Aus ökonomischer Sicht verspricht deren niedrigeres Volumen schnellere Bearbeitungszeiten, Einsparungen in Material- und Lagerkosten sowie eine vereinfachte Verabreichung für den Patienten. Für den Aufreinigungsprozess selbst sind diese konzentrierten Proteinlösungen allerdings eine Herausforderung, da sie zu Proteinaggregation und hoher Viskosität neigen. Proteinaggregation kann einerseits als orthogonaler Aufreinigungsschritt in Form von Kristallisation oder Präzipitation dienen. Unerwünschte Proteinaggregation und hohe Viskosität können andererseits den regulären Verlauf von Prozessschritten, wie Filtration oder Chromatographie, beeinträchtigen. Während unerwünschte Proteinaggregation nicht nur zu Produktverlust führt, sondern auch das Risiko einer Immunantwort für den Patienten darstellt, erschwert hohe Viskosität das Pumpen sowie die Verabreichung durch Spritzen. Für die Prozessentwicklung sind daher grundlegende Kenntnisse über die Aggregationsneigung sowie die Viskosität einer konzentrierten Proteinlösung wichtig, um stabile Prozesse sowie sichere Formulierungen zu gewährleisten. Analytische Methoden, um diese Lösungseigenschaften mit niedrigem Probenvolumen zu bestimmen, sind hierbei von besonderem Interesse.

Auf molekularer Ebene werden die Aggregationsneigung und Viskosität einer Proteinlösung von attraktiven Proteinwechselwirkungen bestimmt. Für hohe Proteinkonzentrationen haben hierbei nicht nur elektrostatische Wechselwirkungen, wie bei verdünnten Lösungen, sondern auch zusätzliche kurzreichweitige Wechselwirkungen, wie van der Waals Wechselwirkungen, Hydratisierungskräfte, hydrophobe und sterische Wechselwirkungen, einen Einfluss. Das Zusammenspiel dieser komplexen Proteinwechselwirkungen begünstigt verschiedene Aggregationsmechanismen. Es bewirkt nicht nur die Bildung dichter Aggregate, sondern auch weitläufiger Netzwerke mit erhöhter Viskosität und verstärkten elastischen Eigenschaften. Analytische Methoden zur Bestimmung dieser Proteinwechselwirkungen sowie die daraus resultierende Aggregationsneigung und Viskosität einer konzentrierten Proteinlösung sind bislang jedoch rar und nicht fest etabliert. Folglich ist wenig bekannt über die Stabilisation und das Verhalten während des Produktionsprozesses von konzentrierten Proteinlösungen.

Diese Arbeit beschäftigt sich deshalb mit der Charakterisierung von Proteinwechselwirkungen, der Proteinaggregation und Viskosität von konzentrierten Proteinlösungen um Strategien für die Entwicklung von sicheren Prozessen und stabilen biopharmazeutischen Formulierungen zu entwickeln. Zur präzisen Bestimmung von rheologischen Eigenschaften konzentrierter Proteinlösungen, wie der dynamischen Viskosität η, wird der Einfluss verschiedener Tracerpartikel auf mikrorheologische Messungen untersucht. Variierende Proteinwechselwirkungen und deren Einfluss auf Proteinaggregation sowie Viskosität werden durch

Änderungen des apparenten Diffusionskoeffizienten D_{app} ermittelt. Um geringeren Probenverbrauch und Arbeitsaufwand während der frühen Entwicklungsphasen zu ermöglichen, wird mithilfe eines Modells basierend auf quantitativer Struktur-Wirkungs-Beziehung (englisch: Quantitative Structure-Activity Relationship (QSAR)) die Vorhersagbarkeit dieses Parameters durch *in silico* bestimmte Proteinstruktureigenschaften geprüft. Die Proteinoberflächenhydrophobizität, deren Einfluss mit steigender Proteinkonzentration wächst, wird durch die Entwicklung einer nichtinvasiven stalagmometrischen Methode erforscht. Um die kolloidale Stabilität konzentrierte Proteinformulierungen zu erhalten, wird der Einfluss von verschiedenen Additiven auf die Aggregationsneigung und Viskosität untersucht. Auf Änderungen der Proteinaggregationsneigung während des Produktionsprozesses wird durch die Konzentrierung verschiedener Proteine bei unterschiedlichen Lösemittelbedingungen mittels Querstromfiltration eingegangen.

Die Ergebnisse dieser Studien bieten Strategien zur besseren Charakterisierung und Stabilisierung von konzentrierten Proteinlösungen. Die Untersuchung verschiedener Tracerpartikel ergab, dass deren Auswahl einen starken Einfluss auf die Genauigkeit mikrorheologischer Messungen hatte. Oberflächenmodifizierte Polystyrolpartikel waren die einzigen Tracerpartikel, die gute Ergebnisse für die dynamische Viskosität und erste Messungen des Speicher- und Verlustmoduls G' und G" erzielten. Es konnte gezeigt werden, dass die Hydrophobizität eines Tracerpartikels einen übergeordneten Einfluss im Vergleich zu dessen Elektrostatik hatte. Um hohe Messgenauigkeiten zu erzielen, wurde diese Oberflächeneigenschaft für die Auswahl von geeigneten Tracerpartikeln als entscheidend identifiziert.

Die Strategie, Änderungen des apparenten Diffusionskoeffizienten D_{app} zur Charakterisierung von Aggregationsneigung und Viskosität von konzentrierten Proteinlösungen zu nutzen, erwies sich als wirkungsvoll. Dieser Parameter ermöglichte es ein breites Spektrum an Proteinwechselwirkungsvariationen abhängig von der Proteinart, Proteinkonzentration, dem pH und der Konzentration an NaCl zu erfassen. Je mehr der apparente Diffusionskoeffizient von seinem linearen Verhalten abhängig der Proteinkonzentration abwich, desto wahrscheinlicher war die Bildung von Proteinaggregaten und hoher Viskosität für die jeweiligen Proben. Während stabile Proben mit relativ niedriger Viskosität ein nahezu lineares Verhalten aufwiesen, wichen Proben mit Aggregationsneigung, wie Präzipitation oder Kristallisation, von dieser Linearität ab. Proben mit hoher Viskosität zeigten besonders hohe Abweichungen. Diese Abweichung des apparenten Diffusionskoeffizienten von seiner konzentrationsabhängigen Linearität war unabhängig von der Proteinart und den Lösemittelbedingungen. Dieser Parameter wies daher das Potenzial auf als Methode zur Prognose der kolloidalen Stabilität von Proteinlösungen dienen zu können.

Seine Vorhersagbarkeit durch *in silico* bestimmte Proteinstruktureigenschaften konnte durch ein QSAR-Modell gezeigt werden. Dieses Modell für den apparenten Diffusionskoeffizienten ergab eine deutliche Korrelation mit einem Bestimmtheitsmaß $R^2 = 0,9$ und einer guten Vorhersagbarkeit für das externe Testset mit einem Bestimmtheitsmaß $R^2 = 0,91$. Die Informationen über den Einfluss von Proteinstruktureigenschaften auf die Proteinwechselwirkungen in Lösung stimmten mit den Experimenten sowie mit der Theorie überein. Desweiteren war das Modell in der Lage ein detailreicheres Bild des Einflusses dieser Eigenschaften auf die wirkenden Proteinwechselwirkungen zu liefern und zeigte eine

vielversprechende Perspektive für das Modellieren von Proteinphasenverhalten durch *in silico* Ansätze auf.

Durch die Entwicklung einer hochauflösenden stalagmometrischen Methode konnten Unterschiede im hydrophoben Charakter von Proteinen aufgelöst werden. Diese Methode zeigte sich der weit verbreiteten spektroskopischen Methode mit Bromophenolblau überlegen, da sie sinnvolle Ergebnisse ohne Einschränkung durch pH oder Proteinart erzielte. Oberflächenspannungen konnten bei niedrigem Probenvolumen (800 µL) und hoher Reproduzierbarkeit ($< 0,1$ ‰ für Wasser) in angemessener Zeit (3,5 min pro Probe) erreicht werden. Das entwickelte pH-abhängige Hydrophobizitätsranking stimmte gut mit der Literatur überein. Für den untersuchten pH-Bereich von 3 bis 9 erwies sich Lysozym aus Hühnereiweiß als am hydrophilsten. α-Lactalbumin bei pH 3 war eindeutig am hydrophobsten.

Um die kolloidale Stabilität konzentrierter Proteinlösungen zu erhalten und gleichzeitig deren Viskosität zu senken, wurde der Einfluss von Additiven auf die Bildung sichtbarer Proteinaggregate, die dynamische Viskosität und die Proteinkonformation betrachtet. Dieser Einfluss war stark vom pH-Wert der Lösung abhängig, da dieser die Proteinwechselwirkungen beeinflusste. Von den untersuchten Additiven war Glycin das einzige, das die konformative und kolloidale Proteinstabilität erhielt und gleichzeitig die dynamische Viskosität senkte. Niedrige Konzentrationen an NaCl zeigten einen ähnlichen Effekt, aber steigende Konzentrationen führten, wie ArgHCl, zu sichtbarer Proteinaggregation. Die Additive PEG 300, PEG 1000 und Glycerin, die nachweislich die Proteinkonformation stabilisieren, erhöhten aufgrund ihrer eigenen Viskosität die dynamische Viskosität der untersuchten konzentrierten Proteinlösungen.

Die Konzentrierung verschiedener Proteinlösungen mittels Querstromfiltration zeigte, dass prozessbedingte Effekte Produktverlust durch die Bildung einer Gelschicht auf der Filtermembran verursachen. Sich ändernde Lösungsbedingungen beeinflussten diesen Aspekt, da stabile Proteinlösungen niedrigere Gelbildung und höhere Ausbeuten ergaben. Prozessbedingte Beanspruchungen, wie Scherung, hatten im Gegensatz zu anderen Publikationen geringen Einfluss auf die Aggregationsneigung der untersuchten Proteinlösungen.

Zusammenfassend wurden in dieser Arbeit Strategien entwickelt, um Proteinwechselwirkungen, Proteinaggregation und die dynamische Viskosität von konzentrierten Proteinlösungen zu charakterisieren und so deren Herstellungsprozess und Formulierung zu verbessern. Das Screening verschiedener Tracerpartikel für mikrorheologische Messungen ermöglichte eine präzise Bestimmung der dynamischen Viskosität konzentrierter Proteinlösungen. Änderungen des apparenten Diffusionskoeffizienten erwiesen sich nicht nur geeignet Proteinwechselwirkungen bei hohen Konzentrationen zu charakterisieren, sondern konnten auch mit konzentrationsabhängigen Änderungen im Phasenverhalten und der dynamischen Viskosität korreliert werden. Die Bildung eines QSAR-Modells verdeutlichte die Vorhersagbarkeit dieses Parameters basierend auf Proteinoberflächeneigenschaften, schaffte ein tieferes mechanistisches Verständnis und eröffnete eine vielversprechende Perspektive für die Modellierung von Proteinphasenverhalten mittels *in silico* Ansätzen. Durch die Entwicklung der stalagmometrischen Methode konnte der Einfluss von hydrophoben Proteinwechselwirkungen ausgewertet werden. Als geeignetes Additiv, das die kolloidale Stabilität und gleichzeitig

die Prozessierbarkeit von konzentrierten Proteinlösungen erhält, wurde Glycin identifiziert. Für die Optimierung der häufig eingesetzten Querstromfiltration konnte gezeigt werden, dass die Bestimmung von stabilen Lösungsbedinungen einen wesentlichen Faktor darstellt, um Proteinaggregation zu vermeiden und hohe Proteinkonzentrationen zu erreichen.

Alle in dieser Arbeit vorgestellten Studien wurden mit verschiedenen Modellproteinen entwickelt und validiert. Eine einfache Übertragbarkeit dieser Strategien auf andere Moleküle sollte allerdings durch ihr niedriges Probenvolumen und ihre Anwendbarkeit für verschiedene Proteine gewährleistet sein. Für die Entwicklung neuer biopharmazeutischer Aufarbeitungsprozesse werden die im Vorausgehenden vorgestellten Ergebnisse wertvolle Informationen für die Schaffung sicherer Formulierungen und stabiler Prozesse konzentrierter Proteinlösungen liefern.

Contents

Acronyms

Notation	Description
ArgHCl	arginine hydrochloride
ATPS	aqueous two-phase systems
BMBF	German Federal Ministry of Education and Research
BPB	bromophenol blue
BPB Na	bromophenol blue sodium salt
BSA	bovine serum albumin
DLS	dynamic light scattering
DWS	diffusing wave spectroscopy
ESP	electrostatic surface potential
FT-IR	Fourier-transformed-infrared
HIC	hydrophobic interaction chromatography
HTP	high throughput
ID	identifier
IR	Infrared
MD	molecular dynamics
MOPSO	3-Morpholino-2-hydroxypropanesulfonic acid
mPES	modified Polyethersulfone
MSD	mean-squared displacement
NWP	Normal Water Permeability
PAV	Piezo Axial Vibrator
PDB	Protein Data Bank
PEG	Polyethylenglycol
PEG-PS	PEGylated polystyrene
PES	Polyethersulfone
pI	isoelectric point

Notation	Description
PLSR	Partial least squares regression
PMMA	Poly(methyl methacrylate)
PS	polystyrene
QSAR	quantitative structure-activity relationship
RMSECV	root mean square error of cross-validation
RP	reversed phase
SEC	size exclusion chromatography
SLS	static light scattering
TFF	tangential flow filtration
TMP	transmembrane pressure
UV	ultraviolet
VIP	variable influence on the projection

List of Symbols

Notation	Description
A	absorption
B_{22}	second virial coefficient
c	concentration
D	diffusion coefficient
D_0	diffusion coefficient at infinite dilution
D_{app}	apparent diffusion coefficient
η	dynamic viscosity
$\eta*$	complex viscosity
f_{inst}	instrumental setup correction factor
G	free energy
g	acceleration of gravity

Notation	Description
G'	storage modulus
G''	loss modulus
γ	surface free energy
k	Boltzmann constant
k_D	diffusion interaction parameter
m	mass
ν	molar volume
Q^2	cross validation square correlation coefficient
R	retention
r	radius
r_h	hydrodynamic radius
R^2	coefficient of determination
S	supersaturation
T	absolute temperature
W	weight
$\tilde{x}$	molar fraction

CHAPTER 1

Introduction

Proteins are therapeutically used in a wide range of therapies for human diseases and conditions, such as diabetes, cancer, hemophilia, myocardial infarction or virial diseases. There are already dozens of protein products on the market and hundreds more in preclincial and clinical development. Before biopharmaceuticals enter clinical research and development to evaluate their therapeutic potential, not only their molecular properties and impurities but also their structural and biological integrity during biopharmaceutical production, storage and delivery need to be extensively characterized. Only if a therapeutic protein can be stabilized and processed adequately, its production will be realized (Chi et al., 2003; Mahler et al., 2009). Being less stable than dilute solutions, this issue is of special importance to concentrated protein solutions. These protein solutions tend to exhibit protein aggregation and high viscosity, which may challenge their developability and manufacturability. Consequently, analytical strategies for the monitoring of these solution characteristics are essential to ensure the successful development of concentrated biopharmaceutical products (W. Wang, 1999). The following chapter presents the fundamentals of protein aggregation and rheological properties of protein solutions. It provides information about the underlying protein interactions, analytical techniques and the consequences of protein aggregation and high viscosity for the biopharamceutical production process.
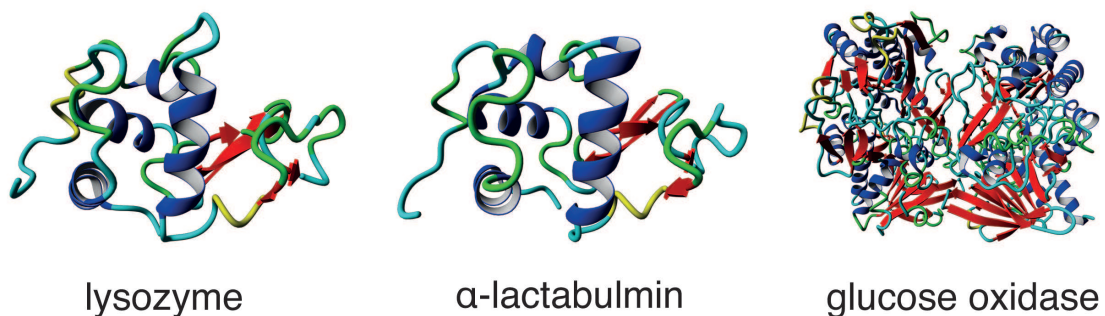

Figure 1.1: Protein structure of lysozyme from chicken egg white, bovine α-lactalbumin apo and glucose oxidase.

1.1 Protein conformation and interactions

Proteins are complex biomolecules with essential tasks in living organisms. Acting as antibodies, enzymes, hormones, or structural components of cells, the functional property of proteins is governed by their unique three-dimensional structure. This three-dimensional structure is primarily determined by the amino acid sequence of the individual polymer chains and their interactions (Pace, Shirley, et al., 1996; Bekard et al., 2011). Each linear polymer chain consists of combinations of 20 amino acids with side chains of different characteristics. These side chains are either basic, acidic, non-polar hydrophobic, and polar hydrophobic. Consequently, electrostatic, hydrophobic, and local peptide interactions, van der Waals forces, and hydrogen bonding contribute to the three-dimensional folding of a protein in its native state. Among all forces involved in protein folding, hydrophobic interactions are the most dominant. These represent repulsive interactions between water and non-polar residues in proteins. Stabilizing the folded state, over 80 % of the peptide groups and non-polar side chains (Ala, Val, Ile, Leu, Met, Phe, Trp, Cys) are buried in the interior of the molecules out of contact with water. Polar side chains (Asn, Glu, Ser, Thr, Tyr) stabilize the protein by building stable hydrogen bonds and intramolecular salt bridges (Pace, Shirley, et al., 1996; W. Wang, 1999; Biswas et al., 2003; Chi et al., 2003; Pace, Treviño, et al., 2004).

On the protein surface, a high propensity of flexible polar and charged side chains (Arg, Lys, His, Asp, Glu) ensure electrostatic interactions with the water molecules stabilizing the protein in solution (Myers et al., 1996; Vieille et al., 1996). These interactions also have a major impact on intermolecular interactions with other protein molecules. Electrostatic protein interactions between two similarly charged macromolecules are usually repulsive and act over long range (Leckband et al., 2001). However, at short-range distances between protein molecules, additional protein interactions, such as van der Waals, hydration, hydrophobic, and steric (excluded volume) interactions, have an impact (Oss, 2003; Liang et al., 2007; Chari et al., 2009; Crommelin et al., 2013). Van der Waals or dispersion forces are attractive electrostatic forces including dipole-dipole, dipole-induced dipole and induced dipole-induced dipole interactions (Chari et al., 2009). Hydration forces capture the solvation forces in water and occure when polar surface groups are dissolved. They are repulsive in nature, because work is required to remove the water molecules from polar surface patches. In contrast, the contact of water molecules with hydrophobic patches on the protein surface is entropically unfavorable. Therefore, hydrophobic protein interactions act attractively (Curtis, Ulrich, et al., 2002; Liang et al., 2007). Acting at short-ranges, van der Waals, hydration and hydrophobic interactions are very sensitive to the local geometry of the proteins (Yadav, Laue, et al., 2012). Steric interactions or excluded volume effects derive from the mutual impenetrability of proteins and are, thus, repulsive in nature (Minton, 2000; Minton, 2005). The overall potential of these forces acting between protein molecules determines the potential of mean force. This force governs the thermodynamic and physical properties of a protein in solution, such as its solubility, aggregation tendency and dynamic viscosity (Curtis, Ulrich, et al., 2002; Saluja and Kalonia, 2008).

In the native state, a high proportion (85 %) of a globular folded protein exists in α-helix or β-sheet or in the turns connecting them (Pace, Shirley, et al., 1996). This three-dimensional

folded state is a fluctuating state of limited number of preferred conformations. The most stable conformation of a protein is usually the native state. However, this native state is only marginally more stable than the large ensemble of unfolded protein conformational states. Relatively small changes in the system environment can already destabilize the structure of a protein and eventually induce its unfolding. When a protein unfolds from the native state, many buried peptide groups and side chains become exposed to water. Promoting hydrophobic interactions, changes in the configuration of the protein surface often result in an increase in attractive protein interactions. Consequently, the colloidal stability of the protein solution as well as its physical properties in solution change (Chi et al., 2003; Pace, Treviño, et al., 2004).

Figure 1.1 displays the structure of the proteins lysozyme from chicken egg white, bovine α-lactalbumin apo and glucose oxidase investigated in this work. Lysozyme and α-lactalbumin apo are homologous in sequence. Both have a molecular weight of about 14 kDa (Palmer et al., 1948; Permyakov et al., 2000). Glucose oxidase is a dimer composed of two identical subunits and has a molecular weight of 160 kDa (O'Malley et al., 1972; Wilson et al., 1992). The distribution of hydrophobic and hydrophilic surface patches on their protein surface is depicted in Figure 1.2. Following the hydrophobicity scale of Bull et al., 1974, the two perspectives are colored from least hydrophobic in blue to most hydrophobic in red.

Figure 1.2: Surface hydrophobicity of lysozyme from chicken egg white, bovine α-lactalbumin apo and glucose oxidase at pH 9 generated in Yasara (Krieger et al., 2002). Following the hydrophobicity scale of Bull et al., 1974, the two perspectives are colored from least hydrophobic in blue to most hydrophobic in red.
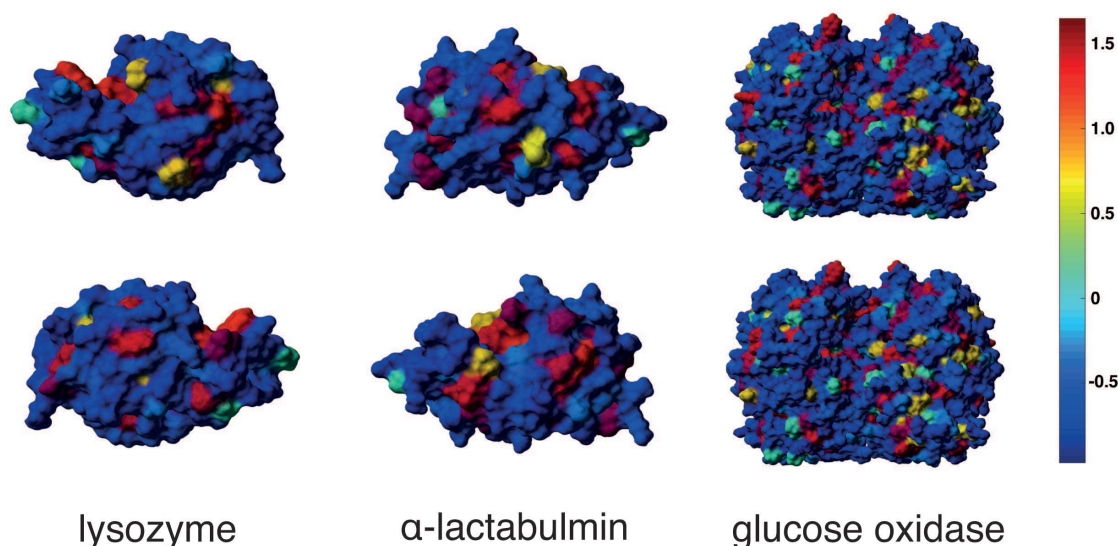
1.2 Protein aggregation

Protein aggregation is a common phenomenon of colloidal instability. In this work, protein aggregation is a universal term for all kinds of multimeric species that are formed by covalent bonds or noncovalent interactions. It summerizes the reversible and irreversible aggregation of native, and non-native proteins respectively (Cromwell et al., 2006; Mahler et al., 2009; Arzenšek et al., 2012).

Thermodynamically, proteins aggregate due to predominating attractive protein interactions minimizing unfavorable interactions between the solvent and exposed side chains. These attractive protein interactions are either generated by modifications or unfolding of the native protein conformation or changes in the physicochemical nature of the protein surface. Changes in protein conformation can either evolve due to chemical or physical degradation. Whereas chemical degradation, such as deamidation, oxidation, and disulfide bond shuffling, modifies the protein structure involving covalent bonds, physical degradation includes protein unfolding. However, due to their flexibility, proteins with intact tertiary structure can also form aggregates. In this case attractive protein interactions result from the physicochemical nature of the protein surface depending on the respective solutions conditions (W. Wang, 1999; Chi et al., 2003).

Before the onset of actual protein aggregation, aggregation pathways require attractive protein interactions to overcome an energy barrier. This barrier results from the free energy required to dissolve the hydration shell around the protein molecules and create a new solid-liquid interface. Classical theory predicts this free energy ΔG to be dependent on the radius r of the cluster:

$$\Delta G = -\frac{4}{3}\pi r^3 \frac{kT}{\nu} lnS + 4\pi r^2 \gamma. \tag{1.1}$$

In this equation, kT is the thermal energy, ν is the molar volume occupied by one protein molecule, γ is the surface free energy, and S is the supersaturation defining the ratio of the actual activity of the solution divided by the activity at equilibrium (Boistelle et al., 1988; Manuel García-Ruiz, 2003). Only when the critical radius, where the energy barrier is highest, is reached, growth of the protein aggregates occurs. During aggregate growth, the size of aggregates increases, while the native protein population is depleted (Chi et al., 2003; W. Wang et al., 2010; Fiorucci et al., 2010).

For protein aggregation, there are a variety of aggregation pathways which may result in different end states (Mahler et al., 2009). These various pathways are determined by the mechanisms of molecular approach, reorientation, and incorporation of native or non-native proteins, which are governed by the strength and range of protein interactions (Chi et al., 2003). These interactions can either result from covalent interactions, such as disulfide bridge formation, or non-covalent interactions, like electrostatic or hydrophobic interactions.

The end state of protein aggregation can be visible or invisible (Cromwell et al., 2006). Depending on its energetic stability, protein aggregation can be reversible or irreversible (Patro et al., 1996) and may lead to different morphologies, such as the formation of precipitate, crystals, gelation or liquid-liquid phase separation (Mahler et al., 2009; W.

Wang et al., 2010; Lewus, Darcy, et al., 2011). Whereas amorphous aggregation results from spontaneous protein precipitation, the formation of ordered, three-dimensional lattices defines protein crystals (Arzenšek et al., 2012). Gelation is associated with the formation of network-like, spacious structures which exhibit elevated viscosity (Fink, 1998; J. Liu et al., 2005; Veerman et al., 2006).

The mechanism proteins aggregate may or may not be accompanied by subtle conformational changes. Due to this impact on protein conformation, protein aggregates may exhibit altered solubility, activity, pharmacokinetics, toxicity, or immunogenicity of the protein molecules (W. Wang, 2005; W. Wang et al., 2010; Saluja and Kalonia, 2008). Moreover, one aggregation mechanism is not mutually exclusive and more than one can occur for the same product (Philo et al., 2009).

1.2.1 Factors influencing protein aggregation

Protein aggregation mechanisms, such as onset, aggregation rate, and the final morphology of the aggregates, have been found to strongly depend on the protein interactions at the respective solution condition. These interactions between the protein molecules can be influenced by temperature, formulation parameters, such as protein concentration, pH, ionic strength and additional additives, or process-related factors, like mechanical stress due to pumping or stirring (Cromwell et al., 2006; Mahler et al., 2009).

Temperature

Among these parameters, temperature is a critical environmental factor. Changing temperature affects protein interactions due to changes in protein conformation as well as colloidal stability. Increasing or decreasing temperature destabilizes the protein structure and can lead to unfolding. Exposed hydrophobic side chains promote attractive protein interactions potentially leading to protein aggregation (Mahler et al., 2009; W. Wang et al., 2010). Furthermore, increasing temperature decreases the colloidal stability of protein solutions because increased diffusion promotes an elevated aggregation rate (Chi et al., 2003; W. Wang, 2005). Throughout this work, temperature was kept constant to exclude its impact.

Protein concentration

Protein concentration plays an essential role for the investigations of concentrated protein solutions presented in this work. Due to changing distances between the molecules, protein interactions are concentration-dependent (Mahler et al., 2009; V. Kumar et al., 2011). In dilute protein solutions, intermolecular distances among molecules are large. Stabilizing the protein molecules in solution, the overall protein interactions are governed by repulsive electrostatic long-range interactions (Saluja and Kalonia, 2008; Chari et al., 2009). With increasing concentrations, average distance among protein molecules decrease while increasing the frequency of encounter and the duration of interaction among them (Chari et al., 2009; Jezek et al., 2011; Mosbæk et al., 2012). Treating protein molecules as impenetrable spheres, excluded volume theory predicts steric interactions to increase the aggregation tendency but also to stabilize the more compact native protein structure against denaturation (Minton, 2000; Minton, 2005). At this state, furthermore, additional attractive short-range van der Waals and hydrophobic interactions are significant (Chari et
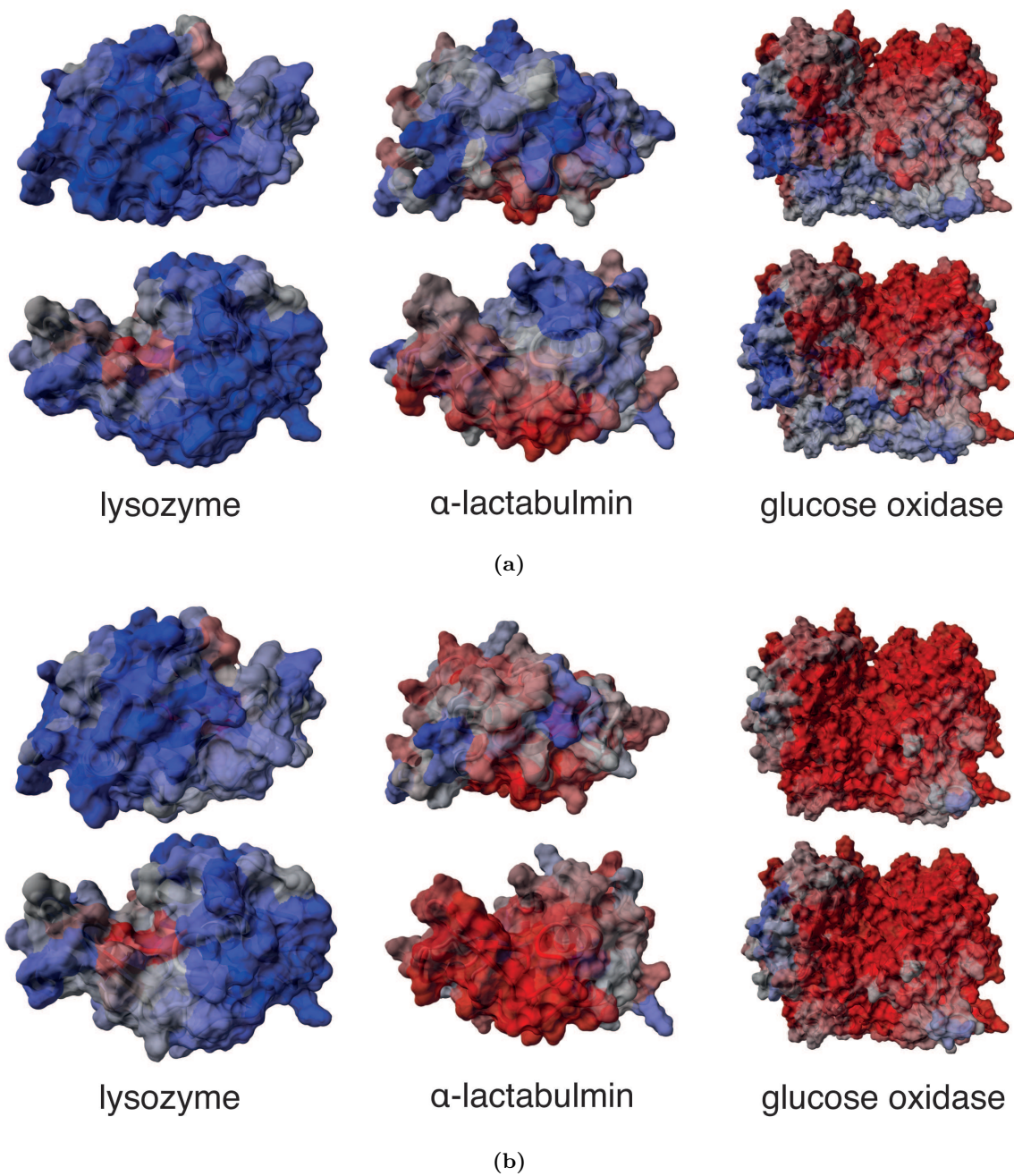
Figure 1.3: Electrostatic surface charge distribution from two perspectives of lysozyme from chicken egg white, bovine α-lactalbumin apo and glucose oxidase at pH 5 (a) and 9 (b). Whereas positively charged surface patches are colored in blue, negatively charged surface patches are displayed in red. Modeling was conducted using Yasara.

al., 2009; Jiao et al., 2010). Their impact can reduce the net repulsion between the protein molecules. Resulting in orientation-dependent intermolecular attractions, the free energy to form a critical nucleus for the initiation of the aggregation process is decreased (W. Wang, 2005; Shire et al., 2004; Yadav, Laue, et al., 2012). This assembly of protein molecules at high protein concentration is often reversible. Due to a more complex interplay of differing protein interactions, aggregation mechanisms may not only result in the formation of dense aggregates but also in spacious networks with elevated viscosity (Shire et al., 2004; Militello et al., 2004; J. Liu et al., 2005; Saluja and Kalonia, 2008; V. Kumar et al., 2011; Jezek et al., 2011; Mosbæk et al., 2012). Yet little is known about the protein interactions involved in network formation. Different types of intermolecular forces are claimed to be dominant for their evolution (J. Liu et al., 2005; V. Kumar et al., 2011; Saito et al., 2012).

Solution conditions

Furthermore, changes to the solution conditions,such as pH, ionic strength and additives, have an impact on the protein interactions governing the aggregation tendency of a protein solution.

pH   Solution pH can strongly affect protein interactions by changing the type and distribution of charges on the protein surface. These changes may not only affect the colloidal stability of a protein solution but also the protein's conformational stability (Mahler et al., 2009; W. Wang et al., 2010). At the isoelectric point (pI), the net charge of a protein is zero. Proteins possess both positively and negatively charged groups. Miniminzing long-range electrostatic protein interactions, this anisotropic charge distribution on the protein surface could give rise to attractive short-range van der Waals and hydrophobic interactions. In such cases, protein interactions could be highly attractive making assembly processes such as aggregation energetically favorable. With further distance from the pI, electrostatic repulsion arises from equally charged groups on the protein surface. At pH values below its pI, the net charge of a protein is positive, above its pI, it is negative (Shaw et al., 2001). These highly charged, repulsive protein interactions stabilize protein solutions colloidally making assembly processes such as aggregation unfavorable (Chi et al., 2003; W. Wang et al., 2010). For the model proteins lysozyme, α-lactalbumin, and glucose oxidase, the distribution of positively (blue) and negatively charged patches (red) on the protein surface at pH 5 and pH 9 are displayed in Figure 1.3(a) and 1.3(b) respectively. Extreme pH can also give rise to destabilizing the native conformation due to increased electrostatic repulsion within the protein and result in partially unfolded states (Chi et al., 2003; Militello et al., 2004; W. Wang et al., 2010). Thus, the exact behavior or a given protein at low pH is a complex interplay between a variety of stabilizing and destabilizing forces (Babu et al., 1997). For the proteins lysozyme and α-lactalbumin investigated in this work, changes in protein conformation have already been published. For lysozyme, a partially unfolded state has been suggested far from equilibrium on the basis of refolding studies (Babu et al., 1997). The acid state of α-lactalbumin at low pH values was found to be a classical molten globule state. Due to increased hydration, its globular shape is swollen from the native state (Permyakov et al., 2000).

Ionic strength   Since pH strongly affects protein interactions, a buffering agent is usually used to maintain an optimum pH for conformational and colloidal stability (W. Wang et al., 2010). Its ionic strength may inhibit protein aggregation due to electrostatic screening of protein surface charges. However, reduction of such interactions could also destabilize the protein, partially expose hydrophobic groups and lead to increased attractive protein interactions (Chi et al., 2003; Jezek et al., 2011). Thus, the overall effect of ionic strength is protein-dependent and can be significantly different in various buffer systems and concentrations (W. Wang et al., 2010; V. Kumar et al., 2011; Saito et al., 2012; Feng et al., 2012).

Neutral additives   Inhibiting protein aggregation, many neutral additives influence protein interactions. A major category of these compounds are sugars and polyols. Their stabilizing effect is demonstrated and widely interpreted as the result of preferential interactions, a widely accepted concept of protein stabilization (Arakawa and Timasheff, 1982; W. Wang, 2005; W. Wang et al., 2010). In presence of a stabilizing additive, the proteins are preferentially hydrated and the additive is preferentially excluded from the protein surface. However, also other stabilization mechanisms, including increased surface tension, increased rate of protein folding, reduction of solvent accessibility and conformational mobility as well as an increase in solvent viscosity were postulated for the effect of these additives (Arakawa and Timasheff, 1982; Ansari et al., 1992; W. Wang et al., 2010; Uribe et al., 2003).

Various polymers have an impact on protein aggregation. Their underlying stabilizing mechanisms are based on their surface activity, preferential exclusion or steric hindrance of protein interactions and increased viscosity limiting protein structural movement (W. Wang, 2005; Liang et al., 2007). Polyethylenglycol (PEG) at different molecular weights is the most common polymer used in the biopharmaceutical industry. PEGs are hydrophobic in nature and may interact with hydrophobic side chains on the protein surface. However, their stabilizing effect seems strongly dependent on its molecular weight. Whereas species with low molecular weight stabilize proteins, species with high molecular weight cause protein aggregation due to osmotic interactions (Minton, 1983). These interactions promote attractive protein interactions by excluding additives between the closely contacting proteins. Protein stabilization by high molecular weight PEG is possible due to their steric hindrance of protein interactions (Chari et al., 2009).

Charged additives   Furthermore, several types of charged additives affect protein aggregation as a result of ionic strength or specific interactions with proteins (Ikeda and Zhong, 2012). Their effect strongly depends on the solution pH, which dictates the charge of ionizable groups on the protein surface.

However, due to complex ionic interactions with the protein surface, the effect of salts on protein aggregation is complex. Salts stabilize, destabilize or have no effect on the protein's conformational or colloidal stability depending on the type and concentration of salt, nature of ionic interactions and charged residues of the protein (Kohn et al., 1997; Crevenna et al., 2012; Chi et al., 2003). At low concentrations, salts cause electrostatic

shielding which can either be stabilizing or destabilizing (Jezek et al., 2011). A stabilizing salting-in effect can evolve due to favorable electrostatic interactions between the salt ions and peptide groups on the protein surface. With increasing salt concentrations, protein interactions become more attractive. Increasing electrostatic shielding of charged surface groups promotes hydrophobic interactions between non-polar residues leading to protein aggregation. This salting-out effect at often correlates with the Hofmeister series and is strongly dependent on the type of salt. As for polymers, osmotic contribution from salt ions resulting in attraction between charged macromolecules can arise in solutions of high salt concentrations (Shih et al., 1992; Kohn et al., 1997; W. Wang, 1999; Curtis, Ulrich, et al., 2002; Curtis, Steinbrecher, et al., 2002). Additionally, binding of salt ions to the protein surface can decrease the thermodynamic stability of the native conformation, promote attractive protein interactions and possibly result in protein aggregation (Chi et al., 2003). In contrast, some positively charged amino acids, such as histidine, arginine, glycine, lysine, either alone or in combination with other additives, are very effective in decreasing attractive protein interactions. Their stabilizing mechanisms are either attributed to shielding of attractive protein interactions or preferential exclusion stabilizing the protein's native conformation (Shire, 2009; W. Wang et al., 2010).

Further additives   Besides the additives presented in this context, further formulation additives were reported to have an impact on protein aggregation and their underlying protein interactions. These additives include surfactants, preservatives, antioxidants, reducing agents, and organic solvents (W. Wang et al., 2010).

Mechanical stress

Another factor influencing protein interactions is mechanical stress due to stirring, pumping or shaking during many routine processing steps. Inducing shear, interfacial effects, caviation or local thermal effects, these types of stress are assumed to have an impact on the proteins' conformational stability. Shear is assumed to expose the hydorphobic areas of proteins causing aggregation (Maa et al., 1996; W. Wang, 2005; Ashton et al., 2009; Bekard et al., 2011). Interfacial effects and cavitation expose the protein to non polar interfaces likely causing them to align at the interface and to change in conformation (Bee et al., 2009; W. Wang et al., 2010).

1.2.2 Analytical strategies for the characterization of protein aggregation

The early detection and characterization of conditions that promote protein aggregation is essential to guarantee stable processing and safe biopharmaceutical formulations. Consequently, analytical strategies monitoring protein aggregation are essential to ensure a successful development of these products (W. Wang, 1999; Amin, Barnett, et al., 2014). Many techniques enable to determine or characterize protein aggregation. In general, protein aggregation can be investigated by determination of either the conformational or colloidal stability of the protein molecules in solution (W. Wang, 2005; Mahler et al., 2009). The conformational stability of a protein solution can be characterized by bioassays based on the activity of the protein or by physical techniques to monitor unfolding, such as Infrared (IR) spectroscopy, Fourier-transformed-infrared (FT-IR) spectroscopy, fluorescence
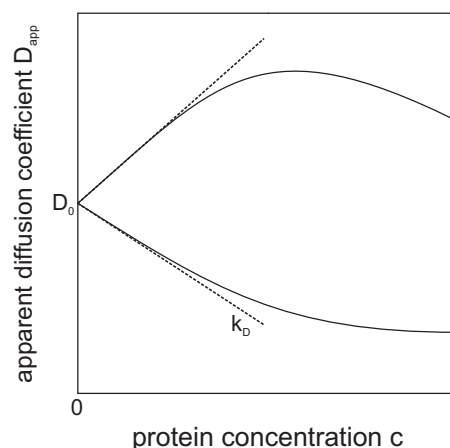
Figure 1.4: Possible changes in the apparent diffusion coefficent depending on protein concentration and the fit for the linear range with its respective slope k_D.

spectroscopy, ultraviolet (UV) spectroscopy, nuclear magnetic resonance spectroscopy, and differential scanning calorimetry. These physical techniques are based on differences in the signal of folded and unfolded states. However, for the identification of protein aggregates these screening methods need to be used with caution, because the determined structural changes solely imply the presence of non-native proteins in the solution investigated but do not consider their colloidal stability (Kondo et al., 1992; W. Wang, 1999; Kong et al., 2007; Amin, Barnett, et al., 2014).

For the investigation of colloidal stability of protein molecules in solution, either aggregates or the aggregation tendency of proteins can be examined. Protein aggregates can be determined by protein phase diagrams, microscopy, polyacylamide gel electrophoresis, size exclusion chromatrography with UV detection, field flow fractionation, analytical ultra-centrifugation, and a variety of light scattering techniques (Shire et al., 2004; W. Wang, 2005; Saluja and Kalonia, 2008; Mahler et al., 2009; Feng et al., 2012; Saito et al., 2012). However, many of these broadly utilized methods have an impact on the solution conditions due to dilution or concentration during or before the analytical process or exposure of the protein to solvent conditions that are very different than the initial formulation composition. This may have considerable impact on the result of the assay since a change in solvent composition or concentration may alter a protein's conformational or colloidal state in a way that is not representative of the initial condition. Thus, the level of protein aggregates measured in samples can be significantly different depending on the sample treatment and analytical procedures utilized (Shire et al., 2004; Mahler et al., 2009; W. Wang et al., 2010).

Methods that allow a direct measurement of protein aggregation in the respective formulation without substantial changes in solution conditions are optical methods, such as the determination of protein phase diagrams, or light scattering techniques. Protein diagrams give basic optical information about the state of a solution. Crystallization, precipitation, gelation and liquid-liquid phase separations can be determined (Baumgartner

et al., 2015; Dumetz et al., 2008). Light scattering techniques are suited to detect and characterize aggregates on a length scale of about 1 - 100 nm. Their principle is based on the scattering of light by every particle in solution. There are many types of light scattering methods available, such as static light scattering (SLS) or dynamic light scattering (DLS). Whereas SLS determines the molar mass of proteins, DLS determines the apparent diffusion coefficient of these macromolecules in solution (Mahler et al., 2009). This parameter allows conclusion on the size of a protein based on the Stokes-Einstein equation (Amin, Barnett, et al., 2014):

$$D = \frac{kT}{6\pi r_h \eta}. \tag{1.2}$$

According to this equation, the diffusion D of proteins or aggregates depends on their hydrodynamic radius r_h, the thermal energy kT and the dynamic viscosity η of the solvent. Thus, the smaller the particles the faster the diffusion.

In order to investigate not only protein aggregates existing in solution but also the aggregation tendency of protein solutions, protein interactions need to be considered (Saluja, Badkar, et al., 2007; Mahler et al., 2009). For concentrated protein solutions, this approach is beneficial because it enables not only the identification of conditions promoting the formation of dense aggregates but also of spacious networks with elevated viscosity (Lehermayr et al., 2011). However, the varying proportions and strengths of protein interactions are not directly accessible (Arzenšek et al., 2012). Thus, other analytical methods reflecting the impact of protein interactions need to be employed. Generally, to access these interactions, resulting colloidal solution characteristics, like thermodynamic properties, such as osmotic pressure (Neal et al., 1998; Moon et al., 2000), or transport parameters (Heinen et al., 2012), such as diffusion (Muschol et al., 1995) or viscosity, are determined (Gaigalas et al., 1995; Neal et al., 1998; Amin, Barnett, et al., 2014; Saluja, Badkar, et al., 2007). Their deviation from ideal behavior defines the overall interactions, the potential of mean force, present in solution (V. Kumar et al., 2011). Minimizing work effort and sample consumption, investigations dealing with the pharmaceutical process development often use concentration independent coefficients of these parameters determined at dilute solution conditions, like the second virial coefficient B_{22} or the diffusion interaction parameter k_D (Saluja and Kalonia, 2008). B_{22} is determined by concentration-dependent virial expansion of the ideal gas law equation (Curtis, Ulrich, et al., 2002; Ahamed et al., 2007; Lehermayr et al., 2011). k_D, which relates to B_{22}, depends on the linearization of data for the apparent diffusion coefficient D_{app} depending on the diffusion coefficient at infinite dilution D_0 and the protein concentration c_P:

$$D_{app,linear} = D_0(1 + k_D c_P) \tag{1.3}$$

(W. Liu et al., 2005; Saluja, Badkar, et al., 2007; Saito et al., 2012; Connolly et al., 2012). Both of these interaction parameters can be assessed by light scattering techniques. Whereas SLS is used to determine B_{22}, k_D results from DLS measurement of the apparent diffusion coefficient (W. Liu et al., 2005; Amin, Barnett, et al., 2014). It is generally understood that positive values of these parameters indicate repulsive protein interactions, while negative

values indicate the presence of attractive protein interactions (Saluja, Badkar, et al., 2007; W. Wang et al., 2010; Saito et al., 2012). Both parameter were shown to correlate with system parameters, like viscosity (Connolly et al., 2012; Neergaard et al., 2013; Saito et al., 2012), but have limitations for high concentrations and, thus, for the prediction of protein aggregation (Saluja, Badkar, et al., 2007; Scherer et al., 2010). Whereas George et al., 1994 found a crystallization slot dependent on B_{22} for model proteins, this approach appeared to be less applicable for antibodies (Lewus, Darcy, et al., 2011; Saito et al., 2012; Lewus, Levy, et al., 2015; Rakel, Bauer, et al., 2015; Rakel, Galm, et al., 2015).

Thus, due to the increasing impact of additional short-range interactions, approaches characterizing protein interactions in concentrated solutions are essential to evaluate their aggregation tendency (Saluja and Kalonia, 2008; Chari et al., 2009; V. Kumar et al., 2011; Amin, Barnett, et al., 2014). These measurement techniques have to be sensitive to weak changes in protein interactions. Due to low product yields in development phase, they need to require low sample volume to achieve high concentrations. To be easily applicable in process development, the interpretation of the data should be clear (Saito et al., 2012). Among these methods fullfilling these requirements, the investigation of rheological parameters has been mostly used (Lefebvre, 1982; Burckbuchler et al., 2010). These parameters, like the complex viscosity $\eta*$ and the storage and loss modulus G' and G'', allow the evaluation of viscosity, protein aggregation and the underlying protein interactions in solution (Saluja, Badkar, et al., 2007; Schermeyer et al., 2016). Another suitable parameter is the apparent diffusion coefficient D_{app}, which enables to acquire the changes in interactions for dilute solutions, represented by k_D, as well as additional short-range interactions for concentrated solutions (Muschol et al., 1995). Avoiding multi-scattering, this measurement of concentrated or even turbid samples is possible due to developments like cross-correlation or measurements from higher ankle and close to the cuvette (Amin, Barnett, et al., 2014). Its correlation to solution characteristics, such as osmotic pressure, suspension viscosity (Gaigalas et al., 1995) and aggregation (Cohen et al., 2005; Zhang et al., 2003) were already shown for protein solutions. Figure 1.4 displays possible changes in the apparent diffusion coefficient for repulsive electrostatic protein interactions with a positive value for k_D and for attractive electrostatic protein interactions with a negative value for k_D (Muschol et al., 1995).

1.3 Rheological properties of protein solutions

Attractive interactions interconnecting proteins with one another, not only enable the formation of aggregates but also the evolution of networks. These network leads to increased viscosity and enhanced elasticity of the protein solutions. Due to a higher complexity of protein interactions, this rheological behavior is often associated with concentrated protein solutions. Whereas solutions with low protein concentration tend to exhibit a Newtonian behavior, concentrated ones, similarly to polymer solutions, exhibit shear-thinning behavior, displayed in Figure 1.5, and show viscoelastic properties. The transition from one behavior to the other is dependent on the protein interactions in solution (Saluja and Kalonia, 2008; Burckbuchler et al., 2010; Jezek et al., 2011; Amin, Rega, et al., 2011; Yadav, Shire, et al., 2011; Schmit et al., 2014). A general molecular understanding of how protein interactions influence the evolution of viscoelastic properties is still largely missing. However, it has

been demonstrated that a number of different types of interactions, including electrostatic, van der Waals, hydrophobic, and steric interactions, contribute to the rheological properties of protein solutions (H. Inoue et al., 1996; J. Liu et al., 2005; Kanai et al., 2008; Shire, 2009; Yadav, Laue, et al., 2012; Amin, Rega, et al., 2011; Saito et al., 2012; W. Cheng et al., 2013).

1.3.1 Rheological techniques for the characterization of protein solutions

Numerous techniques can be used to measure the rheological properties of complex fluids. Besides the basic information about the dynamic viscosity η of the solution, the rheological measurement methods enable the determination of complex rheological parameters, like the storage and loss modulus G' and G''. These can be used to interpret the interactions and structures formed between the particles (Lefebvre, 1982; Veerman et al., 2006; Saluja, Badkar, et al., 2007; Jezek et al., 2011). In the cosmetic, food, and color industry, information obtained from rheological measurements already serve to assure quality criteria with regard to homogenity, sedimentation characteristics, sensation experience, and material haptics (Davis 1973, Brummer and Godersky 1999, Brummer 206, Guaratini 2006). For protein solutions, these rheological properties can help to prevent, predict and manipulate not only high viscosity but also protein aggregation. However, at early downstream process and formulation development the available protein volumes are very low and, therefore, expensive. Only small samples can be used for the analytical screenings of highly concentrated solutions. In comparison to other complex systems like polymer solutions, pharmaceutically relevant protein solutions show a weak network formation and, therefore, the existing elastic behavior is difficult to detect. Frequencies in high kilohertz to megahertz need to be applied (Saluja and Kalonia, 2008).

Methods which enable low sample volumes and measure in the high frequency region are high frequency rheological or microrheological measurements (Amin, Barnett, et al., 2014). These high frequency rheological measurements are based on devices, which are
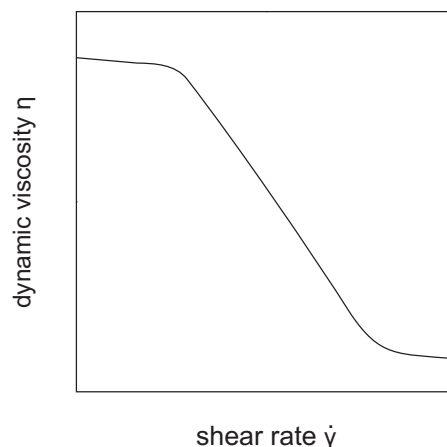

Figure 1.5: Dynamic viscosity of a concentrated protein solution depending on the shear rate (Ikeda and Nishinari, 2001).

able to create frequencies in the kilohertz region. They have already been established for the investigation of proteins. Yet, there are only few suitable devices which all represent prototypes and never got into production (Fritz, Maranzano, et al., 2002; Saluja, Badkar, et al., 2007; Willenbacher et al., 2007). In contrast to these measurements, microrheological measurements can be performed by common DLS or diffusing wave spectroscopy (DWS) devices. Due to the application of very little stress and very small required sample volume, these measurements are specially amenable for the rheological characterization of biological samples. Microrheological measurements utilize the Brownian motion of tracer partices to measure the relation between stress and deformation in materials. This relation is based on the Stokes-Einstein equation (1.2) where the diffusion of a tracer particle D depends on its hydrodynamic radius r_h, the thermal energy kT and the network structure of the surrounding environment. For the determination of the dynamic viscosity η, the Stokes-Einstein equation can directly be applied. For the determination of the complex moduli G' and G'', the mean-squared displacement (MSD) is directly related to the linear frequency-dependent viscous and elastic moduli using the Stokes-Einstein relation. Despite the growing popularity of microrheological techniques, significant technical challenges remain. The main challenge in good microrheological practice is based on a thorough selection of tracer particles. Not having impact on the system investigated, the concentration of these tracer particles chosen must be low. The particles are required to be considerably larger and interaction between the tracers and proteins should be negligible to accurately measure the bulk properties (Valentine et al., 2004; Waigh, 2005; Amin, Rega, et al., 2011).

1.4 Impact of high protein concentrations on the biopharmaceutical downstream process

The production process of a biopharmaceutical is complex and consists of many unit operations. Accomplishing high purity during downstream processing, several orthogonal processing steps are required to effectively remove host cell proteins and other contaminants (Shire, 2009). During these steps, the biopharmaceutical molecule experiences different, sometimes harsh, solution environments and is exposed to process-related stresses (Maa et al., 1996; Bee et al., 2009; Shire, 2009; W. Wang et al., 2010). Whereas upstream is conducted at moderate conditions, cell culture fluid is purified over Protein A chromatography using an acidic solution. Polishing steps typically include cation exchange chromatography, which elutes the protein with high ionic strength solutions and anion exchange chromatogrpahy, which employs high pH conditions to purify the monclonal antibody from process-related impurities. Besides changes in solution conditions, shear is a common process-related stress, which exemplarily occurs when cell culture fluid is harvested by centrifugation, during formulation by tangential flow filtration (TFF), and even during pumping and passage through tubing (Maa et al., 1996; Cromwell et al., 2006; Ashton et al., 2009; Bekard et al., 2011).

Non-optimal conditions during these processing steps can lead to protein conformational or colloidal instabilities promoting protein aggregation (Shire, 2009; Jezek et al., 2011). These protein aggregates could be less efficient and may have immunogenic potential, which makes them generally not acceptable for product release (W. Wang, 1999; W. Wang, 2005; Cromwell et al., 2006; V. Kumar et al., 2011). Thus, developing a protein as a therapeutic agent that maintains its conformational and colloidal intergrity for optimal

efficacy throughout this production process until administration is essential (J. Liu et al., 2005; Jezek et al., 2011).

Aggravating this situation, increasing titers during fermentation and the trend toward highly concentrated formulations require the stabilization of concentrated protein solutions (Shire et al., 2004). From an ideal perspective concentrated protein solutions promise quicker processing, a decrease of storage space and an easier delivery to the patient (E. Rosenberg et al., 2009; Burckbuchler et al., 2010). Particularly when coupled with prefilled syringes and autoinjector device technology, subcutaneous delivery allows for home administration and improved compliance (Shire et al., 2004; Saluja, Badkar, et al., 2007). However, subcutaneous administration is limited to 1.5 mL or less. For monoclonal antibody therapies, especially in the fields of oncology and immunology, this necessitates the development and manufacture of high concentration formulations above 100 mg/mL (Shire, 2009; Chari et al., 2009).

Formulation of these concentrated antibody solutions is challenging as they often exhibit unfavorable phenomena such as increased viscosity and aggregation (Jezek et al., 2011; Lehermayr et al., 2011; Saito et al., 2012). On the one hand, this increased aggregation tendency can be used beneficially as a orthogonal separation step by specific crystallization or precipitation of the target molecule. Crystalline protein formulations, furthermore, provide many advantages, such as higher bioavailability, greater ease of handling, improved stability and varied dissolution characteristics (M. X. Yang et al., 2003; Basu et al., 2004). On the other hand, undesired aggregation and high viscosity make these solutions substantially more difficult to process, prepare and administer (Chari et al., 2009; Burckbuchler et al., 2010; Jezek et al., 2011). Especially formulation by TFF and administration by syringe are affected (Shire et al., 2004; Saluja and Kalonia, 2008; Jezek et al., 2011). During TFF, flow-induced shear together with high local concentration may lead to aggregation and subsequent membrane clogging or other production issues (Jezek et al., 2011). An increase in viscosity may result in such high back pressures that it may exceed the capacity of the pumps and lead to difficulties in removing the final product from the TFF unit resulting in economically unacceptable losses (Shire et al., 2004). For formulation, high viscosity of the protein solution can hinder the delivery by syringe as it affects its injectability (Shire et al., 2004; Burckbuchler et al., 2010; Jezek et al., 2011).

Until now, it is not possible to predict, prevent and stabilize protein aggregation and high viscosity of concentrated protein solutions during processing and delivery (Amin, Barnett, et al., 2014). To address these concerns, an understanding of protein interactions in concentrated solutions is needed. This would aid in establishing strategies to develop solution conditions under which the protein remains most stable and where formulation viscosity does not hinder handling (Chari et al., 2009). Experimental limitations of currently available methods such as sample volume, dilute measurement conditions or special measuring equipment encourage the development of complementary analytical technologies to better understand and predict protein interactions and their impact on solution characteristics of concentrated protein solutions (Shire et al., 2004; Thakkar et al., 2012).

CHAPTER 2

Research proposal

Increasing titers in cell culture and the trend toward highly concentrated formulations require biopharmaceutical downstream processing to cope with concentrated protein solutions. These solutions enable quicker processing, savings in production material and storage space as well as an easier delivery to the patient. However, concentrated protein solutions exhibit elevated aggregation tendency and high viscosity, which may challenge their developability and processability by affecting regular process steps, such as pumping, chromatography, and filtration as well as a delivery by syringe. Both of these solution characteristics depend on attractive protein interactions. Until now, mainly dilute protein solutions have been investigated for changes in protein interactions. However, at high concentrations, protein interactions are more complex. Evolving from electrostatic plus additional short-range interactions, such as van der Waals, hydrophobic, hydration and steric interactions, these can not only promote the formation of dense aggregates but also spacious networks with elevated viscosity and elastic properties. To predict and prevent protein aggregation and high viscosity, protein interactions in concentrated protein solutions have to be understood. Formulation as well as process-related parameters are known to have an impact.

This work deals with strategies for the characterization and stabilization of protein interactions of concentrated protein solutions. It aims to generate a better understanding of their impact on the resulting aggregation tendency and viscosity depending on formulation as well as processing parameters. The knowledge generated should provide valuable information of concentrated protein solutions to guarantee safe processing and stable formulations.

For the determination of dynamic viscosity and rheological properties of concentrated protein solutions, microrheological methods were found to be effective. However, good microrheological practice is based on a thorough selection of tracer particles (Valentine et al., 2004; Waigh, 2005). In order to generate knowledge about suitable tracer particles for measurements of protein solutions, a screening will be conducted. By comparison to high frequency rheological measurements and evaluation of the tracer particles' surface characteristics by means of zeta potential measurements, their impact on the microrheological measurements accuracy will be investigated.

Being able to characterize and prevent protein aggregation and high viscosity in early downstream development, changes in protein interactions need to be considered. Their impact will be studied by looking at changes in the apparent diffusion coefficient. This study will evaluate the relationship between protein aggregation, dynamic viscosity and the apparent diffusion coefficient of protein solutions depending on different formulation parameters and evaluate its capacity as a predictive tool for the biopharmaceutical process

development.

The correlation of this parameter with protein structure properties will be evaluated by quantitative structure-activity relationship (QSAR) modelling which was already successfully used to describe and to predict the experimental behavior of proteins and complex biopharmaceutical products during different chromatography modes (Mazza, Whitehead, et al., 2002; Chung et al., 2010; Ladiwala et al., 2006; Buyel et al., 2013). Furthermore, the ability to create a deeper understanding of the mechanisms affecting protein interactions will be considered.

At high concentrations, besides electrostatics, hydrophobic protein interactions have an impact. Already small changes in the hydrophobic character can provoque changes in solubility and in the aggregation tendency of the molecule (Brems et al., 1988; Nieba et al., 1997). Yet, hydrophobic surface characteristics are difficult to determine, because current methods suffer from serious drawbacks, such as changes in solution conditions or limitations to small peptides. Therefore, a novel non-invase high-throughput stalagmometric approach for the determination of protein surface hydrophobicity based on surface tension will be developed.

In order to prevent protein aggregation and high viscosity, manipulation of protein interactions through the addition of additives was reported as effective (Shire et al., 2004). However, for concentrated protein solutions either the impact of additives on the formation of protein aggregates at low protein concentrations or the dynamic viscosity of concentrated protein solutions was examined (J. Liu et al., 2005; W. Wang et al., 2010). As a consequence, this work will aim to give an overall picture of the impact of additives on attractive protein interactions in concentrated protein solutions. It will investigate the impact of additives on the formation of aggregates as well as high viscosity. Furthermore, the impact of selected additives on the protein conformation will be evaluated by FT-IR spectroscopy.

Changes in aggregation tendency are claimed to not only depend on solution conditions but also process-related effects. Concentration experiments of model proteins via tangential flow filtration will help to evaluate their impact on protein aggregation.

In summary, this work aims to show strategies to characterize and stabilize highly concentrated protein solutions with respect to processing and formulation. In any experimental methods sample volume will be minimized to save product consumption and potential high throughput methods, whenever possible, will be used to reduce time consumption. As the development and validation of these studies are protein consuming, model proteins will be used. However, the developed experimental methods can easily be transferred to any biopharmaceutically relevant protein of interest.

CHAPTER 3

Publications & Manuscripts

This article presents a screening of four different tracer particles for microrheological measurements of protein solutions. Melamine, PMMA, polystyrene and surface modified polystyrene, namely PEG-PS, were selected to find out about their surface characteristics and hence their impact on the microrheological measurement quality at various system conditions. To identify their actual impact on the microrheological measurements, the dynamic viscosity of the samples was determined and compared to results of high frequency rheological measurements. PEG-PS was the only tracer particle that yielded good microrheological results for all tested conditions. The study indicated that the electrostatic surface charge of the tracer particle had a minor impact than its hydrophobicity. This characteristic was the crucial surface property that needs to be considered for the selection of a suitable tracer particle to achieve high measurement accuracy.

This study aims to capture the relationship between protein interactions, aggregation, and viscosity to evaluate the capacity of the apparent diffusion coefficient as a predictive tool for biopharmaceutical process development. For this purpose, diffusion coefficients, the dynamic viscosity and the phase behavior of the model proteins, α-lactalbumin, lysozyme, and glucose oxidase, which vary in structure and size, were determined. Each of these experiments revealed a wide range of variations in protein interactions, which showed to be mirrored by changes in the apparent diffusion coefficient. Whereas stable samples with relatively low viscosity showed an almost linear dependence, the deviation from the concentration-dependent linearity indicated both an increase in the sample viscosity and probability of protein aggregation. This deviation of the apparent diffusion coefficient from concentration-dependent linearity was independent of protein type and solution properties for this study. Thus, this single parameter shows the potential to act as a prognostic tool for colloidal stability of protein solutions.

This article examined the capability of QSAR modeling to predict protein interactions from protein structure properties. For the investigation of protein interactions, the apparent diffusion coefficients of six different globular proteins, namely, α-lactalbumin, lysozyme, β-lactoglobulin, ovalbumin, BSA, and glucose oxidase, with a concentration of 10 mg/mL at varying pH values and NaCl concentrations were determined. This data was used to build a QSAR model, which showed a good correlation between experimental and predicted data with a coefficient of determination $R^2 = 0.9$ and a good predictability for an external test set with $R^2 = 0.91$. The information about the properties affecting protein interactions present in solution was in agreement with experiment and theory. Furthermore, the model was able to give a more detailed picture of the protein properties influencing the diffusion coefficient and the acting protein interactions.

accepted by Biotechnology and Bioengineering (DOI: 10.1002/bit.26210)

In the present study a stalagmometric method was used as a non-invasive high-throughput compatible approach to determine protein hydrophobicity on base of the proteins' surface tension increments. Lysozyme, human lysozyme, BSA, and α-lactalbumin were characterized regarding their hydrophobicity depending on pH. This method occurred to outclass the widely used spectrophotometric method with bromophenol blue sodium salt as it gave reasonable results without restrictions on pH and protein species.

published in Biotechnology and Bioengineering (DOI: 10.1002/bit.25677)

This article investigated the impact of additives on the formation of aggregates as well as high viscosity. For this purpose, additives known to stabilize protein aggregation as well as additives known to modulate the viscosity of concentrated protein solutions were selected. These additives, namely PEG 300, PEG 1000, glycerol, glycine, NaCl, and ArgHCl were examined at different pH values. Their impact on the formation of visible aggregates was investigated by phase behavior experiments. Changes in dynamic viscosity of each sample were determined by microrheological measurements. Furthermore, the impact of selected additives on the protein conformation was evaluated by FT-IR spectroscopy. Of all additives investigated, glycine was the only one that maintained the conformational and colloidal stability of concentrated protein solutions while decreasing their dynamic viscosity.

Low concentrations of NaCl showed the same effect, but increasing concentrations resulted in visible protein aggregation.

3.6 Changes in aggregation tendency of protein solutions by concentration via tangential flow filtration - A study evaluating the impact of process-related effects and solution conditions by comparison to centrifugal concentrators

This manuscript aims to evaluate the impact of process-related effects and protein solution conditions on the changes in aggregation tendency during concentration via tangential flow filtration (TFF). For this purpose, three model proteins already investigated for their aggregation tendency by concentration with centrifugal concentrators were concentrated via TFF at different pH values. The changes in protein aggregation of the protein samples were investigated by dynamic light scattering measurements and phase behavior experiments. An impact of process-related stresses on the conformational stability of the proteins was determined by FT-IR spectroscopy. The results of this study revealed that process-related concentration polarization caused a decrease in yield due to the formation of a dense protein layer on the membrane. Solution conditions influenced this effect, as stable protein solutions resulted in lower gel formation and higher yields. Contrary to other publications, process-related stresses were shown to have minor impact. Besides optimization of concentration processes, the identification of stable solution conditions for concentrated protein solutions could, therefore, be another essential factor to avoid protein aggregation and guarantee smooth processing during concentration via TFF.

in preparation

3.1 Impact of polymer surface characteristics on the microrheological measurement quality of protein solutions - a tracer particle screening

Katharina Christin Bauer[1], Marie-Therese Schermeyer[1], Jonathan Seidel, Jürgen Hubbuch*
[1] Contributed equally

Institute of Engineering in Life Sciences, Section IV: Biomolecular Separation Science, Karlsruhe Institute of Technology (KIT), 76131 Karlsruhe, Germany;
* Corresponding author: telephone: +49-721-608-42557, e-mail: juergen.hubbuch@kit.edu
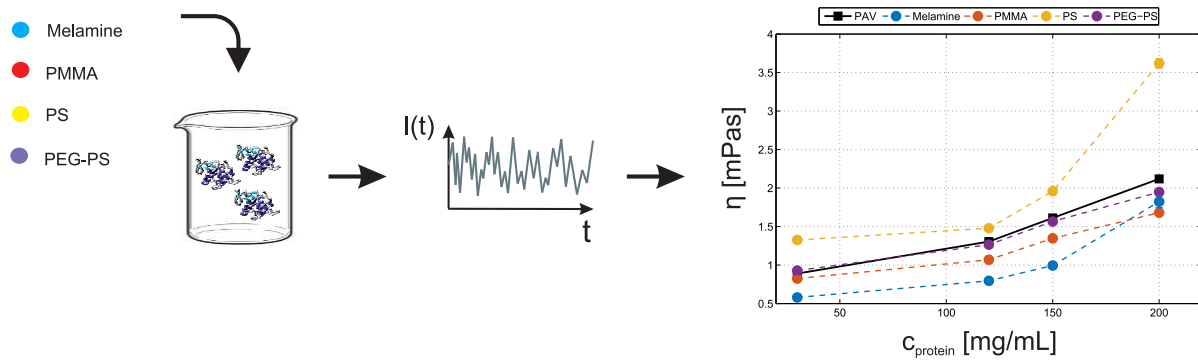
Abstract

Microrheological measurements prove to be suitable to identify rheological parameters of biopharmaceutical solutions. These give information about the flow characteristics but also about the interactions and network structures in protein solutions. For the microrheological measurement tracer particles are required. Due to their specific surface characteristic not all are suitable for reliable measurement results in biopharmaceutical systems. In the present work a screening of melamine, PMMA, polystyrene and surface modified polystyrene as tracer particles were investigated at various protein solution conditions. The surface characteristics of the screened tracer particles were evaluated by zeta potential measurements. Furthermore each tracer particle was used to determine the dynamic viscosity of lysozyme solutions by microrheology and compared to a standard. The results indicate that the selection of the tracer particle had a strong impact on the quality of the microrheological measurement dependent on pH and additive type. Surface modified polystyrene was the only tracer particle that yielded good microrheological results for all tested conditions. The study indicated that the electrostatic surface charge of the tracer particle had a minor impact than its hydrophobicity. This characteristic was the crucial surface property that needs to be considered for the selection of a suitable tracer particle to achieve high measurement accuracy.

Introduction

With the trend towards concentrated biotherapeutics flow characteristics gain increasing relevance for the pharmaceutical process and formulation development. One key issue is the increasing viscosity of these concentrated protein solutions, which affects the outcome of different processing steps like filtration and formulation (Shire et al., 2004). For filtration the viscous solutions are more difficult to pump and can even clog filtration membranes (E. Rosenberg et al., 2009). For formulation the high viscosity of a solution hinders a subcutaneous delivery by syringe (Burckbuchler et al., 2010).

With the help of rheological measurements information about the flow characteristics of protein solutions can be obtained to prevent, predict and manipulate high viscosity. Besides the basic information about the dynamic viscosity of the solution these measurement methods enable the determination of complex rheological parameters like storage and loss modulus, G' and G", which can be used to interpret the interactions and structures formed between the proteins (Jezek et al., 2011; Saluja, Badkar, et al., 2007). In comparison to other complex systems, like polymer solutions, pharmaceutically relevant protein solutions show a weak network formation and therefore the existing elastic behavior is difficult

24

to detect. Hence rheological methods that are able to characterize low elastic behavior are required. Aggravating for the downstream process and formulation development the available protein volumes are very low and therefore expensive. So only small samples can be used for the analytical screenings of highly concentrated solutions. Conventional measurement methods like cone-plate, plate-plate rheometers or capillary viscometers often do not meet these requirements (Saluja, Badkar, et al., 2006). Methods with the possibility to measure in the high frequency region and require low sample volumes are high frequency rheological (Fritz, Pechhold, et al., 2003; Fritz, Maranzano, et al., 2002) or microrheological measurements. High frequency rheological measurements are based on devices, which are able to create frequencies in the kilohertz region. They have already been established for the investigation of proteins Saluja, Badkar, et al., 2006; Schermeyer et al., 2016. Yet there are only few suitable devices, which all represent prototypes and never got into production (Saluja, Badkar, et al., 2007; Willenbacher et al., 2007). In contrast to the high frequency rheological measurements microrheological measurements can be performed by common dynamic light scattering (DLS) or diffusing-wave spectroscopy (DWS) devices. This analytical technique is already established in the biopharmaceutical process development. The principle of this method is based on the diffusion of a particle D dependent on its hydrodynamic radius r_h, the thermal energy kT and the network structure of the surrounding environment. For the determination of the dynamic viscosity η the Stokes-Einstein equation can be applied

$$D = \frac{kT}{6\pi r_h \eta}. \tag{3.1}$$

For the determination of the complex moduli G' and G'' a more complex analysis needs to be performed (Waigh, 2005). In both cases tracer particles of known size are necessary to determine microrheological parameters. These particles are required to be considerably larger than the size of the studied molecule and should not interact with the surrounding solution. Tracer particles smaller in size would not accurately measure the bulk properties. Interactions caused by the surface characteristics of the particle would falsify the measurement data and therefore the rheological information (Waigh, 2005; Breedveld et al., 2003). Currently tracer particles of different material are used to perform microrheological measurements of protein solutions. They consist of materials such as melamine (Amin, Rega, et al., 2011), Poly(methyl methacrylate) (PMMA) (Lazzari et al., 2012), polystyrene (PS) (He, Becker, et al., 2010) or surface modified polymers (Valentine et al., 2004). Amin, Rega, et al., 2011, Valentine et al., 2004 and Gilroy et al., 2011 found that the selection of the tracer particles has an impact on the microrheological measurement quality for protein solutions. One material, which is often reported to interact with its surrounding or with itself, is polystyrene (Breedveld et al., 2003; Gisler et al., 1998). The reason could be found in its surface characteristics. By modification of the surface these particles showed less interaction (Cassidy et al., 1999; Ter Veen et al., 2005). Looking at these findings good microrheological practice is based on a thorough selection of tracer particles. Knowledge to evaluate the functionality are required.

In order to fill this gap we performed a screening of four different tracer particles for

microrheological measurements of lysozyme solutions, used as a model system. Melamine, PMMA, polystyrene and surface modified polystyrene, namely PEG-PS, were selected to find out about their surface characteristics and hence their impact on measurement quality at various system conditions. These conditions were represented by the different lysozyme concentrations, pH-values, plus varying additives. At these conditions the surface characteristics of the tracer particles were studied by zeta potential measurements. The change in the electrostatic potential allowed conclusions about possible interactions in solution. To identify its actual impact on the microrheological measurements the dynamic viscosity of the selected solutions was determined. The results gained with the different tracer particles were compared to results of high frequency rheological measurements. This measurement method was already successfully implemented by several scientific groups (Fritz, Maranzano, et al., 2002; Fritz, Pechhold, et al., 2003; Saluja, Badkar, et al., 2006; Schermeyer et al., 2016) and is therefor used as a standard.

Materials and methods

Chemicals and supplies

The tracer particles used in this study were melamine, polymethylmethacrylate (PMMA), polystyrene and surface modified polystyrene (PEG-PS). Analogous to Amin, Rega, et al., 2011 and Waigh, 2005, their size was carefully chosen in a size range, which should exceed the microstructural length scale of the lysozyme network, because this protein has a comparatively small size of 1.7 nm (Stradner et al., 2006). Polystyrene with a diameter of 0.2 μm and melamine with a diameter of 0.3 μm were both purchased by Alfa Aesar GmbH & Co. KG (Karlsruhe, Germany). PMMA with a diameter of 0.2 μm was purchased by micro particles GmbH (Berlin, Germany). For the surface modified particles with a diameter of 0.22 μm the blank polystyrene particles, described above, were covered with a layer of short length polyethylene glycol (PEG) molecules. Further particle specifications are listed in Table 3.1. The modification of the polystyrene particles followed the PEGylation script of Kim et al. (A. J. Kim et al., 2005). Instead of Pluronic F115 Pluronic F127 (Sigma-Aldrich, St. Louis, USA) was used. The stability of the PEG coating was verified by analytical SEC runs and regular size measurement for each screened buffer condition (data not shown). When using orthogonal PEGylation methods (Nance et al., 2013), the achieved PEG density, which may influence the microrheological measurements, has to be considered. The model protein used in this study was lysozyme from chicken egg white (Hampton Research, Aliso Viejo, CA, USA). It was supplied as a lyophilized powder. The protein has a molecular size of 14.5 kDa, a theoretical pI of 10.7 (Naidu, 2000) and an experimentally determined mass extinction coefficient $E^{1\%}$(280 nm) of 22 L/(g·cm).

The buffer components acetic acid, citric acid, trisodium citrate were purchased form Merck KGaA (Darmstadt, Germany), sodium acetate from Sigma-Aldrich (St. Louis, MO, USA), BisTris propane (1,3-bis(tris(hydroxymethyl)methylamino)propane) from MOLEKULA (München, Germany), 3-Morpholino-2-hydroxypropanesulfonic acid (MOPSO) from AppliChem GmbH (Darmstadt, Germany). Sodium hydroxide and hydrochloric acid for pH-titration and the additives NaCl, $(NH_4)_2SO_4$ came form Merck KGaA, the remaining additives polyethylenglycol (PEG) 300 and 1000 from Sigma-Aldrich. Their specific characteristics are further specified in Table 3.2. Ultrapure water (ISO3696) was used to prepare

all solutions. Buffers were filtered with 0.2 µm cellulose acetate membranes (Sartorius, Göttingen, Germany). Protein solutions were filtered with syringe filters with cellulose acetate membrane (VWR, Radnor, PA, USA). To reduce the residual salt content of the lyophilized lysozyme solution a size exclusion chromatography (SEC) was conducted with Sephadex™ resin from GE Healthcare (Buckinghamshire, Great Britain). The column was manually packed with a diameter of 2.5 cm and a bed height of 23 cm. For the concentration of the protein 20 mL Vivaspin® ultra filtration spin columns (Sartorius) with a molecular weight cut off of 3000 Da were used. For the viscosity measurements ZEN2112 quartz glass cuvettes (Hellma, Müllheim, Germany) were utilized. The zeta potential measurements were performed with folded disposable capillary cells (Malvern Instruments, Malvern, UK) equipped with two electrodes.

Table 3.1: Particle specifications.

Name	Company	Size	Functional groups	Lot
Polystyrene	Alfa Aesar	0.2 µm	Slight anionic charge from surface sulfate groups	T11A024
PMMA	Micro particles GmbH	0.2 µm	-	F-KM255
Melamine	Micro particles GmbH	0.3 µm	-	MF-F-S1902
Pluronic F-127	Sigma Life Sciences	12600 g/mol	-	BCBK9787V

Instrumentation

The buffer exchange was conducted with an ÄKTAprime™ plus system from GE Healthcare. The protein concentration of the lysozyme solutions was determined with the NanoDrop™ 2000c UV-Vis spectrophotometer (Thermo Fisher Scientifc, Waltham, MA, USA). Zetapotentential and microrheological measurements were conducted with the Zetasizer Nano ZSP (Malvern Instruments, Malvern, UK) using dynamic light scattering. With the Non-Invasive Backscatter (NIBS™) optics even turbid samples can be measured without double scattering. The rheological results were compared to results obtained with a squeeze flow rheometer, the Piezo Axial Vibrator (PAV). This instrument was chosen due to its high reproducibility and therefore functions as the standard for this study. The accuracy of this measurement tool could be proven in various publications (Fritz, Pechhold, et al., 2003;

Table 3.2: PEG characteristics.

characteristic	PEG 400	PEG 1000
vapor density	> 1 (vs air)	> 1 (vs air)
vapor pressure	< 0.01 mmHg (20°C)	< 0.01 mmHg (20°C)
autoignition temp.	581 °F	581 °F
mol wt	380 - 420	950 - 1050
refractive index	n20/D 1.467	
viscosity	∼ 120 mPas (20°C)	

Crassous et al., 2005; Vadillo et al., 2010; Pawelzyk et al., 2013).

Sample preparation

Buffers used in this study all had an ionic strength of 100 mM. For the experiments buffers with pH values of 3, 5, 7, and 9 were prepared. The respective buffer components were citric acid and trisodium citrate for pH 3, acetic acid and sodium acetate for pH 5, MOPSO for pH 7 and BisTris Propane for pH 9. Lysozyme of chicken egg white was dissolved in the respective buffer with a starting concentration of 150 mg/mL. To remove residual salts a SEC method followed. Here 5 mL of lysozyme solution with a concentration of 150 mg/mL was purified with a Sephadex™ adsorber. This was packed with a constant flow method. The protein was fractioned in 10 mL Falcon tubes and the concentration measured with an extinction coefficient $E^{1\,\%}(280 \text{ nm})$ of 22 L/(g cm). The concentration of the diluted protein solution to 200 mg/mL was performed in Vivaspins® and a rotational speed of 8000 rad/sec. To have neglectable impact on the studied system tracer particle solutions of 5 w% were induced in a ratio of 1:200 (V(particle solution):V(protein solution)) for the microrheological measurement.

Zeta potential measurements

Depending on the pH and buffer components molecules do have a characteristic surface net charge. This charged surface results in an increased concentration of counter ions close to the particle's surface. The zeta potential is defined as the potential at the boundary, inside which the ions and particles form a stable entity, when the particles move due to an applied electric field. The method used here is based on electrophoretic light scattering. In this case the velocity of particles moving in the electric field is determined by the frequency change of the scattered laser light (Blake et al., 1994; Winzor, 2004). The zeta potential measurements were performed at 25 °C for tracer particles dissolved in buffer and lysozyme solution under conditions mentioned above. A sample volume of 20 µL was pipetted in a disposable cuvettes and measured with the diffusion barrier technique (Corbett et al., 2011). With the correlation to the microrheological results a change of the measurement quality due to electrostatic interactions could be studied.

Determination of the dynamic viscosity and complex moduli using microrheology

In this study passive microrheology was applied. This method extracts rheological properties from the motion of particles undergoing thermal fluctuations. The motion of the particles is measured by dynamic light scattering.

For the calculation of the dynamic viscosity η measured by microrheology the Stokes-Einstein equation, listed as equation 3.1 in this study, was applied. The two unknown parameters r_h and D of the respective tracer particle were determined by two dynamic light scattering measurements. First, r_h of the respective tracer particle was determined in buffer with an estimated viscosity of water at 25 °C. Second, D of the respective tracer particle was determined in lysozyme solution. Considering this approach the dynamic viscosity of protein solutions with melamine, PMMA, polystyrene and PEG-PS as tracer particles was determined using the Zetsizer Nano ZS. The concentration of protein solution was varied within the range of 30 - 200 mg/mL, the pH was shifted from 3 - 9. Additionally

the influence of additive type, namely NaCl, $(NH_4)_2SO_4$, PEG 300 and PEG 1000 on the accuracy of the dynamic viscosity determination was studied. A volume of 40 µL of the sample with the addition of tracer particles in the ratio of 1:200 was directly pipetted into the quartz cuvette and measured at a stable temperature of 25°C.

Microrheological measurements with good results for the dynamic viscosity were further investigated by determination of the complex moduli G' and G". The frequency dependence of the storage (G') and loss modulus (G") were obtained from a thermal energy balance and the measured mean square displacement (Dasgupta et al., 2002). G' and G" were determined over a frequency range of 10 to 100000 rad/sec.

Determination of the dynamic viscosity using high frequency rheology   The high frequency rheological measurements were performed with a squeeze flow rheometer, namely the Piezo Axial Vibrator (PAV), performing a frequency sweep. With frequency sweep measurements one can obtain complex rheological parameters, like the complex storage modulus G' and loss modulus G" as well as the complex viscosity $\eta^\star$.

The complex viscosity can be extrapolated to the zero shear viscosity η_0. The zero shear viscosity obtained with oscillatory measurements can be equated with the dynamic viscosity determined by microrheological measurements, following the Cox-Merz Rule (Metzger, 2012; Kulicke et al., 1980). All measurements were conducted at a temperature of 25°C and a sample volume of 30 µL. The sample was directly pipetted on the measuring head and closed with a thick stainless steel top plate leaving a circular gap with a height of 15 µm in the measurement chamber. A detailed operation of the appliance and a derivation of the required rheological parameters is described in the doctoral thesis of L. Kirschenmann Kirschenmann, 2003.

Results

The measurement quality of microrheological measurements strongly depends on the tracer particles and their specific surface properties in solution. To find the key characteristics of a suitable tracer particle different materials, namely melamine, Poly(methyl methacrylate) (PMMA), polystyrene (PS) and PEGylated polystyrene (PEG-PS) were tested at various conditions. To determine the impact of pH and additives on the electrostatic surface characteristics the zeta potential was determined. Its consequences for the quality of the microrheological measurements were evaluated by the comparison of the determined dynamic viscosity with results of high frequency rheological measurements.

Impact of pH and additives on the zeta potential of the studied tracer particles

Tracer particle surface characteristics are one of the main issues for the quality of a microrheological measurement. These characteristics can induce interactions with the proteins in solution. To better understand the impact of the electrostatic surface characteristics on possible interactions the zeta potential of the respective particle was determined under varying solution conditions. Therefore the influence of pH on the zeta potential of the tracer particles in buffer solution was determined. These results were compared to the same conditions with a constant lysozyme concentration of 150 mg/mL in solution. The deviation of these two values of zeta potential is given by $\delta\zeta$. Analog to this procedure
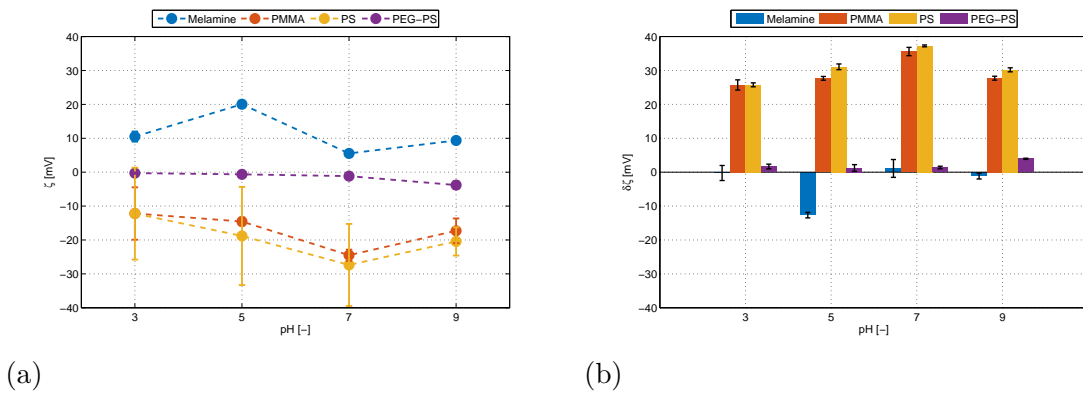
(a)   (b)

Figure 3.1: (a) Zetapotential and calculated standard deviations of the tracer particles melamine, PMMA, poylstyrene (PS) and PEG-PS in buffer and (b) difference between the zetapotential of the tracer particles in buffer and in lysozyme solution at a constant concentration of 150 mg/mL at pH 3, 5, 7 and 9. The depicted standard deviation are calculated for the determined zeta potential in lysozyme solution.
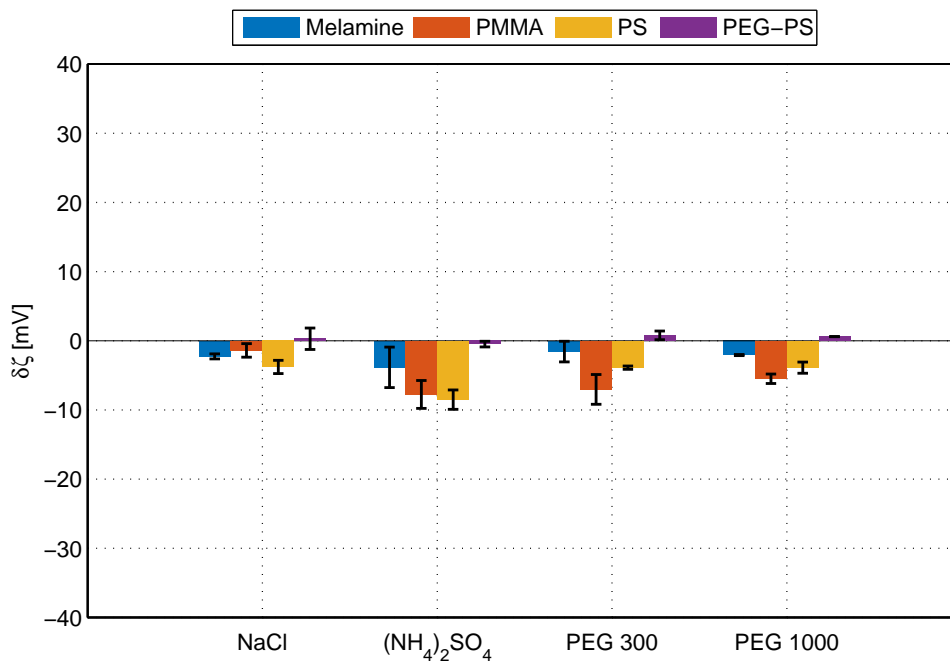

Figure 3.2: Differences of the zeta potential of melamine, PMMA, polystyrene (PS) and PEG-PS in a lysozyme solution with and without addition of NaCl, $(NH_4)_2SO_4$, PEG 300 and PEG 1000 at pH 3.

the impact of additives on protein-particle interactions was studied at pH 3. Here the zeta potential determined for samples with protein in solution were compared to the zeta potential determined for samples with protein and additive in solution.

Figure 3.1(a) displays the zeta potential of melamine, PMMA, polystyrene and PEG-PS tracer particles at pH 3, 5, 7 and 9 in the respective buffer solution. For melamine the surface potential was positive over the studied pH range. At pH 3 and 9 the zeta potential was 11 mV. The highest zeta potential was found at pH 5 with 20 mV, the lowest value at pH 7 with 6 mV. PMMA and polystyrene are both negatively charged and show the same progression of zeta potential over pH. From pH 3 to 7 the zeta potential decreased to a minimum of -25 mV for PMMA and -27 mV for polystyrene. At pH 9 the zeta potential increased to a value around -18 mV for both materials. In comparison to PMMA polystyrene showed high standard deviations for pH 3, 5 and 7. The zeta potential of PEG-PS was determined close to zero for pH 3, 5 and 7. For pH 9 the surface potential decreased to a slightly negative value of -4 mV.

With addition of lysozyme the zeta potential of the tracer particles changed depending on tracer particle type and pH value studied. Figure 3.1(b) shows $\delta\zeta$ for melamine, PMMA, polystyrene and PEG-PS. The zeta potential of melamine stayed constant with addition of lysozyme at pH 3, 7 and 9. At pH 5 the determined zeta potential of the particle decreased. The zeta potential of PMMA and polystyrene increased with addition of lysozyme by a $\delta\zeta > 20$ mV and led to a positive overall surface potential for the studied pH range. In comparison to these two particles the $\delta\zeta$ for PEG-PS was relatively small with the highest value of 3.9 mV at pH 9. This increase led to a neutral surface potential.

In Figure 3.2 the difference of the zeta potential $\delta\zeta$ of the tracer particles in a lysozyme solution with and without additive at pH 3 are shown. This pH-value was chosen due to its low impact on the microrheological measurement accuracy in comparison to pH 5, 7, and 9 (Figure 3.4). At this condition a predominating impact of the additives is expected. In comparison to changes in pH, the chosen additives had a minor impact on the determined zeta potential of the different tracer particles. In general they decreased the zeta potential by a maximum value of 8.5 mV. This value was found for polystyrene with $(NH_4)_2SO_4$ as additive. For PEG-PS $\delta\zeta$ stayed constant with addition of the studied additives. As already observed for the impact of pH in Figure 3.1 the surface potential for this tracer particle is close to 0.

Impact of the tracer particles on the microrheological measurement quality

The following results show the dynamic viscosity of lysozyme solution measured with microrheology in comparison to the results gained by squeeze flow rheology used as standard. Protein concentration, pH and additive type had varying impact on the tracer particles used in this study.

Figure 3.3(a) shows the dynamic viscosity determined by microrheological measurements with tracer particles consisting of melamine, PMMA, polystyrene, PEG-PS and high frequency measurements conducted with the PAV dependent on lysozyme concentration at pH 3. For every measured system the dynamic viscosity increased with increasing concentration. In comparison to the dynamic viscosity determined with the PAV the viscosity derived by microrheological measurements with polystyrene as tracer particle
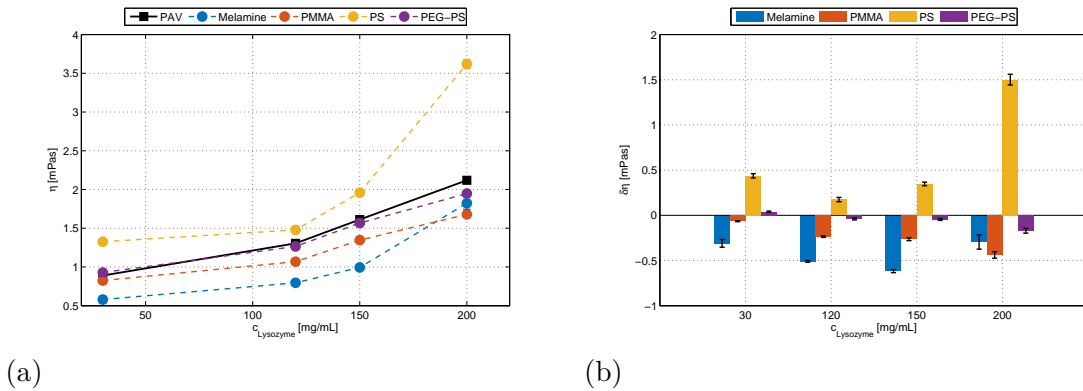
(a)   (b)

Figure 3.3: (a) Dynamic viscosity of a lysozyme solutions determined with the PAV (standard) and microrheological measurements conducted with different tracer particles dependent on concentration at pH 3. (b) Difference to the gold standard for each tracer particle dependent on the lysozyme concentration at pH 3.
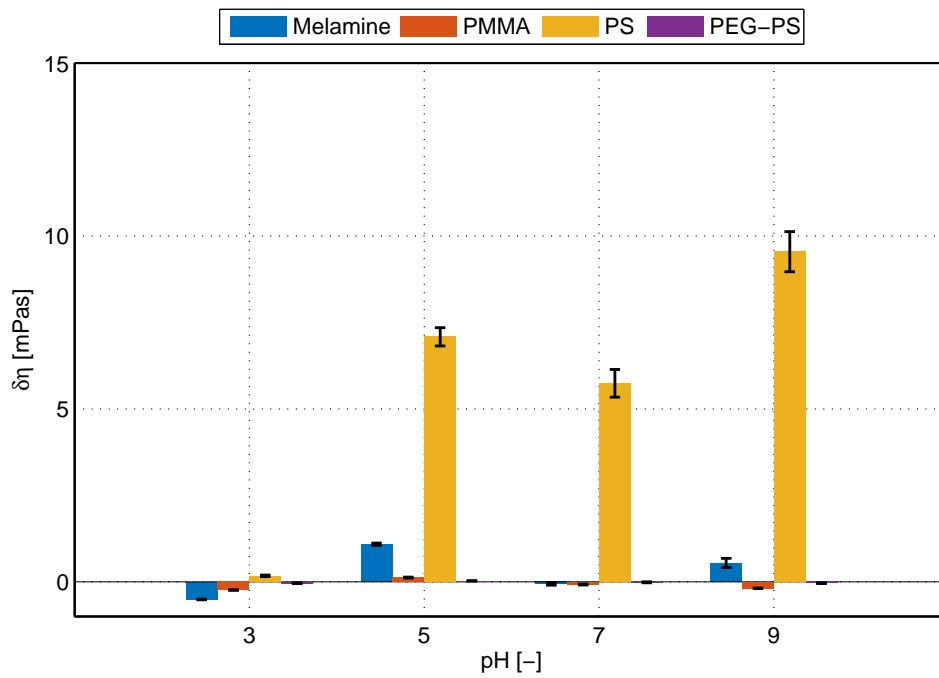

Figure 3.4: Difference to the standard $\delta\eta$ and the standard deviation of the microrheological measurement for each tracer particle dependent on pH at a constant lysozyme concentration of 120 mg/mL.
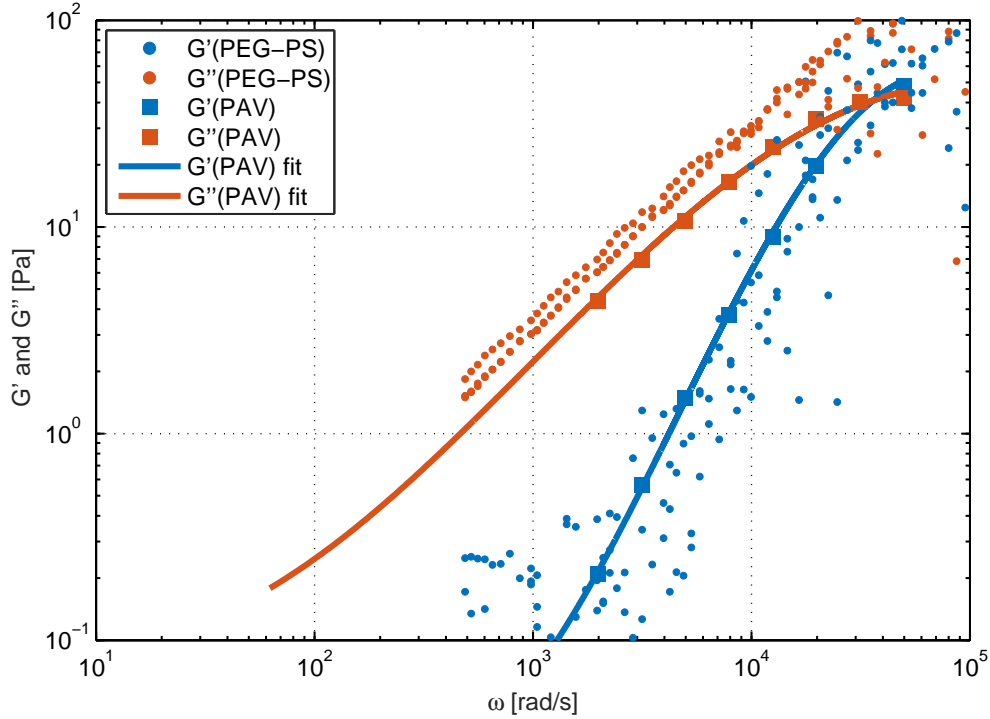
Figure 3.5: Triplicate microrheological measurement with modified polystyrene particles (PEG-PS) of the complex storage and loss modulus (G' and G") in comparison to the standard (PAV) plus its fit (Schermeyer et al., 2016) at pH 7 and a lysozyme concentration of 150 mg/mL.

were overestimated for every studied protein concentration. The results for systems with melamine and PMMA were underestimated. The dynamic viscosity determined with PEG-PS was closest to the values of the chosen standard and had the same progression up to 150 mg/mL.

The difference between the viscosity measured by microrheological measurements and the viscosity determined with the PAV $\delta\eta$ and the standard deviations of the microrheological measurements are shown in Figure 3.3(b). In general the differences increase with increasing protein concentration for all tested particles. The highest $\delta\eta$ was found for polystyrene at a lysozyme concentration of 200 mg/mL. The results for PEG-PS showed high consistency with the PAV. For melamine at a lysozyme concentration of 200 mg/mL $\delta\eta$ decreased, but the standard deviation of the microrheological measurement increased to 7.8 mPas. This was also the highest value of standard deviation determined for this measurement series. Figure 3.4 demonstrates the influence of pH on the difference between the dynamic viscosity determined by microrheological measurements and the standard method at a constant lysozyme concentration of 120 mg/mL. Additionally the standard deviations of the microrheological measurements are displayed. The values of $\delta\eta$ determined with melamine,

PMMA and polystyrene were sensitive to pH. In case of the measurements with melamine no clear trend could be observed. The dynamic viscosity determined for pH 3 and pH 7 was underestimated and thus $\delta\eta$ negative, for pH 5 and pH 9 the dynamic viscosity was overestimated and thus $\delta\eta$ positive. The highest difference for melamine could be found for pH 5 with a value of 1.09 mPas. For PMMA the smallest difference to the standard was detected at pH 7. With a decrease or increase of pH from this point the dynamic viscosity got underestimated and the modulus of $\delta\eta$ increased up to a value of 0.19 mPas. The highest values of $\delta\eta$ as well as the highest standard deviations were determined for polystyrene. For pH 5, pH 7 and pH 9 the dynamic viscosity of the protein solution was overestimated by more than 5 mPas. The standard deviations increased from 0.024 mPas at pH 3 to 0.58 mPas at pH 9. The influence of the pH on PEG-PS was negligibly small and the $\delta\eta$ did not exceeded a modulus of 0.039 mPas.

Also the complex moduli G' and G" determined with PEG-PS particles in triplicate showed a comparable course to the results of the standard. Figure 3.5 shows the raw data of the microrheological measurements and of the PAV as well as its fit by Fourier transformation of second order.

The impact of additives on the dynamic viscosity measured with the different tracer particles can be found in Figure 3.6. Here the differences between the microrheological measurements and the standard induced by added salts and PEG molecules are shown. Two salt types, NaCl and $(NH_4)_2SO_4$, and two PEG molecules of different molecular weight, PEG 300 and PEG 1000, were investigated in this study. Dependent on tracer particle and additive type the measurement quality varied. The dynamic viscosity determined with melamine particles was underestimated with every additive type in solution. The standard deviation calculated for samples containing $(NH_4)_2SO_4$ and melamine as tracer particle in solution was higher than the resulting $\delta\eta$. The difference to the standard $\delta\eta$ with PMMA as tracer particle was negative with sodium chloride and PEG 300 in solution. The addition of $(NH_4)_2SO_4$ resulted in a positive $\delta\eta$. In comparison to the standard the determined viscosity was 13 times higher. PEG 1000 had no significant impact on the measurement accuracy with PMMA as tracer particle. For the microrheological measurements with polystyrene and the two studied salts $\delta\eta$ values were higher than 3 mPas. The addition of PEG revealed a lower determined viscosity. In comparison with the other tracer particles the influence of the chosen additives on the measurement quality with PEG-PS was low. The viscosity was underestimated with addition of sodium chloride, PEG 300 and PEG 1000. $(NH_4)_2SO_4$ resulted in a positive $\delta\eta$ of 0.24 mPas, the highest difference to the standard for this particle.

Discussion

In this work we investigated the suitability of different tracerparticles, namely melamine, PMMA, polystyrene and PEG-PS, for microrheological measurements under various conditions. The results of this investigation showed that the specific particle surface properties dependent on solution conditions like protein concentration, pH as well as the addition of additives had an impact on the measurement quality. The changes on the tracer particle surface and the consequences for the microrheological measurement accuracy are discussed in the following sections.
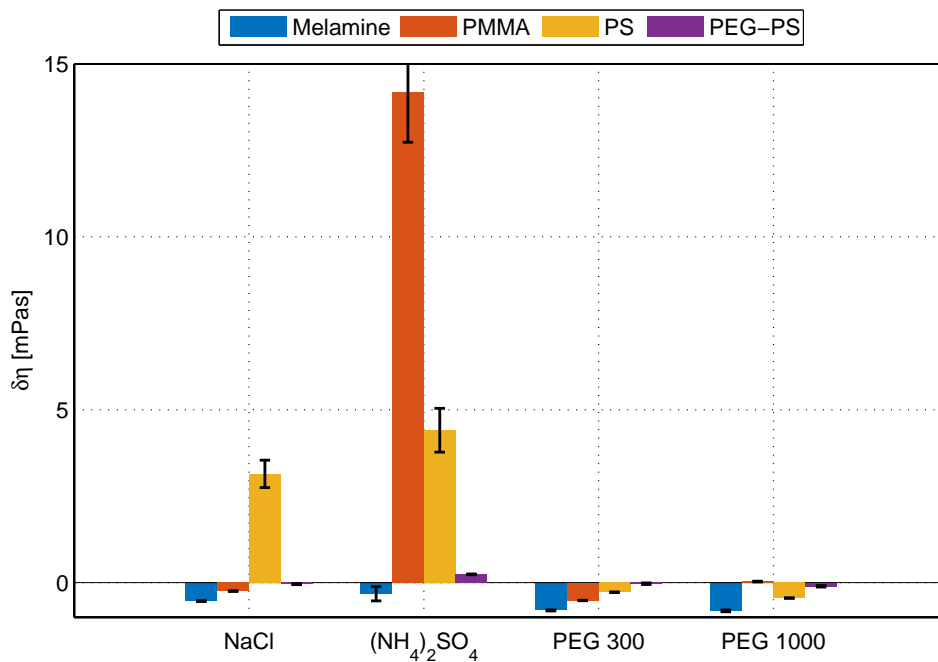
Figure 3.6: Difference to the standard for each tracer particle and the standard deviation of the microrheological measurement dependent on the additives NaCl, $(NH_4)_2SO_4$, PEG 300 and PEG 1000 at pH 3 and lysozyme concentration of 120 mg/mL.

Impact of pH and additives on the zeta potential of the studied tracer particles

To investigate the electrostatic surface characterisitcs and its possible influence on the microrheological measurement quality the zeta potential of the tracer particles melamine, PMMA, polystyrene and PEG-PS was determined under varying conditions. In the following section the impact of pH and additives are discussed.

For the studied pH range the sign of the measured net charge stayed the same for all tested tracer particles. Melamine had a positive zeta potential. This observed surface character is mainly governed by the partial positively charged amine groups, which is in accordance with literature (Olmsted et al., 1997). With addition of lysozyme the observed variance of charge with changing pH is compensated to a constant value of 10 mV. This change in zeta potential for pH 5 implies an interaction of the tracer particles with lysozyme. As both particles are positive in net charge this effect has to be based on hydrophobic interactions with the hydrocarbon segments of the melamine surface (Deryło-Marczewska et al., 2002). For PMMA a negative zeta potential was determined due to the ionized carboxyl groups Baptista et al., 2003. This finding is in good agreement to literature, which reviewed and determined zeta potential data of unmodified PMMA (Kirby et al., 2004; Falahati et al., 2014). At pH 3 comparatively high standard deviation was observed, which could be attributed to its pKa at 4.5. Below this pH-value the carboxyl groups are not ionized. This could lead to a destabilization of the particles. In lysozyme solution the

zeta potential of PMMA became positive, which is due to electrostatic protein-particle interactions between the positively charged protein surface and the negatively charged tracer particle surface. As PMMA polystyrene had a negative zeta potential from pH 3 to 9, which was also seen for the measurements conducted by Ohsawa et al. Ohsawa et al., 2005. In comparison to PMMA the $\delta\zeta$ of polystyrene in protein solution were even higher. This behavior could be explained by the strong hydrophobic character of polystyrene (N. Kumar et al., 2008). Another argument for the strong hydrophobic character are the high standard deviations for the zeta potential measurements, shown in Figure 3.1. The hypothesis, that the polystyrene particles did not reach equilibrium could not be confirmed by repeated measurements after zero, three, and ten hours (data not shown). Here, the motion in the electric field could be influenced by the hydrophobic forces. This may also lead to aggregation of the poorly stabilized polystyrene particles. By addition of lysozyme the strong hydrophobic impact on the standard deviation decreases. This decrease can be explained by the adsorption of lysozyme to the polystyrene surface, which shields the hydrophobic surface patches. In contrast to the other tracer particles the zeta potential of PEG-PS was close to zero for the tested pH range. This implies a uncharged particle surface. As the PEG-PS surface is neither charged nor hydrophobic no protein-particle interactions are anticipated. The determination of the zeta potential with lysozyme in solution confirms this assumption, because only a small $\delta\zeta$ was observed.

The addition of salts or PEGs had less impact than the change in pH on the determined zeta potential of the tracer particles in lysozyme solution. For melamine, PMMA and polystyrene the additives decreased the zeta potential and hereby the surface charge. Regardless if the tracer particle was positively or negatively charged the additives shield the electrostatic groups on the surface. Comparing the two salt types $(NH_4)_2SO_4$ had a higher shielding effect than NaCl due to its higher electron valence (Broide et al., 1996). The different polymer length of PEG 300 and PEG 1000 did not seem to have an impact on the modulus of $\delta\zeta$. The zeta potential of PEG-PS is not influenced by the studied additives due to its uncharged surface.

Impact of tracer particle surface on the microrheological measurement quality

The observed changes in surface characteristics discussed in the section before are evaluated regarding their impact on the quality of the microrheological measurements dependent on lysozyme concentration, pH and additives. The possible interactions of tracer particles in protein solution, which cause these deviations from the ideal value, are also taken into account.

Compared to pH and addition of additives the influence of lysozyme concentration on the microrheological measurement quality at pH 3 was low independent on the tracer particle type used. The maximum value of $\delta\eta$ with changing lysozyme concentration was 1.5 mPas for the measurement with polystyrene as tracer particle. In general $\delta\eta$ increased with increasing protein concentration. This effect is due to the decreasing molecule distances, which promote increasing interactions (Saluja and Kalonia, 2008). Only exceptions were the measurement values of polystyrene at 30 mg/mL of lysozyme and melamine at 200 mg/mL of lysozyme. Whereas this value for polystyrene could be assessed as an outlier the determined value for melamine could be explained by the different ranges of electrostatic and

hydrophobic interactions. Melamine is protonated at pH 3, which causes a positive surface charge. This can be seen in the measured zeta potential in Figure 3.1. This positive charge of the particle and the positive charge of lysozyme at pH 3 (pI of 10.7) lead to repulsive electrostatic interactions and result in an lower determined viscosity. This state seems to apply for lysozyme concentrations up to 150 mg/mL. At higher concentrations shorter distances between the particles and the proteins allow the formation of additional short-range interactions like attractive hydrophobic interactions and hydration forces (Ellis, 2001; Beretta et al., 2000), which could decrease $\delta\eta$. Like for melamine the viscosity values of the lysozyme solutions measured with PMMA as tracer particle were underestimated, although this particle had a contrary charge in comparison to melamine at pH 3. One possible reason could be the adsorption of protein on the particle surface. As shown in Figure 3.1(b) the surface potential of PMMA with addition of lysozyme became positive. This shift could be explained by the formation of an adsorption equilibrium of lysozyme molecules on the PMMA surface. This change in particle surface leads to repulsive interactions with the positively charged lysozyme molecules in solution and thus to a negative $\delta\eta$. In comparison to melamine and PMMA the determined viscosity with polystyrene as tracer particle was overestimated for all lysozyme concentrations. This particle has the same surface potential as PMMA, but also a strongly hydrophobic character. Thus the particle is poorly hydrated, which leads to a bad dispersability in aqueous solutions. For this reason one can expect strong particle-particle and particle-protein interactions (M. Rosenberg, 1981). Both effects might lead to higher determined viscosity values. Short-range hydrophobic interactions between lysozyme and polystyrene intensify with increasing protein concentrations, which might cause the highest $\delta\eta$ of 1.5 mPas at 200 mg/mL of lysozyme for the studied influence of concentration at pH 3. In case of PEG-PS the hydrophobic surface groups of polystyrene are shielded with neutral and hydrophilic PEG molecules. This modification results in a good accordance of the determined viscosity values with the standard, which does not change with addition of lysozyme (Figure 3.1). Due to the neutral surface potential and hydrophilic character of PEG-PS $\delta\eta$ is below |0.17| mPas for the whole measurement range. To summarize the impact of lysozyme concentration on the measured dynamic viscosity values all tracer particles showed the right trend of increasing viscosity with protein concentration. The measurements with PEG-PS showed the highest accuracy.

The pH-value has an impact on the microrheological measurement quality depending on the type of tracer particle used. In comparison to the impact of lysozyme concentration the impact of different pH values on $\delta\eta$ was up to five times higher. The strongest impact could be found for polystyrene at pH 5, 7 and 9. This unacceptably high difference in viscosity and high standard deviations might be due to hydrophobic interactions of the polystyrene particles with each other respectively interactions of the polystyrene particles with lysozyme (Onwu et al., 2011). These interactions may cause aggregation of the particles and adsorption of lysozyme to the particle surface. Both phenomena increase the observed hydrodynamic radius of the tracer particles and therefor lead to inadequate measurement results and calculations. The adsorption of the protein was already observed in a minor dimension with the increase of lysozyme concentration at pH 3 in section 3.1. One could explain the high deviations for pH 5, 7 and 9 with an adsorption of proteins to the surface, but also a denaturing effect of the strongly hydrophobic polystyrene on

the proteins. This property is already used by several research groups to investigate protein unfolding in solution (Miriani et al., 2014). As well as for polystyrene hydrophobic interactions could cause differences of the determined dynamic viscosity with melamine as a tracer particle. This claim can be explained by the comparison of the zeta potential values for melamine in buffer, shown in Figure 3.1, and lysozyme in solution at pH 5. At this condition melamine and lysozyme both have a positive surface potential. Thus, the observed change of the zeta potential of melamine in lysozyme solution in Figure 3.1(b) can not be explained by electrostatics. In this case hydrophobic interactions must cause an adsorption of lysozyme to the particle, which partially shields the positively charged groups of the melamine surface. In comparison to pH 5 $\delta\eta$ is smaller for pH 3 and 9 and no changes in zeta potential were observed. With this considerations one expects hydrophobic interactions but no shielding at these pH values. For PMMA and PEG-PS the impact of pH can be neglected. All values calculated for $\delta\eta$ are below a value of 0.25 mPas. The best accuracy over the investigated pH range was determined for PEG-PS with $\delta\eta < 0.04$ mPas according to a percentage deviation of 3 %. Therefore those two tracer particles are suitable for microrheological measurements in the tested pH range without additive in solution. For PEG-PS this is due to the fact that the particles' surface is uncharged, which is depicted in Figure 3.1. The good accordance of rheological results obtained with PEG-PS with the standard holds true for the determination of complex viscoelastic moduli. Figure 3.5 demonstrates that the course of G' and G" obtained with PEG-PS are in acceptable agreement with values obtained with the PAV. The scattering of the G' values and thus a limited reproduceability of the complex moduli are due to not optimized meaurement settings and have to be improved for future measurements. For this optimization the impact of particle size is of special interest. In contrast to the zero zeta potential of PEG-PS the measurements conducted with PMMA reveal a negative zeta potential within the tested pH range. With the assumptions made so far one would expect a deviation in the determined dynamic viscosity for this tracer particle. Yet the discussed deviations of the dynamic viscosity for melamine and polystyrene had their cause in hydrophobic interactions. PMMA is more hydrophilic in character (Ochoa, 2003; Feldman et al., 1998). This characteristic seems to dominate the quality of microrheological measurements. The changes in electrostatic character, detected by the zeta potential measurements, have a minor impact on the quality of the microrheological measurements. With this knowledge the determination of hydrophobicity should be prioritized over the determination of electrostatic surface characteristics.

Compared to the impact of pH the addition of the selected additives had a minor influence on the measurement quality. The highest deviation could be found for the viscosity determined with PMMA in a 120 mg/mL lysozyme solution with 150 mM $(NH_4)_2SO_4$. Poor solubility of this tracer particle in buffer solution containing additives seem to be the only plausible reason. Conducted size measurements of PMMA revealed aggregation caused by the addition of the studied additives in buffer (Data not shown). For NaCl, PEG 300 and PEG 1000 this impact could be suppressed by the addition of lysozyme. For $(NH_4)_2SO_4$, which is a common precipitating agent for protein solutions (Duong-Ly et al., 2014; Shih et al., 1992), the aggregation was enhanced. Further deviations were found for measurements with polystyrene and the selected salts. As described before the

zeta potential of the polystyrene particles in these two systems shifts to a positive value with addition of lysozyme. This positive zeta potential is reduced by the interaction with the negatively charged salt ions. This reduction in electrostatics promotes the already present hydrophobic interactions between particles and proteins. This increase in attractive interactions results in an increase in $\delta\eta$. The different impact of the two salt types could be explained analog to the change in zeta potential in Figure 3.2 with the different valence of the salt ions. Consequently, polystyrene and PMMA are unsuitable for microrheological measurement with salt as an additive. For melamine and PEG-PS additional salt does not have an influence on the measurement accuracy, which makes them suitable tracer particles for these specific conditions. With an alteration of conditions this observation would need to be reexamined. In comparison to salt the microrheological measurements with PEG 300 and PEG 1000 in solution resulted in adequate viscosity values independent of PEG type and tracer particle used.

Conclusion

Taken all influences on tracer surface characteristics and their impact on the microrheological measurement quality into account PEG-PS was the only suitable tracer particle in this study. It resulted in good agreement for the dynamic viscosity as well as first promising results for the complex moduli. The key factors were its hydrophilic character and uncharged surface. Although PMMA was oppositely charged to lysozyme it showed exclusively high deviations of measurement quality with the addition of $(NH_4)_2SO_4$. The measurement accuracy for melamine was insufficient for high protein concentrations and changes in pH. These deviations could be explained by its charged and hydrophobic character. However, this study was conducted with respect to the pharmaceutically relevant bioproducts. Here the accuracy of analytical measurements is very important. If costs for PEG-PS exceed investigation budget and measurements in ideal, solute solutions are performed, then melamine could be considered as an alternative. The highest deviations to the standard were determined with polystyrene as tracer particle for every varied parameter in this study. The reason could be found in its charged but mainly hydrophobic character. In principle these results reinforce the observations from other publications, which stated that the selection of a suitable tracer particle is one of the key requirements for the accuracy of a microrheological measurement. Our work reveals that electrostatic interactions due to the charged surface of the tracer particles and the protein molecules seems to have a minor impact on the measurement quality of this screening. It suggests that the hydrophobicity of the tracer particle has the major impact on the microrheological measurement quality. This surface property can cause strong interactions with the protein molecules in solution, especially at high concentrations. Consequently this characteristic is the crucial surface property that needs to be considered for the selection of a suitable tracer particle to achieve high measurement accuracy. This allows a better analysis of biopharamceutical solutions in the early process and formulation development.

experimental work.

References

Amin, S., Rega, C. A., and Jankevics, H. (2011). 'Detection of viscoelasticity in aggregating dilute protein solutions through dynamic light scattering-based optical microrheology'. *Rheol. Acta.* Vol. 51(4), pp. 329–342 (cit. on pp. 12–14, 25, 26, 58).

Baptista, R. P., Santos, A. M., Fedorov, A., Martinho, J. M. G., Pichot, C., Elaïssari, A., Cabral, J. M. S., and Taipa, M. A. (2003). 'Activity, conformation and dynamics of cutinase adsorbed on poly(methyl methacrylate) latex particles'. *J. Biotechnol.* Vol. 102(3), pp. 241–249 (cit. on p. 35).

Beretta, S., Chirico, G., and Baldini, G. (2000). 'Short-Range Interactions of Globular Proteins at High Ionic Strengths'. *Macromolecules.* Vol. 33(23), pp. 8663–8670 (cit. on p. 37).

Blake, R. C., Shute, E. A., and Howard, G. T. (1994). 'Solubilization of minerals by bacteria: Electrophoretic mobility of Thiobacillus ferrooxidans in the presence of iron, pyrite, and sulfur'. *Appl. Environ. Microbiol.* Vol. 60(9), pp. 3349–3357 (cit. on p. 28).

Breedveld, V. and Pine, D. J. (2003). 'Microrheology as a tool for high-throughput screening'. *J. Mater. Sci.* Vol. 38(22), pp. 4461–4470 (cit. on pp. 25, 51).

Broide, M. L., Tominc, T. M., and Saxowsky, M. D. (1996). 'Using phase transitions to investigate the effect of salts on protein interactions'. *Phys. Rev. E: Stat., Nonlinear, Soft Matter Phys.* Vol. 53(6), pp. 6325–6335 (cit. on p. 36).

Burckbuchler, V., Mekhloufi, G., Giteau, A. P., Grossiord, J., Huille, S., and Agnely, F. (2010). 'Rheological and syringeability properties of highly concentrated human polyclonal immunoglobulin solutions'. *Eur. J. Pharm. Biopharm.* Vol. 76(3), pp. 351–356 (cit. on pp. 12, 15, 24, 47, 60, 61, 142).

Cassidy, O. E., Rowley, G., Fletcher, I. W., Davies, S. F., and Briggs, D. (1999). 'Surface modification and electrostatic charge of polystyrene particles'. *Int. J. Pharm. (Amsterdam, Neth.).* Vol. 182(2), pp. 199–211 (cit. on p. 25).

Corbett, J. C. W., Connah, M. T., and Mattison, K. (2011). 'Advances in the measurement of protein mobility using laser Doppler electrophoresis - the diffusion barrier technique.' *Electrophoresis.* Vol. 32(14), pp. 1787–94 (cit. on p. 28).

Crassous, J. J., Régisser, R., Ballauff, M., and Willenbacher, N. (2005). 'Characterization of the viscoelastic behavior of complex fluids using the piezoelastic axial vibrator'. *J. Rheol. (Melville, NY, U. S.).* Vol. 49(4), p. 851 (cit. on p. 28).

Dasgupta, B. R., Tee, S.-Y., Crocker, J. C., Frisken, B. J., and Weitz, D. A. (2002). 'Microrheology of polyethylene oxide using diffusing wave spectroscopy and single scattering'. *Phys. Rev. E: Stat., Nonlinear, Soft Matter Phys.* Vol. 65(5), p. 051505 (cit. on p. 29).

Deryło-Marczewska, A., Goworek, J., Pikus, S., Kobylas, E., and Zgrajka, W. (2002). 'Characterization of Melamine-Formaldehyde Resins by XPS, SAXS, and Sorption Techniques'. *Langmuir.* Vol. 18(20), pp. 7538–7543 (cit. on p. 35).

Duong-Ly, K. C. and Gabelli, S. B. (2014). 'Salting out of proteins using ammonium sulfate precipitation'. *Methods Enzymol.* Vol. 541, pp. 85–94 (cit. on p. 38).

Ellis, R. J. (2001). 'Macromolecular crowding: obvious but underappreciated.' *Trends Biochem. Sci.* Vol. 26(10), pp. 597–604 (cit. on p. 37).

Falahati, H., Wong, L., Davarpanah, L., Garg, A., Schmitz, P., and Barz, D. P. J. (2014). 'The zeta potential of PMMA in contact with electrolytes of various conditions: Theoretical and experimental investigation'. *Electrophoresis.* Vol. 35, pp. 870–882 (cit. on p. 35).

Feldman, K., Tervoort, T., Smith, P., and Spencer, N. D. (1998). 'Toward a Force Spectroscopy of Polymer Surfaces'. *Langmuir.* Vol. 14(2), pp. 372–378 (cit. on p. 38).

Fritz, G., Maranzano, B., Wagner, N., and Willenbacher, N. (2002). 'High frequency rheology of hard sphere colloidal dispersions measured with a torsional resonator'. *J. Nonnewton. Fluid Mech.* Vol. 102(2), pp. 149–156 (cit. on pp. 14, 25, 26).

Fritz, G., Pechhold, W., Willenbacher, N., and Wagner, N. J. (2003). 'Characterizing complex fluids with high frequency rheology using torsional resonators at multiple frequencies'. *J. Rheol. (Melville, NY, U. S.).* Vol. 47(2), p. 303 (cit. on pp. 25–27).

Gilroy, E. L., Hicks, M. R., Smith, D. J., and Rodger, A. (2011). 'Viscosity of aqueous DNA solutions determined using dynamic light scattering'. *Analyst (Cambridge, U. K.).* Vol. 136(20), p. 4159 (cit. on p. 25).

Gisler, T. and Weitz, D. A. (1998). 'Tracer microrheology in complex fluids'. *Curr. Opin. Colloid Interface Sci.* Vol. 3(6), pp. 586–592 (cit. on p. 25).

He, F., Becker, G. W., Litowski, J. R., Narhi, L. O., Brems, D. N., and Razinkov, V. I. (2010). 'High-throughput dynamic light scattering method for measuring viscosity of concentrated protein solutions.' *Anal. Biochem.* Vol. 399(1), pp. 141–3 (cit. on p. 25).

Jezek, J., Rides, M., Derham, B., Moore, J., Cerasoli, E., Simler, R., and Perez-Ramirez, B. (2011). 'Viscosity of concentrated therapeutic protein compositions'. *Adv. Drug Delivery Rev.* Vol. 63(13), pp. 1107–1117 (cit. on pp. 5, 7–9, 12–15, 24, 120, 131, 152).

Kim, A. J., Manoharan, V. N., and Crocker, J. C. (2005). 'Swelling-based method for preparing stable, functionalized polymer colloids.' *J. Am. Chem. Soc.* Vol. 127(6), pp. 1592–3 (cit. on pp. 26, 123).

Kirby, B. J. and Hasselbrink, E. F. (2004). 'Zeta potential of microfluidic substrates: 2. Data for polymers'. *Electrophoresis.* Vol. 25(2), pp. 203–213 (cit. on p. 35).

Kirschenmann, L. (2003). 'Aufbau zweier piezoelektrischer Sonden (PRV / PAV) zur Messung der viskoelastischen Eigenschaften weicher Substanzen im Frequenzbereich 0.5 Hz-2 kHz bzw. 0.5 Hz- 7 kHz'. PhD Thesis. Universität Ulm (cit. on p. 29).

Kulicke, W.-M. and Porter, R. S. (1980). 'Relation between steady shear flow and dynamic rheology'. *Rheol. Acta.* Vol. 19(5), pp. 601–605 (cit. on p. 29).

Kumar, N., Parajuli, O., Gupta, A., and Hahm, J. I. (2008). 'Elucidation of protein adsorption behavior on polymeric surfaces: Toward high-density, high-payload protein templates'. *Langmuir.* Vol. 24(6), pp. 2688–2694 (cit. on p. 36).

Lazzari, S., Moscatelli, D., Codari, F., Salmona, M., Morbidelli, M., and Diomede, L. (2012). 'Colloidal stability of polymeric nanoparticles in biological fluids'. *J. Nanopart. Res.* Vol. 14(6), p. 920 (cit. on p. 25).

Metzger, T. G. (2012). *The Rheology Handbook.* 4th ed. Hannover: Vincentz Network, pp. 51–56 (cit. on p. 29).

Minton, A. P. (1997). 'Influence of excluded volume upon macromolecular structure and associations in 'crowded' media'. *Curr. Opin. Biotechnol.* Vol. 8(1), pp. 65–69 (cit. on pp. 47, 58, 61).

Miriani, M., Eberini, I., Iametti, S., Ferranti, P., Sensi, C., and Bonomi, F. (2014). 'Unfolding of beta-lactoglobulin on the surface of polystyrene nanoparticles: Experimental and computational approaches'. *Proteins: Struct., Funct., Bioinf.* Vol. 82(7), pp. 1272–1282 (cit. on p. 38).

Naidu, A. S. (2000). *Natural Food Antimicrobial Systems.* Ed. by Naidu, A. CRC Press, p. 382 (cit. on p. 26).

Nance, E. A., Woodworth, G. F., Sailor, K. A., Shih, T.-Y., Swaminathan, G., Xiang, D., and Eberhart, C. (2013). 'A Dense Poly(Ethylene Glycol) Coating Improves Penetration of Large Polymeric Nanoparticles Within Brain Tissue'. *Sci. Transl. Med.* Vol. 4(149), 149ra119 (cit. on p. 26).

Ochoa, N. (2003). 'Effect of hydrophilicity on fouling of an emulsified oil wastewater with PVDF/PMMA membranes'. *J. Membr. Sci.* Vol. 226(1-2), pp. 203–211 (cit. on p. 38).

Ohsawa, K., Murata, M., and Ohshima, H. (2005). 'Zeta potential and surface charge density of polystyrene-latex; comparison with synaptic vesicle and brush border membrane vesicle'. *Colloid Polym. Sci.* Vol. 264, pp. 1005–1009 (cit. on p. 36).

Olmsted, J. and Williams, G. (1997). *Chemistry: The Molecular Science.* Jones & Bartlett Learning, p. 1189 (cit. on p. 35).

Onwu, F. K. and Ogah, S. (2011). 'Adsorption of lysozyme unto silica and polystyrene surfaces in aqueous medium'. *Afr. J. Biotechnol.* Vol. 10(15), pp. 3014–3021 (cit. on p. 37).

Pawelzyk, P., Herrmann, H., and Willenbacher, N. (2013). 'Mechanics of intermediate filament networks assembled from keratins K8 and K18'. *Soft Matter.* Vol. 9(37), p. 8871 (cit. on p. 28).

Rosenberg, E., Hepbildikler, S., Kuhne, W., and Winter, G. (2009). 'Ultrafiltration concentration of monoclonal antibody solutions: Development of an optimized method minimizing aggregation'. *J. Membr. Sci.* Vol. 342(1-2), pp. 50–59 (cit. on pp. 15, 24, 142, 143, 151, 152).

Rosenberg, M. (1981). 'Bacterial adherence to polystyrene: a replica method of screening for bacterial hydrophobicity.' *Appl. Envir. Microbiol.* Vol. 42(2), pp. 375–377 (cit. on p. 37).

Saluja, A., Badkar, A. V., Zeng, D. L., Nema, S., and Kalonia, D. S. (2006). 'Application of high-frequency rheology measurements for analyzing protein-protein interactions in high protein concentration solutions using a model monoclonal antibody (IgG2)'. *J. Pharm. Sci.* Vol. 95(9), pp. 1967–1983 (cit. on pp. 25, 26).

– (2007). 'Ultrasonic storage modulus as a novel parameter for analyzing protein-protein interactions in high protein concentration solutions: correlation with static and dynamic light scattering measurements.' *Biophys. J.* Vol. 92(1), pp. 234–44 (cit. on pp. 11–15, 24, 25, 48, 51, 75, 77, 86).

Saluja, A. and Kalonia, D. S. (2008). 'Nature and consequences of protein-protein interactions in high protein concentration solutions.' *Int. J. Pharm. (Amsterdam, Neth.).* Vol. 358(1-2), pp. 1–15 (cit. on pp. 2, 5, 7, 10–13, 15, 36, 46–48, 58, 59, 61, 62, 75).

Schermeyer, M.-T., Sigloch, H., Bauer, K. C., Oelschlaeger, C., and Hubbuch, J. (2016). 'Squeeze flow rheometry as a novel tool for the characterization of highly concentrated protein solutions'. *Biotechnol. Bioeng.* Vol. 113(3), pp. 576–587 (cit. on pp. 12, 25, 26, 33, 48, 52).

Shih, Y. C., Prausnitz, J. M., and Blanch, H. W. (1992). 'Some characteristics of protein precipitation by salts'. *Biotechnol. Bioeng.* Vol. 40, pp. 1155–1164 (cit. on pp. 9, 38, 133).

Shire, S. J., Shahrokh, Z., and Liu, J. (2004). 'Challenges in the development of high protein concentration formulations.' *J. Pharm. Sci.* Vol. 93(6), pp. 1390–402 (cit. on pp. 7, 10, 15, 18, 24, 46, 74, 120, 121, 129, 133, 142, 143, 149).

Stradner, A., Cardinaux, F., and Schurtenberger, P. (2006). 'A Small-Angle Scattering Study on Equilibrium Clusters in Lysozyme Solutions'. *J. Phys. Chem. B.* Vol. 110(42), pp. 21222–21231 (cit. on p. 26).

Ter Veen, R., Fromell, K., and Caldwell, K. D. (2005). 'Shifts in polystyrene particle surface charge upon adsorption of the Pluronic F108 surfactant'. *J. Colloid Interface Sci.* Vol. 288(1), pp. 124–128 (cit. on p. 25).

Vadillo, D. C., Tuladhar, T. R., Mulji, A. C., and Mackley, M. R. (2010). 'The rheological characterization of linear viscoelasticity for ink jet fluids using piezo axial vibrator and torsion resonator rheometers'. *J. Rheol. (Melville, NY, U. S.).* Vol. 54(4), p. 781 (cit. on p. 28).

Valentine, M., Perlman, Z., Gardel, M., Shin, J., Matsudaira, P., Mitchison, T., and Weitz, D. (2004). 'Colloid Surface Chemistry Critically Affects Multiple Particle Tracking Measurements of Biomaterials'. *Biophys. J.* Vol. 86(6), pp. 4004–4014 (cit. on pp. 14, 17, 25).

Waigh, T. A. (2005). 'Microrheology of complex fluids'. *Rep. Prog. Phys.* Vol. 68(3), pp. 685–742 (cit. on pp. 14, 17, 25, 26, 51).

Willenbacher, N. and Oelschlaeger, C. (2007). 'Dynamics and structure of complex fluids from high frequency mechanical and optical rheometry'. *Curr. Opin. Colloid Interface Sci.* Vol. 12(1), pp. 43–49 (cit. on pp. 14, 25).

Winzor, D. J. (2004). 'Determination of the net charge (valence) of a protein: a fundamental but elusive parameter'. *Anal. Biochem.* Vol. 325(1), pp. 1–20 (cit. on p. 28).

3.2 Concentration-dependent changes in apparent diffusion coefficients as indicator for colloidal stability of protein solutions

Katharina Christin Bauer, Mathias Göbel, Marie-Luise Schwab, Marie-Therese Schermeyer, Jürgen Hubbuch*

Institute of Engineering in Life Sciences, Section IV: Biomolecular Separation Science, Karlsruhe Institute of Technology (KIT), 76131 Karlsruhe, Germany;
* Corresponding author: telephone: +49-721-608-42557, e-mail: juergen.hubbuch@kit.edu

dynamic viscosity

phase behavior

apparent diffusion coefficient
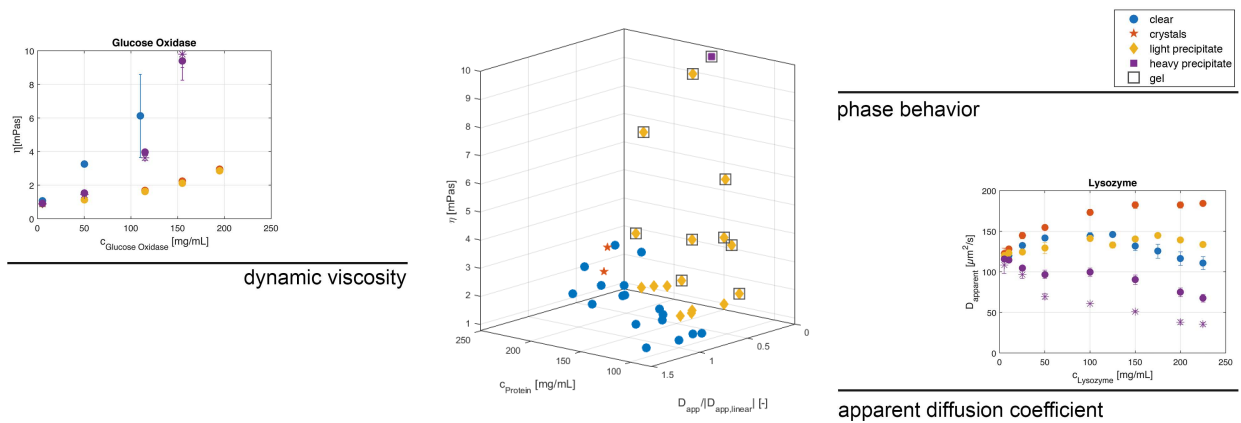
Abstract

The colloidal stability of a protein solution during downstream processing, formulation, and storage is a key issue for the biopharmaceutical production process. Thus, knowledge about colloidal solution characteristics, such as the tendency to form aggregates or high viscosity, at various processing conditions is of interest. This work correlates changes in the apparent diffusion coefficient as a parameter of protein interactions with observed protein aggregation and dynamic viscosity of the respective protein samples. For this purpose, the diffusion coefficient, the protein phase behavior, and the dynamic viscosity in various systems containing the model proteins α-lactalbumin, lysozyme, and glucose oxidase were studied. Each of these experiments revealed a wide range of variations in protein interactions depending on protein type, protein concentration, pH, and the NaCl concentration. All these variations showed to be mirrored by changes in the apparent diffusion coefficient in the respective samples. Whereas stable samples with relatively low viscosity showed an almost linear dependence, the deviation from the concentration-dependent linearity indicated both an increase in the sample viscosity and probability of protein aggregation. This deviation of the apparent diffusion coefficient from concentration-dependent linearity was independent of protein type and solution properties for this study. Thus, this single parameter shows the potential to act as a prognostic tool for colloidal stability of protein solutions.

Introduction

The colloidal stability of a protein solution is essential for the successful outcome of a biopharmaceutical production process. Especially with increasing product titers in fermentation and the trend towards highly concentrated formulations, this key issue becomes more relevant to the pharmaceutical industry and, thus, to its downstream processing (Shire, 2009; Gronemeyer et al., 2014). From an economic perspective, more concentrated protein solutions provide quicker processing times, a decrease in storage space, and an easier delivery to the patient. However, for downstream processing, these solutions are challenging regarding their susceptible colloidal stability, which can lead to the formation of aggregates and high viscosity (Shire et al., 2004; Saluja and Kalonia, 2008; Philo et al., 2009). From a molecular point of view, these solution characteristics correlate strongly with protein interactions. Whereas repulsive protein interactions stabilize protein solutions, attractive protein interactions, resulting from variation of solution parameters or changes in the proteins' conformational stability, can cause protein aggregation. Publications often find protein aggregation to be irreversible. In contrast, protein self-association denotes the

assembly of reversible multimers from native proteins (Cromwell et al., 2006; Arzenšek et al., 2012). A clear distinction of these two phenomenons, however, is difficult, as protein aggregation or protein self-association mechanisms may not be mutually exclusive (Philo et al., 2009). Hence, this work defines the term protein aggregation to capture any formation of reversible or irreversible multimeric species evolved from native or non-native protein molecules (Mahler et al., 2009).

This approach is beneficial, because various aggregation mechanisms with different end states can occure at high protein concentrations. Due to smaller distances between the protein molecules, attractive protein interactions are more complex than at the dilute state. Besides electrostatic interactions, additional short-range interactions, such as charge fluctuations, hydrophobic interactions, hydrogen bonding (Crommelin et al., 2013; Oss, 2003; V. Kumar et al., 2011; Burckbuchler et al., 2010), and the impact of excluded volume effects have to be considered (Zimmerman et al., 1993; Minton, 1997; Minton, 2000). This complex interplay of attractive interactions can not only lead to the formation of dense protein aggregates, but may also result in spacious networks with elevated viscosity, which were reported to be reversible by J. Liu et al., 2005.

Thus, to prevent protein aggregation and high viscosity in order to guarantee the development of stable and processable biopharmaceutical products, their colloidal stability has to be considered carefully with every change in solution condition (W. Wang, 1999). Analytical methods indicating these colloidal solution characteristics of a protein solution are, therefore, of special interest (Prausnitz, 2003).

Yet, there are various approaches which provide information about the tendency of protein solutions to form aggregates or high viscosity. Phenomenological information can be gained by evaluating phase transitions, such as precipitation or gelation, through protein phase diagrams (Baumgartner et al., 2015; Dumetz et al., 2008). More quantitative information can be determined by the investigation of intermolecular protein interactions (Amin, Barnett, et al., 2014).

Generally, to access these interactions, resulting colloidal solution characteristics, like thermodynamic properties, such as the osmotic pressure (Neal et al., 1998; Moon et al., 2000), or transport parameters (Heinen et al., 2012), such as diffusion (Muschol et al., 1995) or viscosity, are determined (Gaigalas et al., 1995). Their deviation from ideal behavior defines the overall interactions, the so-called potential of mean force, present in solution. Publications dealing with the pharmaceutical process development often use concentration-independent coefficients of these parameters, to minimize work effort and sample consumption (Saluja and Kalonia, 2008). These parameters, like the second virial coefficient B_{22} (Curtis, Ulrich, et al., 2002; Ahamed et al., 2007) or the diffusion interaction parameter k_D (Connolly et al., 2012), are determined in the dilute state. They were shown to correlate with system parameters, like viscosity (Connolly et al., 2012; Neergaard et al., 2013; Saito et al., 2012), but have limitations for high concentrations (Scherer et al., 2010) and the prognosis of aggregation. Whereas George et al., 1994 found a crystallization slot depending on B_{22} for model proteins, this approach appeared to be less applicable to antibodies (Lewus, Darcy, et al., 2011; Rakel, Bauer, et al., 2015; Rakel, Galm, et al., 2015; Saito et al., 2012). In order to reduce these restrictions arising from analyzing dilute solutions, other approaches account for additional short-range interactions. With

these approaches, colloidal solution characteristics are determined depending on protein concentration (Chari et al., 2009; Saluja and Kalonia, 2008). One approach is based on the determination of rheological parameters, like the complex viscosity $\eta*$ and the storage and loss moduli G' and G''. These parameters allow the evaluation of viscosity as well as the network-like structure with its underlying protein interactions in solution (Saluja, Badkar, et al., 2007). By means of the crossover point of the two moduli G' and G'', Schermeyer et al., 2016 found a correlation to the phase behavior of lysozyme. For the investigation of dilute as well as concentrated protein solutions, the apparent diffusion coefficient D_{app} seems particularly suitable, because it enables to acquire the changes in interactions for dilute solutions, represented by k_D, as well as additional short-range interactions for concentrated solutions (Muschol et al., 1995). Its correlation to solution characteristics, such as osmotic pressure and suspension viscosity (Gaigalas et al., 1995) or aggregation (Cohen et al., 2005; Zhang et al., 2003) for protein solutions was already shown. Yet, the capability of the apparent diffusion coefficient as a indicative tool for the colloidal stability of protein solutions with respect to aggregation and viscosity has not been evaluated so far.

This work aims to capture this relationship between protein interactions, aggregation, and viscosity and evaluate the capacity of the apparent diffusion coefficient as a prognostic tool for biopharmaceutical process development. For this purpose, the diffusion coefficients of the model proteins, α-lactalbumin, lysozyme, and glucose oxidase, which vary in structure and size, were determined by dynamic light scattering (DLS) experiments. Capturing a wide range of protein interactions, these experiments were conducted at different pH values, protein concentrations up to 225 mg/mL, and with addition of NaCl. DLS was also used to determine the dynamic viscosity of the protein solutions by microrheology. The aggregation tendency of the samples was examined by phase diagrams. As a final step, the results of all measurements were compared and correlated to resolve the relationship of colloidal stability and changes in the apparent diffusion coefficient.

Materials and Methods

To evaluate the correlation of changes in protein diffusion with the aggregation tendency and the dynamic viscosity for a wide scope of conditions and protein properties, the model proteins α-lactalbumin, lysozyme, and glucose oxidase were investigated. These were studied at pH 3, 5, 7, and 9, protein concentrations of up to 225 mg/mL, and NaCl concentrations of up to 200 mM. The isoelectric point (pI) and molecular weight of each protein is listed in Table 3.3. The following section describes the preparation of the buffers and protein solutions, the determination of the phase diagrams, as well as the investigation of the apparent diffusion coefficient and dynamic viscosity by DLS.

Buffers and protein solutions

Buffer solutions of 100 mM ionic strength were prepared for pH 3, 5, 7, and 9. The respective buffer components were citric acid (Merck KGaA, Darmstadt, Germany) and sodium citrate (Sigma-Aldrich, St. Louis, MO, USA) for pH 3, acetic acid (Merck KGaA) and sodium acetate (Sigma-Aldrich) for pH 5, 3-Morpholino-2-hydroxypropanesulfonic acid (MOPSO) (AppliChem GmbH, Darmstadt, Germany) for pH 7, and BisTris propane

(Molekula Limited, Newcastle upon Tyne, UK) for pH 9. For the buffer stock solution with NaCl (Merck KGaA), a concentration of 2 M was added to the buffer components. The pH was controlled and corrected by titration of NaOH or HCl (Merck KGaA) with a five-point calibrated pH meter (HI-3220, Hanna® Instruments, Woonsocket, RI, USA) equipped with a SenTix® 62 pH electrode (Xylem Inc., White Plains, NY, USA). Each pH adjustment was conducted with an accuracy of +/- 0.05 pH units. The buffers were filtered with a 0.2 µm membrane consisting of Supor® Polyethersulfone (PES) (Pall Corporation, Port Washington, NY, USA) for pH 9 and cellulose acetate (Sartorius AG, Göttingen, Germany) for all other pH values. The buffers were used at constant pH 24 h after preparation and stored at room temperature.

Lysozyme from chicken egg white was purchased from Hampton Research (Aliso Viejo, CA, USA), α-lactalbumin from bovine milk, the calcium-depleted apo form and its holo form, as well as glucose oxidase were purchased from Sigma-Aldrich. The lyophilized proteins were weighted in and diluted in the buffer solution at the respective pH. Each protein solution was filtered with a 0.2 µm syringe filter (PES for pH 9, cellulose acetate for all other pH values (VWR, Radnor, PA, USA)). Production-related additives were removed by size exclusion chromatography, which was performed at a ÄKTAprime™ plus chromatography system using a Sephadex resin (GE Healthcare, Uppsala, Sweden). After size exclusion, the protein solutions were concentrated to the desired concentration with Vivaspin® centrifugal concentrators (Sartorius AG). The concentration was determined by a NanoDrop™ 2000c UV-Vis spectrophotometer (Thermo Fisher Scientific, Waltham, MA, USA). The respective extinction coefficients were $E^{1\%}(280\,\text{nm}) = 16.81\ \text{L}\,\text{g}^{-1}\,\text{cm}^{-1}$ for α-lactalbumin, $E^{1\%}(280\,\text{nm}) = 22.00\ \text{L}\,\text{g}^{-1}\,\text{cm}^{-1}$ for lysozyme, and $E^{1\%}(280\,\text{nm}) = 12.00\ \text{L}\,\text{g}^{-1}\,\text{cm}^{-1}$ for glucose oxidase.

Table 3.3: Isoelectric point (pI) and molecular weight of the studied model proteins α-lactalbumin apo and holo, lysozyme, and glucose oxidase.

Protein	Molecular weight [kDa]	pI [ ]
α-Lactalbumin apo & holo (Permyakov et al., 2000; Bramaud et al., 1997)	14	4.2
Lysozyme (Palmer et al., 1948; Donev, 2011)	13.9	11.3
Glucose oxidase (Tsuge et al., 1975; Wilson et al., 1992)	160	4.2

Phase diagrams

The phase diagrams of each protein at concentrations between 0 and 225 mg/ml, pH 3, 5, 7, and 9, and NaCl concentrations from 0 to 200 mM were prepared as described in the publication by Baumgartner et al., 2015 on a Freedom EVO® 100 fully automated robotic liquid handling station (Tecan Group Ltd., Männedorf, Switzerland). This station is equipped with fixed tips and 250 µL dilutors. It is controlled by Freedom EVOware® 2.4 SP3 (Tecan Group Ltd.). To maintain high protein concentrations for the samples, 2.4 µL of the respective pre-diluted buffer solution were mixed with 21.6 µL of the respective

pre-diluted protein solution on the MRC Under Oil 96 Well Crystallization Plate (SWISSCI AG, Neuheim, Switzerland). Whereas the dilution of the respective buffer stock solution of 2 M NaCl was performed on the robotic handling station, the protein stock solution was diluted manually. The studied concentration range of the protein stock solutions was reliant on the solubility of the protein at the respective pH. To avoid evaporation, the crystallization plate was covered with Duck® Brand HD Clear sealing tape (ShurTech® brands, Avon, OH, USA). The plates were incubated in the RockImager 54 (Formulatrix, Bedford, MA, USA) at room temperature and evaluated optically for the phase states clear solution, crystals, light and heavy precipitate after 40 days. Exemplary pictures of these phase state are displayed in Figure 3.7. Each sample that could not be pipetted at this time was scored as gel.
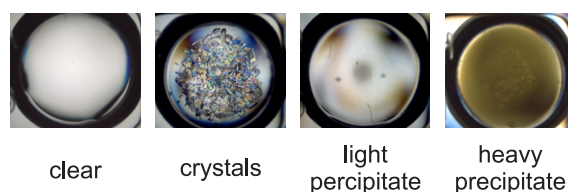

| clear | crystals | light percipitate | heavy precipitate |

Figure 3.7: Exemplary pictures for the phase states clear solution, crystals, light and heavy precipitate scored after 40 days. For the score clear solution 225 mg/mL lysozyme at pH 5, for crystals 175 mg/mL lysozyme at pH 3 with 100 mM NaCl, for light percipitate 150 mg/mL α-lactalbumin apo at pH 9, and for heavy percipitate 175 mg/mL glucose oxidase at pH 9 with 100 mM NaCl is displayed.

Dynamic light scattering

The apparent diffusion coefficients and the dynamic viscosity of the protein samples at concentrations between 0 and 225 mg/mL, pH 3, 5, 7, and 9, and with addition of NaCl at pH 9 were determined by dynamic light scattering (DLS). These measurements were conducted with the ZetaSizer Nano ZSP (Malvern Instruments, Worcestershire, UK). Each sample was determined in triplicate with the Non-Invasive Back Scatter (NIBS®) optics at 25 °C. The protein solutions were prepared right before the measurement. For α-lactalbumin apo and holo, the addition of 200 mM, for lysozyme 150 mM, and for glucose oxidase 100 mM NaCl at pH 9 were investigated. These concentrations of NaCl were chosen due to having a maximum effect on the phase behavior independent of pH for the respective protein displayed in Figure 3.8. For preparation of the samples, 4.5 µL of the respective buffer solution and 40.5 µL of the pre-diluted respective protein solution were mixed in a ZEN2112 quartz cuvette (Hellma® GmbH & Co. KG, Müllheim, Germany).

Apparent diffusion coefficient   For determination of the apparent diffusion coefficient, the size measurement consisted of three replicates with automatic duration. The diffusion coefficient, evaluated by the cumulant fit of the protein analysis model, was used for further interpretation of the results and is referred to as apparent diffusion coefficient D_{app} in the following sections of this article.

In order to derive the diffusion interaction parameter k_D for the proteins and conditions investigated in this study, the linear dependence of the apparent diffusion coefficient was

fitted to the following equation valid for the dilute state:

$$D_{app,linear} = D_0(1 + k_D c_P). \tag{3.2}$$

In this equation, D_0 is the diffusion coefficient at infinite dilution and c_P the protein concentration (Saluja, Badkar, et al., 2007; V. Kumar et al., 2011; Connolly et al., 2012). To account for good accuracy of the data, each fit was set for protein concentrations that did fulfill the range of $0.96 < R^2 < 1$ for the coefficient of determination. For higher protein concentrations where D_{app} deviates from linearity, an extrapolated linear apparent diffusion coefficient $D_{app,linear}$ was calculated depending on the respective protein concentration and protein interaction coefficient k_D by Equation 3.2. By building the ratio $\frac{D_{app}}{|D_{app,linear}|}$, the deviation of each sample from concentration-dependent linearity was evaluated.

Dynamic viscosity   The dynamic viscosity of the samples right after preparation was determined by microrheological measurements based on DLS. Following previous investigations (Bauer, Schermeyer, et al., 2016), PEGylated polystyrene (PEG-PS) particles (5 wt%) were added to the samples at a volume ratio of 1:200 (V(Particle solution):V(Sample)) and their size was determined. The size measurement consisted of three replicates with an automatic measurement duration on condition that the particles were the only scatterers detected. The diffusion coefficient, evaluated by the cumulant fit of the protein analysis model, was then applied to calculate the dynamic viscosity of each sample based on the Stokes-Einstein equation. The experimentally determined hydrodynamic radius of the PEG-PS particles in the respective buffer and the dynamic viscosity of water at 25 °C were used as a reference (Breedveld et al., 2003; Waigh, 2005).

Results

To evaluate a potential correlation of the changes in the apparent diffusion coefficient with the aggregation tendency and viscosity of proteins solutions, the proteins α-lactalbumin, lysozyme, and glucose oxidase were investigated at various conditions. The results for their phase behavior, dynamic viscosity and apparent diffusion coefficient are described in the following.

Phase behavior

The phase behavior of proteins is a function of solution conditions. In this study, a wide variety of phase transitions was observed. In general, already small changes in the solution conditions or in the protein structure properties had an impact. Figure 3.8 illustrates the influence of pH, protein concentration, and sodium chloride for each of the proteins investigated. The pH varied from pH 3 to 9 and protein concentration from 0 to 225 mg/mL with the highest value being depending on the solubility of each protein. The NaCl concentration added ranged from 0 to 175 mM for lysozyme and from 0 to 200 mM for α-lactalbumin and glucose oxidase.

α-lactalbumin apo reached different solubility limits depending on pH. At pH 3, above 75 mg/mL gelation appeared. Instead of gelation, α-lactalbumin apo precipitated by addition of NaCl. At pH 5, the protein precipitation started at concentrations above 11 mg/mL.
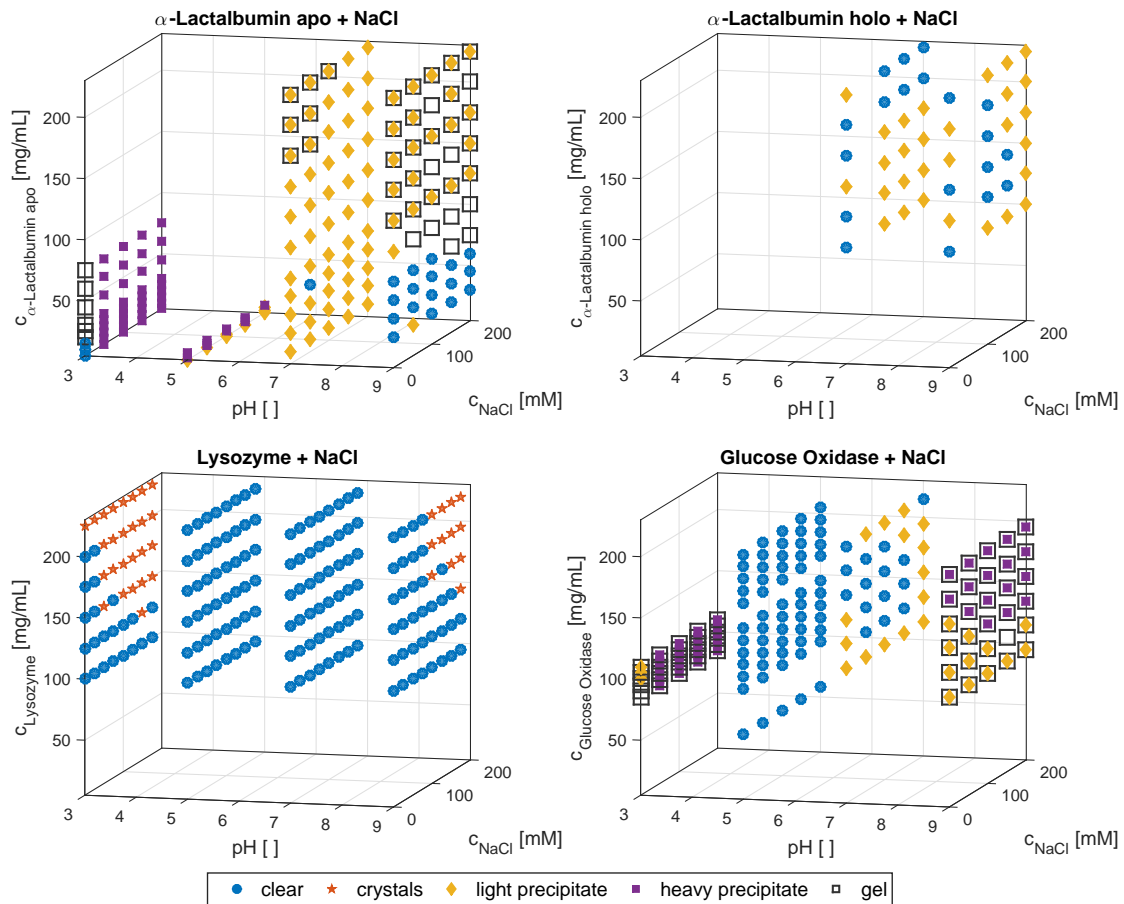
Figure 3.8: Phase diagrams of α-lactalbumin, the apo and holo form, lysozyme (Schermeyer et al., 2016), and glucose oxidase depending on pH, protein, and NaCl concentration.

At pH 7 and 9, α-lactalbumin apo could be concentrated to 225 mg/mL. At pH 7, the solutions showed light precipitate for all protein and NaCl concentrations. For high protein and low NaCl concentrations, gelation was determined. For pH 9, gelation occurred above 125 mg/mL. With addition of NaCl, this phase state shifted to lower protein concentrations as far as 75 mg/mL with 200 mM NaCl. Below 75 mg/mL, the solutions were clear, at higher concentrations, light precipitate was found. For α-lactalbumin holo, only the highly soluble concentrations at pH 7 and 9 were studied. In contrast to the apo form, only clear solutions or solutions with light precipitate were detected.

The results for lysozyme were published earlier by Schermeyer et al., 2016. Lysozyme was the only protein, that formed crystals for the studied conditions. For pH 3 at 225 mg/mL, crystals were determined, for pH 9 at 175 mg/mL crystallization started with addition of 100 mM NaCl. With increasing amount of NaCl, the crystallization area for both pH values became broader by shifting first crystallization conditions to lower protein concentrations. No phase transition was found for pH 5 and 7. At these pH values, the lysozyme solutions

were clear for all studied protein and NaCl concentrations.

For glucose oxidase at pH 5, the protein solutions stayed clear irrespective of the protein and NaCl concentrations. Light precipitate and clear solutions were detected at pH 7. For pH 3 and 9, gelation was determined for all studied conditions. For pH 3, in the studied area from 85 to 110 mg/mL and at a NaCl concentration from 0 to 200 mM, nearly all conditions showed additional heavy precipitate. For pH 9, light precipitate was found for protein concentrations up to 155 mg/mL. For higher concentrations, the protein formed heavy precipitate. With increasing NaCl concentration, this state of heavy precipitate expanded to lower protein concentrations.

Dynamic viscosity

Protein interactions not only govern the phase behavior, but also the viscosity of a protein solution during processing and storage (Neergaard et al., 2013; Connolly et al., 2012). To determine the dynamic viscosity for the protein solutions studied, microrheological measurements were conducted directly after preparation. Figure 3.9 shows the results with standard deviations for α-lactalbumin apo and holo, lysozyme, and glucose oxidase at pH 3, 5, 7, and 9 and the effect of NaCl at pH 9. This effect of NaCl was investigated by adding a salt concentration of 200 mM for α-lactalbumin apo and holo, 150 mM for lysozyme, and 100 mM NaCl for glucose oxidase to the protein samples.

For all proteins studied, the dynamic viscosity depended on the protein concentration. The effect of NaCl on the dynamic viscosity at pH 9 was negligibly small. For α-lactalbumin apo and glucose oxidase, additionally a clear dependence on pH was observed. For 225 mg/mL α-lactalbumin at pH 9 with NaCl, no value could be determined due to spontaneous precipitation of this solution. The highest viscosity of 9.7 mPas was determined for glucose oxidase at pH 9. This and two other values above 6 mPas had standard deviations above 16 %. In comparison, the standard deviation of the determined values under 6 mPas was below 10 %.

For α-lactalbumin apo at pH 3, a distinct increase in dynamic viscosity ($\eta > 2$ mPas) was determined at 50 mg/mL, at pH 9 a comparable increase was reached at 175 mg/mL, for pH 7 at 225 mg/mL. This dependence of the determined dynamic viscosity for the apo form at pH 7 corresponded to the ones of the holo form at pH 7 and 9. In contrast to α-lactalbumin holo, differences in the slope of the dynamic viscosity were found for lysozyme above 150 mg/mL with varying pH. At 225 mg/mL, the dynamic viscosity decreased from pH 9 to 3, followed by the lowest values at pH 5 and 7. For glucose oxidase at pH 3, a distinct increase in dynamic viscosity was determined at 50 mg/mL. Values above 2 mPas were determined for pH 9 at 125 mg/mL, for pH 5 and 7 at 150 mg/mL.

Apparent diffusion coefficient

For the determination of protein interactions in solution, the apparent diffusion coefficients of α-lactalbumin apo and holo, lysozyme, and glucose oxidase were determined depending on protein concentration under various conditions. Analogous to the phase behavior shown in Figure 3.8, the apparent diffusion coefficient depended on the protein type, its concentration, and the respective solution condition.

The results for the apparent diffusion coefficient with standard deviations of the proteins
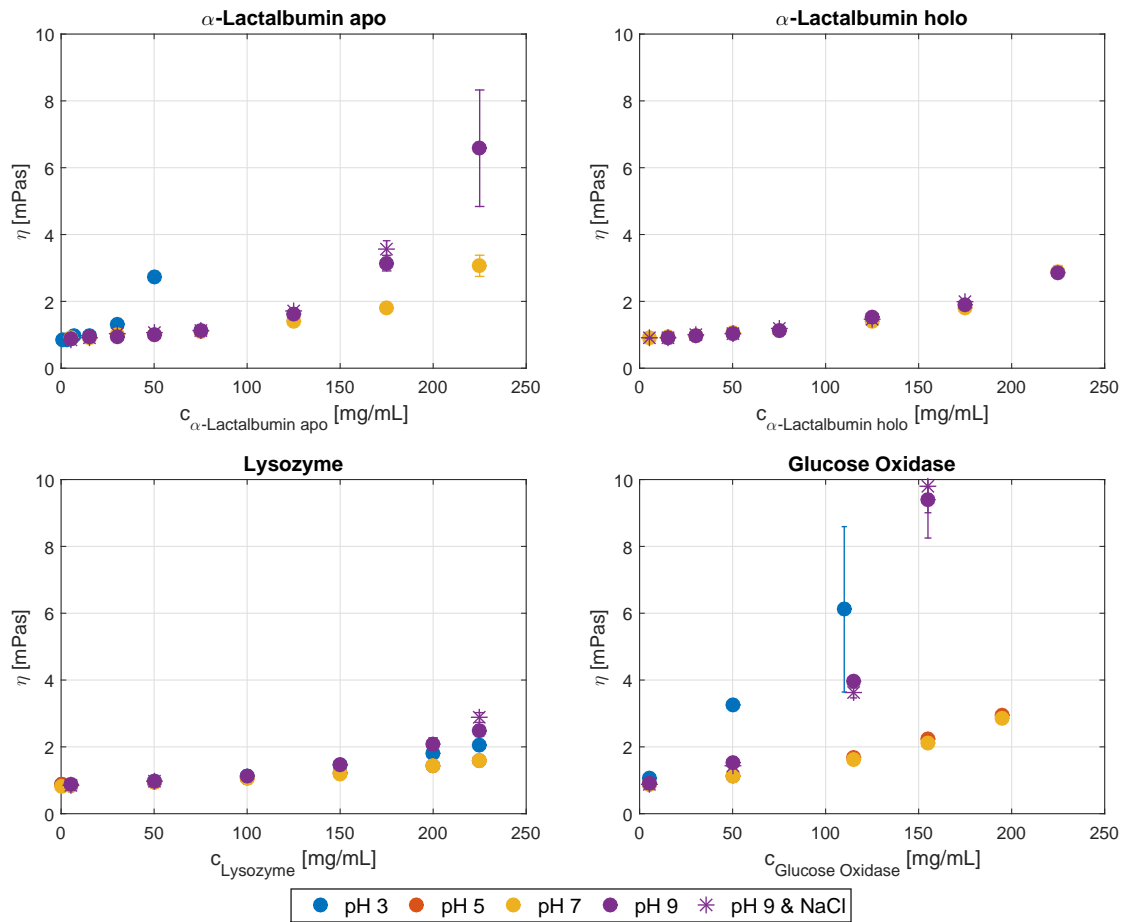
Figure 3.9: Dynamic viscosity of α-lactalbumin, the apo and holo form, lysozyme, and glucose oxidase depending on protein concentration, pH, and NaCl at pH 9.

studied at pH 3, 5, 7, and 9 and the effect of NaCl at pH 9 are shown in Figure 3.10. For the samples with NaCl, the same concentrations as for the measurements of the dynamic viscosity in Section 3.2, namely 200 mM NaCl for α-lactalbumin, 150 mM NaCl for lysozyme, and 100 mM NaCl for glucose oxidase, were added. Values with high standard deviations for the diffusion coefficient could be found for low concentrations of α-lactalbumin apo at pH 5 and 9, for the holo form at pH 9, for lysozyme at pH 9 with NaCl and glucose oxidase at pH 3 and 9. Apart from these, the determined standard deviations were below 7.2 %. For α-lactalbumin apo at pH 3, the apparent diffusion coefficient decreased continuously with increasing protein concentration. As for the phase diagrams, the highest reachable concentration was 75 mg/mL. Measurements at pH 5 could only be conducted at low protein concentrations and resulted in very low apparent diffusion coefficients with high standard deviations. At pH 7 and 9, the determined diffusion coefficients resulted in a maximum value of 102 μm^2/s at a concentration of 30 mg/mL, respectively 96 μm^2/s at 10 mg/mL. At pH 7, the following decreasing slope was less steep than for the samples
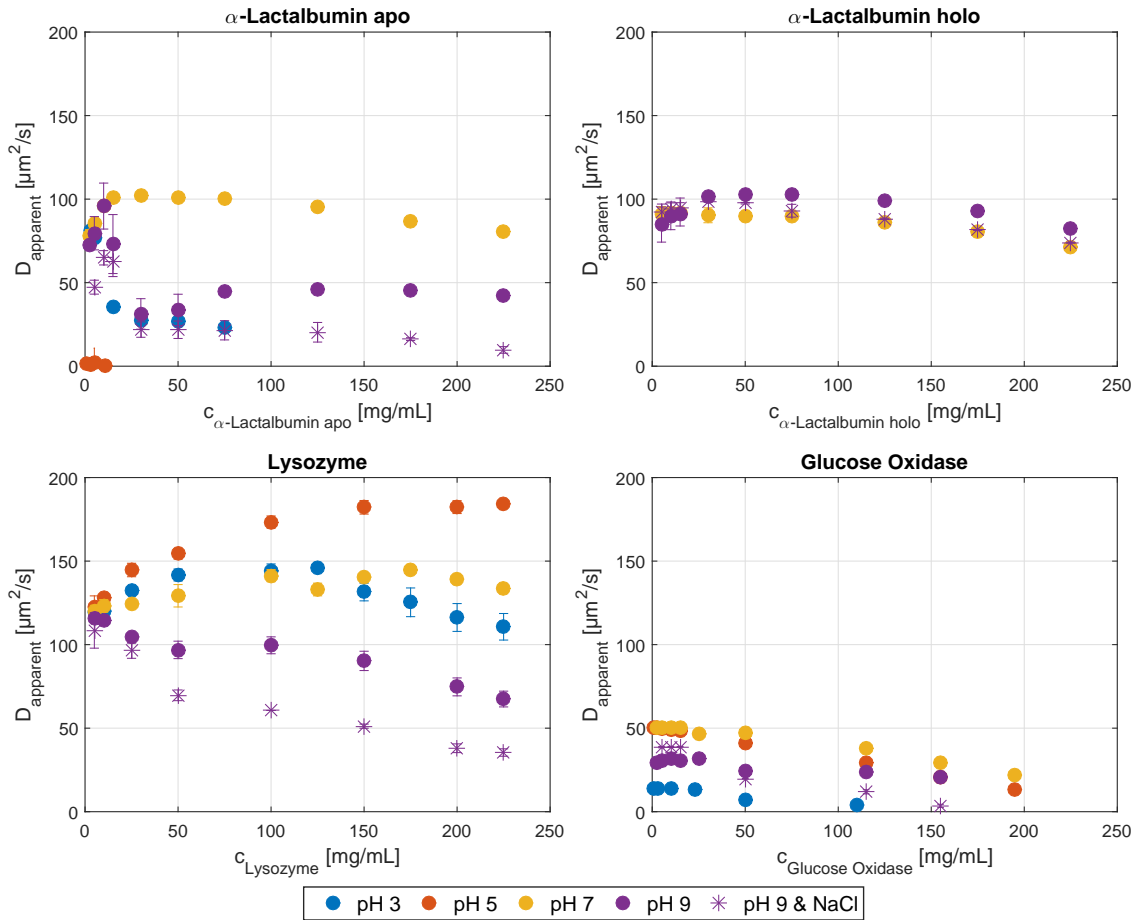
Figure 3.10: Apparent diffusion coefficient of α-lactalbumin, the apo and holo form, lysozyme, and glucose oxidase depending on protein concentration, pH, and NaCl at pH 9.

at pH 9. At pH 9 without NaCl, an additional minimum at 30 mg/mL and an almost constant value of 45 µm^2/s above 75 mg/mL were determined. When looking at the apparent diffusion coefficients of α-lactalbumin holo at pH 7 and 9, the values were most comparable to the high diffusion coefficients of the apo form at pH 7. At pH 7, the apparent diffusion coefficients stayed almost constant up to 75 mg/mL, then decreased continuously. A maximum could be found at pH 9. Due to strong changes at low concentrations of α-lactalbumin, a linear dependence for the values of the apparent diffusion coefficient could only be determined for concentrations lower than 15 mg/mL.

For lysozyme, a more linear behavior depending on protein concentration and higher values for the apparent diffusion coefficient were found. At pH 3, 5, and 7, the values increased at low concentrations. At pH 3 and 125 mg/mL, the diffusion coefficient reached a maximum value of 146 µm^2/s, for pH 5 from 150 mg/mL, the diffusion coefficient was almost constant at 180 µm^2/s, at pH 7 from 125 mg/mL, it varied around the value of 139 µm^2/s. At pH 9, the apparent diffusion coefficients decreased continuously with concentration. With

addition of NaCl, this dependence was shifted to lower values.

For glucose oxidase, all determined apparent coefficients were below 51 µm²/s. In contrast to the other proteins, the values for the apparent diffusion coefficient at low concentrations differed considerably from each other. The highest values were found for pH 5 and 7, followed by values for pH 9 and 3. For pH 5, the apparent diffusion coefficient decreased linearly with increasing protein concentration. For pH 7, the values for the apparent diffusion coefficient almost followed the same trend but showed a plateau for low protein concentrations. At pH 9, the addition of NaCl shifted the apparent diffusion coefficients to higher values until 50 mg/mL. For higher protein concentrations, this ratio reversed, because the apparent diffusion coefficients with NaCl decreased continuously, whereas the values without salt stayed almost constant at about 23 µm²/s. Apparent diffusion coefficients at pH 3 above 110 mg/mL and at 9 above 155 mg/mL could not be obtained, because, as for the phase diagrams in Figure 3.8, these solutions showed heavy precipitation and gelation. For this protein, pH 3, 7, and 9 showed linear behavior below 30 mg/mL. Contrary to the changing dependence at these pH values, the apparent diffusion coefficients at pH 5 showed a linear behavior for the complete concentration range.
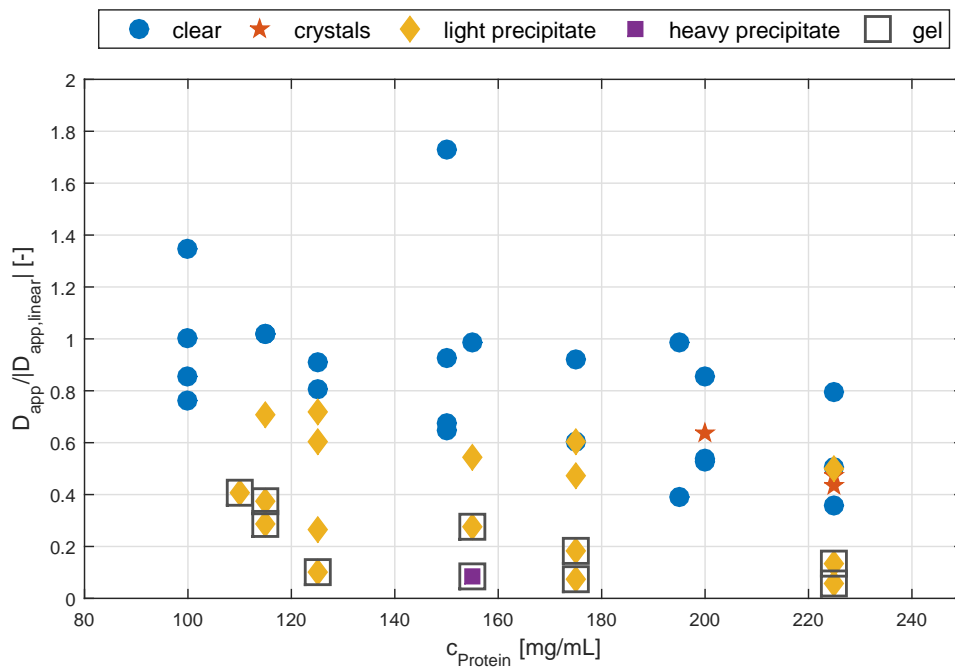

Figure 3.11: Deviation from linearity $\frac{D_{app}}{|D_{app,linear}|}$ depending on protein concentration.
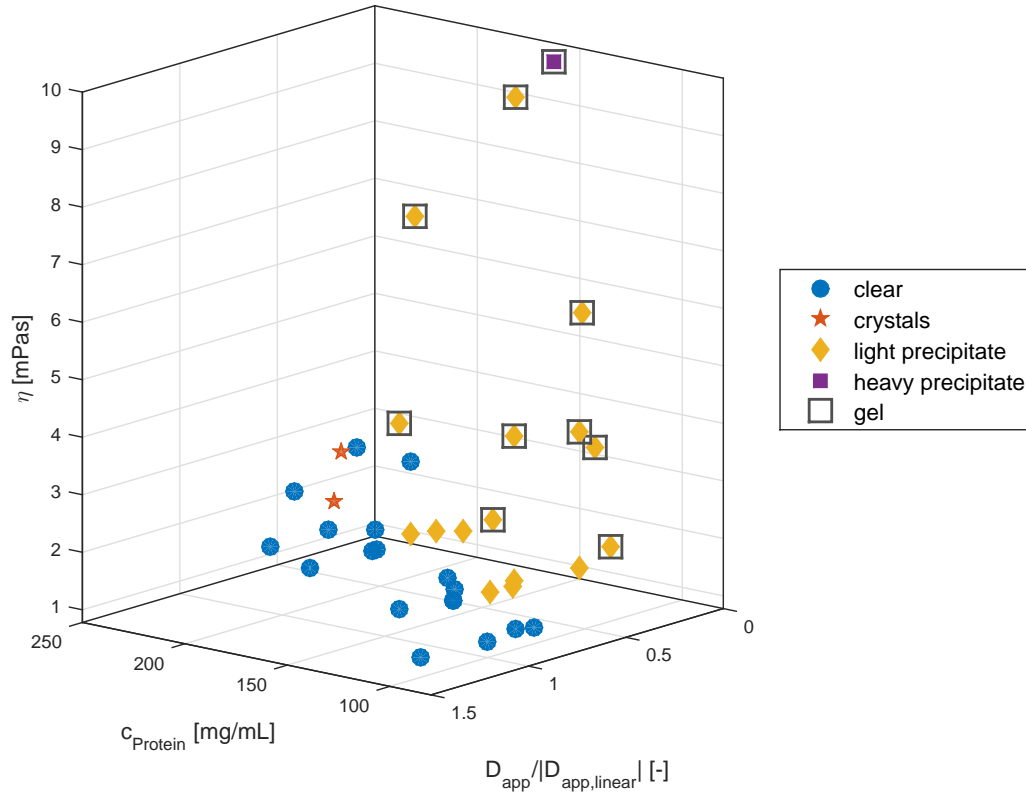
Figure 3.12: Deviation from linearity $\frac{D_{app}}{|D_{app,linear}|}$ depending on protein concentration and dynamic viscosity.

Correlation of concentration dependent changes in diffusion with the aggregation tendency and viscosity

In order to examine the correlation of changes in protein diffusion with the stability and processability of a protein solution, the deviation from linearity for the apparent diffusion coefficient was compared to the aggregation tendency and dynamic viscosity of the respective samples. For this purpose, a specific term for the deviation from linearity was introduced by building the ration $\frac{D_{app}}{|D_{app,linear}|}$ of the determined apparent diffusion coefficient D_{app} and the linear apparent diffusion coefficient at the respective condition and protein concentration. This linear apparent diffusion coefficient $D_{app,linear}$ was calculated by extrapolation of the fit for the dilute state at the respective condition and protein concentration depending on Equation 3.2. Figure 3.11 shows the result for the correlation of this term with the phase behavior for all studied proteins at various conditions depending on protein concentration. The phase states of the protein samples were taken from the results determined by the phase diagrams for the respective protein and solution condition. For protein samples with clear solution, the determined apparent diffusion coefficient D_{app} deviated less from the linear dependence. This resulted in a $\frac{D_{app}}{|D_{app,linear}|}$ close to 1. For

$\frac{D_{app}}{|D_{app,linear}|} < 0.8$, samples with changes in phase behavior were determined. Samples with crystallization and light precipitate were found for higher values of $\frac{D_{app}}{|D_{app,linear}|}$ than heavy precipitation and gelation. These limits depended on protein concentration. Whereas conditions with light precipitate had a value of around 0.7 and gelation of 0.4 or below for $\frac{D_{app}}{|D_{app,linear}|}$ at 115 mg/mL, conditions with light precipitate or crystals were below 0.5 and gelation below 0.1 for 225 mg/mL. Accounting for the relationship between aggregation, viscosity, and changes in protein diffusion, the results for the dynamic viscosity of the protein solutions were included in Figure 3.12. Besides the different phase states and $\frac{D_{app}}{|D_{app,linear}|}$, as shown in Figure 3.11, the dynamic viscosity of the samples depending on protein concentration is displayed. This correlation indicated, that high viscosity ($\eta > 3$ mPas) correlated to gelating conditions for the phase behavior of the protein solutions, and thus values of $\frac{D_{app}}{|D_{app,linear}|} < 0.4$. Conditions that stayed clear or formed light precipitate or crystals, resulted in lower viscosity ($\eta < 3$ mPas).

Discussion

Aggregation tendency, viscosity, and diffusion depend on protein interactions present in solution (Amin, Barnett, et al., 2014). In order to provide an overall picture of their relationship and evaluate the prognostic potential of changes in the apparent diffusion coefficient for the aggregation tendency and viscosity of protein solutions, phase diagrams, the dynamic viscosity, and the apparent diffusion coefficient were determined. For a correlation with a wide scope of conditions and protein properties, the proteins α-lactalbumin apo and holo, lysozyme, and glucose oxidase were investigated at pH 3, 5, 7, and 9. An addition of NaCl had rather similar effect on the dynamic viscosity and the apparent diffusion coefficient determined for the various samples in this study. For this reason, only values for pH 9 are displayed. The respective results, their correlation to protein interactions, and the capacity of changes in protein diffusion as a tool to indicate the stability and processability of a protein solution are discussed in the following.

Phase behavior

The phase behavior of the studied proteins α-lactalbumin apo and holo, lysozyme, and glucose oxidase, depicted in Figure 3.8, varied with protein type, protein concentration, pH as well as NaCl concentration. These parameters influence the protein interactions in solution and therefore govern the respective phase behavior of the sample (Dumetz, 2007). In general, the increase in protein concentration promotes the impact of excluded volume effects (Zimmerman et al., 1993; Minton, 1997; Minton, 2000) and additional attractive short-range interactions (Chari et al., 2009; Saluja and Kalonia, 2008). In our study, their impact was detected by the formation of aggregates or gel-like states for α-lactalbumin apo at pH 3, 7, and 9, lysozyme at pH 3 and 9, and glucose oxidase at pH 3 and 9.

The impact of pH depends on the specific surface configuration of each protein and, thus, its resulting isoelectric point (pI), listed in Table 3.3. Close to this pH value, at which the net charge of the protein is close to zero, attractive short-range interactions, such as van der Waals or hydrophobic forces, are more dominant (Papadopoulos, 2008). These interactions promote a higher tendency towards aggregation (Amin, Rega, et al., 2011) or

highly viscous gelation (Desbrières, 2000; Saluja and Kalonia, 2008). In our study, their impact could be found for α-lactalbumin apo at pH 3 and 5 and for glucose oxidase at pH 3. A strong impact of hydrophobic forces for α-lactalbumin at pH 3 can, furthermore, be explained by the molten globule state of the protein under this condition. Within this state, the protein surface becomes more hydrophobic due to its increased hydration (Permyakov et al., 2000; Amrhein, Bauer, et al., 2015). Interestingly, glucose oxidase showed its most stable phase behavior close to its pI at pH 5. This result is consistent with the high activity reported for this pH (Pazur et al., 1964; Singh et al., 2014). In theory, protein phase behavior is stabilized with further distance to the pI due to predominating repulsive electrostatic interactions (Papadopoulos, 2008; Shaw et al., 2001). These interactions account for a higher solubility and lower aggregation tendency (Cromwell et al., 2006; Tardieu et al., 2002). In our study, these effects were determined for α-lactalbumin apo at pH 7, α-lactalbumin holo at pH 7 and 9, lysozyme at pH 5 and 7 as well as glucose oxidase at pH 7. Contrary to this theory, phase states that imply predominating attractive interactions were determined at pH values far from pI. For α-lactalbumin apo at pH 9, gelation and light precipitation, for lysozyme at pH 3, crystals, and for glucose oxidase at pH 9 gelation plus light or heavy precipitate were detected. In this case, hydrophobic interactions have a considerable impact due to the strong protonation of the protein surface (D. Guo et al., 1986). Hydrophobicity measurements conducted by Amrhein, Bauer, et al., 2015 for lysozyme and α-lactalbumin apo further underline this consideration.

The addition of salt is known to promote attractive hydrophobic protein interactions due to the shielding of electrostatic charges (Curtis, Ulrich, et al., 2002; Lindman et al., 2006; Kuehner, Engmann, et al., 1999). Therefore, the addition of NaCl promoted unstable phase behavior for lysozyme at pH 9 and glucose oxidase at pH 3. An increase in NaCl concentration shifted these conditions to lower protein concentrations, like for α-lactalbumin apo at pH 9, for lysozyme at pH 3 and 9, and glucose oxidase at pH 9. In contrast, for α-lactalbumin apo at pH 3 and 7 the addition of NaCl prevented gelation, which is associated with the formation of network-like states with elevated viscosity. This suggests changed or even reduced attractive interactions. In comparison to other publications, this effect within the same NaCl concentration range was also observed for casein (P. Harris, 2012). Besides protein concentration and solution conditions, the protein surface composition itself had an impact on the phase behavior, because α-lactalbumin apo and holo, which only differ by the binding of a calcium ion (Permyakov et al., 2000), resulted in different phase behavior. Different aggregation mechanisms for the similarly structured lysozyme and α-lactalbumin due to a different amino acid composition on the protein surface reinforced this conclusion (Amrhein, Bauer, et al., 2015).

In summary, the phase behavior of the protein varied depending on the protein type, protein concentration, the present solution condition, and the resulting molecule properties. Electrostatic as well as additional short-range interactions, such as excluded volume effects and hydrophobic interactions, played a role for the samples investigated in this study. Consequently, for the discussion in the following sections, this wide scope of results provides a good foundation to extensively investigate the relationship between protein interactions, protein aggregation, and dynamic viscosity as well as the capability of the apparent diffusion coefficient as a prognostic tool to capture these changes.

Dynamic viscosity

Whereas the protein phase behavior was scored after 40 days, the dynamic viscosity was determined directly after preparation. This experiment was conducted to consider the viscosity of the protein solutions during processing but also its correlation to phase behavior and the underlying protein interactions. The results show that the dynamic viscosity, like the protein phase behavior, is governed by the protein concentration, the protein size but also the respective solution condition.

According to theory (Connolly et al., 2012; Yadav, Shire, et al., 2011; Saito et al., 2012), protein concentration was the driving force of changes in dynamic viscosity for the studied proteins depicted in Figure 3.10. The decreasing intermolecular distances promote the impact of additional attractive short-range interactions and excluded volume effects. Due to the impact of molecule size (Lefebvre, 1982), glucose oxidase yielded in comparably higher values for the dynamic viscosity of similar samples depending on protein concentration. For our study, no differences for the determined dynamic viscosity at concentrations below 150 mg/mL could be distinguished, except for conditions that resulted in gelation due to the impact of attractive short-range forces, especially hydrophobic interactions. These conditions could be assigned to α-lactalbumin and glucose oxidase at pH 3 and 9 and were already discussed in Section 3.2. Analogous to this observation, other publications considered the impact of short-range hydrophobic interactions on high viscosity (Hall et al., 1984; Kamerzell et al., 2013; Desbrières, 2000; W. Cheng et al., 2013; Connolly et al., 2012), which due to J. Liu et al., 2005 is based on reversible self-association. However, J. Liu et al., 2005 attributed this effect to electrostatic interactions.

For this study, the presence of predominating electrostatic interactions was determined for conditions with a more moderate increase in viscosity. However, the phase state, meaning if these solutions stayed clear, formed crystals or precipitate, could not be distinguished by the increase in dynamic viscosity and is in agreement with other publications (J. Liu et al., 2005; Burckbuchler et al., 2010).

Contrary to the determined phase behavior and results of other publication (N. Wang et al., 2009; Kanai et al., 2008; N. Inoue et al., 2014a; Salinas et al., 2010), the addition of NaCl at pH 9 had a minor effect. Regarding our study, dynamic viscosity seems to be less sensitive to the shielding of electrostatic interactions. An argument for the discrepancy to phase behavior could be the direct measurement after preparation and, thus, an impact of the association kinetics of proteins (V. Kumar et al., 2011; Sheinerman et al., 2000; Roberts, 2007). Especially for gel formations, such as for α-lactalbumin and glucose oxidase at pH 9 with addition of NaCl, inhibited association kinetics are plausible (Bryant et al., 2000; Veerman et al., 2006). Differing protein types as well as the high buffer capacity used in this study could have an impact on the discrepancy to other publications.

In summary, the increase in dynamic viscosity, determined in our study as well as in other publications, mainly depended on the protein concentration but also on attractive short-range hydrophobic forces. Their predominating impact promoted strong increases in viscosity and the formation of gels for the phase behavior. Other attractive interactions, which promoted light precipitation or crystals, did not change the dynamic viscosity markedly.

Apparent diffusion coefficient

The apparent diffusion coefficient depends on the hydrodynamic radius of the protein, based on the Stokes-Einstein equation (Young et al., 1980) as well as on protein-solvent and protein interactions (Rallison et al., 1986). Whereas the hydrodynamic radius and protein-solvent interactions govern the diffusion of the protein at infinite dilution, protein interactions govern the changes depending on protein concentration (Giannopoulou et al., 2007; Kuehner, Heyer, et al., 1997). In general, an increase in the diffusion coefficient indicates predominating repulsive interactions whereas a decrease indicates predominating attractive interactions (Connolly et al., 2012; V. Kumar et al., 2011). Thus, as also already stated by Gaigalas et al., 1995, the protein type, its concentration, the pH value, and the ionic strength have an impact on changes in the apparent diffusion coefficients of proteins. For this study, at infinite dilution, changes due to the differing molecular weights, depicted in Table 3.3, but also changes in protein-solvent interactions due to changes in pH or ionic strength were detected. α-Lactalbumin and lysozyme with lower molecular weight and, thus, smaller hydrodynamic radii showed higher apparent diffusion coefficients compared to glucose oxidase with a higher molecular weight. The difference at infinite dilution between the same sized α-lactalbumin and lysozyme and the differences for glucose oxidase due to changes in pH and ionic strength could be explained by their differing protein-solvent interactions. These are based on the specific surface configuration under the respective solution condition (Grigsby et al., 2000; Halle, 2004). With increasing protein concentration, moreover, changes in protein interactions due to electrostatic as well as additional short-range interactions were determined.

In this study, the impact of predominating electrostatic interactions was determined at dilute concentrations, which is in agreement with other published work (Chari et al., 2009; Muschol et al., 1995). In order to capture the impact of these interactions by the diffusion interaction parameter k_D, the dependence of the apparent diffusion coefficient was fitted linearly, as described in Section 3.2. It is notable that for samples with stable phase behavior and low viscosity, like lysozyme and glucose oxidase at pH 5, a wide concentration range could be fitted. In comparison, conditions with precipitation or gelation, like glucose oxidase at pH 3, 7, and 9 or α-lactalbumin, could only be fitted for concentrations of up to 30 mg/mL. At higher concentrations, the impact of additional short-range effects could be captured because with decreasing distances between the protein molecules, the consideration of a linear dependence and thus solely acting electrostatic interactions is no longer valid (Saluja and Kalonia, 2008; Zimmerman et al., 1993). In our study, these were captured by stagnating or decreasing diffusion coefficients, which was also observed by Muschol et al., 1995. Several publications accounted this impact to sterically driven molecular crowding (Zimmerman et al., 1993; Minton, 1997; Minton, 2000). However, other publications pointed out that the sole consideration of electrostatics and excluded volume is insufficient (Minton, 1983). Muschol et al., 1995 as well as Burckbuchler et al., 2010 suggested the consideration of additional short-range interactions, like charge fluctuations, hydrophobic interactions, and hydrogen bonding. The results of this study further underline their suggestion because conditions associated with hydrophobic interactions for the protein phase behavior resulted in the highest deviations from the linear dependence at high protein

concentrations. Solely steric considerations would have been insufficient to explain the varying deviations of the apparent diffusion coefficient depending on pH for the same sized lysozyme and α-lactalbumin. Due to this impact of additional short-range interactions at high concentrations, several publications (Saluja and Kalonia, 2008; Scherer et al., 2010) question the predictability of concentration-independent coefficients, like k_D or B_{22}. Regarding the results of this study, some samples correlated to the theoretical considerations for k_D, others contradicted them. For glucose oxidase at pH 5, k_D was negative although it was stable for the full concentration range. Furthermore, the positive k_D for α-lactalbumin as well as glucose oxidase at pH 7 and 9 did not match with the detected precipitation and gelation under these conditions.

In this study, a more convenient approach investigating the stability of the studied protein samples was found to be the consideration of the deviation from linearity for the apparent diffusion coefficient depending on protein concentration. With reference to the phase behavior of this study, this parameter captured the discussed impact of the attractive and repulsive electrostatic interactions as well as additional attractive short-range interactions in a reasonable way. In comparison to the determined dynamic viscosity, changes in electrostatic interactions by means of changes in the apparent diffusion coefficient could be determined at low protein concentrations and with addition of NaCl. Whereas linear or dependence with low deviations from linearity could be correlated to more stable conditions, strong deviations from linearity could be correlated to unstable conditions regarding the protein phase behavior. In the following section, this information is further used to investigate the correlation of concentration-dependent changes in the apparent diffusion coefficient with aggregation tendency and dynamic viscosity of protein solutions.

Correlation of concentration-dependent changes in protein diffusion with stability and viscosity

For the correlation of concentration-dependent changes in the apparent diffusion coefficient with the aggregation tendency and dynamic viscosity of the protein solutions, a term for its deviation from linearity was considered. Therefore, each determined diffusion coefficient D_{app} was related to its extrapolated linear apparent diffusion coefficient $D_{app,linear}$ at the respective protein concentration. The determination of this term $\frac{D_{app}}{|D_{app,linear}|}$ is described in Section 3.2. Figure 3.11 depicts the correlation of its value with the protein phase behavior for the common concentration range of 80 to 225 mg/mL. The lower the term for the deviation from linearity, the less stable were the protein samples. Regarding protein interactions, the more the protein interactions at the dilute state deviated from the ones at high concentrations, the more plausible was aggregation or, for further deviations, highly viscous gelation. This correlation seems generally applicable to this study because it could be applied to all proteins studied with different size and structural properties under various conditions. For the studied protein samples, it demonstrated the serious impact of additional short-range interactions on aggregation (W. Wang, 1999) and even more on viscosity, also displayed in Figure 3.12. In contrast to other findings (Lindman et al., 2006; Bhaskar et al., 1991; J. Liu et al., 2005), it highlights the importance of predominating electrostatic interactions for colloidal stability and low viscosity of protein solutions by reference to the linear dependence of the diffusion coefficient. Interestingly, at higher concentrations, stronger deviations from linearity were possible without changing

the stability of the protein solution. This observation can be supported by the increasing impact of excluded volume effects, for which Minton, 2000 found a stabilizing effect with increasing protein concentrations.

However, differences between conditions for light precipitation or crystallization could not be distinguished for the changes in the apparent diffusion coefficient. Therefore, the conformation homogeneity of the protein surface seems to be an important factor (Derewenda, 2004). This characteristic cannot be captured because the apparent diffusion coefficient only reflects the overall potential of interactions (Lounnas et al., 1994).

Still, in the end, changes in the apparent diffusion coefficient allowed the correlation of protein interactions with aggregation and high dynamic viscosity of concentrated protein solutions. Being independent of protein type, size, and structure in this study, this parameter shows the potential to compare and indicate the colloidal stability of various samples. However, to verify this prognostic capacity of changes in the apparent diffusion coefficient, further proteins at different conditions should be studied. The only requirement for determination of parameter is the determination of a linear fit for the apparent diffusion coefficient at the dilute state, which is compared to selected concentrated samples of the respective condition. Therefore, this approach would prevent expanded studies of samples with high concentrations and enable less sample consumption and work effort.

Conclusion and Outlook

The apparent diffusion coefficient captured the impact of protein interactions affecting the aggregation tendency and viscosity of the protein solutions in this study. Electrostatic, but also additional short-range interactions, like excluded volume effects and hydrophobic interactions, were identified to have an impact on the changes depending on protein concentration, pH as well as NaCl concentration. The evaluation of the apparent diffusion coefficient by means of its concentration-dependent deviation from linearity resulted in a good correlation with this varying impact of interactions. Samples with a dependence for the apparent diffusion coefficient close to linearity showed colloidal stability, whereas deviations from linearity implied the impact of additional short-range interactions and, thus, aggregation, like precipitation or crystallization. Stronger deviations, which could be associated with the impact of hydrophobic interactions, furthermore resulted in gelating samples which already had a high viscosity after preparation and therefore present a risk to downstream processing. This deviation of the apparent diffusion coefficient from concentration-dependent linearity was independent of protein type and solution properties for this study. Consequently, to ensure the colloidal stability of a protein solution, changes in the apparent diffusion coefficient, determined directly after preparation of the samples, not only allow the correlation to the aggregation tendency and viscosity, but also show potential for their indication. With the required measurements in the dilute state for a linear fit and selected conditions for higher concentrations, this approach enables wide studies with regard to information about the aggregation tendency and viscosity by simultaneously saving sample volume and work effort. An automatization of this method would furthermore enable a promising high throughput (HTP) screening procedure for the stability and processability of biopharmaceuticals.

References

Ahamed, T., Esteban, B. N. A., Ottens, M., Dedem, G. W. K. van, Wielen, L. A. M. van der, Bisschops, M. A. T., Lee, A., Pham, C., and Thömmes, J. (2007). 'Phase behavior of an intact monoclonal antibody.' *Biophys. J.* Vol. 93(2), pp. 610–9 (cit. on pp. 11, 47, 75).

Amin, S., Barnett, G. V., Pathak, J. A., Roberts, C. J., and Sarangapani, P. S. (2014). 'Protein aggregation, particle formation, characterization & rheology'. *Curr. Opin. Colloid Interface Sci.* Vol. 19(5), pp. 438–449 (cit. on pp. 9–13, 15, 47, 58).

Amin, S., Rega, C. A., and Jankevics, H. (2011). 'Detection of viscoelasticity in aggregating dilute protein solutions through dynamic light scattering-based optical microrheology'. *Rheol. Acta.* Vol. 51(4), pp. 329–342 (cit. on pp. 12–14, 25, 26, 58).

Amrhein, S., Bauer, K. C., Galm, L., and Hubbuch, J. (2015). 'Non-invasive high throughput approach for protein hydrophobicity determination based on surface tension'. *Biotechnol. Bioeng.* Vol. 112(12), pp. 2485–2494 (cit. on p. 59).

Arakawa, T. and Timasheff, S. N. (1987). 'Abnormal solubility behavior of β-lactoglobulin: salting-in by glycine and sodium chloride'. *Biochemistry.* Vol. 26(16), pp. 5147–5153 (cit. on p. 133).

Arzenšek, D., Kuzman, D., and Podgornik, R. (2012). 'Colloidal interactions between monoclonal antibodies in aqueous solutions'. *J. Colloid Interface Sci.* Vol. 384(1), pp. 207–216 (cit. on pp. 4, 5, 11, 47).

Basu, S. K., Govardhan, C. P., Jung, C. W., and Margolin, A. L. (2004). 'Protein crystals for the delivery of biopharmaceuticals'. *Expert Opin. Biol. Ther.* Vol. 4(3), pp. 301–317 (cit. on p. 15).

Bauer, K. C., Schermeyer, M.-T., Seidel, J., and Hubbuch, J. (2016). 'Impact of polymer surface characteristics on the microrheological measurement quality of protein solutions - A tracer particle screening'. *Int. J. Pharm. (Amsterdam, Neth.).* Vol. 505(1-2), pp. 246–254 (cit. on pp. 51, 123).

Baumgartner, K., Galm, L., Nötzold, J., Sigloch, H., Morgenstern, J., Schleining, K., Suhm, S., Oelmeier, S. A., and Hubbuch, J. (2015). 'Determination of protein phase diagrams by microbatch experiments: Exploring the influence of precipitants and pH'. *Int. J. Pharm. (Amsterdam, Neth.).* Vol. 479(1), pp. 28–40 (cit. on pp. 10, 47, 49, 82, 132).

Bhaskar, K. R., Gong, D. H., Bansil, R., Pajevic, S., Hamilton, J. A., Turner, B. S., and LaMont, J. T. (1991). 'Profound increase in viscosity and aggregation of pig gastric mucin at low pH.' *Am. J. Physiol.* Vol. 261(5 Pt 1), G827–32 (cit. on p. 62).

Bramaud, C., Aimar, P., and Daufin, G. (1997). 'Whey protein fractionation: Isoelectric precipitation of α-lactalbumin under gentle heat treatment'. *Biotechnol. Bioeng.* Vol. 56, pp. 391–397 (cit. on p. 49).

Breedveld, V. and Pine, D. J. (2003). 'Microrheology as a tool for high-throughput screening'. *J. Mater. Sci.* Vol. 38(22), pp. 4461–4470 (cit. on pp. 25, 51).

Bryant, C. and McClements, D. (2000). 'Influence of NaCl and CaCl2 on Cold-Set Gelation of Heat-denatured Whey Protein'. *J. Food Sci.* Vol. 65(5), pp. 801–804 (cit. on p. 60).

Burckbuchler, V., Mekhloufi, G., Giteau, A. P., Grossiord, J., Huille, S., and Agnely, F. (2010). 'Rheological and syringeability properties of highly concentrated human polyclonal immunoglobulin solutions'. *Eur. J. Pharm. Biopharm.* Vol. 76(3), pp. 351–356 (cit. on pp. 12, 15, 24, 47, 60, 61, 142).

Chari, R., Jerath, K., Badkar, A. V., and Kalonia, D. S. (2009). 'Long- and short-range electrostatic interactions affect the rheology of highly concentrated antibody solutions.' *Pharm. Res.* Vol. 26(12), pp. 2607–18 (cit. on pp. 2, 5, 8, 12, 15, 48, 58, 61, 120).

Cheng, W., Joshi, S. B., Jain, N. K., He, F., Kerwin, B. A., Volkin, D. B., and Middaugh, C. R. (2013). 'Linking the solution viscosity of an IgG2 monoclonal antibody to its structure as a function of pH and temperature'. *J. Pharm. Sci.* Vol. 102, pp. 4291–4304 (cit. on pp. 13, 60).

Cohen, Y., Avram, L., and Frish, L. (2005). 'Diffusion NMR spectroscopy in supramolecular and combinatorial chemistry: an old parameter–new insights.' *Angew. Chem. Int. Ed. Engl.* Vol. 44(4), pp. 520–54 (cit. on pp. 12, 48).

Connolly, B. D., Petry, C., Yadav, S., Demeule, B., Ciaccio, N., Moore, J. M. R., Shire, S. J., and Gokarn, Y. R. (2012). 'Weak interactions govern the viscosity of concentrated antibody solutions: high-throughput analysis using the diffusion interaction parameter.' *Biophys. J.* Vol. 103(1), pp. 69–78 (cit. on pp. 11, 12, 47, 51, 53, 60, 61, 75).

Crommelin, D. J. A., Sindelar, R. D., and Meibohm, B. (2013). *Pharmaceutical Biotechnology: Fundamentals and Applications*. SpringerLink : Bücher. Springer New York (cit. on pp. 2, 47, 75, 86).

Cromwell, M. E. M., Hilario, E., and Jacobson, F. (2006). 'Protein aggregation and bioprocessing.' *AAPS J.* Vol. 8(3), E572–9 (cit. on pp. 4, 5, 14, 47, 59).

Curtis, R. A., Ulrich, J., Montaser, A., Prausnitz, J. M., and Blanch, H. W. (2002). 'Protein-protein interactions in concentrated electrolyte solutions.' *Biotechnol. Bioeng.* Vol. 79(4), pp. 367–80 (cit. on pp. 2, 9, 11, 47, 59, 129).

Derewenda, Z. S. (2004). 'Rational Protein Crystallization by Mutational Surface Engineering'. *Structure.* Vol. 12(4), pp. 529–535 (cit. on p. 63).

Desbrières, J. (2000). 'Thermogelation of methylcellulose: rheological considerations'. *Polymer (Guildf).* Vol. 41(7), pp. 2451–2461 (cit. on pp. 59, 60).

Donev, R. (2011). *Advances in Protein Chemistry and Structural Biology.* Academic Press. Academic Press (cit. on p. 49).

Dumetz, A. C. (2007). *Protein Interactions and Phase Behavior in Aqueous Solutions: Effects of Salt, Polymer, and Organic Additives.* University of Delaware, p. 284 (cit. on pp. 58, 87).

Dumetz, A. C., Chockla, A. M., Kaler, E. W., and Lenhoff, A. M. (2008). 'Protein phase behavior in aqueous solutions: crystallization, liquid-liquid phase separation, gels, and aggregates.' *Biophys. J.* Vol. 94(2), pp. 570–83 (cit. on pp. 11, 47).

Gaigalas, A., Reipa, V., Hubbard, J., Edwards, J., and Douglas, J. (1995). 'A non-perturbative relation between the mutual diffusion coefficient, suspension viscosity, and osmotic compressibility: Application to concentrated protein solutions'. *Chem. Eng. Sci.* Vol. 50(7), pp. 1107–1114 (cit. on pp. 11, 12, 47, 48, 61).

George, A. and Wilson, W. W. (1994). 'Predicting protein crystallization from a dilute solution property'. *Acta Crystallogr. Sect. D Biol. Crystallogr.* Vol. 50(4), pp. 361–365 (cit. on pp. 12, 47, 75).

Giannopoulou, A., Aletras, A. J., Pharmakakis, N., Papatheodorou, G. N., and Yannopoulos, S. N. (2007). 'Dynamics of proteins: Light scattering study of dilute and dense colloidal suspensions of eye lens homogenates'. *J. Chem. Phys.* Vol. 127(20), pp. 1–24 (cit. on p. 61).

Grigsby, J. J., Blanch, H. W., and Prausnitz, J. M. (2000). 'Diffusivities of Lysozyme in Aqueous MgCl 2 Solutions from Dynamic Light-Scattering Data: Effect of Protein and Salt Concentrations'. *J. Phys. Chem. B.* Vol. 104(15), pp. 3645–3650 (cit. on p. 61).

Gronemeyer, P., Ditz, R., and Strube, J. (2014). 'Trends in Upstream and Downstream Process Development for Antibody Manufacturing'. *Bioengineering.* Vol. 1(4), pp. 188–212 (cit. on p. 46).

Guo, D., Mant, C. T., Taneja, A. K., Parker, J., and Rodges, R. S. (1986). 'Prediction of peptide retention times in reversed-phase high-performance liquid chromatography I. Determination of retention coefficients of amino acid residues of model synthetic peptides'. *J. Chromatogr. A.* Vol. 359(8), pp. 499–518 (cit. on pp. 59, 86, 111).

Hall, C. G. and Abraham, G. N. (1984). 'Reversible self-association of a human myeloma protein. Thermodynamics and relevance to viscosity effects and solubility.' *Biochemistry.* Vol. 23(22), pp. 5123–9 (cit. on p. 60).

Halle, B. (2004). 'Protein hydration dynamics in solution: a critical survey'. *Philos. Trans. R. Soc. B Biol. Sci.* Vol. 359(1448), pp. 1207–1224 (cit. on p. 61).

Harris, P. (2012). *Food Gels.* Elsevier Applied Food Science Series. Springer Netherlands (cit. on p. 59).

Heinen, M., Zanini, F., Roosen-Runge, F., Fedunová, D., Zhang, F., Hennig, M., Seydel, T., Schweins, R., Sztucki, M., Antalík, M., Schreiber, F., and Nägele, G. (2012). 'Viscosity and diffusion: crowding and salt effects in protein solutions'. *Soft Matter.* Vol. 8(5), pp. 1404–1419 (cit. on pp. 11, 47).

Inoue, N., Takai, E., Arakawa, T., and Shiraki, K. (2014a). 'Arginine and lysine reduce the high viscosity of serum albumin solutions for pharmaceutical injection.' *J. Biosci. Bioeng.* Vol. 117(5), pp. 539–43 (cit. on pp. 60, 121, 132, 133).

Kamerzell, T. J., Pace, A. L., Li, M., Danilenko, D. M., McDowell, M., Gokarn, Y. R., and Wang, Y. J. (2013). 'Polar solvents decrease the viscosity of high concentration IgG1 solutions through hydrophobic solvation and interaction: Formulation and biocompatibility considerations'. *J. Pharm. Sci.* Vol. 102(4), pp. 1182–1193 (cit. on p. 60).

Kanai, S., Liu, J. U. N., Patapoff, T. W., and Shire, S. J. (2008). 'Reversible Self-Association of a Concentrated Monoclonal Antibody Solution Mediated by Fab-Fab Interaction That Impacts Solution Viscosity'. *J. Pharm. Sci.* Vol. 97(10), pp. 4219–4227 (cit. on pp. 13, 60).

Kim, A. J., Manoharan, V. N., and Crocker, J. C. (2005). 'Swelling-based method for preparing stable, functionalized polymer colloids.' *J. Am. Chem. Soc.* Vol. 127(6), pp. 1592–3 (cit. on pp. 26, 123).

Kuehner, D. E., Heyer, C., Rämsch, C., Fornefeld, U. M., Blanch, H. W., and Prausnitz, J. M. (1997). 'Interactions of lysozyme in concentrated electrolyte solutions from dynamic light-scattering measurements.' *Biophys. J.* Vol. 73(6), pp. 3211–24 (cit. on pp. 61, 77).

Kuehner, D. E., Engmann, J., Fergg, F., Wernick, M., Blanch, H. W., and Prausnitz, J. M. (1999). 'Lysozyme Net Charge and Ion Binding in Concentrated Aqueous Electrolyte Solutions'. *J. Phys. Chem. B.* Vol. 103(8), pp. 1368–1374 (cit. on p. 59).

Kumar, V., Dixit, N., Zhou, L., and Fraunhofer, W. (2011). 'Impact of short range hydrophobic interactions and long range electrostatic forces on the aggregation kinetics of a monoclonal antibody and a dual-variable domain immunoglobulin at low and high concentrations'. *Int. J. Pharm. (Amsterdam, Neth.).* Vol. 421(1), pp. 82–93 (cit. on pp. 5, 7, 8, 11, 12, 14, 47, 51, 60, 61, 90).

Lefebvre, J. (1982). 'Viscosity of concentrated protein solutions'. *Rheol. Acta.* Vol. 21(4-5), pp. 620–625 (cit. on pp. 12, 13, 60, 131).

Lewus, R. A., Darcy, P. A., Lenhoff, A. M., and Sandler, S. I. (2011). 'Interactions and phase behavior of a monoclonal antibody'. *Biotechnol. Prog.* Vol. 27(1), pp. 280–289 (cit. on pp. 5, 12, 47, 74).

Lindman, S., Xue, W.-F., Szczepankiewicz, O., Bauer, M. C., Nilsson, H., and Linse, S. (2006). 'Salting the Charged Surface: pH and Salt Dependence of Protein G B1 Stability'. *Biophys. J.* Vol. 90(8), pp. 2911–2921 (cit. on pp. 59, 62).

Liu, J., Nguyen, M. D., Andya, J. D., and Shire, S. J. (2005). 'Reversible Self-Association Increases the Viscosity of a Concentrated Monoclonal Antibody in Aqueous Solution'. *J. Pharm. Sci.* Vol. 94(9), pp. 1928–1940 (cit. on pp. 5, 7, 13, 15, 18, 47, 60, 62, 120, 121, 129, 131, 143).

Lounnas, V., Pettitt, B. M., and Phillips, G. N. (1994). 'A global model of the protein-solvent interface.' *Biophys. J.* Vol. 66(3 Pt 1), pp. 601–14 (cit. on p. 63).

Mahler, H.-C., Friess, W., Grauschopf, U., and Kiese, S. (2009). 'Protein aggregation: Pathways, induction factors and analysis'. *J. Pharm. Sci.* Vol. 98(9), pp. 2909–2934 (cit. on pp. 1, 4, 5, 7, 9–11, 47, 120, 131, 143).

Minton, A. P. (1983). 'The effect of volume occupancy upon the thermodynamic activity of proteins: some biochemical consequences'. *Mol. Cell. Biochem.* Vol. 55(2), pp. 119–140 (cit. on pp. 8, 61).

Minton, A. P. (1997). 'Influence of excluded volume upon macromolecular structure and associations in 'crowded' media'. *Curr. Opin. Biotechnol.* Vol. 8(1), pp. 65–69 (cit. on pp. 47, 58, 61).

Minton, A. P. (2000). 'Implications of macromolecular crowding for protein assembly.' *Curr. Opin. Struct. Biol.* Vol. 10(1), pp. 34–9 (cit. on pp. 2, 5, 47, 58, 61, 63, 131).

Moon, Y., Anderson, C., Blanch, H., and Prausnitz, J. (2000). 'Osmotic pressures and second virial coefficients for aqueous saline solutions of lysozyme'. *Fluid Phase Equilib.* Vol. 168(2), pp. 229–239 (cit. on pp. 11, 47).

Muschol, M. and Rosenberger, F. (1995). 'Interactions in undersaturated and supersaturated lysozyme solutions: Static and dynamic light scattering results'. *J. Chem. Phys.* Vol. 103(24), p. 10424 (cit. on pp. 11, 12, 47, 48, 61, 75, 77, 84).

Neal, B. L., Asthagiri, D., and Lenhoff, A. M. (1998). 'Molecular origins of osmotic second virial coefficients of proteins.' *Biophys. J.* Vol. 75(5), pp. 2469–77 (cit. on pp. 11, 47).

Neergaard, M. S., Kalonia, D. S., Parshad, H., Nielsen, A. D., Møller, E. H., and Weert, M. van de (2013). 'Viscosity of high concentration protein formulations of monoclonal antibodies of the IgG1 and IgG4 subclass - prediction of viscosity through protein-protein interaction measurements.' *Eur. J. Pharm. Sci.* Vol. 49(3), pp. 400–10 (cit. on pp. 12, 47, 53).

Oss, C. J. van (2003). 'Long-range and short-range mechanisms of hydrophobic attraction and hydrophilic repulsion in specific and aspecific interactions'. *J. Mol. Recognit.* Vol. 16(4), pp. 177–190 (cit. on pp. 2, 47, 75).

Palmer, K. J., Ballantyne, M., and Galvin, J. A. (1948). 'The molecular weight of lysozyme determined by the X-ray diffraction method.' *J. Am. Chem. Soc.* Vol. 70(3), pp. 906–908 (cit. on pp. 3, 49).

Papadopoulos, K. N. (2008). *Food Chemistry Research Developments.* Nova Science Publishers (cit. on pp. 58, 59).

Pazur, J. H. and Kleppe, K. (1964). 'The Oxidation of glucose and related compounds by glucose oxidase from Aspergillus niger'. *Biochemistry.* Vol. 3, pp. 578–583 (cit. on p. 59).

Permyakov, E. A. and Berliner, L. J. (2000). 'α-Lactalbumin: structure and function'. *FEBS Lett.* Vol. 473(3), pp. 269–274 (cit. on pp. 3, 7, 49, 59, 80, 111).

Philo, J. S. and Arakawa, T. (2009). 'Mechanisms of protein aggregation.' *Curr. Pharm. Biotechnol.* Vol. 10(4), pp. 348–51 (cit. on pp. 5, 46, 47).

Prausnitz, J. M. (2003). 'Molecular thermodynamics for some applications in biotechnology'. *J. Chem. Thermodyn.* Vol. 35(1), pp. 21–39 (cit. on p. 47).

Rakel, N., Bauer, K. C., Galm, L., and Hubbuch, J. (2015). 'From osmotic second virial coefficient (B 22) to phase behavior of a monoclonal antibody'. *Biotechnol. Prog.* Vol. 31(2), pp. 438–451 (cit. on pp. 12, 47).

Rakel, N., Galm, L., Bauer, K. C., and Hubbuch, J. (2015). 'Influence of macromolecular precipitants on phase behavior of monoclonal antibodies'. *Biotechnol. Prog.* Vol. 31(1), pp. 145–153 (cit. on pp. 12, 47).

Rallison, J. M. and Hinch, E. J. (1986). 'The effect of particle interactions on dynamic light scattering from a dilute suspension'. *J. Fluid Mech.* Vol. 167, p. 131 (cit. on p. 61).

Roberts, C. J. (2007). 'Non-native protein aggregation kinetics'. *Biotechnol. Bioeng.* Vol. 98(5), pp. 927–938 (cit. on p. 60).

Saito, S., Hasegawa, J., Kobayashi, N., Kishi, N., Uchiyama, S., and Fukui, K. (2012). 'Behavior of monoclonal antibodies: relation between the second virial coefficient (B (2)) at low concentrations and aggregation propensity and viscosity at high concentrations.' *Pharm. Res.* Vol. 29(2), pp. 397–410 (cit. on pp. 7, 8, 10–13, 15, 47, 60).

Salinas, B. A., Sathish, H. A., Bishop, S. M., Harn, N., Carpenter, J. F., and Randolph, T. W. (2010). 'Understanding and modulating opalescence and viscosity in a monoclonal antibody formulation'. *J. Pharm. Sci.* Vol. 99(1), pp. 82–93 (cit. on p. 60).

Saluja, A., Badkar, A. V., Zeng, D. L., Nema, S., and Kalonia, D. S. (2007). 'Ultrasonic storage modulus as a novel parameter for analyzing protein-protein interactions in high protein concentration solutions: correlation with static and dynamic light scattering measurements.' *Biophys. J.* Vol. 92(1), pp. 234–44 (cit. on pp. 11–15, 24, 25, 48, 51, 75, 77, 86).

Saluja, A. and Kalonia, D. S. (2008). 'Nature and consequences of protein-protein interactions in high protein concentration solutions.' *Int. J. Pharm. (Amsterdam, Neth.).* Vol. 358(1-2), pp. 1–15 (cit. on pp. 2, 5, 7, 10–13, 15, 36, 46–48, 58, 59, 61, 62, 75).

Scherer, T. M., Liu, J., Shire, S. J., and Minton, A. P. (2010). 'Intermolecular interactions of IgG1 monoclonal antibodies at high concentrations characterized by light scattering.' *J. Phys. Chem. B.* Vol. 114(40), pp. 12948–57 (cit. on pp. 12, 47, 62).

Schermeyer, M.-T., Sigloch, H., Bauer, K. C., Oelschlaeger, C., and Hubbuch, J. (2016). 'Squeeze flow rheometry as a novel tool for the characterization of highly concentrated protein solutions'. *Biotechnol. Bioeng.* Vol. 113(3), pp. 576–587 (cit. on pp. 12, 25, 26, 33, 48, 52).

Shaw, K. L., Grimsley, G. R., Yakovlev, G. I., Makarov, A. A., and Pace, C. N. (2001). 'The effect of net charge on the solubility, activity, and stability of ribonuclease Sa'. *Protein Sci.* Vol. 10(6), pp. 1206–1215 (cit. on pp. 7, 59).

Sheinerman, F. B., Norel, R., and Honig, B. (2000). 'Electrostatic aspects of protein-protein interactions'. *Curr. Opin. Struct. Biol.* Vol. 10(2), pp. 153–159 (cit. on p. 60).

Shire, S. J. (2009). 'Formulation and manufacturability of biologics'. *Curr. Opin. Biotechnol.* Vol. 20, pp. 708–714 (cit. on pp. 9, 13–15, 46, 121, 143, 149).

Shire, S. J., Shahrokh, Z., and Liu, J. (2004). 'Challenges in the development of high protein concentration formulations.' *J. Pharm. Sci.* Vol. 93(6), pp. 1390–402 (cit. on pp. 7, 10, 15, 18, 24, 46, 74, 120, 121, 129, 133, 142, 143, 149).

Singh, V. and Singh, D. (2014). 'Glucose oxidase immobilization on guar gum-gelatin dual-templated silica hybrid xerogel'. *Ind. Eng. Chem. Res.* Vol. 53(10), pp. 3854–3860 (cit. on p. 59).

Tardieu, A., Bonneté, F., Finet, S., and Vivarès, D. (2002). 'Understanding salt or PEG induced attractive interactions to crystallize biological macromolecules'. *Acta Crystallogr. Sect. D Biol. Crystallogr.* Vol. 58, pp. 1549–1553 (cit. on p. 59).

Tsuge, H. J., Natsuaki, O., and Ohashi, K. (1975). 'Purification, properties, and molecular features of glucose oxidase from Aspergillus niger.' *J. Biochem.* Vol. 78, pp. 835–843 (cit. on p. 49).

Veerman, C., Rajagopal, K., Palla, C. S., Pochan, D. J., Schneider, J. P., and Furst, E. M. (2006). 'Gelation kinetics of β-hairpin peptide hydrogel networks'. *Macromolecules.* Vol. 39(19), pp. 6608–6614 (cit. on pp. 5, 13, 60).

Waigh, T. A. (2005). 'Microrheology of complex fluids'. *Rep. Prog. Phys.* Vol. 68(3), pp. 685–742 (cit. on pp. 14, 17, 25, 26, 51).

Wang, N., Hu, B., Lonescu, R., Mac, H. H., Sweeney, J., Hamm, C., Kirchmeier, M. J., and Meyer, B. K. (2009). 'Opalescence of an IgGi monoclonal antibody formulation is mediated by ionic strength and excipients'. *BioPharm Int.* Vol. 22(4), pp. 36–47 (cit. on p. 60).

Wang, W. (1999). 'Instability, stabilization, and formulation of liquid protein pharmaceuticals'. *Int. J. Pharm. (Amsterdam, Neth.).* Vol. 185(2), pp. 129–188 (cit. on pp. 1, 2, 4, 9, 10, 14, 47, 62, 120, 129, 131, 133, 143, 149).

– (2005). 'Protein aggregation and its inhibition in biopharmaceutics.' *Int. J. Pharm. (Amsterdam, Neth.).* Vol. 289(1-2), pp. 1–30 (cit. on pp. 5, 7–10, 14, 132).

Wilson, R. and Turner, A. (1992). 'Glucose oxidase: an ideal enzyme'. *Biosens. Bioelectron.* Vol. 7(3), pp. 165–185 (cit. on pp. 3, 49).

Yadav, S., Laue, T. M., Kalonia, D. S., Singh, S. N., and Shire, S. J. (2012). 'The influence of charge distribution on self-association and viscosity behavior of monoclonal antibody solutions'. *Mol. Pharm.* Vol. 9, pp. 791–802 (cit. on pp. 2, 7, 13).

Yadav, S., Shire, S. J., and Kalonia, D. S. (2011). 'Viscosity analysis of high concentration bovine serum albumin aqueous solutions.' *Pharm. Res.* Vol. 28(8), pp. 1973–83 (cit. on pp. 12, 60, 131).

Young, M. E., Carroad, P. A., and Bell, R. L. (1980). 'Estimation of diffusion coefficients of proteins'. *Biotechnol. Bioeng.* Vol. 22(5), pp. 947–955 (cit. on pp. 61, 77).

Zhang, J. and Liu, X. Y. (2003). 'Effect of protein-protein interactions on protein aggregation kinetics'. *J. Chem. Phys.* Vol. 119(20), p. 10972 (cit. on pp. 12, 48, 75).

Zimmerman, S. B. and Minton, A. P. (1993). 'Macromolecular crowding: biochemical, biophysical, and physiological consequences.' *Annu. Rev. Biophys. Biomol. Struct.* Vol. 22, pp. 27–65 (cit. on pp. 47, 58, 61).

3.3 Influence of structure properties on protein-protein interactions - QSAR modeling of changes in diffusion coefficients

Katharina Christin Bauer[1], Frank Hämmerling[1], Jörg Kittelmann, Cathrin Dürr, Fabian Görlich, Jürgen Hubbuch*
[1] Contributed equally

Institute of Engineering in Life Sciences, Section IV: Biomolecular Separation Science, Karlsruhe Institute of Technology (KIT), 76131 Karlsruhe, Germany;
* Corresponding author: telephone: +49-721-608-42557, e-mail: juergen.hubbuch@kit.edu
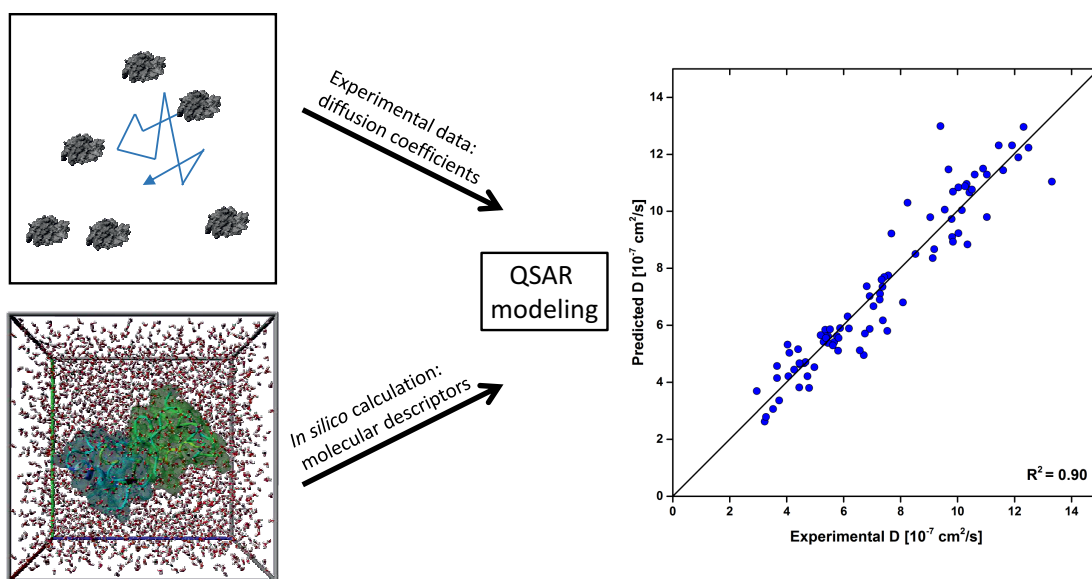
Abstract

Information about protein-protein interactions provides valuable knowledge about the phase behavior of protein solutions during the biopharmaceutical production process. Up to date it is possible to capture their overall impact by an experimentally determined potential of mean force. For the description of this potential, the second virial coefficient B_{22}, the diffusion interaction parameter k_D, the storage modulus G', or the diffusion coefficient D is applied. *In silico* methods do not only have the potential to predict these parameters, but also to provide deeper understanding of the molecular origin of the protein-protein interactions by correlating the data to the protein's three-dimensional structure. This methodology furthermore allows a lower sample consumption and less experimental effort. Of all *in silico* methods, QSAR modeling, which correlates the properties of the molecule's structure with the experimental behavior, seems to be particularly suitable for this purpose. To verify this, the study reported here dealt with the determination of a QSAR model for the diffusion coefficient of proteins. This model consisted of diffusion coefficients for six different model proteins at various pH values and NaCl concentrations. The generated QSAR model showed a good correlation between experimental and predicted data with a coefficient of determination $R^2 = 0.9$ and a good predictability for an external test set with $R^2 = 0.91$. The information about the properties affecting protein-protein interactions present in solution was in agreement with experiment and theory. Furthermore, the model was able to give a more detailed picture of the protein properties influencing the diffusion coefficient and the acting protein-protein interactions.

Introduction

Protein-protein interactions govern the phase behavior, or more precisely, physical properties such as solubility or viscosity of a biopharmaceutical protein solution. Already small changes in these properties can affect the outcome of each process step until the final product is obtained. A decrease in solubility, for example, can provoke aggregation, whereas an increase of viscosity can inhibit processability. In both of these cases, product loss can be the consequence (Lewus, Darcy, et al., 2011; Shire et al., 2004). To predict or prevent these changes, protein as well as protein-solvent interactions have to be understood. On a molecular level, protein-protein interactions are based on the protein's configuration as well as on its surface patches with their specific properties, meaning its electrostatic charge and hydrophobicity. Depending on the solution conditions, these specific surface patches change

74

and interact differently with their surrounding (Y.-C. Cheng et al., 2008). Electrostatic interactions can act attractively or repulsively over long-range distance. At short-range distance additional interactions can have an impact. These interactions are attractive van der Waals and hydrophobic interactions as well as repulsive hydration forces (Oss, 2003; Liang et al., 2007; Crommelin et al., 2013). Yet researchers are able to experimentally determine an overall potential of all these acting forces, called the potential of mean force (Saluja and Kalonia, 2008). The potential of mean force can be derived from one physical solution property and its deviation from ideality. This deviation is usually represented by parameters, such as the second virial coefficient B_{22} (George et al., 1994; Ahamed et al., 2007) or the diffusion interaction parameter k_D (Connolly et al., 2012) for dilute solutions, the storage modulus G' (Saluja, Badkar, et al., 2007) for highly concentrated solutions, or the mutual diffusion coefficient D (Zhang et al., 2003; Muschol et al., 1995; Bauer, Göbel, et al., 2016) for dilute, represented by k_D, as well as highly concentrated protein solutions. Using this approach, scientists can capture the overall change in interactions, but they cannot correlate them to their origin on the protein surface (Saluja and Kalonia, 2008). Computational methods, so-called *in silico* methods, which use the protein structure as basic information, have the potential to fill this gap by correlating the three-dimensional molecule structure to the overall potential gained in experiments. A highly suitable approach is to use quantitative structure-activity relationship (QSAR). The principal aim of this method is to predict experimental properties of a compound based on the molecular structure. QSARs work on the assumption that structurally similar compounds have similar activities and therefore have predictive abilities (Dehmer et al., 2012). QSARs still are mainly applied for small molecules during the development of bioactive compounds (Mazza, Sukumar, et al., 2001). During the last two decades, QSAR models were successfully used to describe and to predict the experimental behavior of proteins and complex biopharmaceutical products during ion-exchange (Mazza, Sukumar, et al., 2001; Mazza, Whitehead, et al., 2002), mixed-mode (T. Yang et al., 2007; Chung et al., 2010) and hydrophobic interaction (Ladiwala et al., 2006) chromatography. Buyel et al., 2013 used QSAR to predict the chromatographic separation of tobacco host cell proteins out of a complex feedstock.

This work aimed at extending use of QSAR modeling for proteins from chromatography to stability and processability of protein solutions during downstream processing and storage. For this purpose, the capability of QSAR modeling to predict protein-protein interactions from protein structure properties was examined. Furthermore, the ability to create a deeper understanding of the mechanisms affecting protein-protein interactions was considered. For the investigation of protein-protein interactions, the apparent diffusion coefficients of six different globular proteins, namely, α-lactalbumin, lysozyme, β-lactoglobulin, ovalbumin, BSA, and glucose oxidase, with a concentration of 10 mg/mL at varying pH values and NaCl concentrations were determined. These data were used to build a QSAR model. Apart from the predictive capacity of this QSAR model, its information about the protein-protein interactions having an impact on the value of the apparent diffusion coefficient was evaluated.

Materials and Methods

In this section the materials and methods for building a QSAR model to describe and predict the diffusion coefficient of different proteins at various pH values and NaCl concentrations are explained. It covers the preparation of the buffers as well as protein solutions, the determination of the diffusion coefficient by dynamic light scattering, and the QSAR modeling.

Buffers and Protein Solutions

Buffer stock solutions with and without NaCl were prepared for pH 3, 5, 7, and 9. The buffer components were citric acid (Merck KGaA, Darmstadt, Germany) and sodium citrate (Sigma-Aldrich, St. Louis, MO, USA) for pH 3, acetic acid (Merck KGaA) and sodium acetate (Sigma-Aldrich, St. Louis, MO, USA) for pH 5, MOPSO (AppliChem GmbH, Darmstadt, Germany) for pH 7, and BisTris (Sigma-Aldrich) for pH 9. Without addition of NaCl, each buffer stock solution had an ionic strength of 100 mM. For the stock solutions with NaCl, 2.5 M NaCl (Merck KGaA) were weighed in with the rest of the components. The pH was controlled using a five-point calibrated pH meter (HI-3220, Hanna® Instruments, Woonsocket, RI, USA) equipped with a SenTix® 62 pH electrode (Xylem Inc., White Plains, NY, USA) and corrected by titration of hydrochloric acid or sodium hydroxide with an accuracy of ±0.05. Both chemicals were purchased from Merck (Darmstadt, Germany). Each buffer was filtrated with a 0.22 μm cellulose acetate membrane (Sartorius AG, Göttingen, Germany). The buffers were used at constant pH 24 h after preparation. Lysozyme from chicken egg-white was purchased from Hampton Research (Aliso Viejo, CA, USA). α-lactalbumin from bovine milk, β-lactoglobulin from bovine milk, ovalbumin, bovine serum albumin (BSA), and glucose oxidase were purchased from Sigma-Aldrich. Each protein was weighed in and diluted with the buffer stock solution without salt at the respective pH. The protein solutions were filtered through 0.22 μm syringe filters with cellulose acetate membrane (VWR, Radnor, PA, USA). By centrifugation with Vivaspin® centrifugal concentrators (Sartorius AG) with polyethersulfone membrane, the solutions were desalted until 99.9 % of the solution were exchanged and then concentrated. Protein concentration was determined photometrically with a NanoDrop™ 2000c UV-Vis spectrophotometer (Thermo Fisher Scientific, Waltham, MA, USA). The respective extinction coefficients were $E^{1\%}(280\text{ nm}) = 20.01$ L g^{-1} cm^{-1} for α-lactalbumin, $E^{1\%}(280\text{ nm}) = 22.00$ L g^{-1} cm^{-1} for lysozyme, $E^{1\%}(280\text{ nm}) = 7.65$ L g^{-1} cm^{-1} for β-lactoglobulin, $E^{1\%}(280\text{ nm}) = 6.90$ L g^{-1} cm^{-1} for ovalbumin, $E^{1\%}(280\text{ nm}) = 5.72$ L g^{-1} cm^{-1} for BSA, and $E^{1\%}(280\text{ nm}) = 16.07$ L g^{-1} cm^{-1} for glucose oxidase. The samples of 10 mg/mL at different pH values and NaCl concentrations were prepared by mixing the protein stock solution with the buffer stock solutions with or without NaCl of the respective pH.

Dynamic Light Scattering

Dynamic light scattering (DLS) measurements are based on the interference of the scattered light by diffusing particles in solution. This method is mainly used to determine the size

and size distribution of these diffusing particles based on the Stokes-Einstein equation:

$$D = \frac{k_B T}{4\pi r_h \eta_S}. \tag{3.3}$$

In this equation for the ideal dilute state the diffusion coefficient D of a scattering particle depends on its hydrodynamic radius r_h, the viscosity of the surrounding solution η_S and the thermal energy $k_B T$. For a non-ideal solution, such as protein solutions, intermolecular interactions have an additional impact on the diffusion coefficient. For this purpose the diffusion coefficient is expanded by a term representing protein-protein interactions:

$$D = D_0(1 + k_D c_P). \tag{3.4}$$

In this equation D_0 is the diffusion coefficient of the protein at infinite dilution, c_P the protein concentration, and k_D the diffusion interaction parameter summarizing all protein-protein interactions (Kuehner, Heyer, et al., 1997; Lehermayr et al., 2011).

Principle of Determining Changes in Interactions by DLS As described in the previous section the principle of determining changes in interactions by dynamic light scattering is based on the changes of the determined diffusion coefficient due to protein-protein interactions. In general, a decrease in the apparent diffusion coefficient can be interpreted as predominating attractive interactions, an increase suggests predominating repulsive interactions in solution (Muschol et al., 1995). For the purpose of our work, we determined diffusion coefficients at a constant concentration of 10 mg/mL for different proteins, namely, α-lactalbumin, lysozyme, β-lactoglobulin, ovalbumin, BSA, and glucose oxidase at pH 3, 5, 7, and 9 and NaCl concentrations between 0 and 1.82 M. By the changes of the diffusion coefficient depending on the respective condition, changes of present interactions in solution were determined.

To exclude that observed changes in diffusion coefficient D are solely the effect of a perturbation on the diffusion coefficient at infinite dilution D_0, this parameter was calculated and determined experimentally for selected proteins and conditions. $D_{0,calc}$ was determined with the correlation that relates D to the molecular weight published by Young et al., 1980. The experimentally determined $D_{0,exp}$ was extrapolated to infinite dilute protein concentration from diffusion coefficients determined at several protein concentrations according to Saluja, Badkar, et al., 2007. At each pH the respective values of D_0 for all investigated NaCl concentrations were averaged and the standard deviation was calculated.

DLS Measurements Dynamic light scattering (DLS) measurements of the protein solutions were conducted in triplicate with the high-throughput compatible Wyatt Technology DynaPro™ Plate Reader (Wyatt Technology Corporation, Santa Barbara, CA, USA). For each measurement, the sample volume of 30 μL was pipetted into one well of a Corning® Low Volume 384 Well Microplate NBS™ (Corning Incorporated, Tewksbury, MA, USA) and covered by silicon oil WACKER® AK 20 (Wacker Chemie AG, Munich, Germany) to prevent evaporation. Each measurement consisted of 10 acquisitions for 5 s at 23 °C. The

apparent diffusion coefficient of the respective protein was determined by the distributional result of the DYNAMICS® Software Version 7.1.7.16 (Wyatt Technology Corporation) and averaged over the three measured wells of the same sample.

QSAR Modeling

Structure Preparation   According to protein name and organism, the UniProtID for all proteins was obtained from UniProt (The Uniprot Consortium, 2015). All Protein Data Bank (PDB) files were downloaded from the RCSB Protein Data Bank (Berman, 2000). The specific IDs can be found in Table 3.4. In Yasara (Krieger et al., 2002), a software for visualization, modeling of molecules, and molecular dynamics simulations, a protein structure reflecting the conditions in solution was generated. Therefor the structures were checked for completeness and, if necessary, missing residues or intramolecular disulfide bonds were added manually. The hydrogen bonding network was optimized and an energy minimization experiment was conducted using the Amber03 force field (Duan et al., 2003). Heteroatoms were separated from the protein structure and the protonation of amino acids was executed in H++ (Anandakrishnan et al., 2012) according to the respective pH value and ionic strength. After protonation of amino acid residues, the heteroatoms were inserted again. Using the Amber03 force field another energy minimization and molecular dynamics (MD) simulation experiment were performed. The 10 ps MD simulation experiment was carried out at 298 K, the size of the simulation box was extended 10 Å on every side of the protein, periodic boundaries were chosen and snapshots were taken every 1 ps and averaged afterwards. This averaged structure was then used for the calculation of molecular descriptors. Glucose oxidase, which exists as a dimer under the studied conditions, was assembled by two monomers with the help of SWISS-MODEL (Biasini et al., 2014).

Calculation of Molecular Descriptors   The 'mantoQSAR' software developed in-house was used for the calculation of molecular descriptors based on the averaged PDB structure after the MD simulation. It accounts for molecular structure, electrostatic and hydrophobic properties of the proteins at distinct pH values and ionic strengths. The group of molecular structure properties descriptors include all descriptors derived from geometric data of proteins, such as protein size, number of amino acids, protein shape and others. The hydrophobic properties are calculated using the hydropathy score published by Kyte et al., 1982. For a detailed breakdown of each of these properties, four different types of

Table 3.4: PDB identifier (ID), pI, and molecular weight of the proteins used in this study.

Protein Name	PDB ID	pI	Molecular weight [kDa]
α-Lactalbumin	1F6S	4.5	14.2
Lysozyme	1LYZ	11.0	14.9
β-Lactoglobulin	2AKQ	4.9	18.4
Ovalbumin	1OVA	4.5	44.3
BSA	3V03	4.9	66.4
Glucose oxidase*	1CF3	4.2	160.0

*Dimer created with SWISS-MODEL (http://swissmodel.expasy.org)

descriptors are defined:

1. Full molecule descriptors: This set of descriptors comprises the complete molecule and calculates properties for the overall molecule's structure.

2. Plane descriptors: A number of 120 planes is tangentially approached to the protein molecule's surface until a set distance of 5 Å between the protein and the plane. This distance is adapted from previous work published by Dismer et al., 2010 and Lang et al., 2015. For this study a set of 120 plane orientations, randomly distributed along the protein surface, was chosen and respective descriptors calculated for each orientation.

3. Patch descriptors: Patch descriptors only account for a part of the molecule and only calculate the values for the selected part ("patch") of the molecule. The size of the protein surface patch considered for calculation of the patch descriptors was derived from the calculated planes: based on the orientation of the planes, solvent-accessible protein surface area within a distance below 20 Å was taken into account for calculation of molecular descriptors and thus only parts of the molecule are represented.

4. Shell descriptors: The calculated descriptor values obtained from all 120 plane orientations are summed up to gain a 'shell projection', representing the properties at a distance of 5 Å around the molecule.

Multi-variate Data Analysis & Modeling Partial least squares regression (PLSR) was used for QSAR modeling of the diffusion coefficient D. For this purpose, the complete data set with 94 observations and the associated descriptor values from mantoQSAR was split into a training and a test set. The training set containing 84 observations was used to build a QSAR model. This resulting model was then applied to the test set containing 10 observations. The experiments for the test set were randomly chosen, considering that the observations were located within the borders of the PLSR score scatter plot. During the first step, all 251 molecular descriptors were used to calculate an initial crude model with the training set data. Descriptors with a significant influence on protein diffusion coefficients were chosen according to the value of the variable influence on the projection (VIP). The VIP is a parameter that summarizes the importance of the X-variables to the X- and Y-models. Descriptors with a VIP value > 1 are deemed to contribute strongly to the resulting PLSR model (Eriksson, Byrne, et al., 2013). Based on the 68 selected descriptors of the first crude model with a VIP value > 1, a final PLS model was created and then applied to predict the diffusion coefficients of the training set. This model had its own new VIP values, whose interpretation allowed for the generation of a mechanistic understanding. To exclude a random correlation of the selected molecular descriptors and the diffusion coefficients, a response permutation (Y-scrambling) with the final QSAR model was performed. The X-dataset, including the descriptors, was left intact, while the Y-dataset, including the observations, was randomly re-ordered 100 times. For each of the 100 Y-permutations, the data were PLSR-modeled. The correlation of X- and Y-data

was assessed through the resulting coefficients of determination R^2 and the predictive capabilities of the respective model through the value of Q^2 (Eriksson, Jaworska, et al., 2003; Tropsha et al., 2003).

Results

This section presents the results for the diffusion coefficients as well as the QSAR model for the different proteins at various pH values and NaCl concentrations. The results for the QSAR model cover the training and the test. To underline the correlation between the surface properties of the proteins, captured by 68 descriptors, and the diffusion coefficient, the permutation plot is depicted.

Diffusion Coefficients

To examine protein-protein interactions, the diffusion coefficient was determined. Figure 3.13 displays the diffusion coefficients as well as calculated and experimentally determined diffusion coefficients $D_{0,calc}$ and $D_{0,exp}$ of α-lactalbumin and lysozyme at selected conditions. $D_{0,calc}$ had a value of $10.1 \cdot 10^{-7}$ cm^2/s for α-lactalbumin and $9.9 \cdot 10^{-7}$ cm^2/s for lysozyme. The values for $D_{0,exp}$ varied depending on protein and pH value. For α-lactalbumin these were 12.6, 13.2, and $12.9 \cdot 10^{-7}$ cm^2/s for pH 5, 7, and 9, for lysozyme 11.5, 11.7, and $11.1 \cdot 10^{-7}$ cm^2/s for pH 3, 5, and 7. The standard deviation for all these values was below $0.6 \cdot 10^{-7}$ cm^2/s. The determined diffusion coefficients for α-lactalbumin and lysozyme varied dependent on protein type, pH and NaCl concentration. These values are also displayed in Figure 3.14 that shows the apparent diffusion coefficient of the studied proteins, namely, α-lactalbumin, lysozyme, β-lactoglobulin, ovalbumin, BSA, and glucose oxidase, with a concentration of 10 mg/mL at pH 3, 5, 7, and 9 and NaCl concentrations between 0 and 1.82 M. In these experiments the diffusion coefficient decreased with increasing NaCl concentration at constant pH. Furthermore, the diffusion coefficient varied depending on the pH value. In all experiments the standard deviation was below $1.47 \cdot 10^{-7}$ cm^2/s. This maximum value was determined for ovalbumin at pH 5 with 1.82 M NaCl. By looking at the results individually the diffusion coefficient of α-lactalbumin at 0 M NaCl had a value around $11 \cdot 10^{-7}$ cm^2/s for pH 5, 7 and 9. The values for pH 3 were neglected, because the protein formed a molten globule state (Permyakov et al., 2000). These changes in tertiary and quaternary structure can not be described by *in silico* simulation experiments. For high NaCl concentrations, this protein precipitated at all studied pH values. For this reason, no diffusion coefficients were determined. For lysozyme, the values of D at 0 M NaCl were within the same range as for α-lactalbumin, but precipitation could only be observed at pH 3. For β-lactoglobulin, the values at 0 M NaCl were lower and varied with pH. The highest value was measured at pH 7, followed by pH 3 and pH 9. Precipitation occurred for high NaCl concentrations at pH 3. At pH 5, β-lactoglobulin was not soluble, which is why no values were obtained. Ovalbumin at 0 M NaCl showed diffusion coefficients around $6.6 \cdot 10^{-7}$ cm^2/s with a maximum value of $7.6 \cdot 10^{-7}$ cm^2/s for pH 7. In comparison to β-lactoglobulin, these values were lower. For pH 5, the value of the diffusion coefficients depending on NaCl concentration was nearly constant. The values for pH 3 had to be neglected for the same reason as for α-lactalbumin. The molten globule state of ovalbumin under this condition (Tatsumi et al., 1997) could not be modeled by Yasara. For BSA, no
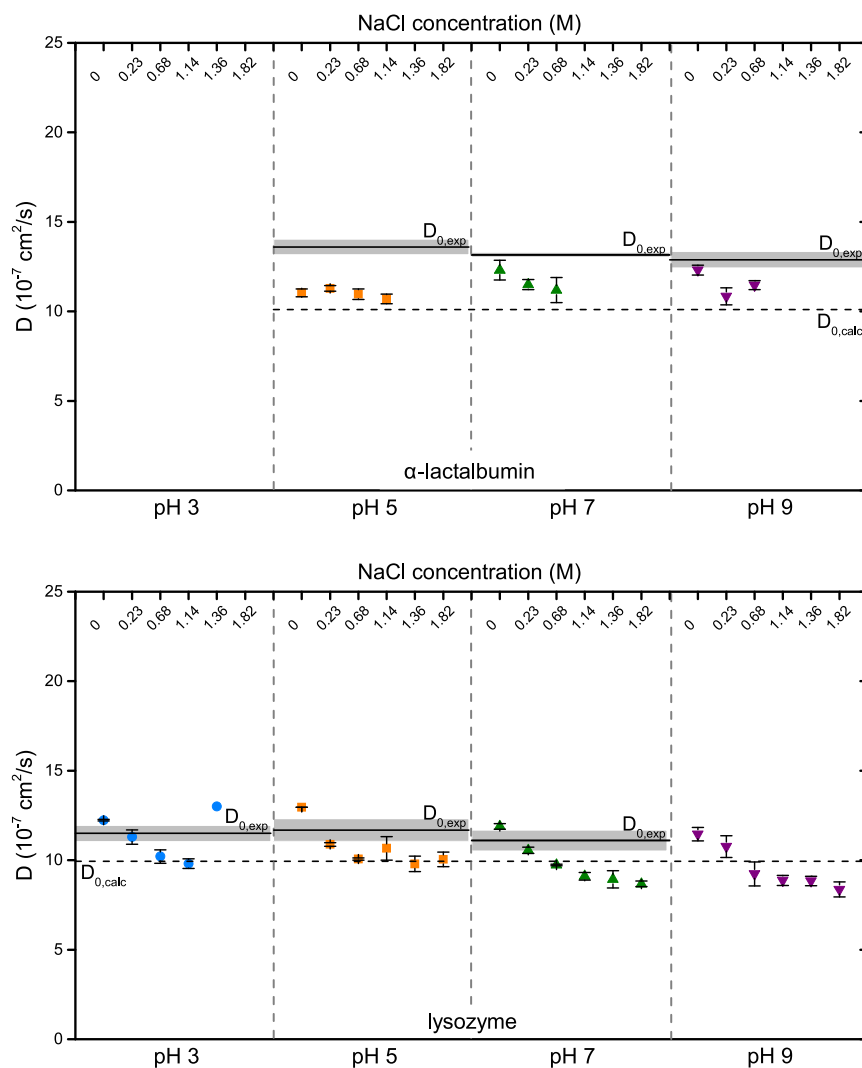
Figure 3.13: Diffusion coefficients at infinite dilution D_0 and a protein concentration of 10 mg/mL of α-lactalbumin and lysozyme at selected conditions. The solid line represents the experimentally determined $D_{0,exp}$ and the standard deviation colored in grey, and the dashed line the calculated $D_{0,calc}$.

strong influence of pH and NaCl concentration could be detected, with the exception of pH 3. Under this condition, precipitation could be observed at high NaCl concentrations. Almost the same behavior was found for glucose oxidase. For this protein, no data is shown for pH 3, because precipitation occurred directly upon addition of NaCl (Baumgartner et al., 2015).

QSAR Modeling

A QSAR model was built as described in section 3.3 with the molecular descriptors and the experimentally determined diffusion coefficients from section 3.3. The best resulting model contained 68 molecular descriptors and consisted of four PLS components. Comparison of experimental and predicted data of the training set is shown in Figure 3.15 with a coefficient of determination R^2 of 0.91 and a predictability Q^2 of 0.88. The R^2 value is considered as a measure for the strength of the association between the observed and predicted observations, while the cross validation square correlation coefficient Q^2 is a measure for the predictability of the model. The root mean square error of cross-validation (RMSECV) was $0.98 \cdot 10^{-7}$ cm^2/s. This model was used for the prediction of the diffusion coefficients from the external test set, consisting of ten experiments that had been excluded from the training set. Figure 3.16 shows the experimental and the predicted data for these 10 conditions with a coefficient of determination R^2 of 0.91. For an additional assessment of the statistical significance of the predictive power, a response permutation (Y-scrambling) was performed. Randomization of Y-data while keeping the X-data intact results in the generation of 100 "scrambled" models, each with a respective R^2 and Q^2 that are displayed in Figure 3.17. Both values for the scrambled models were compared with the values of the real model. All values for R^2 and Q^2 are lower for the scrambled models. In order to evaluate the descriptors with the highest impact on the model, a VIP plot was created. It shows the VIP values and the respective regression coefficient for each descriptor in Figure 3.18. Descriptors with a VIP > 1.0 are considered to have a strong influence on the target figure. Descriptors with values below 1.0 have a minor impact (Eriksson, Byrne, et al., 2013). The sign of the regression coefficient indicates the direction of the influence. Descriptors with a positive regression coefficient are proportional to the value of the diffusion coefficient, negative regression coefficients are inversely proportional (Kessler, 2007). The three descriptors with the highest VIP value were found to represent the electrostatic surface potential (ESP), the total surface area of the protein, and the solvent-accessible surface area of the protein patch with the lowest hydrophobicity. The 20 descriptors with VIP values > 1.0 are listed and explained in Table 3.5.

Discussion

As mentioned in the Introduction, several parameters can be used to describe protein-protein interactions in solution. For this study, the diffusion coefficient was selected to directly correlate a physical solution property to protein structure properties without further manipulation of data. To avoid an additional uncertainty that downgrades the quality of the QSAR model, the diffusion interaction parameter k_D was not considered as an alternative. The use of this parameter would require concentration-dependent linearity of the diffusion coefficient. Especially at conditions where additional short-range interactions

Table 3.5: Descriptors with a VIP value > 1.0 included in the final QSAR model and their descriptions.

No.	Descriptor	Definition
1	sumSurfA_ShellEsp	Sum of ESP of surface points projected on a shell around the molecule with a distance of 4.2 Å
2	totalSurf	Surface area of the protein in Å^2
3	totalSurf_PatchHydLow	Solvent-accessible surface area of the protein surface patch with the lowest hydrophobicity value in Å^2
4	nAtom	Number of atoms of the protein
5	mass	Molecular weight of the molecule
6	nAAcid	Chain length of the protein
7	shapeMin	Value for the sphericity of the protein: (minimum distance between mass center and protein surface)/(mean distance between mass center and protein surface)
8	totalSurf_PatchEspLow	Solvent-accessible surface area of the protein surface patch with the lowest ESP value in Å^2
9	totalSurf_PatchHydHigh	Solvent-accessible surface area of the protein surface patch with the highest hydrophobicity value in Å^2
10	shapeMax	Value for the sphericity of the protein: (maximum distance between mass center and protein surface)/(mean distance between mass center and protein surface)
11	binAbs_SurfHyd_3	Number of points with low hydrophobicity on the protein surface
12	nPos_SurfHyd	Number of hydrophobic surface points on the protein surface
13	relPos_SurfEsp	Ratio of positively charged surface points on the protein surface
14	relPos_PatchEspHigh	Ratio of positively charged surface points on the protein patch with the highest ESP value
15	sumSurf_PatchEspLow	Sum of ESP on the protein patch with the lowest ESP value
16	sumNeg_PatchEspLow	Sum of negative charge on the surface patch with the lowest ESP value
17	nPos_ShellEsp	Number of positively charged surface points projected on a shell around the molecule with a distance of 4.2 Å
18	relPos_PatchEspLow	Ratio of positively charged surface points on the protein surface patch with the lowest ESP value
19	mean_PatchHydHigh	Mean hydrophobicity on the protein surface patch with the highest hydrophobicity
20	sumPos_SurfHyd	Sum of points with positive hydropathy score on the protein surface
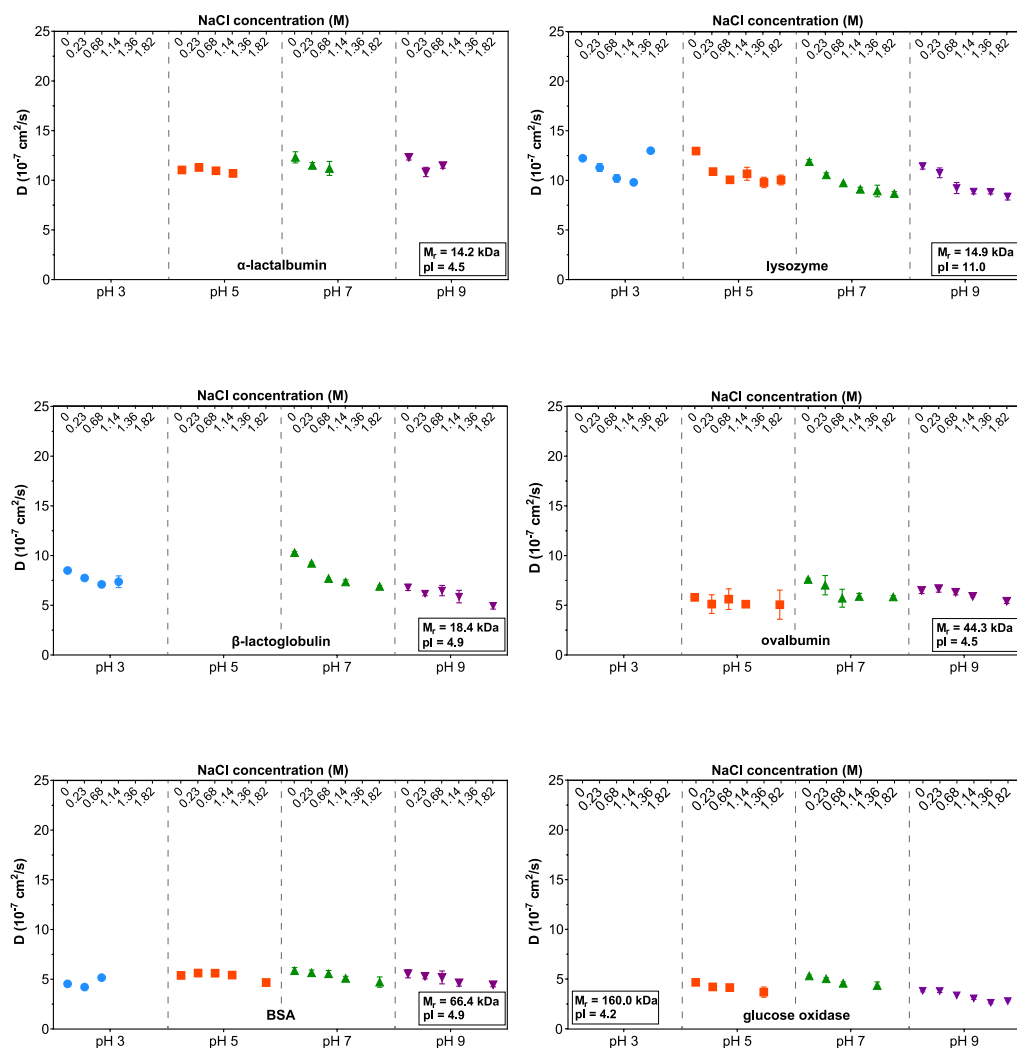
Figure 3.14: Diffusion coefficients of α-lactalbumin, lysozyme, β-lactoglobulin, ovalbumin, BSA, and glucose oxidase at 10 mg/mL for NaCl concentrations between 0 and 1.82 M and pH 3, 5, 7, and 9.

have an impact, such as for high protein or salt concentrations, this state of ideal dilution and, thus, concentration-dependent linearity cannot be commonly assumed (Muschol et al., 1995; Velev et al., 1998; Bauer, Göbel, et al., 2016).

Protein-protein Interactions Obtained by Determination of Diffusion Coefficients

When looking at the diffusion coefficients and the impact of protein-protein interactions, all parameters that can have an impact on these values need to be considered. According to the Stokes-Einstein relation, the diffusion coefficient depends on the hydrodynamic radius of the protein, the temperature, and the viscosity of the solvent (Equation 3.3). Whereas temperature and viscosity of the solvent were constant in this study, the hydrodynamic radius, which depends on the shape and size of the protein, could have an impact. As we
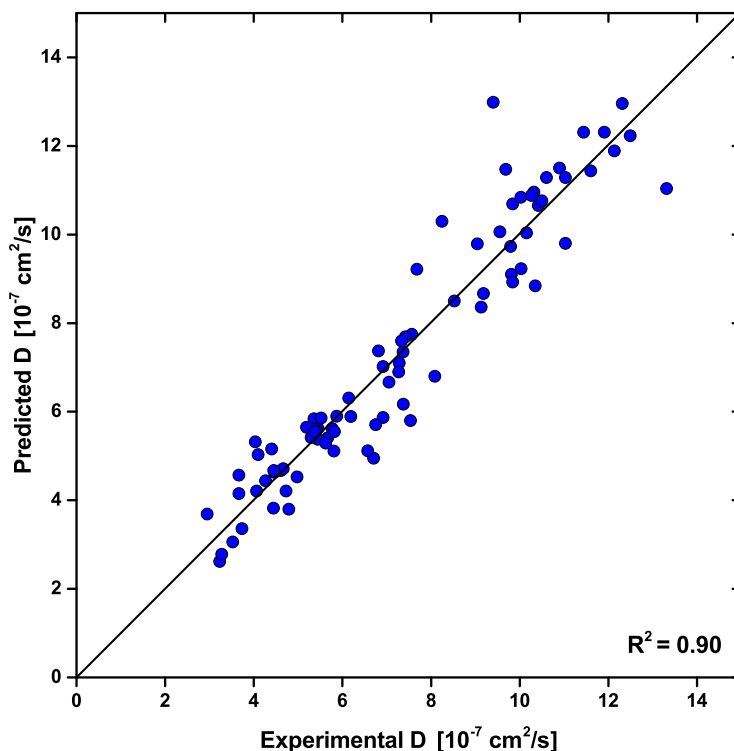
Figure 3.15: QSAR model of the training set: Experimental vs. predicted values of the diffusion coefficient.

only used globular proteins, the shape was supposed to have a negligible impact when interpreting the investigated data. In this study, the proteins with a higher molecular weight showed a lower diffusion coefficient compared to those with a lower molecular weight, following the Stokes-Einstein equation.

For protein solutions, apart from these influencing parameters for the ideal state reflected by Stokes-Einstein, interactions have to be taken into account. For this purpose this diffusion coefficient for the ideal state is complemented by a virial expansion resulting in Equation 3.4 where D_0 is the diffusion coefficient of one particle in solution at infinite dilution. This parameter exclusively is a function of particle size, shape, and the surrounding solvent (Felderhof, 1978; Lehermayr et al., 2011). D_0 is fairly constant for one protein under the conditions investigated in this study. The values for D at 10 mg/mL differ significantly from D_0 and its perturbation. Therefor the observed differences in the diffusion coefficients displayed in Figure 3.13 are due to changes in the diffusion interaction parameter k_D. These interactions varied when changing the pH or adding NaCl. In theory, variation in pH changes the electrostatic charge distribution on the protein surface by protonation or deprotonation of amino acid side chains. Far from isoelectric point (pI), at dilute state, electrostatic interactions predominate. Due to their long-range repulsive nature, these interactions prevail over short-range interactions and cause an increase of the diffusion coefficient. Nevertheless, short-range interactions are present and also influence
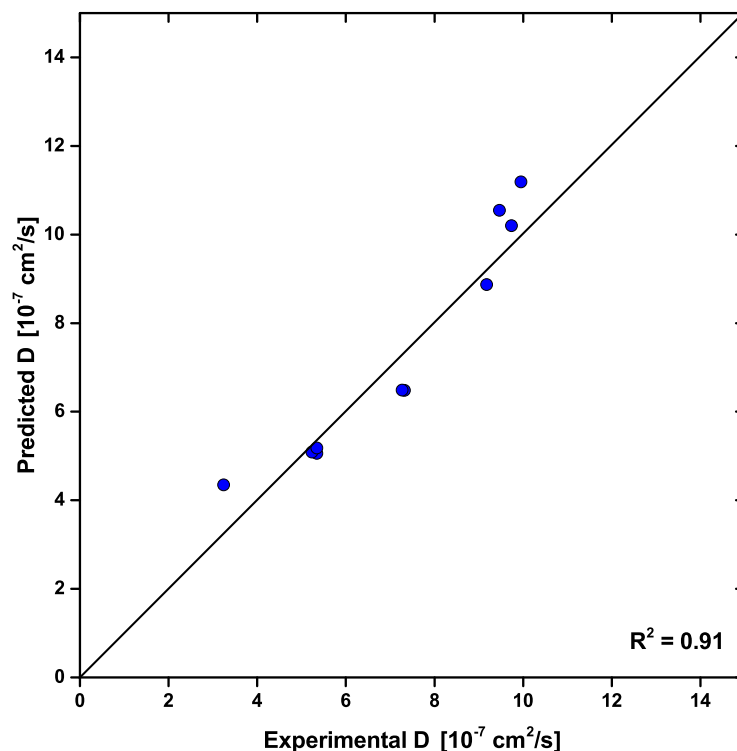
Figure 3.16: External validation of the QSAR model with the training set: Experimental vs. predicted values of the diffusion coefficient.

the diffusion coefficients of the proteins. These interactions include attractive van der Waals and hydrophobic interactions as well as repulsive hydration forces (Liang et al., 2007). Close to the pI, the electrostatic net charge of a protein is close to zero. Here, attractive short-range interactions have an increasing impact. The overall potential of these forces can cause an attraction of the proteins, which is reflected by a lower diffusion coefficient (Crommelin et al., 2013; Saluja, Badkar, et al., 2007). For the experimental data of this study, this theoretical decrease of repulsive interaction towards the pI was observed at 0 M NaCl for α-lactalbumin from pH 7 to pH 5, lysozyme from pH 5 to pH 7, and for ovalbumin, BSA, and glucose oxidase from pH 7 to pH 5. In contrast, pH values far from the pI deviated from this theory. The values for the diffusion coefficient for lysozyme at pH 3 and for β-lactoglobulin, ovalbumin, BSA, and glucose oxidase at pH 9 did not further increase, which indicates an increase in attractive interactions under this conditions. One reason for this increase far from the pI could be the strong deprotonation or protonation of the protein surface, which promotes an increase in hydrophobic surface area (D. Guo et al., 1986).

In contrast to the changes in pH, variation of NaCl concentration causes electrostatic shielding of the charged surface patches. As a result, electrostatic interactions decrease and the impact of short-range interactions, such as hydrophobic interactions, are promoted (Curtis, Steinbrecher, et al., 2002). This effect is reflected by a decrease in the value of
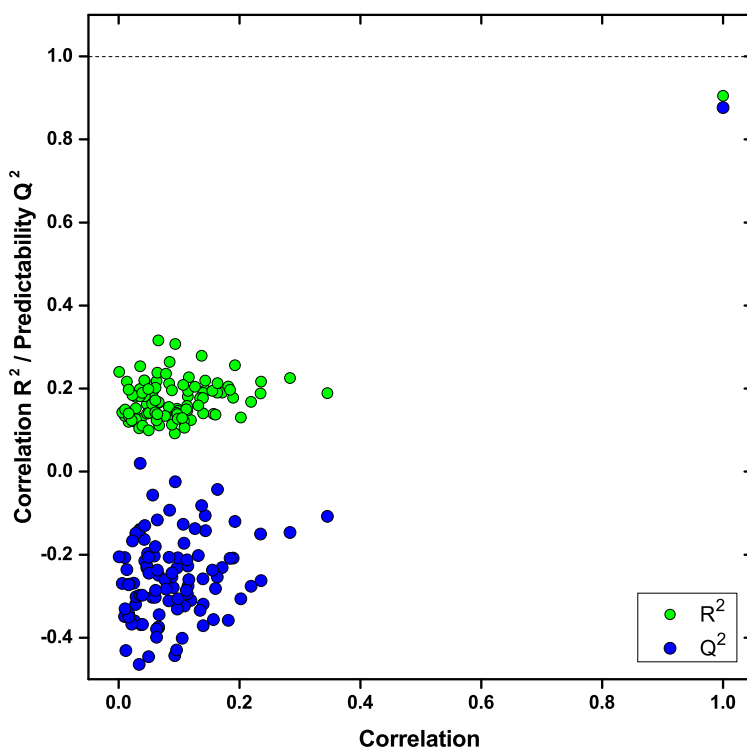
Figure 3.17: Permutation plot for the randomized Y-vector displaying the respective correlation R^2 and predictability Q^2.

the diffusion coefficient with increasing NaCl concentration (Parmar et al., 2009). For the diffusion coefficients determined in this study, this observation could be seen for all proteins at constant pH. Precipitation caused by strong attractive interactions (Dumetz, 2007) occurred for α-lactalbumin at pH 9 and for lysozyme as well as BSA at pH 3.

In summary, the results for the diffusion coefficient in this study provided valuable information about the interactions in solution for each protein and its respective condition. With their variety in proteins, their size, pH values, and NaCl concentrations, the data seemed suitable for building a sound QSAR model.

Evaluation of QSAR Modeling

For the description of the diffusion coefficient by QSAR modeling, the calculated molecular descriptors are considered to take into account all protein properties as well as changes in pH and ionic strength. For this study, a set of 68 descriptors represented the molecular properties, which determined the value of the diffusion coefficient of the respective protein. For the training set, the results for the predicted values of the diffusion coefficient compared with the experimentally determined values were taken from Figure 3.15. With a coefficient of determination R^2 of 0.90, prediction agreed well with the experimental data. Predictability Q^2 was 0.88 and determined by internal cross-validation. Still, the quality of the model could be improved any further by decreasing the experimental error. Predicted values for two conditions deviated in model response compared to experimental data. Those were
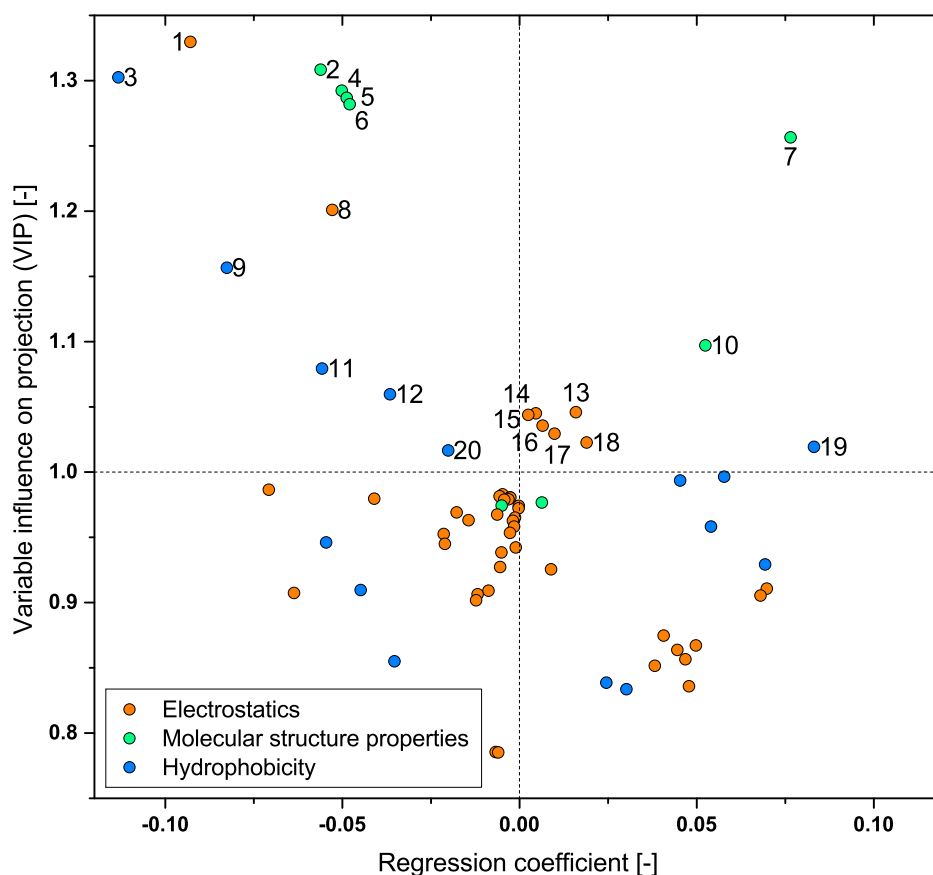
Figure 3.18: VIP values and regression coefficients for all 68 descriptors of the final QSAR model. The 20 descriptors with a VIP value > 1 are numbered and described in Table 3.5.

lysozyme at pH 3, 1.46 M NaCl and α-lactalbumin at pH 5, 0.1 M NaCl. This could be due to unstable conditions, caused by approximation to the solubility line or the pI.

Besides internal validation, within the training set, the final QSAR model was also applied and validated with an external test set including 10 observations (Figure 3.16). The results of this external validation indicate that the predicted values for the diffusion coefficient were in good agreement with the experimental data. The high value of $R^2 = 0.91$ for the test set suggests that the resulting QSAR model has a high predictive ability. This means that the QSAR model also allows for the accurate prediction of diffusion coefficients under new conditions excluded the training set.

For an additional assessment of the statistical significance of the predictive power, a response permutation (Y-scrambling) was performed (Figure 3.17). It can be seen clearly that all values for R^2 and Q^2 are significantly lower for the scrambled models. This reflects a clear statistical significance of the estimated predictive power of the QSAR model and its validity. A random correlation between the descriptors and the experimental data can therefor be excluded.

Influence of Protein Structure Properties on Protein-protein Interactions

The resulting QSAR model did not only allow the prediction of the diffusion coefficient, but also provided mechanistic insight into the properties influencing the diffusion coefficient. In this study the impact of the molecular size and shape as well as protein-protein interactions were captured by the 68 molecular descriptors of the QSAR model. The importance of each descriptor to the model can be evaluated by the VIP value. Descriptors with a VIP > 1.0 are considered to have a strong influence on the target figure. Descriptors with values below 1.0 have a minor impact (Eriksson, Byrne, et al., 2013). Figure 3.18 shows the VIP value and the regression coefficient for each descriptor. The sign of the regression coefficient indicates the direction of the influence. Descriptors with a positive regression coefficient are proportional to the value of the diffusion coefficient, negative regression coefficients are inversely proportional (Kessler, 2007).

Using this model for the diffusion coefficient, descriptors with information about electrostatic surface and molecular structure properties showed the highest VIP values. Five of seven descriptors with a VIP > 1.25 were connected to protein structure properties, the remaining ones to electrostatics. This strong influence of molecular structure properties was also obvious from the experimental data. This is in accordance with the Stokes-Einstein equation and contributes to D_0, the diffusion coefficient at infinite dilution included in the virial expansion of D. In the Stokes-Einstein equation the parameter for molecular structure properties is represented by the hydrodynamic radius r_h. Its inversely proportional impact was also captured by the model through negative regression coefficients for the descriptors 2, 4, 5, and 6, as is displayed in Table 3.5. In contrast to this, descriptor 7 had a positive regression coefficient, although it belonged to the same set. The reason is the missing correlation to r_h. The descriptor describes the influence of the molecule's shape on the diffusion coefficient. The more spherical the molecule, the higher is the value for this descriptor, which results in a higher diffusion coefficient. This correlation is in agreement with theory, because the non-spherical shape of a molecule increases the friction coefficient and, thus, results in a decrease of the diffusion coefficient (Jackson, 2006). Although this study was conducted with globular proteins only, it is obvious that this model was sensitive to changes in molecular shape. By looking at the values of this descriptor for the proteins used in this study, it can be seen that BSA and glucose oxidase deviate most strongly from a spherical shape. Besides descriptors for molecular structure properties, descriptors representing protein-protein interactions accounted for VIP values > 1.25. These protein-protein interactions are captured by the diffusion interaction parameter k_D included in the virial expansion of D. Descriptor 1, which had the highest VIP value in this model, represented the strong influence of electrostatic surface potential and, thus, the important impact of electrostatic interactions. Under the screened conditions, these long-range interactions revealed a strong influence for many conditions investigated in this study. Descriptor 3 represents the surface area of the protein surface patch with the lowest hydrophobicity. This property further underlines the strong influence of electrostatics under the studied conditions, because a large area with low hydrophobicity results in a mainly electrostatic effect.

In contrast to the descriptors mentioned above, descriptors 8 to 20 with a VIP value between

1.0 and 1.25 captured electrostatic, but also short-range interactions, e.g. hydrophobic properties. For this group, no clear correlation with the experimental data could be made. Nevertheless, the main effects of the descriptors describing the same property could be pointed out. For the descriptors describing hydrophobic properties, a negative regression coefficient was determined. This is in accordance with theory, because hydrophobic interactions always have an attractive character and, hence, result in a decrease of the diffusion coefficient (Liang et al., 2007). For the protein concentration used in this study, however, the VIP > 1 for these descriptors was remarkable. It showed that although electrostatic interactions dominate over short-range interactions under dilute conditions, the latter contribute to the value of the diffusion coefficient. According to theory, this most likely occurs at conditions close to the pI of the proteins or at high NaCl concentrations causing charge shielding effects and therefor promoting short-range interactions, such as hydrophobic interactions (Curtis, Steinbrecher, et al., 2002; Chi et al., 2003). Another more unlikely reason could be that for the studied proteins with a high molecular weight, namely, ovalbumin, BSA, and glucose oxidase, a protein concentration of 10 mg/mL exceeded the dilute state. According to the findings of Kumar et al., this would promote the impact of hydrophobic interactions (V. Kumar et al., 2011). By exemplarily taking a closer look at descriptor 9, this assumption was maintained: The impact of the descriptor was particularly important to proteins with high molecular weight (data not shown).

For the descriptors describing electrostatic properties (descriptors 13-18), slightly positive regression coefficients were found. In contrast to descriptors 1 and 8, they have an influence in opposite direction. Additionally, it is remarkable that four of these descriptors were related to positively charged surface points, although mainly proteins with negative net charge under the studied conditions were used in this work. These contrasts underline the complexity of the electrostatic impact on protein-protein interactions in solution. Electrostatic interactions can be influenced by a multitude of parameters (Wisz et al., 2003). In the presented model, these were the pH value, ionic strength through addition of NaCl, and surface charge of the protein. For the description of their synergetic effects on the impact of electrostatics, a variety of descriptors is necessary. This also includes oppositely directed descriptors, as can be seen for descriptors 1 and 8 with a negative regression coefficient, which probably capture the influence of negative charge, and descriptors 13 to 18 with positive values, which capture the influence of positive charge. These descriptors with positive regression coefficient values might be considered as a compensation of strong negative influence of the descriptors 1 and 8.

Among the descriptors with VIP values between 1.0 and 1.25, one descriptor capturing molecular structure properties could be found. This descriptor again underlines the strong impact of protein shape on the value of D, which was already observed for descriptor 7.

Taking all observations together, the diffusion coefficient is a result of various properties depending on the protein's structure. The size of the molecule and electrostatic interactions were found to be the properties with the main impact for this study. Further interactions that play a role for the overall potential could be identified. For other experimental setups, e.g. for concentrated protein solutions, differing results of QSAR modeling due to changes in underlying interactions could be expected. In this study, it was also shown that there is a complex relationship between the acting forces, which can also influence each other.

Thus, QSAR modeling does not only enable the prediction of protein-protein interactions by determination of the diffusion coefficient, but also provides insights into the fundamental understanding of the properties influencing this parameter.

Conclusion and Outlook

Determination of the diffusion coefficient by QSAR modeling did not only reveal the predictive capacity of this method, but also its ability to improve mechanistic understanding on a molecular basis. The diffusion coefficients determined in this study showed clear correlations to the protein-protein interactions in solution. The QSAR model based on these results and the three-dimensional structure properties of the proteins was able to determine and predict these values with a coefficient of determination R^2 of 0.9 and a predictability Q^2 of 0.88. In accordance with the experimental data, it described the strong impact of the protein size. Regarding protein-protein interactions, which experimentally can only be captured by an overall potential, the VIP value for each descriptor of the final model agreed with theory and reflected the predominant impact of electrostatic interactions under the studied dilute conditions. It also provided deeper insight, as it accounted for the shape and additional short-range interactions of the molecules, such as hydrophobic forces. With this promising results, QSAR modeling cannot only be used to gain more information with less sample consumption and working effort, but also improves mechanistic understanding of various parameters in biotherapeutics associated with the protein's three-dimensional structure.

So far, QSAR has only been used to describe and predict the chromatographic behavior of large biomolecules during purification processes. This work is the first application of QSAR beyond chromatography and the results demonstrate the potential of this methodology for future applications in the field of protein phase behavior and understanding the underlying mechanisms and interactions. Future work in this field could focus on the generation of QSAR models for other parameters reflecting protein-protein interactions, such as the second virial coefficient B_{22}, the diffusion interaction parameter k_D, or the storage modulus G'. Additionally, the implementation of non-globular proteins and the generation of advanced models sensitive to protein concentration could be topic of further research. This option mentioned last might enable to overcome the drawback that QSAR models have only been valid for the respective protein concentration so far.

Acknowledgments

References

Ahamed, T., Esteban, B. N. A., Ottens, M., Dedem, G. W. K. van, Wielen, L. A. M. van der, Bisschops, M. A. T., Lee, A., Pham, C., and Thömmes, J. (2007). 'Phase behavior of an intact monoclonal antibody.' *Biophys. J.* Vol. 93(2), pp. 610–9 (cit. on pp. 11, 47, 75).

Anandakrishnan, R., Aguilar, B., and Onufriev, A. V. (2012). 'H++ 3.0: automating pK prediction and the preparation of biomolecular structures for atomistic molecular modeling and simulations'. *Nucleic Acids Res.* Vol. 40(W1), W537–W541 (cit. on p. 78).

Bauer, K. C., Göbel, M., Schwab, M.-L., Schermeyer, M.-T., and Hubbuch, J. (2016). 'Concentration-dependent changes in apparent diffusion coefficients as indicator for colloidal stability of protein solutions'. *Int. J. Pharm. (Amsterdam, Neth.).* Vol. 511(1), pp. 276–287 (cit. on pp. 75, 84, 129, 146, 148, 150, 151).

Baumgartner, K., Galm, L., Nötzold, J., Sigloch, H., Morgenstern, J., Schleining, K., Suhm, S., Oelmeier, S. A., and Hubbuch, J. (2015). 'Determination of protein phase diagrams by microbatch experiments: Exploring the influence of precipitants and pH'. *Int. J. Pharm. (Amsterdam, Neth.).* Vol. 479(1), pp. 28–40 (cit. on pp. 10, 47, 49, 82, 132).

Berman, H. M. (2000). 'The Protein Data Bank'. *Nucleic Acids Res.* Vol. 28(1), pp. 235–242 (cit. on p. 78).

Biasini, M., Bienert, S., Waterhouse, A., Arnold, K., Studer, G., Schmidt, T., Kiefer, F., Cassarino, T. G., Bertoni, M., Bordoli, L., and Schwede, T. (2014). 'SWISS-MODEL: modelling protein tertiary and quaternary structure using evolutionary information'. *Nucleic Acids Res.* Vol. 42(W1), W252–W258 (cit. on p. 78).

Buyel, J., Woo, J., Cramer, S., and Fischer, R. (2013). 'The use of quantitative structure-activity relationship models to develop optimized processes for the removal of tobacco host cell proteins during biopharmaceutical production'. *J. Chromatogr. A.* Vol. 1322, pp. 18–28 (cit. on pp. 18, 75).

Cheng, Y.-C., Bianco, C. L., Sandler, S. I., and Lenhoff, A. M. (2008). 'Salting-Out of Lysozyme and Ovalbumin from Mixtures: Predicting Precipitation Performance from Protein-Protein Interactions'. *Ind. Eng. Chem. Res.* Vol. 47(15), pp. 5203–5213 (cit. on p. 75).

Chi, E. Y., Krishnan, S., Randolph, T. W., and Carpenter, J. F. (2003). 'Physical stability of proteins in aqueous solution: mechanism and driving forces in nonnative protein aggregation.' *Pharm. Res.* Vol. 20(9), pp. 1325–36 (cit. on pp. 1–5, 7–9, 90, 129).

Chung, W. K., Hou, Y., Holstein, M., Freed, A., Makhatadze, G. I., and Cramer, S. M. (2010). 'Investigation of protein binding affinity in multimodal chromatographic systems using a homologous protein library'. *J. Chromatogr. A.* Vol. 1217(2), pp. 191–198 (cit. on pp. 18, 75).

Connolly, B. D., Petry, C., Yadav, S., Demeule, B., Ciaccio, N., Moore, J. M. R., Shire, S. J., and Gokarn, Y. R. (2012). 'Weak interactions govern the viscosity of concentrated antibody solutions: high-throughput analysis using the diffusion interaction parameter.' *Biophys. J.* Vol. 103(1), pp. 69–78 (cit. on pp. 11, 12, 47, 51, 53, 60, 61, 75).

Crommelin, D. J. A., Sindelar, R. D., and Meibohm, B. (2013). *Pharmaceutical Biotechnology: Fundamentals and Applications.* SpringerLink : Bücher. Springer New York (cit. on pp. 2, 47, 75, 86).

Curtis, R. A., Steinbrecher, C., Heinemann, M., Blanch, H. W., and Prausnitz, J. M. (2002). 'Hydrophobic forces between protein molecules in aqueous solutions of concentrated electrolyte.' *Biophys. Chem.* Vol. 98(3), pp. 249–65 (cit. on pp. 9, 86, 90).

Curtis, R. A., Ulrich, J., Montaser, A., Prausnitz, J. M., and Blanch, H. W. (2002). 'Protein-protein interactions in concentrated electrolyte solutions.' *Biotechnol. Bioeng.* Vol. 79(4), pp. 367–80 (cit. on pp. 2, 9, 11, 47, 59, 129).

Dehmer, M., Varmuza, K., and Bonchev, D. (2012). *Statistical Modelling of Molecular Descriptors in QSAR/QSPR*. Ed. by Dehmer, M., Varmuza, K., and Bonchev, D. Weinheim, Germany: Wiley-VCH Verlag GmbH & Co. KGaA (cit. on p. 75).

Dismer, F. and Hubbuch, J. (2010). '3D structure-based protein retention prediction for ion-exchange chromatography'. *J. Chromatogr. A.* Vol. 1217(8), pp. 1343–1353 (cit. on p. 79).

Duan, Y., Wu, C., Chowdhury, S. S., Lee, M. C., Xiong, G., Zhang, W., Yang, R., Cieplak, P., Luo, R., Lee, T., Caldwell, J., Wang, J., and Kollman, P. (2003). 'A point-charge force field for molecular mechanics simulations of proteins based on condensed-phase quantum mechanical calculations.' *J. Comput. Chem.* Vol. 24(16), pp. 1999–2012 (cit. on p. 78).

Dumetz, A. C. (2007). *Protein Interactions and Phase Behavior in Aqueous Solutions: Effects of Salt, Polymer, and Organic Additives*. University of Delaware, p. 284 (cit. on pp. 58, 87).

Eriksson, L., Byrne, T., Johansson, E., Trygg, J., and Wikström, C. (2013). *Multi- and Megavariate Data Analysis: Part I: Basic Principles and Applications*. MKS Umetrics AB, p. 425 (cit. on pp. 79, 82, 89).

Eriksson, L., Jaworska, J., Worth, A. P., Cronin, M. T., McDowell, R. M., and Gramatica, P. (2003). 'Methods for Reliability and Uncertainty Assessment and for Applicability Evaluations of Classification- and Regression-Based QSARs'. *Environ. Health Perspect.* Vol. 111(10), pp. 1361–1375 (cit. on p. 80).

Felderhof, B. U. (1978). 'Diffusion of interacting Brownian particles'. *J. Phys. A. Math. Gen.* Vol. 11(5), pp. 929–937 (cit. on p. 85).

George, A. and Wilson, W. W. (1994). 'Predicting protein crystallization from a dilute solution property'. *Acta Crystallogr. Sect. D Biol. Crystallogr.* Vol. 50(4), pp. 361–365 (cit. on pp. 12, 47, 75).

Guo, D., Mant, C. T., Taneja, A. K., Parker, J., and Rodges, R. S. (1986). 'Prediction of peptide retention times in reversed-phase high-performance liquid chromatography I. Determination of retention coefficients of amino acid residues of model synthetic peptides'. *J. Chromatogr. A.* Vol. 359(8), pp. 499–518 (cit. on pp. 59, 86, 111).

Jackson, M. B. (2006). *Molecular and Cellular Biophysics*. Cambridge University Press (cit. on p. 89).

Kessler, W. (2007). *Multivariate Datenanalyse.* Weinheim, Germany: Wiley-VCH Verlag GmbH & Co. KGaA, p. 340 (cit. on pp. 82, 89).

Krieger, E., Koraimann, G., and Vriend, G. (2002). 'Increasing the precision of comparative models with YASARA NOVA-a self-parameterizing force field'. *Proteins Struct. Funct. Bioinforma.* Vol. 47(3), pp. 393–402 (cit. on pp. 3, 78).

Kuehner, D. E., Heyer, C., Rämsch, C., Fornefeld, U. M., Blanch, H. W., and Prausnitz, J. M. (1997). 'Interactions of lysozyme in concentrated electrolyte solutions from dynamic light-scattering measurements.' *Biophys. J.* Vol. 73(6), pp. 3211–24 (cit. on pp. 61, 77).

Kumar, V., Dixit, N., Zhou, L., and Fraunhofer, W. (2011). 'Impact of short range hydrophobic interactions and long range electrostatic forces on the aggregation kinetics of a monoclonal antibody and a dual-variable domain immunoglobulin at low and high concentrations'. *Int. J. Pharm. (Amsterdam, Neth.).* Vol. 421(1), pp. 82–93 (cit. on pp. 5, 7, 8, 11, 12, 14, 47, 51, 60, 61, 90).

Kyte, J. and Doolittle, R. F. (1982). 'A simple method for displaying the hydropathic character of a protein'. *J. Mol. Biol.* Vol. 157(1), pp. 105–132 (cit. on pp. 78, 99).

Ladiwala, A., Xia, F., Luo, Q., Breneman, C. M., and Cramer, S. M. (2006). 'Investigation of protein retention and selectivity in HIC systems using quantitative structure retention relationship models.' *Biotechnol. Bioeng.* Vol. 93(5), pp. 836–50 (cit. on pp. 18, 75).

Lang, K. M. H., Kittelmann, J., Dürr, C., Osberghaus, A., and Hubbuch, J. (2015). 'A comprehensive molecular dynamics approach to protein retention modeling in ion exchange chromatography'. *J. Chromatogr. A.* Vol. 1381, pp. 184–193 (cit. on p. 79).

Lehermayr, C., Mahler, H.-C., Mäder, K., and Fischer, S. (2011). 'Assessment of Net Charge and Protein-Protein Interactions of Different Monoclonal Antibodies'. *J. Pharm. Sci.* Vol. 100(7), pp. 2551–2562 (cit. on pp. 11, 15, 77, 85).

Lewus, R. A., Darcy, P. A., Lenhoff, A. M., and Sandler, S. I. (2011). 'Interactions and phase behavior of a monoclonal antibody'. *Biotechnol. Prog.* Vol. 27(1), pp. 280–289 (cit. on pp. 5, 12, 47, 74).

Liang, Y., Hilal, N., Langston, P., and Starov, V. (2007). 'Interaction forces between colloidal particles in liquid: Theory and experiment'. *Adv. Colloid Interface Sci.* Vol. 134-135, pp. 151–166 (cit. on pp. 2, 8, 75, 86, 90, 131).

Mazza, C. B., Sukumar, N., Breneman, C. M., and Cramer, S. M. (2001). 'Prediction of protein retention in ion-exchange systems using molecular descriptors obtained from crystal structure.' *Anal. Chem.* Vol. 73(22), pp. 5457–61 (cit. on p. 75).

Mazza, C. B., Whitehead, C. E., Breneman, C. M., and Cramer, S. M. (2002). 'Predictive quantitative structure retention relationship models for ion-exchange chromatography'. *Chromatographia.* Vol. 56(3-4), pp. 147–152 (cit. on pp. 18, 75).

Muschol, M. and Rosenberger, F. (1995). 'Interactions in undersaturated and supersaturated lysozyme solutions: Static and dynamic light scattering results'. *J. Chem. Phys.* Vol. 103(24), p. 10424 (cit. on pp. 11, 12, 47, 48, 61, 75, 77, 84).

Oss, C. J. van (2003). 'Long-range and short-range mechanisms of hydrophobic attraction and hydrophilic repulsion in specific and aspecific interactions'. *J. Mol. Recognit.* Vol. 16(4), pp. 177–190 (cit. on pp. 2, 47, 75).

Parmar, A. S. and Muschol, M. (2009). 'Hydration and Hydrodynamic Interactions of Lysozyme: Effects of Chaotropic versus Kosmotropic Ions'. *Biophys. J.* Vol. 97(2), pp. 590–598 (cit. on p. 87).

Permyakov, E. A. and Berliner, L. J. (2000). 'α-Lactalbumin: structure and function'. *FEBS Lett.* Vol. 473(3), pp. 269–274 (cit. on pp. 3, 7, 49, 59, 80, 111).

Saluja, A., Badkar, A. V., Zeng, D. L., Nema, S., and Kalonia, D. S. (2007). 'Ultrasonic storage modulus as a novel parameter for analyzing protein-protein interactions in high protein concentration solutions: correlation with static and dynamic light scattering measurements.' *Biophys. J.* Vol. 92(1), pp. 234–44 (cit. on pp. 11–15, 24, 25, 48, 51, 75, 77, 86).

Saluja, A. and Kalonia, D. S. (2008). 'Nature and consequences of protein-protein interactions in high protein concentration solutions.' *Int. J. Pharm. (Amsterdam, Neth.).* Vol. 358(1-2), pp. 1–15 (cit. on pp. 2, 5, 7, 10–13, 15, 36, 46–48, 58, 59, 61, 62, 75).

Schermeyer, M.-T., Sigloch, H., Bauer, K. C., Oelschlaeger, C., and Hubbuch, J. (2016). 'Squeeze flow rheometry as a novel tool for the characterization of highly concentrated protein solutions'. *Biotechnol. Bioeng.* Vol. 113(3), pp. 576–587 (cit. on pp. 12, 25, 26, 33, 48, 52).

Shire, S. J., Shahrokh, Z., and Liu, J. (2004). 'Challenges in the development of high protein concentration formulations.' *J. Pharm. Sci.* Vol. 93(6), pp. 1390–402 (cit. on pp. 7, 10, 15, 18, 24, 46, 74, 120, 121, 129, 133, 142, 143, 149).

Tatsumi, E. and Hirose, M. (1997). 'Highly ordered molten globule-like state of ovalbumin at acidic pH: native-like fragmentation by protease and selective modification of Cys367 with dithiodipyridine.' *J. Biochem.* Vol. 122, pp. 300–308 (cit. on p. 80).

The Uniprot Consortium (2015). 'UniProt: a hub for protein information'. *Nucleic Acids Res.* Vol. 43(D1), pp. D204–D212 (cit. on p. 78).

Tropsha, A., Gramatica, P., and Gombar, V. (2003). 'The Importance of Being Earnest: Validation is the Absolute Essential for Successful Application and Interpretation of QSPR Models'. *QSAR Comb. Sci.* Vol. 22(1), pp. 69–77 (cit. on p. 80).

Velev, O. D., Kaler, E. W., and Lenhoff, A. M. (1998). 'Protein interactions in solution characterized by light and neutron scattering: comparison of lysozyme and chymotrypsinogen.' *Biophys. J.* Vol. 75(6), pp. 2682–97 (cit. on p. 84).

Wisz, M. S. and Hellinga, H. W. (2003). 'An empirical model for electrostatic interactions in proteins incorporating multiple geometry-dependent dielectric constants'. *Proteins Struct. Funct. Genet.* Vol. 51(3), pp. 360–377 (cit. on p. 90).

Yang, T., Breneman, C. M., and Cramer, S. M. (2007). 'Investigation of multi-modal high-salt binding ion-exchange chromatography using quantitative structure-property relationship modeling'. *J. Chromatogr. A.* Vol. 1175(1), pp. 96–105 (cit. on p. 75).

Young, M. E., Carroad, P. A., and Bell, R. L. (1980). 'Estimation of diffusion coefficients of proteins'. *Biotechnol. Bioeng.* Vol. 22(5), pp. 947–955 (cit. on pp. 61, 77).

Zhang, J. and Liu, X. Y. (2003). 'Effect of protein-protein interactions on protein aggregation kinetics'. *J. Chem. Phys.* Vol. 119(20), p. 10972 (cit. on pp. 12, 48, 75).

3.4 Non-invasive high throughput approach for protein hydrophobicity determination based on surface tension

Sven Amrhein[1], Katharina Christin Bauer[1], Lara Galm[1], Jürgen Hubbuch*
[1] Contributed equally

Institute of Engineering in Life Sciences, Section IV: Biomolecular Separation Science, Karlsruhe Institute of Technology (KIT), 76131 Karlsruhe, Germany;
* Corresponding author: telephone: +49-721-608-42557, e-mail: juergen.hubbuch@kit.edu
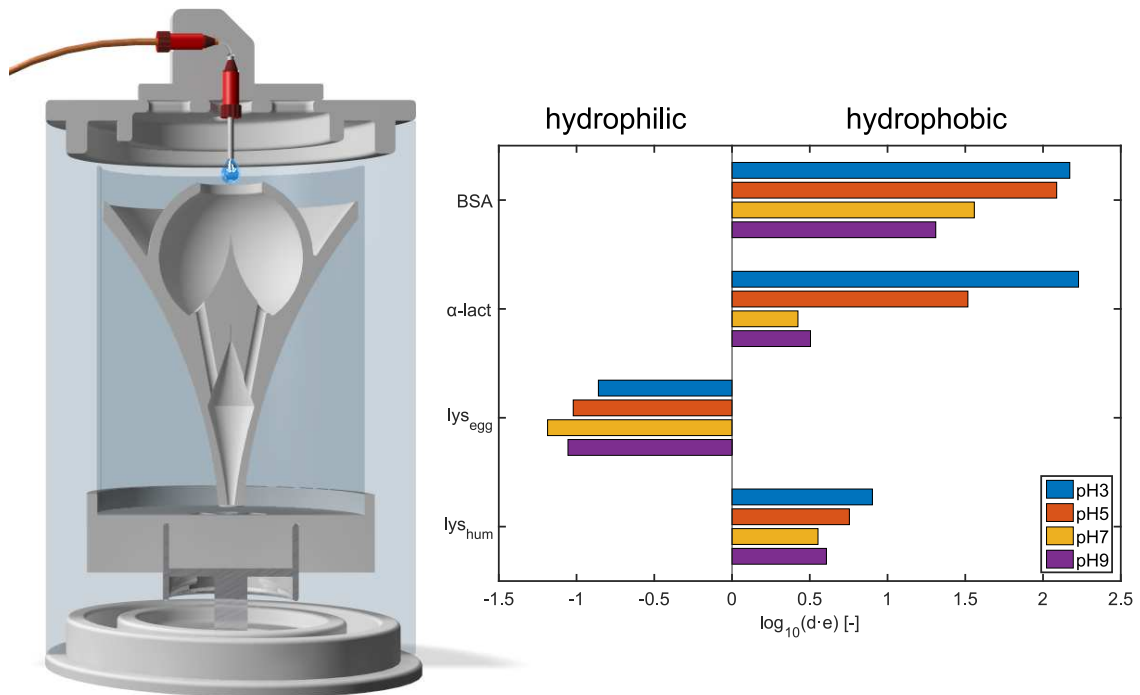
Abstract

The surface hydrophobicity of a protein is an important factor for its interactions in solution and thus the outcome of its production process. Yet most of the methods are not able to evaluate the influence of these hydrophobic interactions under natural conditions. In the present work we have established a high resolution stalagmometric method for surface tension determination on a liquid handling station, which can cope with accuracy as well as high throughput requirements. Surface tensions could be derived with a low sample consumption (800 µL) and a high reproducibility (< 0.1 ‰ for water) within a reasonable time (3.5 min per sample). This method was used as a non-invasive HTP compatible approach to determine surface tensions of protein solutions dependent on protein content. The protein influence on the solutions' surface tension was correlated to the hydrophobicity of lysozyme, human lysozyme, BSA, and α-lactalbumin. Differences in proteins' hydrophobic character depending on pH and species could be resolved. Within this work we have developed a pH-dependent hydrophobicity ranking, which was found to be in good agreement with literature. For the studied pH range of 3 to 9 lysozyme from chicken egg white was identified to be the most hydrophilic. α-lactalbumin at pH 3 exhibited the most pronounced hydrophobic character. The stalagmometric method occurred to outclass the widely used spectrophotometric method with bromophenol blue sodium salt as it gave reasonable results without restrictions on pH and protein species.

Keywords: *stalagmometer, bromophenol blue, hydrophilicity, protein solution, protein-solvent interaction*

Introduction

Hydrophobic interactions play a key role in the outcome of the production process of biopharmaceutical therapeutics passing through fermentation, the purification process, formulation and storage. During protein expression in fermentation hydrophobic forces regulate the formation of the globular protein molecule (Tanford, 1962; Dill, 1990). The resulting surface characteristics and the protein concentration govern its solubility for all following production steps. Already small changes in the hydrophobic character can provoque changes in solubility and in the aggregation tendency of the molecule (Brems et al., 1988; Nieba et al., 1997). Undesired aggregation during the process or storage can cause denaturation and thus product loss. However, for the purification process this changes regarding solubility can also be turned into advantage in terms of protein crystallization or precipitation as purification steps. The hydrophobic character of a protein can additionally be exploited to separate complex protein mixtures by using aqueous two-phase systems (ATPS) (Andrews et al., 2005; Diederich et al., 2013; Asenjo et al., 2011), reversed phase (RP) chromatography or hydrophobic interaction chromatography (HIC) (Janson, 2012). The knowledge of protein surface hydrophobicity therefore helps to predict, control and manipulate the influence of hydrophobic interactions during processing and storage.

98

Within the last decades a huge research effort has been spend on the development of experimental and *in silico* approaches for assessing protein surface hydrophobicity and the identification of highly hydrophobic proteins. In experiments most frequently protein hydrophobicity has been adapted from the hydrophobicity of single amino acids, that are ranked in different hydrophobicity scales (Janin, 1979; Kyte et al., 1982; Eisenberg, 1984; Black et al., 1991; Rose et al., 1993). This amino acid hydrophobicity has been measured mainly in terms of their solubility in organic and denaturant solutions (Whitney et al., 1962; Nozaki et al., 1963; Nozaki et al., 1965; Nozaki et al., 1970; Nozaki et al., 1971; Dooley et al., 1972) or their partition between an aqueous and an organic phase (Fendler et al., 1975; Radzicka et al., 1988).

Efforts have been made on hydrophobicity rankings of whole proteins based on partitioning in aqueous two-phase systems (Shanbhag et al., 1975), retention factors in HIC (Keshavarz et al., 1979) or using hydrophobic dyes (Kato et al., 1980; Cardamone et al., 1992; Hendriks et al., 2002; Bertsch et al., 2003; Hawe et al., 2008). Yet most experimental methods are invasive and not adequate to consider the influence of solution characteristics on the protein. In most cases organic liquids are inevitable which may influence the tertiary structure of the protein or even denature it.

In silico methods apply experimentally determined hydrophobicity scales to quantify protein hydrophobicity. These methods calculate the protein hydrophobicity either based on the amino acid sequence (Salgado et al., 2005) or based on the three-dimensional structure (Miller et al., 1987; Lijnzaad et al., 1996; Chennamsetty et al., 2009). Salgado et al. (Salgado et al., 2006a; Salgado et al., 2006b) found that methods based on the three-dimensional structure show a better predictive performance for protein adsorption mechanisms in HIC than the ones based on the amino acid sequence. Sophisticated approaches based on QSAR (Mahn et al., 2004; Chen et al., 2007) or molecular dynamics (MD) simulations (Amrhein, Oelmeier, et al., 2014; Reißer et al., 2014) give the most detailed description of the protein surface. However, these sophisticated *in silico* approaches require either an enormous computational effort or use theoretical hydrophobicity scales as described above and thus cannot account for the influence of the solvent. Generally, approaches using theoretically derived hydrophobicity scales are highly influenced by the selected hydrophobicity scale (Trinquier et al., 1998; Biswas et al., 2003).

One promising way of considering the environmental dependency is to measure hydrophobicity via surface tension. This experimental method is able of capturing the environmental dependency because it is non-invasive. The existence of a correlation between surface or interfacial tension and hydrophobicity of single amino acids or macromolecules is known for a long time (Bull et al., 1974; Keshavarz et al., 1979; Kato et al., 1980; Absolom et al., 1987). Bull et al., 1974 pointed out the potency of sorting amino acids by hydrophobicity according to their surface tension increment. According to this, hydrophobic amino acids reduce the surface tension with increasing concentration. Conversely, hydrophilic amino acids increase the surface tension.

Keshavarz et al., 1979 could show a significant negative correlation between the effective hydrophobicities of bovine serum albumin, ovalbumin, lysozyme, γ-globulin, myoglobin, β-lactoglobulin, trypsin, conalbumin, and α-chymotrypsin and interfacial tension. The more hydrophobic the protein, the greater the depression in the interfacial tension. Recently

Genest et al., 2013 found a correlation between the depression of the surface tension and the polymer hydrophobicity.

There are quite a number of methods for the determination of surface tensions such as the Capillary rise method, the Wilhelmy plate method, pendant and sessile drop methods, and the stalagmometric method. This method combines low sample consumption and compatibility to high throughput liquid-handling devices. Additionally, we are confident that this gravimetric approach is superior to imaging approaches in terms of precision and robustness.

In the present work we chose the stalagmometric method and developed a high resolution experimental setup which can be integrated into HTP work flow by a liquid handling station. This method was used as a non-invasive high throughput compatible approach to determine protein hydrophobicity on base of the proteins' surface tension increments. Lysozyme, human lysozyme, BSA, and α-lactalbumin were characterized regarding hydrophobicity dependent on pH value. This set of proteins covers a wide range of molecular weight, isoelectric points and includes two similar lysozyme species differing in amino acid composition. The hydrophobicity values for BSA derived from this approach were found to be in good agreement to values obtained by the widely used method of absorption difference spectroscopy of bromophenol blue sodium salt (BPB Na). Instead of this pH and protein species dependent absorption method the developed stalagmometric method was able to cover the full pH range in a completely automated way by considering the environmental protein complexity.

Materials and Methods

Stalagmometric method for determination of surface tension

The stalagmometric method was chosen for the determination of the surface tension due to its ability to be transformed into a fully automated procedure. In this method the specific fluid is purged very slowly through a needle in a vertical direction in order to form drops. The drop grows up to a specific maximum volume and falls onto a high precision mass balance. The Tate's law (Tate, 1864) expresses the correlation between the drop's weight W_{drop} and its surface tension γ at the moment the drop falls from the needle with an outer radius r:

$$W_{drop} = 2\pi r\gamma. \tag{3.5}$$

However, the instrumental setup has an influence on the drop size and the registered weight will be W'_{drop}. W_{drop} and W'_{drop} are correlated by an instrumental setup correction factor f_{inst}. Considering this correction factor the surface tension γ can be expressed as

$$\gamma = \frac{m_{drop}g}{2\pi r f_{inst}}, \tag{3.6}$$

where m_{drop} represents the mass of the drop, g the acceleration of gravity, r the radius of the needle, and f_{inst} the correction factor. By using a liquid with a known surface tension γ_{ref}, resulting in a specific drop mass $m_{drop,ref}$, the correction factor can be evaluated and the surface tension γ_{sample} of the liquid of interest can be determined by applying equation

3.7 to its specific drop mass $m_{drop,sample}$.

$$\frac{\gamma_{ref}}{m_{drop,ref}} = \frac{\gamma_{sample}}{m_{drop,sample}}. \tag{3.7}$$

Automation of stalagmometric method for the purpose of HTP

In the following the automation of this stalagmometric method, which principle can be found in subsection 3.4, is described. This method was optimized towards analysis speed, accuracy and precision. The validation was conducted using liquids with a wide range of surface tension values.

Automation using a liquid handling station This method was established on a fully automated robotic liquid handling station, namely *EVO 100 Freedom* purchased from Tecan (Crailsheim, Germany), equipped with stainless steel fixed tips and 1 mL dilutors. The liquid handling station was controlled using Evoware 2.4 SP3. The complete experimental setup, as is illustrated schematically by a partially section view in Figure 3.19, consisted of two major subunits, namely a *Tip2World* interface mounted on a docking station and the stalagmometric setup, interconnected via a capillary tubing (PEEK, ID: 0.25 mm). The *Tip2World* interface enables to supply liquid samples with a robotic liquid handling arm via connected standard capillary tubings and is described in detail elsewhere (Amrhein, Schwab, et al., 2014).
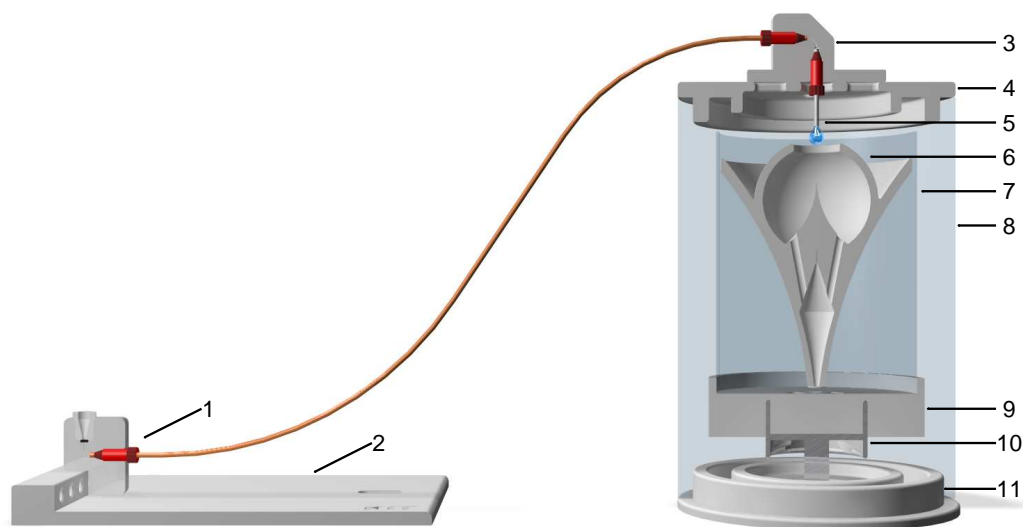
Figure 3.19: Illustration in partially section view of the setup of the stalagmometer, consisting of (1) *Tip2World* interface, (2) docking station, (3) the distribution block with a standard input 10-32 port, (4) a lid for fixation and centering of the distribution block, (5) a stainless steel needle in vertical orientation, (6) a drop trap, (7) a trough to collect and weight the drops, (8) a glass cylinder for evaporation protection, (9) a carrier, (10) balance unit, and (11) bottom part with water trough.

The stalagmometric system setup consisted of the distribution block, connecting the capillary tubing coming from the *Tip2World* interface with the drop generating needle, and a 250 mL container to collect the drops (Azlon® Specimen, SciLabware Limited, Stoke-on-Trent, United Kingdom). This container was placed on an Excellence WXTS205DU high performance balance unit (Mettler Toledo, Greifensee, Switzerland). The distribution block possesses a standard 10-32 coned input port and a vertically aligned standard 10-32 coned output port, where the drop generating stainless steel needle was fixed. This needle had an inner diameter of 0.5 mm and an outer diameter of 1.6 mm. Both ports were connected by an internal capillary (ID: 0.5 mm). The container held a drop trap to collect the falling drops in a gentle way. This was realized by a customized design shown in Figure 3.19 and enhanced the balance signal stability. To prevent the drop from evaporation a cylindrical evaporation trap was developed. This consisted of a cylinder, which was placed on a bottom ring with a water trough and a lid. All components were custom designed and 3D printed. Apart from bottom and lid (Sculpteo, Issy-les-Moulineaux, France) they were manufactured by a high resolution 3D printer (Stratasys, Minneapolis, USA). The construction work was carried out with the 2D/3D CAD software SolidEdge (Siemens PLM Software, Plano, USA). For the surface tension determination all samples were stored at room temperature in 1.3 mL 96-well Deep Well plates (Nalgene Nunc, Rochester, NY, USA) and sealed with a pre-slit well cap (Nalgene Nunc, Rochester, NY, USA), in order to minimize evaporation. The sample to be analyzed was pumped with a flow rate of 5 µL/s using the *Tip2World* interface to the stalagmometer through a PEEK capillary tubing with a diameter of 0.25 mm. The falling drop masses were recorded continuously via serial communication realized by automated routines written in Matlab® R2013b (The Mathworks, Natick, ME, USA). By evaluating the step profile of the balance signal, the distinguished masses of each drop were calculated. In order to increase the accuracy, instabilities of the weight signal were sorted out. Processing of the experimental results of the stalagmometric method was performed by means of fully automated routines written in Matlab® R2013b (The Mathworks, Natick, ME, USA).

Validation of surface tension determination The stalagmometric approach for surface tension determination was tested with respect to reproducibility by measuring 70 samples of ultrapure water with a volume of 800 µL each. For the validation of the procedure, surface tension measurements were performed with aqueous mixtures of sodium chloride (NaCl) and ethylene glycol solutions in order to cover a wide range of surface tensions. In particular, NaCl solutions were used with a molar fraction of 0 % to about 10 %. Ethylene glycol solutions were used within a molar fraction range of 0 % to 26 %. NaCl, analysis grade, was purchased from Merck KGaA (Darmstadt, Germany). Ethylene glycol, analysis grade, was purchased from VWR International (Radnor, PA, USA). Ethylene glycol and NaCl solutions were prepared by mixing the respective masses of ethylene glycol or NaCl with ultrapure water in order to reach the desired mass fractions. Ultrapure water was used as reference liquid. Cross contamination of samples was minimized by purging the tubing with air. All liquids were analyzed 8-fold with a volume of 800 µL each.

Correlation of surface tension and hydrophobicity

In order to test the applicability of using the surface tension increment of an analyte to deduce its hydrophobicity, polyethylene glycol (PEG) with varying molecular weights were used. PEG is known to expose increased hydrophobicity with increasing molecular weight (J. M. Harris, 1992). The polymer sample preparation is described in detail in 3.4. The method then was applied to protein solutions. These solutions varied in protein species, pH and buffer composition as explained in 3.4. The derived hydrophobicity measures were compared to hydrophobicity values derived from an orthogonal colorimetric method using BPB Na as described in section 3.4.

Stalagmometric determination of polymer hydrophobicity   The surface tension increments of PEG species with a molecular weight of 200, 300, 400, 600 and 1000 Da were determined by measuring aqueous PEG solutions with molar fractions varying from 0.02 to 0.11 %. These concentrations correlate to mass fractions from 0.2 to 1.2 % (w/w) for PEG 200, PEG 300 and PEG 400; from 0.4 to 2 % (w/w) for PEG 600 and from 0.8 to 4 % (w/w) for PEG 1000. Samples were prepared by mixing the respective masses of PEG with ultrapure water. 800 µL of each solution were measured 8-fold. All PEG species were of analysis grade and purchased from Merck KGaA (Darmstadt, Germany).

Determination of protein hydrophobicity

Sample Preparation   The used buffer substances were citric acid (Merck, Darmstadt, Germany) and sodium citrate (Sigma-Aldrich, St. Louis, MO, USA) for pH 3, sodium acetate (Sigma-Aldrich, St. Louis, MO, USA) and acetic acid (Merck, Darmstadt, Germany) for pH 5, MOPSO (AppliChem, Darmstadt, Germany) for pH 7 and Bis-Tris propane (Molekula, Dorset, UK) for pH 9. Buffer capacity was 100 mM for all buffers. Hydrochloric acid and sodium hydroxide for pH adjustment were obtained from Merck (Darmstadt, Germany). pH adjustment was performed using a five-point calibrated pH-meter (HI-3220, Hanna Instruments, Woonsocket, RI, USA) equipped with a SenTix® 62 pH electrode (Xylem Inc., White Plains, NY, USA). pH was adjusted with the appropriate titrant with an accuracy of $\pm$ 0.05 pH units. All buffers were filtered through 0.2 µm cellulose acetate filters (Sartorius, Göttingen, Germany). Buffers were used at the earliest one day after preparation and repeated pH verification. Lysozyme from chicken egg white was purchased from Hampton Research (Aliso Viejo, CA, USA), human lysozyme, bovine serum albumin (BSA), and calcium depleted α-lactalbumin were purchased from Sigma-Aldrich (St. Louis, MO, USA). To set up the protein stock solutions, protein was weighed in and dissolved in the appropriate buffer yielding the desired concentration. All protein solutions were filtered through 0.2 µm syringe filters with cellulose acetate membrane (VWR, Radnor, PA, USA) and further desalted via size exclusion chromatography using a HiTrap Desalting Column (GE Healthcare, Uppsala, Sweden) on an ÄKTAprime™ plus system (GE Healthcare, Uppsala, Sweden). The desired concentration was achieved by using Vivaspin centrifugal concentrators (Sartorius, Göttingen, Germany) with PES membranes. Protein concentration determination of the collected fractions was conducted using a NanoDrop2000c UV-Vis spectrophotometer (Thermo Fisher Scientific, Waltham, MA, USA). (Extinction

coefficients were $E^{1\%}(280 \text{ nm})_{\text{lysozyme}} = 22.00$, $E^{1\%}(280 \text{ nm})_{\text{human lysozyme}} = 16.00$, $E^{1\%}(280 \text{ nm})_{\text{BSA}} = 6.70$, $E^{1\%}(280 \text{ nm})_{\alpha\text{-lactalbumin}} = 16.81$).

Stalagmometric determination of protein hydrophobicity   Buffers and protein stock solutions of lysozyme, human lysozyme, BSA, and α-lactalbumin were prepared as described above. Protein solutions were prepared by dilution of the protein stock solutions with the respective buffer. The following solutions were laid eightfold in a 1.3 mL 96-well Deep Well plate: for reference ultrapure water and the respective buffer, protein solutions varying in protein molar fractions from $5.6{\cdot}10^{-6}$ to $1{\cdot}10^{-2}$ % for lysozyme and from $1.4{\cdot}10^{-6}$ to $3.9{\cdot}10^{-5}$ % for human lysozyme, BSA, and α-lactalbumin. 800 µL of each of the 96 samples were pumped to the stalagmometer with a flow rate of 5 µL/s. The surface tension of all samples was analyzed according to 3.4 in 8-fold replicates.

Spectrophotometric determination of protein hydrophobicity   The determination of protein hydrophobicity using bromophenol blue sodium salt (BPB Na) as a hydrophobicity sensitive dye was conducted for lysozyme, human lysozyme, BSA, and α-lactalbumin. Buffers and protein stock solutions were prepared as described earlier. BPB Na, purchased from Sigma-Aldrich (St. Louis, MO, USA), was dissolved in the respective buffer to reach a dye concentration of 0.02 mg/mL for the BPB Na stock solution. The spectrophotometric method was conducted according to Bertsch et al., 2003. No measurements were conducted at pH 3, because BPB Na is a well known pH indicator dye within the pH range of 3.0 to 4.6. Protein stock solutions were diluted using the respective buffers and mixed with a fixed volume of BPB Na stock solution, yielding protein solutions with a BPB Na concentration of 7.99 µM and protein molar fractions up to $3.3{\cdot}10^{-5}$ % for BSA and up to $4.9{\cdot}10^{-3}$ % for lysozyme, human lysozyme, and α-lactalbumin. The absorption spectra of a BPB Na solution without protein and of the BPB Na solutions with added protein were measured between 550 and 650 nm in 1 nm steps using an Infinite® M200 microplate reader (Tecan, Crailsheim, Germany). The measurements of each solution were conducted in triplicate. In contrast to Bertsch et al. we examined the shift of the absorption maximum $\Delta A_{\max}$ in dependency of the protein concentration instead of the absorption difference at 620 nm ΔA_{620}. The value of the absorption maximum shift was calculated as mean value from the triplicate spectrophotometric measurements. The shift of the absorption maximum $\Delta A_{\max}$ (in nm) was fitted using a Box Lucas model

$$\Delta A_{max} = a \cdot (1 - e^{-b\tilde{x}}), \tag{3.8}$$

where $\tilde{x}$ reflects the protein molar fraction, a and b are adjustable constants. Parameter a describes the limit of absorption maximum shift, $a \cdot b$ can be interpreted as relative surface hydrophobicity. It reflects the slope of the fitted curve for a protein molar fraction $\tilde{x}$ approaching zero. The higher $a \cdot b$ the higher the protein surface hydrophobicity.

Results

Development of HTP compatible stalagmometric method for surface tension determination

We were able to create HTP compatibility of the stalagmometric method by connecting the stalagmometer to the prior developed *Tip2World* interface (Amrhein, Schwab, et al., 2014). As mentioned in section 3.4 the HTP compatible stalagmometric method was tested for reproducibility using 70 samples of ultrapure water. These measurements showed a standard deviation of less than 0.1 ‰ which correlates to a 99.7 % confidence interval ($\pm 3\sigma$), which equals a deviation of less than $\pm$ 0.2 mN/m for water. The validation, described in section 3.4, was conducted by comparison of derived surface tensions with published data (Tsierkezos et al., 1998; Jańczuk et al., 1989; Melinder, 2007). The experimentally obtained surface tensions were in good agreement with reported data as illustrated in Figure 3.20. Ethylene glycol exposed a decreasing impact on the surface tension, NaCl increased the surface tension following a linear trend within the studied concentration interval. Thus the developed HTP compatible stalagmometric method showed high accuracy and covered a wide range of surface tensions from 57 to 82 mN/m. The developed method required about 3.5 minutes per sample resulting in less than 5.5 hours for analyzing a set of 96 samples without requiring sophisticated instrumentation and man power.

Stalagmometric determination of hydrophobicity

Hydrophobicity of polymers   The influence of polyethylene glycol (PEG) on the surface tension was studied to assess hydrophobicity. PEG species of different molecular weights starting from 200 to 1000 Da were studied. All surface tensions were normalized on ultrapure water. As illustrated in Figure 3.21 all surface tensions could be derived precisely with relative standard deviations less than 1.5 ‰ throughout all PEG samples. It is apparent from Figure 3.21 that all studied PEG species followed a decreasing trend with increasing concentration. The higher the PEG molecular weight, the higher the decrease in surface tension.

Hydrophobicity of proteins   Surface tensions of lysozyme, human lysozyme, BSA, and α-lactalbumin were analyzed in dependency of protein concentration and pH in order to characterize their hydrophobicity within the respective buffer system. Figure 3.22 illustrates the normalized profiles of the surface tensions of these proteins. The surface tensions were normalized on the respective pure buffer. Human lysozyme, BSA as well as α-lactalbumin decreased the surface tension even at very low molar fractions of less than $4 \cdot 10^{-5}$ %. It is apparent from Figure 3.22 that the decrease of surface tension is highly influenced by the pH value.

In particular, for BSA pH 3 had the highest influence on surface tension followed by pH 5, 7, and 9. The normalized surface tension profiles of pH 3 and 5 and the ones of pH 7 and 9 were close to each other. Regarding α-lactalbumin, the most distinctive decrease of the surface tension was observed at pH 3, followed by pH 5. The slopes of the normalized surface tensions at pH 7 and 9 were similar and slightly negative. In contrast to pH 3 and 5, the normalized surface tension of pH 7 and 9 followed a rather linear trend within the studied concentration range. In comparison to BSA and α-lactalbumin the influence of pH
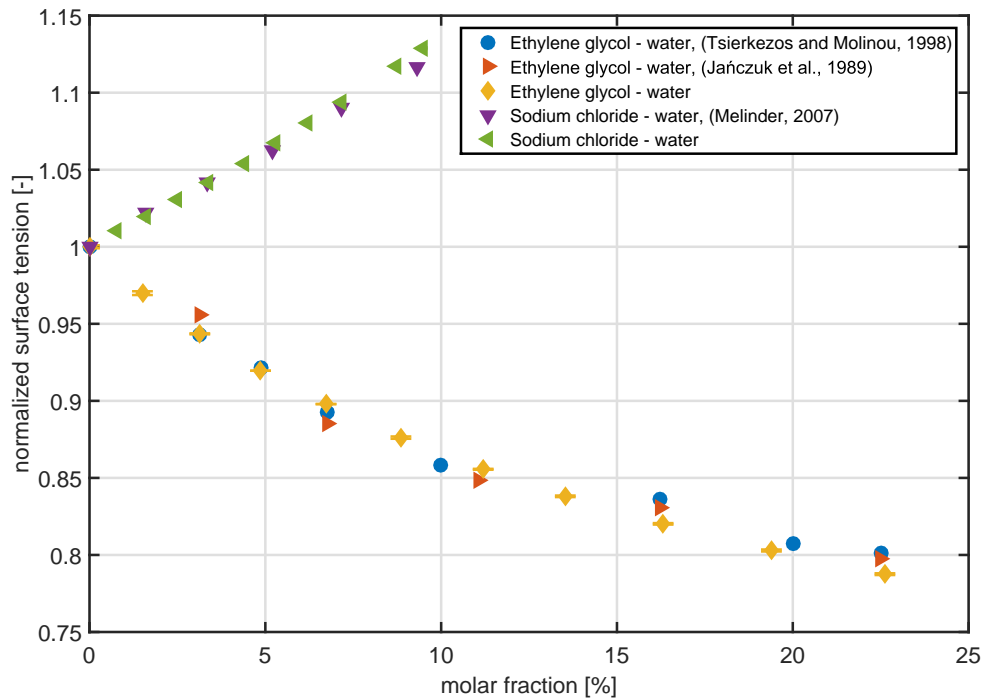
Figure 3.20: Comparison of experimentally determined surface tensions with literature values (Tsierkezos et al., 1998; Jańczuk et al., 1989; Melinder, 2007). The error bars refer to the 95 % confidence interval ($\pm 2\sigma$).

on the surface tension of human lysozyme was clearly lower, whereas the strongest decrease was observed at pH 3 again.

Lysozyme in contrast to BSA, α-lactalbumin, and human lysozyme showed less impact on the surface tension. For lysozyme a significant reduction in surface tension could only be observed at molar fractions 300 times higher. The profiles were similar for all pH values with the strongest reduction of surface tension to 0.92 at pH 3 for a molar fraction of 10^{-2} % within the studied concentration range.

In order to derive a hydrophobicity scale from the surface tension profiles they were fitted to equation 3.9

$$\gamma_{norm} = 1 - \frac{d \cdot e \cdot (\tilde{x} + c)}{1 + e \cdot (\tilde{x} + c)}, \tag{3.9}$$

where γ_{norm} stands for the normalized surface tension, $\tilde{x}$ represents the molar protein fraction. The fitting parameters d and e could be calculated for all profiles within this study with a coefficient of correlation larger than 0.98. Exclusively in case of α-lactalbumin the normalized surface tension of pure buffer and the lowest concentrated sample were excluded from the calculation, which was considered by setting the parameter c properly. For all other proteins, parameter c was set to zero. Equation 3.9 describes a saturation
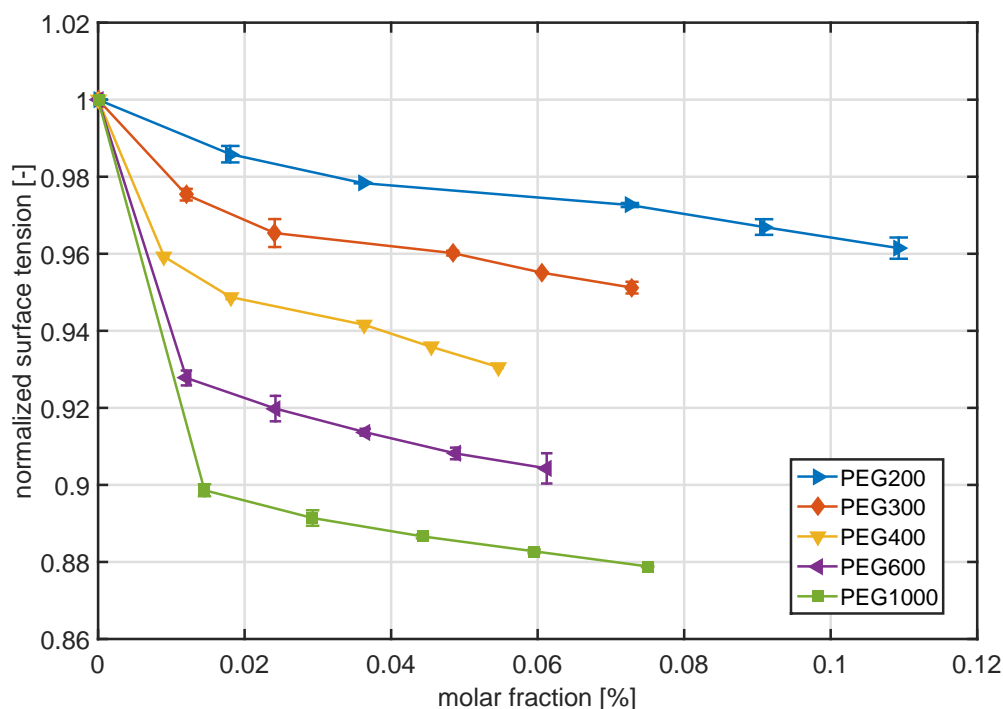
Figure 3.21: Normalized surface tension profiles of PEG varying in molecular weight. Surface tensions were normalized to ultrapure water. The error bars correlate to the 95 % confidence intervall ($\pm 2\sigma$).

function of the normalized surface tension regression, where $d \cdot e$ can be interpreted as the surface activity of the protein and e as the maximal regression of the normalized surface tension. By means of the surface activity, the studied proteins can be ranked according to their hydrophobic character as illustrated in Figure 3.23.

Spectrophotometric determination of hydrophobicity

The shift of the absorption maximum ΔA_{max} of BPB Na in presence of BSA was measured at pH 5, pH 7, and pH 9 and is illustrated in Figure 3.24. There is a clear pH dependency of ΔA_{max} as function of the BSA molar fraction. The change of ΔA_{max} in the range between 0 and $1 \cdot 10^{-5}$ % was strongest for pH 5, followed by pH 7 and 9. The same order applied for the upper limit of ΔA_{max}. The data points could be fitted using equation 3.8 with a coefficient of correlation better than 0.97. This dye method was also used to compare different proteins. In addition to BSA, human lysozyme, α-lactalbumin, and lysozyme were investigated at pH 5, 7, and 9. For these proteins the molar fractions had to be increased 150 fold compared to BSA in order to identify significant shifts of the absorption maximum. For all of the investigated proteins a pH dependency of the absorption maximum shift was detected. A comparison between the four proteins at pH 7 is exemplarily shown in Figure 3.25. BSA showed a significantly steeper slope and higher upper limit of the fitted
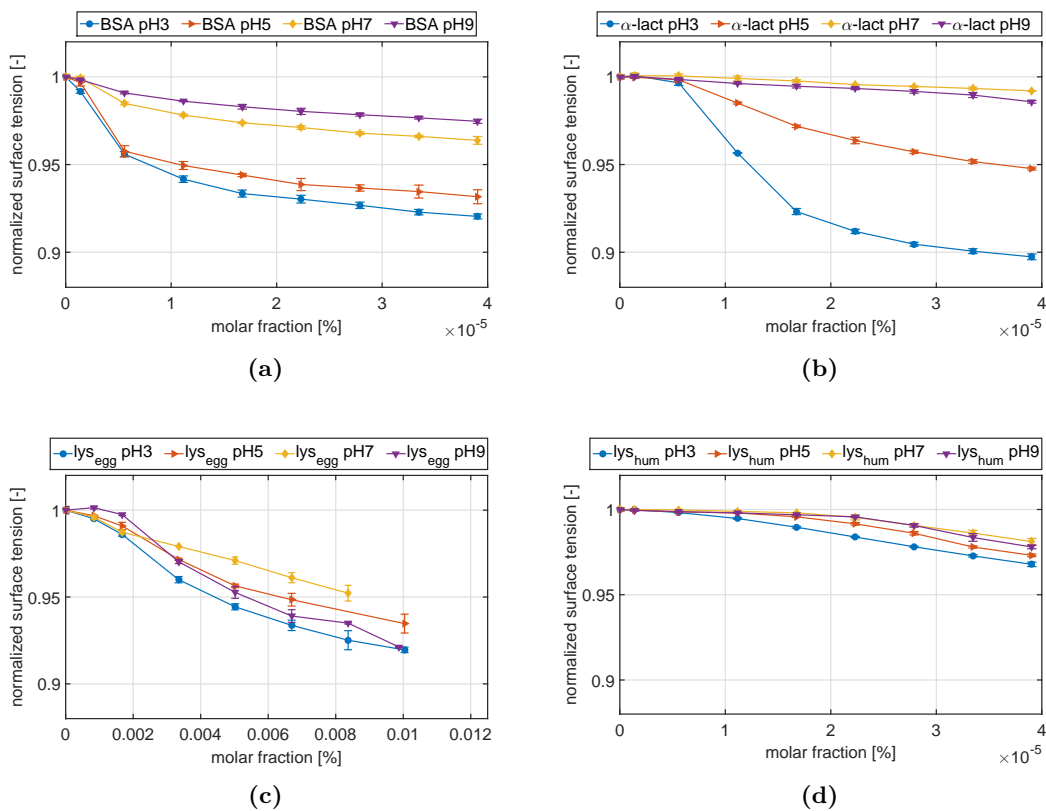
Figure 3.22: Surface tension profiles of (a) bovine serum albumin (BSA), (b) α-lactalbumin (α-lact), (c) lysozyme (lys$_{\text{egg}}$), and (d) human lysozyme (lys$_{\text{hum}}$). The error bars refer to the 95 % confidence interval ($\pm 2\sigma$)

curve compared to human lysozyme, α-lactalbumin, and lysozyme. Apart from BSA the highest values of ΔA_{max} were reached by human lysozyme and α-lactalbumin. However, the slope of the fitted curve of lysozyme was steepest.

Discussion

Development of HTP compatible stalagmometric method for surface tension determination

In the presented work a highly accurate, robust and HTP compatible stalagmometric method was established onto a liquid handling station using a high precision mass balance and two custom made subunits, the *Tip2World* interface and the stalagmometric setup in particular. Both subunits can be produced using 3D printing technology with a high precision and to a reasonable price. The method was validated with solutions containing NaCl or ethylene glycol. According to literature NaCl increases the surface tension of water (Pegram et al., 2007). Due to its lower polar character compared to water ethylene glycol exposes attractive interactions with the air-water interface and thus reduces its surface tension. With these two additives we were able to show the validity of the stalagmometric method for a wide range of surface tension values from 57 to 82 mN/m. The sample
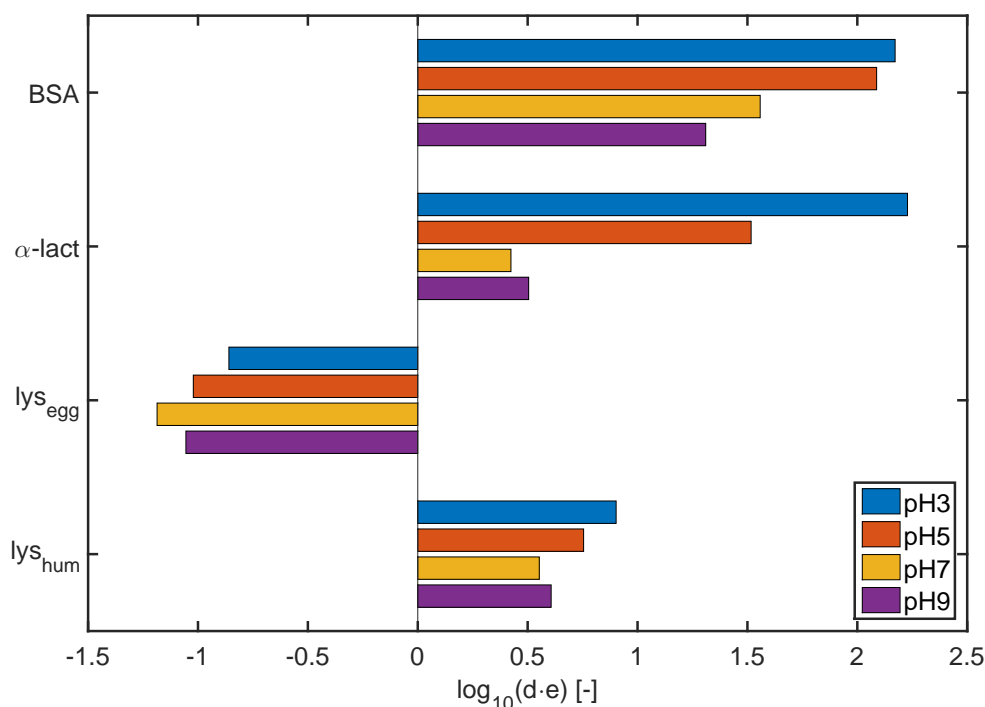
Figure 3.23: Hydrophobicity ranking of bovine serum albumin (BSA), α-lactalbumin (α-lact), lysozyme (lys$_{egg}$), and human lysozyme (lys$_{hum}$) by means of the surface activity

throughput of the used design was about 18 samples per hour. As mentioned before this results in an operation time of 5.5 hours for analyzing a set of 96 samples. It is important to note, that in this work we only used one tip of the liquid handling arm at a time and the setup allows the integration of multiple stalagmometric devices. Thus, using the full span of 8 tips of the liquid handling arm in combination with eight stalagmometric devices in parallel would speed up the measurement 8 fold resulting in a throughput of 144 samples per hour.

Stalagmometric Determination of Hydrophobicity

Polymers' hydrophobicity   To examine the correlation between surface tension and hydrophobicity PEG of different molecular weight was used. PEG species of higher molecular weight are known to be more hydrophobic (J. M. Harris, 1992). From our stalagmometric measurements we observed a stronger decrease of surface tension with increasing molecular weight and thus conclude that this is caused by the increase of hydrophobicity. This is in agreement with the findings of Genest et al., 2013 on hydrophobically modified polyelectrolytes that also exhibited lower surface tension values the more hydrophobic they were. Thus, the presented stalagmometric method is capable of deducing an analytes' hydrophobicity from its influence on the surface tension. Distinct differences in surface tensions and thus in hydrophobicity could even be identified for small changes in molecular
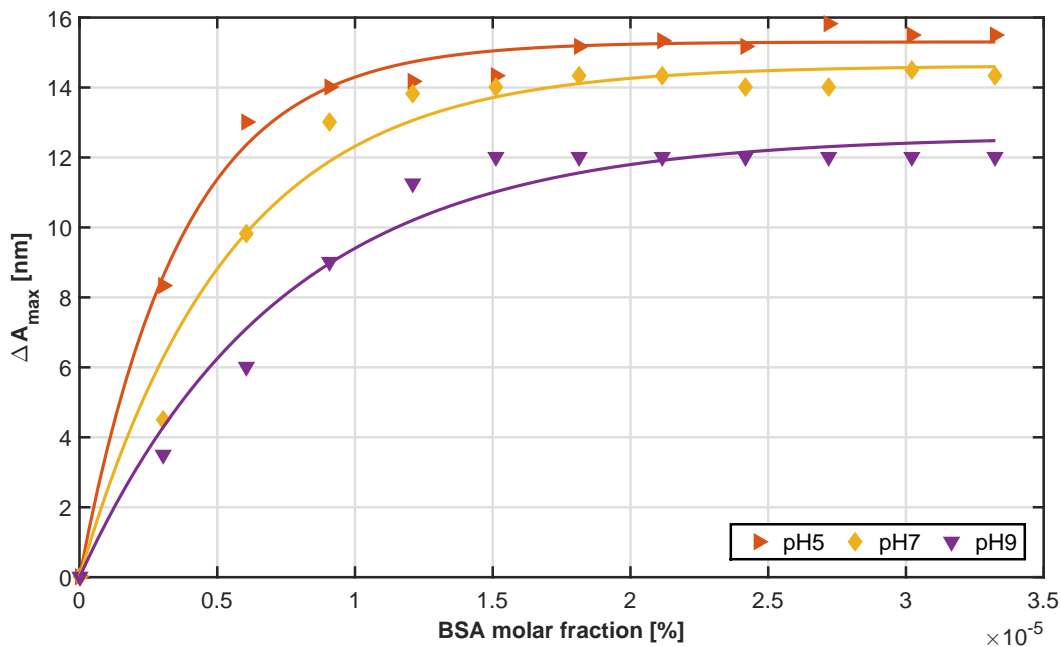
Figure 3.24: Comparison of absorption maximum shift (ΔA_{max}) of BPB Na in presence of bovine serum albumin (BSA) at pH 5, 7, and 9 and its corresponding fits

weight by 100 Da, as could be seen for PEG 200, PEG 300 and PEG 400 in Figure 3.21. This highlights the sensitivity of this stalagmometric approach. Moreover, the change of surface tension dependent on PEG molar fraction demonstrates the high resolution and precision of the developed HTP stalagmometric method. As it could be proved that the here designed HTP stalagmometric setup is able to capture polymer hydrophobicity with a high sensitivity, resolution and precision and was applied to protein solutions.

Proteins' Hydrophobicity In order to estimate the influence of protein species and pH we studied the surface tension increments of lysozyme, human lysozyme, BSA and α-lactalbumin at pH 3, 5, 7, and 9. For each protein we observed an influence of pH on the surface tension increment. This is reasonable as the pH influences the protonation of ionizable amino acids and thus the charge distribution on the protein surface what causes an impact on hydrophobic surface patches. Like for PEG an increase in hydrophobic surface character favors the interaction of the protein molecule with the less polar air-water interface. This results in a decrease of the surface tension. The derived ranking for the investigated proteins and pH values starts with α-lactalbumin at pH 3 as the sample with the most pronounced hydrophobic character. This pronounced hydrophobic character of α-lactalbumin at pH 3 can be explained by transformation of α-lactalbumin into a so called molten globule state where the protein is partially unfolded and inner hydrophobic patches
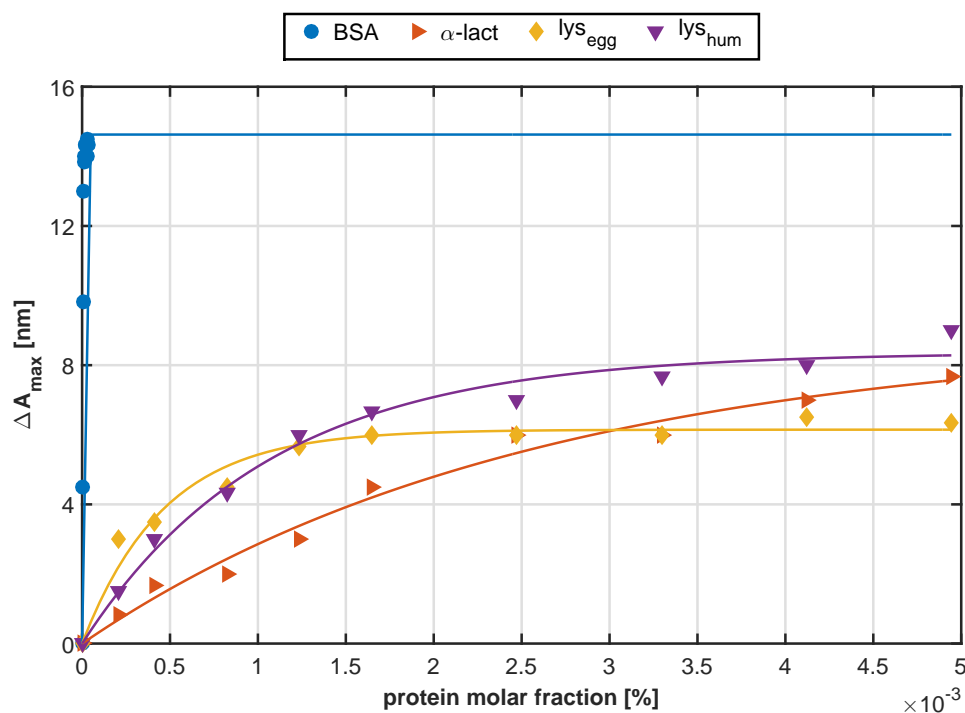
Figure 3.25: Comparison of absorption maximum shift (ΔA_{max}) of BPB Na in presence of bovine serum albumin (BSA), α-lactalbumin (α-lact), lysozyme (lys$_{egg}$) and human lysozyme (lys$_{hum}$) at pH 7 and its corresponding fits

are exposed on the protein surface (Permyakov et al., 2000). The ranking continues with decreasing hydrophobic character as can be seen in Figure 3.23. For each of the investigated proteins the hydrophobic character is highest at pH 3. This might be due to a modification of the charge distribution on the protein surface resulting from the protonation of amino acids. For example at pH 3 the amino acids Glu and Asp are protonated in contrast to pH 5. The protonation of the respective amino acids results in a loss of a negative charge and leads to a more pronounced hydrophobic character of the surface patches and a less favored hydration (D. Guo et al., 1986). In addition, the protonation of these amino acids influences the H-bond-network and thus could lead to minor effects on the formation of secondary structures such as α-helix and β-sheet. These minor structural changes might result in slightly different interactions with the solvent, which we were able to resolve with the presented approach. Major structural changes such as partial unfolding due to the acidic pH which would potentially result in a much stronger influence on hydrophobicity and thus surface tension could be excluded by FT-IR analysis (data not shown). Highest hydrophobic character was not always exhibited nearest to the isoelectric points of the investigated proteins as was shown for lysozyme and human lysozyme. Both exhibited the highest hydrophobic character far away from their isoelectric points. Thus, protein surface charge also influences surface tension but is not the critical factor.

It is important to point out that the differences between the surface tension profiles and thus the pH-dependent hydrophobic character of lysozyme were much smaller compared to BSA, α-lactalbumin and human lysozyme. Additionally, significant changes for the normalized surface tension could be found only at molar fractions 300 times higher than for the other proteins. Hence, lysozyme occurred to be much less hydrophobic compared to BSA, α-lactalbumin and human lysozyme. This significant different hydrophobic character of lysozyme is in agreement with Bigelow, 1967 who found BSA and α-lactalbumin to be very hydrophobic and lysozyme to be only weakly hydrophobic. The discrepancy between the structural similar lysozyme species (root means square deviation of backbone atoms less than 1 Å) underlines the strong impact of the amino acid composition on the protein surface (sequence identity less than 65 %).

In summary, the presented HTP stalagmometric setup emerged as promising approach for deducing the hydrophobic character of whole protein molecules in their three-dimensional conformation and in aqueous solution. Differences in the hydrophobic character depending on pH and protein species could be resolved.

Spectrophotometric determination of hydrophobicity

The dye measurements for BSA resulted in the highest hydrophobicity at pH 5, followed by pH 7 and 9. This hydrophobicity order is in agreement with our findings using the stalagmometric method. For lysozyme, human lysozyme and α-lactalbumin we had to increase the molar fraction 150 fold to see a distinct and reproducible shift of the absorption maximum. Despite the high molar fractions ΔA_{max} of BPB Na caused by lysozyme, human lysozyme and α-lactalbumin reached only half the value of ΔA_{max} for BSA. Additionally, the course of ΔA_{max} depending on lysozyme, human lysozyme and α-lactalbumin molar fraction were very similar.

Though BPB and BPB Na are well-known polarity sensitive dyes (Bertsch et al., 2003) they were so far mainly used for investigation of BSA and HSA (Bertsch et al., 2003; Cao et al., 2003; Wei et al., 1996; Tayyab et al., 1990; Murakami et al., 1981; Kragh-Hansen et al., 1974; Bjerrum, 1968; Waldmann-Meyer et al., 1956). It has been shown before, that the affinity for BPB and BPB Na is highly dependent on protein species (Cao et al., 2003; Flores, 1978; Waldmann-Meyer et al., 1956). Cao et al., 2003 observed a great difference between the magnitude of the redshift of the BPB absorption maximum by BSA and Chitosan, a biopolymer 6 times smaller than BSA. However, protein size is not the only factor influencing the BPB-protein interaction. Investigations of Flores, 1978 and Waldmann-Meyer et al., 1956 showed that even big proteins like ovalbumin and γ-globulin exhibited a significantly lower affinity for BPB and thus a significantly lower redshift in consequence. Likewise, small proteins like cytochrome c and myoglobin (Mayburd et al., 2000; Flores, 1978) were shown to cause pronounced redshifts. Consequently, the BPB Na method seems to be feasible for protein molecules with a high affinity to BPB Na like BSA. In this case a pH dependent hydrophobic character could be resolved. For lysozyme, human lysozyme and α-lactalbumin the dye method turned out to be inappropriate. For these proteins the dye method yielded in very similar results independent of the protein species and a low hydrophobic character compared to BSA, which is in disagreement with literature (Bigelow, 1967) and the results of our stalagmometric method. Thus, spectrophotometric

determination of protein hydrophobicity is highly dependent on protein-dye interactions and not an universally applicable method (Alizadeh-Pasdar et al., 2000). In contrast, the stalagmometric method is able to characterize small hydrophobic and hydrophilic proteins and no limitations regarding solution composition need to be considered.

Conclusions

In the present work we have developed a high throughput stalagmometric method which is able to measure surface tensions in a highly accurate way and can be operated by liquid handling stations and thus be integrated into high throughput work flow. This method was used to develop an innovative non-invasive approach for characterization of protein hydrophobicity on base of its impact on surface tension. The correlation between surface activity and hydrophobicity was validated using PEG of different molecular weights and applied to four different proteins, namely lysozyme, human lysozyme, BSA, and α-lactalbumin at four pH values. It was possible to rank protein hydrophobicity in dependency of the pH. Lysozyme was found to be hydrophilic, whereas α-lactalbumin turned out to be the most hydrophobic at pH 3. The derived ranking was in good agreement with literature and theoretical considerations regarding pH depending charge distributions.

The stalagmometric method was compared to an orthogonal and established spectrophotometric method for estimating protein hydrophobicity. Results of the spectrophotometric method regarding pH dependency of BSA were in agreement with the stalagmometric method. Spectrophotometric results for lysozyme, human lysozyme, and α-lactalbumin could not be used to derive protein hydrophobicity, as only BSA caused reasonable shifts of the absorption maximum of BPB Na. Dye based methods are often restricted by pH and protein size and are highly influenced by the aromatic and aliphatic nature of the dye molecule.

Contrary, the stalagmometric method is non-invasive and not restricted by pH and protein size. Differences in the hydrophobic character of proteins depending on protein species and pH could be resolved. Thus, we are convinced that the presented approach is an appropriate way to determine protein hydrophobicity in a non-invasive and highly accurate way.

Acknowledgment

References

Absolom, D. R., Zingg, W., and Neumann, A. W. (1987). 'Protein adsorption to polymer particles: role of surface properties.' *J. Biomed. Mater. Res.* Vol. 21(2), pp. 161–171 (cit. on p. 99).

Alizadeh-Pasdar, N. and Li-Chan, E. C. Y. (2000). 'Comparison of Protein Surface Hydrophobicity Measured at Various pH Values Using Three Different Fluorescent Probes'. *J. Agric. Food Chem.* Vol. 48(2), pp. 328–334 (cit. on p. 113).

Amrhein, S., Oelmeier, S. A., Dismer, F., and Hubbuch, J. (2014). 'Molecular dynamics simulations approach for the characterization of peptides with respect to hydrophobicity.' *J. Phys. Chem. B.* Vol. 118(7), pp. 1707–1714 (cit. on p. 99).

Amrhein, S, Schwab, M.-L., Hoffmann, M., and Hubbuch, J. (2014). 'Characterization of aqueous two phase systems by combining lab-on-a-chip technology with robotic liquid handling stations'. *J. Chromatogr. A.* Vol. 1367(0), pp. 68–77 (cit. on pp. 101, 105).

Andrews, B. A., Schmidt, A. S., and Asenjo, J. A. (2005). 'Correlation for the partition behavior of proteins in aqueous two-phase systems: Effect of surface hydrophobicity and charge'. *Biotechnol. Bioeng.* Vol. 90(3), pp. 380–390 (cit. on p. 98).

Asenjo, J. A. and Andrews, B. A. (2011). 'Aqueous two-phase systems for protein separation: A perspective'. *J. Chromatogr. A.* Vol. 1218(49), pp. 8826–8835 (cit. on p. 98).

Bertsch, M., Mayburd, A. L., and Kassner, R. J. (2003). 'The identification of hydrophobic sites on the surface of proteins using absorption difference spectroscopy of bromophenol blue.' *Anal. Biochem.* Vol. 313(2), pp. 187–195 (cit. on pp. 99, 104, 112).

Bigelow, C. C. (1967). 'On the average hydrophobicity of proteins and the relation between it and protein structure.' *J. Theor. Biol.* Vol. 16(2), pp. 187–211 (cit. on p. 112).

Biswas, K. M., DeVido, D. R., and Dorsey, J. G. (2003). 'Evaluation of methods for measuring amino acid hydrophobicities and interactions'. *J. Chromatogr. A.* Vol. 1000, pp. 637–655 (cit. on pp. 2, 99).

Bjerrum, O. J. (1968). 'Interaction of Bromphenol Blue and Bilirubin with Bovine and Human Serum Albumin Determined by Gel Filtration'. *Scand. J. Clin. Lab. Investig.* Vol. 22(1), pp. 41–48 (cit. on p. 112).

Black, S. D. and Mould, D. R. (1991). 'Development of hydrophobicity parameters to analyze proteins which bear post- or cotranslational modifications.' *Anal. Biochem.* Vol. 193(1), pp. 72–82 (cit. on p. 99).

Brems, D. N., Plaisted, S. M., Havel, H. A., and Tomich, C. S. (1988). 'Stabilization of an associated folding intermediate of bovine growth hormone by site-directed mutagenesis.' *Proc. Natl. Acad. Sci. U. S. A.* Vol. 85(10), pp. 3367–3371 (cit. on pp. 18, 98).

Bull, H. B. and Breese, K. (1974). 'Surface tension of amino acid solutions: A hydrophobicity scale of the amino acid residues'. *Arch. Biochem. Biophys.* Vol. 161(2), pp. 665–670 (cit. on pp. 3, 99).

Cao, W. G., Jiao, Q. C., Fu, Y., Chen, L., and Liu, Q. (2003). 'Mechanism of the Interaction Between Bromophenol Blue and Bovine Serum Albumin'. *Spectrosc. Lett.* Vol. 36(3), pp. 197–209 (cit. on p. 112).

Cardamone, M. and Puri, N. K. (1992). 'Spectrofluorimetric assessment of the surface hydrophobicity of proteins.' *Biochem. J.* Vol. 282, pp. 589–593 (cit. on p. 99).

Chen, J., Yang, T., Luo, Q., Breneman, C. M., and Cramer, S. M. (2007). 'Investigation of protein retention in hydrophobic interaction chromatographic (HIC) systems using the preferential interaction theory and quantitative structure property relationship models'. *React. Funct. Polym.* Vol. 67(12), pp. 1561–1569 (cit. on p. 99).

Chennamsetty, N., Helk, B., Voynov, V., Kayser, V., and Trout, B. L. (2009). 'Aggregation-prone motifs in human immunoglobulin G.' *J. Mol. Biol.* Vol. 391(2), pp. 404–413 (cit. on p. 99).

Diederich, P., Amrhein, S., Hämmerling, F., and Hubbuch, J. (2013). 'Evaluation of PEG/phosphate aqueous two-phase systems for the purification of the chicken egg white protein avidin by using high-throughput techniques'. *Chem. Eng. Sci.* Vol. 104(0), pp. 945–956 (cit. on p. 98).

Dill, K. A. (1990). 'Dominant forces in protein folding'. *Biochemistry.* Vol. 29(31), pp. 7133–7155 (cit. on p. 98).

Dooley, K. H. and Castellino, F. J. (1972). 'Solubility of amino acids in aqueous guanidinium thiocyanate solutions.' *Biochemistry.* Vol. 11(10), pp. 1870–1874 (cit. on p. 99).

Eisenberg, D. (1984). 'Three-dimensional structure of membrane and surface proteins'. *Annu. Rev. Biochem. Biochem.* Vol. 53, pp. 595–623 (cit. on p. 99).

Fendler, J. H., Nome, F., and Nagyvary, J. (1975). 'Compartmentalization of Amino Acids in Surfactant Aggregates'. *J. Mol. Evol.* Vol. 6, pp. 215–232 (cit. on p. 99).

Fink, A. L. (1998). 'Protein aggregation: folding aggregates, inclusion bodies and amyloid'. *Fold. Des.* Vol. 3(1), R9–R23 (cit. on p. 5).

Flores, R. (1978). 'A Rapid and Reproducible Assay for Quantitative Estimation of Proteins using Bromophenol Blue'. *Anal. Biochem.* Vol. 88, pp. 605–611 (cit. on p. 112).

Genest, S., Schwarz, S., Petzold-Welcke, K., Heinze, T., and Voit, B. (2013). 'Characterization of highly substituted, cationic amphiphilic starch derivatives: Dynamic surface tension and intrinsic viscosity'. *Starch/Stärke.* Vol. 65, pp. 999–1010 (cit. on pp. 100, 109).

Guo, D., Mant, C. T., Taneja, A. K., Parker, J., and Rodges, R. S. (1986). 'Prediction of peptide retention times in reversed-phase high-performance liquid chromatography I. Determination of retention coefficients of amino acid residues of model synthetic peptides'. *J. Chromatogr. A.* Vol. 359(8), pp. 499–518 (cit. on pp. 59, 86, 111).

Harris, J. M. (1992). *Poly(Ethylene Glycol) Chemistry: Biotechnical and Biomedical Applications.* Ethylene Glycol Chemistry: Biotechnical and Biomedical Applications. Springer (cit. on pp. 103, 109).

Hawe, A., Sutter, M., and Jiskoot, W. (2008). 'Extrinsic fluorescent dyes as tools for protein characterization.' *Pharm. Res.* Vol. 25(7), pp. 1487–1499 (cit. on p. 99).

Hendriks, J., Gensch, T., Hviid, L., Horst, M. A. van der, Hellingwerf, K. J., and Thor, J. J. van (2002). 'Transient exposure of hydrophobic surface in the photoactive yellow protein monitored with Nile Red.' *Biophys. J.* Vol. 82(3), pp. 1632–1643 (cit. on p. 99).

Jańczuk, B., Białopiotrowicz, T., and Wójcik, W. (1989). 'The components of surface tension of liquids and their usefulness in determinations of surface free energy of solids'. *J. Colloid Interface Sci.* Vol. 127(1), pp. 59–66 (cit. on pp. 105, 106).

Janin, J. (1979). 'Surface and inside volumes in globular proteins'. *Nature.* Vol. 277, pp. 491–492 (cit. on p. 99).

Janson, J.-C. (2012). *Protein purification: principles, high resolution methods, and applications.* Vol. 151. John Wiley & Sons (cit. on p. 98).

Kato, A. and Nakai, S. (1980). 'Hydrophobicity determined by a fluorescence probe method and its correlation with surface properties of proteins'. *Biochim. Biophys. Acta.* Vol. 624, pp. 13–20 (cit. on p. 99).

Keshavarz, E. and Nakai, S. (1979). 'The relationship between hydrophobicity and interfacial tension of proteins.' *Biochim. Biophys. Acta.* Vol. 576(2), pp. 269–279 (cit. on p. 99).

Kragh-Hansen, U., Møller, J. V., and Lind, K. E. (1974). 'Relation between binding of phenolsulfophtalein dyes and other ligands with a high affinity for human serum albumin'. *Biochim. Biophys. Acta.* Vol. 365, pp. 360–371 (cit. on p. 112).

Kyte, J. and Doolittle, R. F. (1982). 'A simple method for displaying the hydropathic character of a protein'. *J. Mol. Biol.* Vol. 157(1), pp. 105–132 (cit. on pp. 78, 99).

Lijnzaad, P., Berendsen, H. J. C., and Argos, P. (1996). 'A method for detecting hydrophobic patches on protein surfaces.' *Proteins.* Vol. 26(2), pp. 192–203 (cit. on p. 99).

Mahn, A., Lienqueo, M. E., and Asenjo, J. A. (2004). 'Effect of surface hydrophobicity distribution on retention of ribonucleases in hydrophobic interaction chromatography'. *J. Chromatogr. A.* Vol. 1043(1), pp. 47–55 (cit. on p. 99).

Mayburd, A. L., Tan, Y., and Kassner, R. J. (2000). 'Complex formation between Chromatium vinosum ferric cytochrome c' and bromophenol blue.' *Arch. Biochem. Biophys.* Vol. 378(1), pp. 40–44 (cit. on p. 112).

Melinder, Å. (2007). 'Thermophysical properties of aqueous solutions used as secondary working fluids'. PhD thesis. School of Industrial Engineering and Management, Royal Institute of Technology, KTH Stockholm (cit. on pp. 105, 106).

Miller, S., Janin, J., Lesk, A. M., and Chothia, C. (1987). 'Interior and surface of monomeric proteins.' *J. Mol. Biol.* Vol. 196, pp. 641–656 (cit. on p. 99).

Murakami, K., Sano, T., and Yasunaga, T. (1981). 'Kinetic Studies of the Interaction of Bromophenol Blue with Bovine Serum Albumin by Pressure-jump Method'. *Bull. Chem. Soc. Jpn.* Vol. 54(3), pp. 862–868 (cit. on p. 112).

Nieba, L., Honegger, A., Krebber, C., and Plückthun, A. (1997). 'Disrupting the hydrophobic patches at the antibody variable/constant domain interface: improved in vivo folding and physical characterization of an engineered scFv fragment.' *Protein Eng.* Vol. 10(4), pp. 435–444 (cit. on pp. 18, 98).

Nozaki, Y. and Tanford, C. (1971). 'The solubility of amino acids and two glycine peptides in aqueous ethanol and dioxane solutions'. *J. Biol. Chem.* Vol. 246(7), pp. 2211–2217 (cit. on p. 99).

Nozaki, Y. and Tanford, C. (1963). 'The Solubility of Amino Acids and Related Compounds in Aqueous Urea Solutions'. *J. Biol. Chem.* Vol. 238, pp. 4074–4081 (cit. on p. 99).

– (1965). 'The solubility of amino acids and related compounds in equeous ethylene glycol solutions'. *J. Biol. Chem.* Vol. 240, pp. 3568–3573 (cit. on p. 99).

– (1970). 'The solubility of amino acids, diglycine, and triglycine in aqueous guanidine hydrochloride solutions'. *J. Biol. Chem.* Vol. 245, pp. 1648–1652 (cit. on p. 99).

Pegram, L. M. and Record, M. T. (2007). 'Hofmeister Salt Effects on Surface Tension Arise from Partitioning of Anions and Cations between Bulk Water and the Air-Water Interface'. *J. Phys. Chem. B.* Vol. 111(19), pp. 5411–5417 (cit. on p. 108).

Permyakov, E. A. and Berliner, L. J. (2000). 'α-Lactalbumin: structure and function'. *FEBS Lett.* Vol. 473(3), pp. 269–274 (cit. on pp. 3, 7, 49, 59, 80, 111).

Radzicka, A. and Wolfenden, R. (1988). 'Comparing the polarities of the amino acids: side-chain distribution coefficients between the vapor phase, cyclohexane, 1-octanol, and neutral aqueous solution'. *Biochemistry.* Vol. 27(5), pp. 1664–1670 (cit. on p. 99).

Reißer, S., Strandberg, E., Steinbrecher, T., and Ulrich, A. S. (2014). '3D Hydrophobic Moment Vectors as a Tool to Characterize the Surface Polarity of Amphiphilic Peptides'. *Biophys. J.* Vol. 106(11), pp. 2385–2394 (cit. on p. 99).

Rose, G. D. and Wolfenden, R. (1993). 'Hydrogen bonding, hydrophobicity, packing, and protein folding'. *Annu. Rev. Biophys. Biomol. Struct.* Vol. 22, pp. 381–415 (cit. on p. 99).

Salgado, J. C., Rapaport, I., and Asenjo, J. A. (2005). 'Is it possible to predict the average surface hydrophobicity of a protein using only its amino acid composition?' *J. Chromatogr. A.* Vol. 1075(1), pp. 133–143 (cit. on p. 99).

– (2006a). 'Predicting the behaviour of proteins in hydrophobic interaction chromatography: 1: Using the hydrophobic imbalance (HI) to describe their surface amino acid distribution'. *J. Chromatogr. A.* Vol. 1107(1), pp. 110–119 (cit. on p. 99).

– (2006b). 'Predicting the behaviour of proteins in hydrophobic interaction chromatography 2. Using a statistical description of their surface amino acid distribution'. *J. Chromatogr. A.* Vol. 1107(1), pp. 120–129 (cit. on p. 99).

Shanbhag, V. P. and Axelsson, C.-G. (1975). 'Hydrophobic interaction determined by partition in aqueous two-phase systems'. *Eur. J. Biochem.* Vol. 60, pp. 17–22 (cit. on p. 99).

Tanford, C. (1962). 'Contribution of hydrophobic interactions to the stability of the globular conformation of proteins'. *J. Am. Chem. Soc.* Vol. 84(22), pp. 4240–4247 (cit. on p. 98).

Tate, T. (1864). 'On the magnitude of a drop of liquid formed under different circumstances'. *London, Edinburgh, Dublin Philos. Mag. J. Sci.* Vol. 27(181), pp. 176–180 (cit. on p. 100).

Tayyab, S. and Qasim, M. (1990). 'Binding of bromophenol blue to bovine serum albumin and its succinylated forms'. *Int. J. Biol. Macromol.* Vol. 12(1), pp. 55–58 (cit. on p. 112).

Trinquier, G. and Sanejouand, Y.-H. (1998). 'Which effective property of amino acids is best preserved by the genetic code?' *Protein Eng.* Vol. 11(3), pp. 153–169 (cit. on p. 99).

Tsierkezos, N. G. and Molinou, I. E. (1998). 'Thermodynamic Properties of Water + Ethylene Glycol at 283.15, 293.15, 303.15, and 313.15 K'. *J. Chem. Eng. Data.* Vol. 43(6), pp. 989–993 (cit. on pp. 105, 106).

Vagenende, V., Yap, M. G. S., and Trout, B. L. (2009). 'Mechanisms of protein stabilization and prevention of protein aggregation by glycerol'. *Biochemistry.* Vol. 48(46), pp. 11084–11096 (cit. on p. 121).

Waldmann-Meyer, H. and Schilling, K. (1956). 'The Interaction of Bromophenol Blue with Serum Albumin and γ-Globulin in Acid Medium'. *Arch. Biochem. Biophys.* Vol. 64, pp. 291–301 (cit. on p. 112).

Wei, Y.-J., Li, K.-A., and Tong, S.-Y. (1996). 'The interaction of Bromophenol Blue with proteins in acidic solution'. *Talanta.* Vol. 43(1), pp. 1–10 (cit. on p. 112).

Whitney, P. L., Tanford, C., W, P. L., and Tanford, C. (1962). 'Solubility of amino acids in aqueous urea solutions and its implications for the denaturation of proteins by urea'. *J. Biol. Chem.* Vol. 237, pp. 1735–1737 (cit. on p. 99).

3.5 Impact of additives on the formation of protein aggregates and viscosity in concentrated protein solutions

Katharina Christin Bauer, Susanna Suhm, Anna Katharina Wöll, Jürgen Hubbuch

Institute of Engineering in Life Sciences, Section IV: Biomolecular Separation Science, Karlsruhe Institute of Technology (KIT), 76131 Karlsruhe, Germany;
* Corresponding author: telephone: +49-721-608-42557, e-mail: juergen.hubbuch@kit.edu
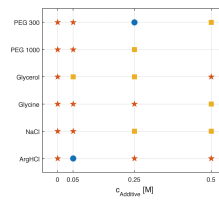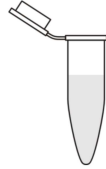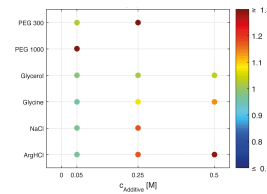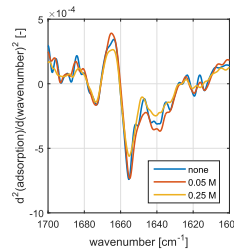
Abstract

In concentrated protein solutions attractive protein interactions may not only cause the formation of undesired aggregates but also of gel-like networks with elevated viscosity. To guarantee stable biopharmaceutical processes and safe formulations, both phenomenons have to be avoided as these may hinder regular processing steps. This work screens the impact of additives on both phase behavior and viscosity of concentrated protein solutions. For this purpose, additives known for stabilizing proteins in solution or modulating the dynamic viscosity were selected. These additives were PEG 300, PEG 1000, glycerol, glycine, NaCl and ArgHCl. Concentrated lysozyme and glucose oxidase solutions at pH 3 and 9 served as model systems. Fourier-transformed-infrared spectroscopy was chosen to determine the conformational stability of selected protein samples. Influencing protein interactions, the impact of additives was strongly dependent on pH. Of all additives investigated, glycine was the only one that maintained protein conformational and colloidal stability while decreasing the dynamic viscosity. Low concentrations of NaCl showed the same effect, but increasing concentrations resulted in visible protein aggregates.

Introduction

Increasing titers in fermentation (Chon et al., 2011) and the trend towards highly concentrated formulations (Shire et al., 2004) require biopharmaceutical downstream processing to cope with concentrated protein solutions. Their tendency to form protein aggregates and high viscosity impacts judgment on developability and manufacturability - pumping, filtration or chromatography - of the target molecule as well as its syringeability (Shire et al., 2004; Jezek et al., 2011; Z. Guo et al., 2012). From a molecular point of view, the aggregation tendency and viscosity of a protein solution are governed by attractive protein interactions. Depending on the physicochemical nature of the protein surface, the complexity of attractive protein interactions may lead to various aggregation mechanisms and result in differing aggregate morphology. The multimers formed through assembly of native or non-native protein monomers can be reversible or irreversible, visible or invisible as well as soluble or insoluble (Mahler et al., 2009). At high concentrations, not only electrostatic interactions but also short-range van der Waals, hydration, hydrophobic and steric interactions influence protein aggregation which may either result in the formation of dense aggregates or spacious networks with elevated viscosity (W. Wang, 1999; J. Liu et al., 2005; Chari et al., 2009). Thus, in order to preserve the colloidal stability of concentrated protein solutions and guarantee reliable processing and safe formulations, attractive protein interactions resulting in aggregate formation as well as high viscosity need to be prevented

(Shire, 2009; Patro et al., 1996). This can be achieved by manipulating protein interactions through the addition of additives which either induce changes in proteins' conformational or colloidal stability in solution (Shire et al., 2004). The specific impact of additives on protein interactions can strongly vary and is usually dependent on additive type, additive concentration, protein type, protein concentration and pH.

Their impact on the formation of protein aggregates was already extensively investigated for solutions with low protein concentration. PEGs (Kozer et al., 2007), sugars (Arakawa and Timasheff, 1982), polyols (Vagenende et al., 2009) and amino acids (Arakawa, Ejima, et al., 2007) were found to have a stabilizing impact due to preferential interactions (Arakawa and Timasheff, 1985). The effect of salts on protein aggregation is more complex. Their impact depends on complex ionic interactions with the protein surface. Salts can either stabilize, destabilize or have no effect on protein aggregation depending on the type and concentration of salt. At low concentrations, salts were shown to stabilize due to electrostatic shielding of attractive forces (Hamada et al., 2009).

The impact of additives on concentrated protein solutions was considered by investigating their dynamic viscosity. Salts and amino acids were published to have a lowering effect on this parameter. Du et al., 2011 found so-called hydrophobic salts to have a strong decreasing impact on concentrated bovine serum albumin and γ-globulin solutions. N. Inoue et al., 2014a showed amino acids, such as glycine and argine, to decrease the dynamic viscosity of concentrated bovine and human serum albumin solutions.

Influencing protein interactions due to changes in the physicochemical nature of the protein surface, pH has been shown to additionally influence the impact of additives (Kohn et al., 1997). Galm et al., 2015 published PEG 1000, glycerol, and glycine to either have an impact on changes in protein conformation or in protein solubility. A pH-dependent impact of additives on dynamic viscosity was published investigating the gelation of soy proteins with sugar and $CaCl_2$ (Alvarez et al., 2008).

Hence, until now, either the impact of additives on the formation of protein aggregates at low protein concentrations or the dynamic viscosity of concentrated protein solutions was examined. However, for concentrated protein solutions different aggregation mechanisms can either lead to the formation of dense protein aggregates or spacious networks with high viscosity (J. Liu et al., 2005; W. Wang et al., 2010).

As a consequence, this work aims to provide a picture of the impact of additives on attractive protein interactions in concentrated protein solutions by investigating the impact on the formation of aggregates as well as viscosity. For this purpose, additives known to stabilize protein aggregation as well as additives known to modulate the viscosity of concentrated protein solutions were selected. These additives, namely PEG 300, PEG 1000, glycerol, glycine, sodium chloride (NaCl), and arginine hydrochloride (ArgHCl) were examined at different pH values. Changes in protein interactions depending on pH and the impact of selected additives on the protein conformation were evaluated by Fourier-transformed-infrared (FT-IR) spectroscopy. The formation of visible aggregates and changes in dynamic viscosity of each sample were determined by phase behavior experiments and microrheological measurements.

Materials and Methods

To investigate the impact of additives on attractive protein interactions in concentrated protein solutions, the phase behavior and the dynamic viscosity were determined. The additives selected were PEG 300, PEG 1000, glycerol, glycine, NaCl, and ArgHCl. Concentrated lysozyme and glucose oxidase solutions at pH 3 and 9 served as model system. Changes in secondary structure of these proteins were investigated for selected additives. This section presents the preparation of the buffers as well as the additive and protein solutions applied in this study. It also contains information about the methods, such as the examination of structural changes by FT-IR spectroscopy, the phase behavior experiments, and the microrheological measurements.

Buffers and protein solutions

All buffers had an ionic strength of 100 mM. The respective components for pH 3 were citric acid (Merck KGaA, Darmstadt, Germany) and sodium citrate (Sigma-Aldrich, St. Louis, MO, USA). For pH 9, BisTris propane (Molekula Limited, Newcastle upon Tyne, UK) was used. The additives investigated were PEG 300, PEG 1000, glycine (Sigma-Aldrich), glycerol (Alfa Aesar®, Ward Hill, MA, USA), NaCl, and ArgHCl (Merck KGaA). For each additive, a stock solution was prepared. These additive solution contained the buffer components at the respective pH and an additive concentration of 0.6 M for PEG 300, PEG 1000, glycerol, or 1 M for glycine, NaCl and ArgHCl. The pH of the buffers and additive solutions was determined with a five-point calibrated pH meter (HI-3220, Hanna® Instruments, Woonsocket, RI, USA) equipped with a SenTix® 62 pH electrode (Xylem Inc., White Plains, NY, USA) and corrected by titration of NaOH or HCl (Merck KGaA) with an accuracy of +/- 0.5 pH units. After titration, the buffers were filtered with 0.2 μm membranes consisting of cellulose acetate (Sartorius AG, Göttingen, Germany) for pH 3 and Supor® Polyethersulfone (PES) (Pall Corporation, Port Washington, NY, USA) for pH 9. Each solution was first used 24 hours after preparation. They were stored at room temperature and regularly checked for constant pH. Lyophilized lysozyme (Hampton Research, Aliso Viejo, CA, USA) and glucose oxidase (Sigma-Aldrich) were weight in and dissolved in the respective buffer without additive. The protein solutions were filtered with 0.2 μm syringe filters (cellulose acetate for pH 3, PES for pH 9 (VWR, Radnor, PA, USA)). Production related salts were removed by size exclusion chromatography with a HiTrap Desalting column (GE Healthcare, Uppsala, Sweden) on an ÄKTAprime™ plus chromatography system (GE Healthcare). Afterwards, the solutions were concentrated with Vivaspin® centrifugal concentrators (Sartorius AG). For lysozyme at pH 3 and 9, the protein stock solution had a concentration of 360 mg/mL. For glucose oxidase at pH 3, a concentration of 100 mg/mL, and at pH 9, a concentration of 260 mg/mL was reached. These protein concentrations were determined by a NanoDrop™ 2000c UV-Vis spectrophotometer (Thermo Fisher Scientific, Waltham, MA, USA). The respective extinction coefficients were $E^{1\%}$(280 nm) = 22.00 $L\,g^{-1}\,cm^{-1}$ for lysozyme and $E^{1\%}$(280 nm) = 12.00 $L\,g^{-1}\,cm^{-1}$ for glucose oxidase. The samples with constant protein concentrations of 180 mg/mL for lysozyme, 50 mg/mL for glucose oxidase at pH 3 and 130 mg/mL at pH 9 were prepared by mixing the correct volume of buffer, protein stock solution and additive solution.

FT-IR spectroscopy

Changes in the conformational stability of selected protein samples were determined by FT-IR spectroscopy. This measurement was performed with a Nicolet™ iS5 and an iD7 ATR detector (Thermo Fisher Scientific). The absorbance of each sample was scanned 150 times with a spectral resolution of 2 cm^{-1} from 3500 to 1000 cm^{-1}. Background spectra at the respective additive concentration and pH were recorded with 256 scans. All measurements were conducted in duplicate with a sample volume of 5 μL. The OMNIC software (Thermo Fisher Scientific) was used for recording and processing of the FT-IR spectra. Processing steps were atmospheric suppression to delete the impact of water vapor bands and the calculation of the second derivative to investigate the protein conformation. For the formation of the second derivative Savitzky-Golay with 25 points and third polynomial order was applied. The wavenumber bands relevant for the conformational stability of a protein lie within a range of 1700 - 1600 cm^{-1} and can be assigned to α-helix (1658 - 1650 cm^{-1}), β-sheet (1695 - 1670 cm^{-1} and 1640 - 1620 cm^{-1}) and random coil (1650 - 1640 cm^{-1}) (Byler et al., 1986; Dong et al., 1997).

Phase behavior experiments

The formation of visible protein aggregates for the samples investigated in this study was determined by phase behavior experiments. Therefor, 30 μL of each sample were pipetted on MRC Under Oil 96 Well Crystallization Plates (SWISSCI AG, Neuheim, Switzerland) and sealed with Duck® Brand HD Clear sealing tape (ShurTech® brands, Avon, OH, USA) to avoid evaporation. The plates were incubated in the automated chrystallographer RockImager 54 (Formulatrix, Bedford, MA, USA) for 40 days at 20 °C. After this time, a photograph of each sample was taken to evaluate optical phase transitions. These transitions were classified visually into clear solution, crystals and precipitate.

Microrheological measurements

The dynamic viscosity of the protein samples was determined by microrheological measurements using dynamic light scattering with a ZetaSizer Nano ZSP (Malvern Instruments, Worcestershire, UK). Following previous investigations (Bauer, Schermeyer, et al., 2016), PEGylated particles (5 wt%) were added to the prepared samples. The particles were synthesized in house with Pluronic F-127 (Sigma-Aldrich) and polystyrene latex particles (0.2 micron (Alfa Aesar®), 1.0 micron (Polysciences Inc., Warrington, PA, USA)) described in the publication of A. J. Kim et al., 2005. To ensure that the particles were the only scatterers detected, particles of a diameter of 0.22 and 1.15 micron, were used for samples containing lysozyme and glucose oxidase respectively. These particles were added to the samples with a ratio of 1:200 (V$_{particle\ solution}$:V$_{sample}$). The samples were prepared right before the measurement. The size measurement required a sample volume of 45 μL and consisted of three measurements with automated duration at 25 °C. The diffusion coefficients determined by the distribution result were used for the calculation of the dynamic viscosity of each sample based on the Stokes-Einstein equation.

Results

In this study, the impact of additives on different protein aggregation pathways of concentrated protein solutions was investigated. The chosen additives were PEG 300, PEG 1000, glycerol, glycine, NaCl, and ArgHCl. Changes in protein interactions depending on pH and the impact of selected additives on the protein conformation were investigated by FT-IR spectroscopy. To carve out the effect of the additives on the formation of aggregates and high viscosity, both the phase behavior and the dynamic viscosity of concentrated lysozyme and glucose oxidase solutions were determined. Throughout the study, the protein concentration for each protein at the respective pH was held constant. These protein concentrations were chosen according to experiments conducted prior to our studies, which reflect the concentration achievable after a centrifugation time of 3 hours using the method set forth in Section 3.5. The lysozyme solutions had a protein concentration of 180 mg/mL at pH 3 and 9, for the glucose oxidase solutions a protein concentration of 50 mg/mL at pH 3 and of 130 mg/mL at pH 9 could be reached. The additive concentrations were chosen analogous to previous publications (Du et al., 2011; Z. Guo et al., 2012; Galm et al., 2015) and adapted to the same concentration range for easier comparability. The results determined for varying pH values and additive concentrations are presented in the following section.

Additive induced changes in conformational stability

Changes in the conformational stability of a protein alter protein interactions and, thus, the aggregation tendency of a protein solution. The following results of the FT-IR spectra present differences in the secondary structure of lysozyme and glucose oxidase at pH 3 and 9 and the impact of the selected additives glycine, NaCl and ArgHCl. Whereas Figure 3.26 depicts the second derivative of the FT-IR spectra determined for lysozyme at pH 3 and 9, the second derivative spectra for glucose oxidase at these pH values is displayed in Figure 3.27. Both proteins resulted in varying FT-IR spectra depending on pH, additive type and concentration.

Lysozyme as well as glucose oxidase had different native spectra as a function of pH. For both protein, a decrease of peak depth and, thus, a reduction of ordered structures at pH 3 in comparison to pH 9 could be determined. With addition of additives, all spectra showed slight deviations from the spectra without additive. At pH 9, stronger deviations from the spectra without additive were determined with increasing concentration of NaCl and ArgHCl. Contrarily, the spectra determined with addition of glycine showed high accordance to the spectra without additive. Only 0.25 M glycine caused slight changes in the α-helice region of glucose oxidase.

In summary, the conformational stability of lysozyme and glucose oxidase changed with pH, additive type and concentration. For both proteins, a decrease in ordered structures could be determined at pH 3. Whereas for pH 3 all additives caused slight deviations in the second derivative of the FT-IR spectra, the addition of glycine at pH 9 maintained the native spectra of the proteins. The spectra determined with addition of NaCl and ArgHCl at pH 9 deviated.
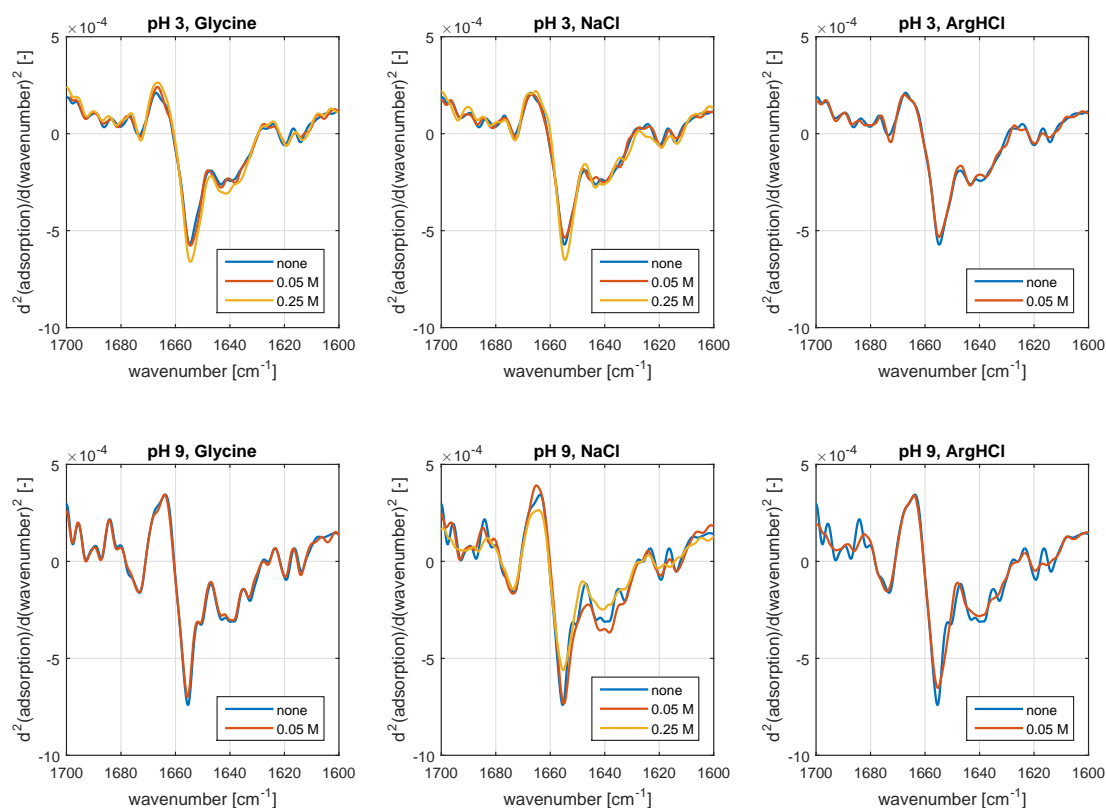
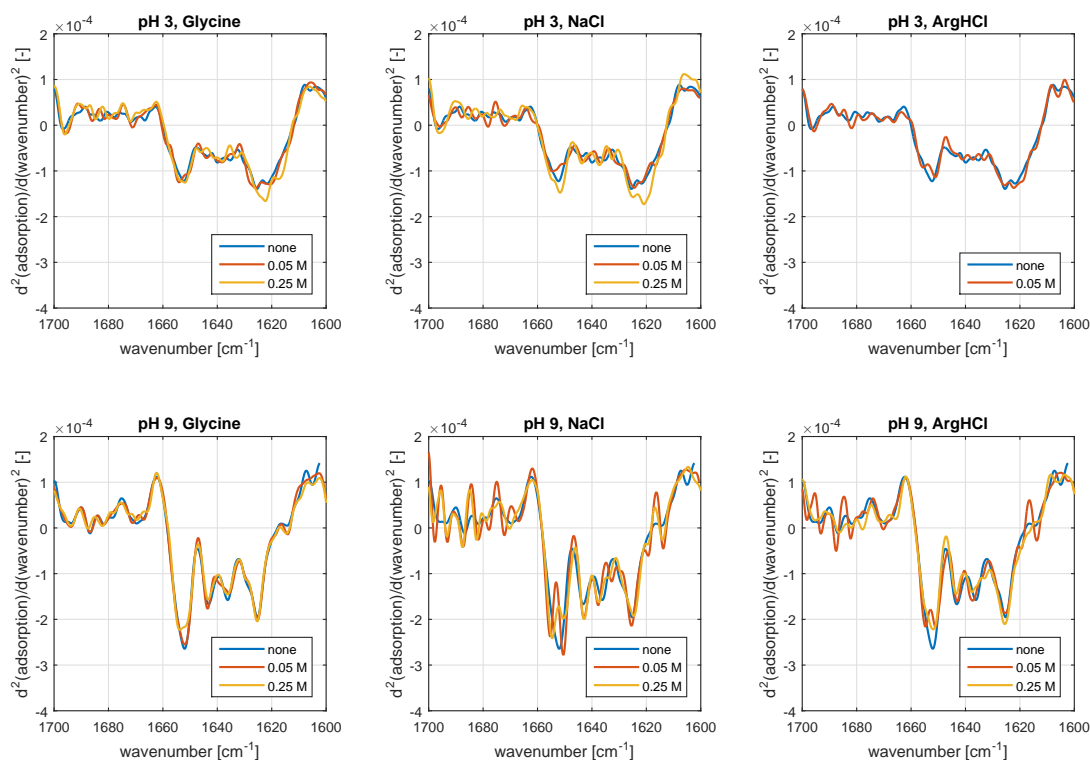**Figure 3.26:** Second derivative FT-IR spectra of 180 mg/mL lysozyme at pH 3 and 9 without additive and with addition of glycine, NaCl, and ArgHCl.

Additive induced changes in phase behavior

The impact of the additives PEG 300, PEG 1000, glycerol, glycine, NaCl, and ArgHCl on the phase behavior of concentrated protein solutions was investigated by determining the evolution of or changes in visible aggregates, such as crystals or precipitate. Figure 3.28(a) and 3.29(a) display the phase transitions of the lysozyme and glucose oxidase solutions at pH 3 and 9 depending on additive type and concentration. The phase transitions investigated in this study varied with protein type and solution composition. Whereas samples of lysozyme resulted in the formation of crystals or precipitate, glucose oxidase solely precipitated. Lysozyme already showed different phase behavior with varying pH. At pH 3, 180 mg/mL lysozyme formed crystals, at pH 9 the solution stayed clear. The glucose oxidase solutions at pH 3 and 9 were clear.

Further changes were detected with addition of additives for both protein solutions. The specific outcome of each sample was dependent on the protein type, the respective pH, the additive type and its concentration. For lysozyme at pH 3, 0.25 M PEG 300 and 0.05 M ArgHCl generated clear solutions. For lysozyme at pH 9 and glucose oxidase at pH 3 and 9, PEG 300 and glycine maintained clear solutions for the whole investigated range

Figure 3.27: Second derivative FT-IR spectra of 50 mg/mL glucose oxidase at pH 3 and 130 mg/mL at pH 9 without additive and with addition of glycine, NaCl, and ArgHCl.

of additive concentrations. Glycerol also met this condition for glucose oxidase at pH 3. Visible aggregates with increasing additive concentrations were determined for PEG 1000, glycerol, NaCl and ArgHCl. Due to strong precipitation no homogeneous samples could be prepared at high PEG 1000 concentrations. For these samples no result was displayed.

In summary, the impact of additives clearly changed the phase behavior of the protein solutions investigated in this study. The specific outcome of each sample, was influenced by the protein type, pH, the additive type, and the additive concentration. Only 0.25 M PEG 300 and 0.05 M ArgHCl were able to stabilize an aggregating protein sample. Clear protein solutions were maintained by PEG 300 and glycine. The additives PEG 1000, glycerol, NaCl, and ArgHCl promoted the formation of visible aggregates for the investigated protein solutions with increasing additive concentration.

Additive induced changes in dynamic viscosity

Figure 3.28(b) and 3.29(b) display the impact of the additives studied on the dynamic viscosity η of concentrated lysozyme and glucose oxidase solutions at pH 3 and 9. To assess the effect of the additives investigated in this study on modulating solution viscosity, the term $\delta\eta$ is shown. This term captures the ratio between the dynamic viscosity of the protein solution with additive $\eta_{with\,additive}$ and the one without additive $\eta_{without\,additive}$.
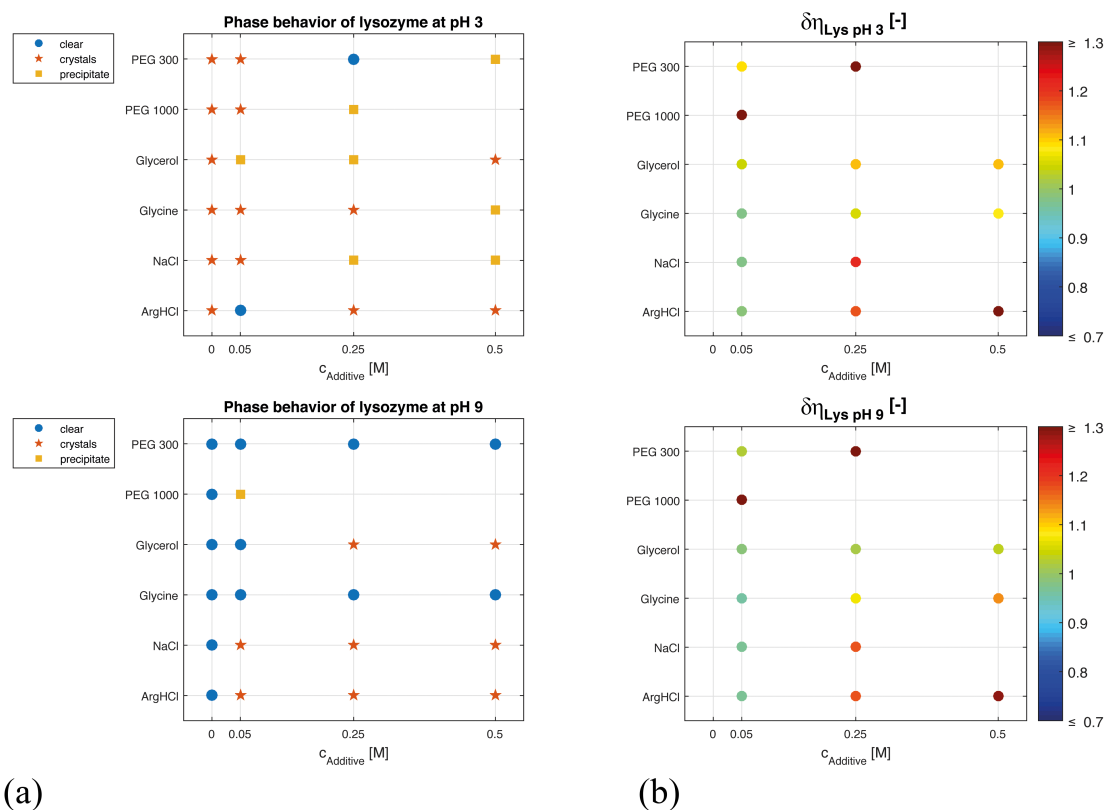
Figure 3.28: Impact of additives on the phase behavior (a) and the dynamic viscosity represented by $\delta\eta$ (b) of a lysozyme solution with a protein concentration of 180 mg/mL at pH 3 and 9. PEG 300, PEG 1000, glycerol, glycine, NaCl, and ArgHCl had concentrations of 0.05, 0.25, and 0.5 M. The term $\delta\eta$ captured the ratio between the protein solution's viscosity with additive $\eta_{with\,additive}$ and the one without additive $\eta_{without\,additive}$.

Whereas values for $\delta\eta < 1$ imply a decrease, values for $\delta\eta > 1$ imply an increase of the dynamic viscosity with addition of additives. In this study, the results for $\delta\eta$ varied with protein type, pH, additive type and concentration.

The pure buffer solutions had a dynamic viscosity close to water, which in general increased with addition of the various additives. The viscosity values of the buffers and the buffers with 0.25 M additive are displayed in Table 3.6.

In this study, protein type and pH governed the initial dynamic viscosity of the protein solutions without additive. Hence, all lysozyme solutions investigated in this study had a lower dynamic viscosity than the glucose oxidase solutions. 180 mg/mL lysozyme had a dynamic viscosity of 1.7 mPas at pH 3 and of 1.6 mPas at pH 9. The solutions containing glucose oxidase at pH 3 and 9 had a dynamic viscosity of 2.6 mPas. For lysozyme, these values could be determined with a standard deviation below 0.1 mPas. For glucose oxidase, the standard deviation was 0.5 mPas at pH 3 and 0.1 mPas at pH 9.

This initial dynamic viscosity of the protein solutions was decreased, maintained or increased with varying concentrations of the additives PEG 300, PEG 1000, glycerol, glycine, NaCl,

(a)   (b)
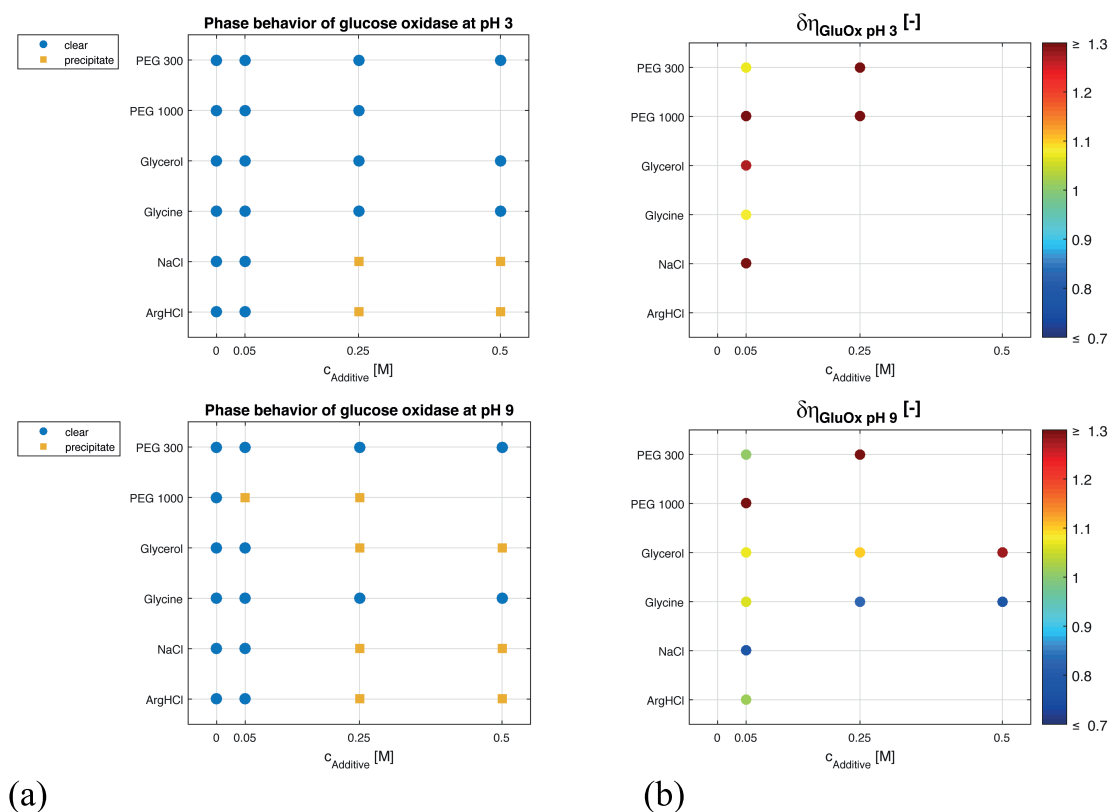
Figure 3.29: Impact of additives on the phase behavior (a) and dynamic viscosity represented by $\delta\eta$ (b) of a glucose oxidase solution with a protein concentration of 50 mg/mL at pH 3 and 130 mg/mL at 9. PEG 300, PEG 1000, glycerol, glycine, NaCl, and ArgHCl had concentrations of 0.05, 0.25, and 0.5 M. The term $\delta\eta$ captured the ratio between the protein solution's viscosity with additive $\eta_{with\ additive}$ and the one without additive $\eta_{without\ additive}$.

or ArgHCl. A decreasing effect due to $\delta\eta\ <1$ could be determined for glycine and NaCl. However, this effect was limited to glucose oxidase at pH 9. Glycine decreased the dynamic viscosity starting at 0.25 M. With addition of 0.5 M glycine, a dynamic viscosity of 2.1 mPas was reached. Referring to the dynamic viscosity of the protein solution without additive, which reflects a dynamic viscosity of 0.9 mPas for water at 25 °C and an increase in dynamic viscosity of 1.7 mPas due to the proteins and buffer components, this value represented a decrease in initial dynamic viscosity of about 30 %. The relative standard deviation for these values was below 13 %. With addition of 0.05 M NaCl the most significant decrease, a dynamic viscosity of 1.8 mPas with a relative standard deviation of 2 %, was reached. For lysozyme at pH 9, slightly decreased values for $\delta\eta$ in the range of $0.96 <\ \delta\eta\ < 0.97$ could be determined for 0.05 M gylcine, NaCl and ArgHCl. However, this range was within the relative standard deviation of 4 % for the dynamic viscosity of the lysozyme samples investigated in this study. All other samples resulted in either values for $\delta\eta > 1$, thus, an increase in dynamic viscosity, or spontaneous aggregation. PEG 300, PEG 1000 and glycerol had an increasing effect for all protein samples investigated. At high additive

concentrations PEG 300, PEG 1000, NaCl, and ArgHCl precipitated the protein solutions in several cases, in particular for glucose oxidase at pH 3. Influencing the accuracy of the microrheological measurements, no results could be determined. For these samples no $\delta\eta$ is shown.

In summary, additives change the dynamic viscosity of protein solutions. These changes were dependent on protein type, pH, additive type, and additive concentration. Decreasing the dynamic viscosity of glucose oxidase at pH 9, glycine and NaCl had a lowering effect. Low concentrations of these additives and ArgHCl also showed slightly decreasing impact on lysozyme at pH 9, but where within the perturbation of the measurement values. At pH 3, no decrease in dynamic viscosity by the addition of additives could be achieved. PEG 300, PEG 1000, and glycerol increased the dynamic viscosity of the protein solutions investigated in this study. In many cases, the microrheological measurement accuracy was low due to precipitation of the protein. In particular, for glucose oxidase at pH 3, this phenomenon could be observed with increasing additive concentrations.

Discussion

Evolving from changes in conformational or colloidal stability, attractive protein interactions can cause proteins to aggregate via differing mechanisms. At high protein concentrations, these interactions not only promote the formation of dense aggregates but also spacious networks with elevated viscosity (W. Wang, 1999; J. Liu et al., 2005). For the biopharmaceutical production process, both of these phenomenons have to be prevented to guarantee stable processes and safe formulations. This can be achieved by manipulating protein interactions through the addition of additives (Shire et al., 2004). Galm et al., 2015 already found additives to influence protein solubility depending on their conformational stability. This study aims to complement these findings by evaluating the impact of additives on the colloidal stability and dynamic viscosity of concentrated protein solutions. For this purpose, the conformational stability, the phase behavior as well as the dynamic viscosity was evaluated. All additives investigated in this study were either reported to decrease the aggregation tendency or high viscosity of protein solutions. Showing high tendency to aggregation respectively high viscosity in former studies (Bauer, Göbel, et al., 2016), lysozyme and glucose oxidase at pH 3 and 9 were used as model systems. The results for the experiments conducted are discussed in the following section.

Additive induced changes in the conformational stability of proteins

Protein interactions and, thus, protein aggregation mechanisms vary with changes in the protein's conformational stability. This stability is known to depend on pH as well as additives dissolved in solution. Galm et al., 2015 found additives to influence protein solubility only for conformationally stable proteins. Several additives of this study, namely PEG 300 (Remmele Jr. et al., 1998), PEG 1000 (Galm et al., 2015), glycerol (Scopes, 2013), and glycine (Arakawa and Timasheff, 1985) were already shown to increase the conformational stability of proteins. However, salts, such as NaCl and ArgHCl, can either stabilize or destabilize the protein conformation (Curtis, Ulrich, et al., 2002; Chi et al., 2003; Crevenna et al., 2012; Komaromy et al., 2015). FT-IR spectroscopy was conducted to evaluate the impact of pH as well as NaCl and ArgHCl on the conformational stability

Table 3.6: Viscosity results for the buffers, the buffers with 0.25 M additive, the protein solutions, and the protein solutions with 0.25 M additive at pH 3 and 9.

Sample	$\eta_{without\,protein}$ [mPas]	$\eta_{with\,protein}$ [mPas]
Lysozyme pH 3	0.89	1.65
+ PEG 300	1.15	2.34
+ PEG 1000	3.48	-
+ Glycerol	0.97	1.84
+ Glycine	0.92	1.73
+ NaCl	0.89	1.99
+ ArgHCl	0.99	1.94
Lysozyme pH 9	0.89	1.61
+ PEG 300	1.23	2.27
+ PEG 1000	3.66	-
+ Glycerol	0.94	1.62
+ Glycine	0.93	1.73
+ NaCl	0.93	1.88
+ ArgHCl	0.95	1.89
Glucose oxidase pH 3	0.89	2.39
+ PEG 300	1.15	4.01
+ PEG 1000	3.48	7.18
+ Glycerol	0.97	-
+ Glycine	0.92	-
+ NaCl	0.89	-
+ ArgHCl	0.99	-
Glucose oxidase pH 9	0.89	2.38
+ PEG 300	1.23	3.19
+ PEG 1000	3.66	-
+ Glycerol	0.94	2.63
+ Glycine	0.93	1.97
+ NaCl	0.93	-
+ ArgHCl	0.95	-

of the proteins investigated in this study. For comparison, the impact of the stabilizing additive glycine on the secondary structure was also determined.

The evaluation of the FT-IR spectra of both proteins showed a visible dependence on pH. For lysozyme at pH 3, a slight decrease in ordered structures in comparison to pH 9 and no changes with addition of glycine, NaCl or ArgHCl could be determined. Other studies found lysozyme at this pH to be conformationally unstable. Galm et al., 2015 reported conformational instability due to increasing NaCl concentrations. Moreover, Goto et al., 1989 as well as W. Wang et al., 2010 underline that proteins tend to (partially) unfold at pH values far from pI which could correlate to a conformational instability of lysozyme at this condition. For glucose oxidase at pH 3, a distinct decrease in ordered structures in comparison to pH 9 implied deviations from the native state. This conclusion could be

supported by the findings of Bright et al., 1969, who determined no detectable activity for glucose oxidase at this pH. The addition of additives resulted in no conformational changes.

For lysozyme and glucose oxidase at pH 9, no changes in the secondary structure were determined for glycine concentrations below 0.25 M. In contrast, NaCl and ArgHCl had an impact on the protein conformation and, thus, seemed to decrease the colloidal stability of the protein solutions with increasing salt concentrations.

In summary, FT-IR measurements and additional information from other publications indicate the protein conformation of lysozyme and glucose oxidase to be more stable at pH 9 than at pH 3. For the selected additives investigated in this study, the already reported stabilizing additive glycine showed the potential to maintain the conformational stability of both proteins at pH 9. NaCl and ArgHCl influenced their conformational stability at this pH.

Additives induced changes in phase behavior and viscosity

Attractive protein interactions can promote the formation of protein aggregates as well as networks with high viscosity (W. Wang, 1999; J. Liu et al., 2005). Manipulating these protein interactions, additives are reported as effective. This study investigated the impact of additives on the colloidal stability of concentrated protein solutions by determining the phase behavior and dynamic viscosity.

The results showed, that protein type, pH, additive type and additive concentration have an impact on the protein interactions affecting the aggregation tendency and viscosity of the protein solutions. For this study, lysozyme more likely aggregated, whereas glucose oxidase solution resulted in high viscosity. The underlying reasons for this disparity are the varying size and surface properties that govern the interplay of complex interactions between the protein molecules. In the concentrated state, electrostatic long range interactions as well as additional short range interactions, such as van der Waals, hydration, hydrophobic and steric interactions, like excluded volume effects, have an impact (W. Wang, 1999; Liang et al., 2007). Dependent on their composition, protein interactions promote different aggregation mechanisms (Mahler et al., 2009). Due to its bigger size and shorter distances between the protein molecules attractive short range interactions should be more dominant for glucose oxidase. Whereas excluded volume effects lead to a decrease in molecular mobility, hydrophobic and van der Waals interactions could promote stronger attractive interactions (Minton, 2000; Jezek et al., 2011). Promoting the formation of a network-like state, these interactions contribute to the higher viscosity of glucose oxidase. In contrast, lysozyme is smaller in size and therefor less hindered by excluded volume effects. Due to its high mobility, attractive protein interactions promote the formation of dense aggregates for this protein. Changes in dynamic viscosity of concentrated lysozyme solutions were, therefore, less obvious (Yadav, Shire, et al., 2011; Minton, 2005). An impact of entanglement, which was published for antibodies, could be neglected for the globular proteins investigated in this study due to the absence of unfolding. This consideration could also explain the lower viscosity values determined in comparison with other publications dealing with concentrated antibody solutions (Lefebvre, 1982; Schmit et al., 2014).

Analogous to Galm et al., 2015, FT-IR spectroscopy was used to evaluate the conformational

stability of lysozyme and glucose oxidase at pH 3 and 9. In this study only the solubility of conformationally stable proteins could be influenced by additives. Thus, with respect to the present results of the FT-IR measurements and information from other publications, changes in aggregation tendency and dynamic viscosity with addition of additives were rather expected for pH 9, because at pH 3 lysozyme as well as glucose oxidase are potentially conformationally unstable.

Taking into account the additives investigated, the following conclusions for the aggregation tendency and dynamic viscosity of the protein solutions could be drawn.

PEGs were already shown to inhibit protein aggregation (Galm et al., 2015; Baumgartner et al., 2015). However, this stabilizing effect is partially associated with increasing the dynamic viscosity of protein solutions (W. Wang, 2005; Kozer et al., 2007). PEG 300 was chosen to keep this impact on dynamic viscosity low. Analogous to publications (Remmele Jr. et al., 1998; Kozer et al., 2007), PEG 300 stabilized the protein in solution for the samples investigated in this study. However, excluded volume effects in solution plus additional attractive short range interaction decreased the mobility of the protein in solution and, thus, increased the dynamic viscosity. For PEG 1000, an increase in dynamic viscosity could already be detected at low concentrations. Although this additive was shown to stabilize lysozyme solutions (Galm et al., 2015), attractive depletion forces promoted the formation of aggregates for lysozyme and glucose oxidase solutions investigated in this study (Baumgartner et al., 2015). At high PEG 300 and PEG 1000 concentrations, these strong attractive protein interactions inhibited the preparation of homogeneous samples for the phase behavior experiments and microrheological measurements. Due to spontaneous precipitation, no results were shown for these samples.

Glycerol is known to achieve increased conformational stability by inducing preferential hydration of the proteins (Timasheff, 2002). Galm et al., 2015 could, moreover, show an increase in colloidal stability for conformationally stable systems with this additive. However, analogous to PEG, its effect is also associated with increasing the dynamic viscosity of protein solutions (Uribe et al., 2003; Meyer et al., 1989; Scopes, 2013). For this study, glycerol promoted the formation of aggregates for lysozyme at pH 3 and 9 as well as glucose oxidase at pH 9 due to attractive depletion interactions (Kozer et al., 2007). Regarding its impact on dynamic viscosity, glycerol had no lowering effect on the studied protein solutions. This trend is in agreement with further publications (Meyer et al., 1989; Gonnelli et al., 1993; Uribe et al., 2003; Scopes, 2013) as well as findings by He, Woods, et al., 2011, who studied the impact of related sugars on the dynamic viscosity of mAb2 solutions.

Glycine was already investigated with respect to aggregation as well as viscosity. These publications report glycine to decrease attractive protein interactions preventing the formation of aggregates (Arakawa and Timasheff, 1985) and high dynamic viscosity (N. Inoue et al., 2014a). These findings could be confirmed for the conformationally stable protein condition of lysozyme and glucose oxidase at pH 9. However, for lysozyme at pH 9, due to its low viscosity discussed before, only slightly decreasing changes at low glycine concentrations within the pertubation of the measurement values could be determined. Glycine, hence, presented a suitable additive to be applied as stabilizing agent in concentrated and conformationally stable protein solutions to maintain colloidal

stability and decrease dynamic viscosity. An effect of this zwitterion could possibly be attributed to changes in electrostatic protein interactions but this impact should be rather minimal. Preferential hydration of the proteins due to the preferential interaction theory is, therefore, more plausible. According to the findings of N. Inoue et al., 2014a, glycine had less lowering effect on the dynamic viscosity than salts. Due to this reason, NaCl and ArgHCl were also investigated in this study.

NaCl is known to stabilize the phase behavior of protein solutions at low salt concentrations and destabilize it at high salt concentrations (Arakawa and Timasheff, 1987; W. Wang, 1999; Shih et al., 1992). In this study, increasing concentrations of NaCl promoted visible protein aggregation due to attractive protein interactions, which could be induced by shielding repulsive electrostatic interactions. Another additional aspect could be changing protein interactions depending on possible changes in the conformational stability of the protein shown by the FT-IR measurements. At a low NaCl concentration of 0.05 M, analogous to the publication of Shire et al., 2004, a decreasing impact on the dynamic viscosity without the formation of protein aggregates could be found. This effect could only be determined for the conformationally stable glucose oxidase at pH 9 but had a stronger impact than glycine. For lysozyme, like with glycine, slightly decreasing changes within the perturbation of the measurement values could be detected. Thus, at this state, the shielding of attractive electrostatic interactions is predominant.

The dynamic viscosity of the pure buffer solutions was in general increased by addition of the various additives. This, furthermore, underlines the ability of glycine and NaCl to decrease the attractive protein interactions present in solution.

Another salt already investigated for its lowering effect on viscosity is ArgHCl (N. Inoue et al., 2014b; N. Inoue et al., 2014a). Its cation, the amino acid arginine is also known to suppress the formation of protein aggregates (Arakawa and Tsumoto, 2003; Arakawa, Ejima, et al., 2007). On the phase behavior of glucose oxidase low ArgHCl concentrations had no impact. For lysozyme at pH 3, 0.05 M of ArgHCl the formation of crystals could be prevented due to a shielding impact on attractive electrostatic interactions. Analogous to NaCl, increasing ArgHCl concentrations resulted in visible protein aggregation. Although ArgHCl was reported to decrease the dynamic viscosity of protein solutions, only slightly lower viscosity could be determined for lysozyme at pH 9. Thus, with respect to preserving colloidal stability and decreasing the dynamic viscosity of concentrated protein solutions, NaCl and ArgHCl seemed most likely suitablefor low salt concentrations.

In summary, the additives, PEG 300, PEG 1000, and glycerol, stabilized the protein solutions investigated in this study by increasing their dynamic viscosity. Additives decreasing attractive protein interactions with respect to the formation of aggregates and high viscosity were glycine as well as low concentrations of NaCl. Analogous to the findings of Galm et al., 2015 maintenance of colloidal stability and a decrease in dynamic viscosity could be determined for conformationally stable proteins. For NaCl, only low salt concentrations did not influence the colloidal stability. For higher NaCl concentrations, visible protein aggregation occurred. Contrary to the study of Z. Guo et al., 2012, ArgHCl did not conclusively decrease the dynamic viscosity but resulted in visible aggregation at salt concentrations higher than 0.05 M for the protein solutions investigated.

Conclusion

Maintaining the colloidal stability while decreasing the dynamic viscosity of a concentrated protein solution, an additive must meet special demands. It needs to decrease attractive protein interactions promoting the formation of dense aggregates as well as spacious networks. Furthermore, a destabilizing impact on the conformational stability of a protein needs to be excluded. For this study, glycine was the only additive that met these requirements. Low concentrations of NaCl showed promising results for the phase behavior and dynamic viscosity of investigated samples. However, for high salt concentrations, NaCl and ArgHCl caused visible protein aggregation. Those additives known to stabilize the protein conformation, PEG 300, PEG 1000, and glycerol, increased the dynamic viscosity of the concentrated protein solutions investigated due to their own viscosity. Thus, for the selection of an appropriate additive stabilizing the colloidal stability of concentrated protein solutions with respect to the formation of protein aggregates and high dynamic viscosity, the conformational stability of the protein, the impact of the additive on the colloidal stability and the additive's solution viscosity itself have to be considered.

Acknowledgments

References

Alvarez, P. A., Ramaswamy, H. S., and Ismail, A. A. (2008). 'High pressure gelation of soy proteins: Effect of concentration, pH and additives'. *J. Food Eng.* Vol. 88(3), pp. 331–340 (cit. on p. 121).

Amrhein, S., Bauer, K. C., Galm, L., and Hubbuch, J. (2015). 'Non-invasive high throughput approach for protein hydrophobicity determination based on surface tension'. *Biotechnol. Bioeng.* Vol. 112(12), pp. 2485–2494 (cit. on p. 59).

Arakawa, T., Ejima, D., Tsumoto, K., Obeyama, N., Tanaka, Y., Kita, Y., and Timasheff, S. N. (2007). 'Suppression of protein interactions by arginine: A proposed mechanism of the arginine effects'. *Biophys. Chem.* Vol. 127, pp. 1–8 (cit. on pp. 121, 133).

Arakawa, T. and Timasheff, S. N. (1982). 'Stabilization of protein structure by sugars.' *Biochemistry.* Vol. 21(25), pp. 6536–44 (cit. on pp. 8, 121).

– (1985). 'The stabilization of proteins by osmolytes.' *Biophys. J.* Vol. 47(3), pp. 411–4 (cit. on pp. 121, 129, 132).

– (1987). 'Abnormal solubility behavior of β-lactoglobulin: salting-in by glycine and sodium chloride'. *Biochemistry.* Vol. 26(16), pp. 5147–5153 (cit. on p. 133).

Arakawa, T. and Tsumoto, K. (2003). 'The effects of arginine on refolding of aggregated proteins: Not facilitate refolding, but suppress aggregation'. *Biochem. Biophys. Res. Commun.* Vol. 304(1), pp. 148–152 (cit. on p. 133).

Basu, S. K., Govardhan, C. P., Jung, C. W., and Margolin, A. L. (2004). 'Protein crystals for the delivery of biopharmaceuticals'. *Expert Opin. Biol. Ther.* Vol. 4(3), pp. 301–317 (cit. on p. 15).

Bauer, K. C., Göbel, M., Schwab, M.-L., Schermeyer, M.-T., and Hubbuch, J. (2016). 'Concentration-dependent changes in apparent diffusion coefficients as indicator for colloidal stability of protein solutions'. *Int. J. Pharm. (Amsterdam, Neth.).* Vol. 511(1), pp. 276–287 (cit. on pp. 75, 84, 129, 146, 148, 150, 151).

Bauer, K. C., Schermeyer, M.-T., Seidel, J., and Hubbuch, J. (2016). 'Impact of polymer surface characteristics on the microrheological measurement quality of protein solutions - A tracer particle screening'. *Int. J. Pharm. (Amsterdam, Neth.).* Vol. 505(1-2), pp. 246–254 (cit. on pp. 51, 123).

Baumgartner, K., Galm, L., Nötzold, J., Sigloch, H., Morgenstern, J., Schleining, K., Suhm, S., Oelmeier, S. A., and Hubbuch, J. (2015). 'Determination of protein phase diagrams by microbatch experiments: Exploring the influence of precipitants and pH'. *Int. J. Pharm. (Amsterdam, Neth.).* Vol. 479(1), pp. 28–40 (cit. on pp. 10, 47, 49, 82, 132).

Bhaskar, K. R., Gong, D. H., Bansil, R., Pajevic, S., Hamilton, J. A., Turner, B. S., and LaMont, J. T. (1991). 'Profound increase in viscosity and aggregation of pig gastric mucin at low pH.' *Am. J. Physiol.* Vol. 261(5 Pt 1), G827–32 (cit. on p. 62).

Bright, H. J. and Appleby, M. (1969). 'The pH Dependence of the Individual Steps in the Glucose Oxidase Reaction The pH Dependence of the Individual Glucose Oxidase Reaction*'. *J. Biol. Chem.* Vol. 244(13), pp. 3625–3634 (cit. on p. 131).

Byler, D. M. and Susi, H. (1986). 'Examination of the secondary structure of proteins by deconvolved FTIR spectra.' *Biopolymers.* Vol. 25(3), pp. 469–487 (cit. on p. 123).

Chari, R., Jerath, K., Badkar, A. V., and Kalonia, D. S. (2009). 'Long- and short-range electrostatic interactions affect the rheology of highly concentrated antibody solutions.' *Pharm. Res.* Vol. 26(12), pp. 2607–18 (cit. on pp. 2, 5, 8, 12, 15, 48, 58, 61, 120).

Cheng, W., Joshi, S. B., Jain, N. K., He, F., Kerwin, B. A., Volkin, D. B., and Middaugh, C. R. (2013). 'Linking the solution viscosity of an IgG2 monoclonal antibody to its structure as a function of pH and temperature'. *J. Pharm. Sci.* Vol. 102, pp. 4291–4304 (cit. on pp. 13, 60).

Chi, E. Y., Krishnan, S., Randolph, T. W., and Carpenter, J. F. (2003). 'Physical stability of proteins in aqueous solution: mechanism and driving forces in nonnative protein aggregation.' *Pharm. Res.* Vol. 20(9), pp. 1325–36 (cit. on pp. 1–5, 7–9, 90, 129).

Chon, J. H. and Zarbis-Papastoitsis, G. (2011). 'Advances in the production and downstream processing of antibodies'. *N. Biotechnol.* Vol. 28(5), pp. 458–463 (cit. on p. 120).

Crevenna, A. H., Naredi-Rainer, N., Lamb, D. C., Wedlich-Söldner, R., and Dzubiella, J. (2012). 'Effects of hofmeister ions on the α-helical structure of proteins'. *Biophys. J.* Vol. 102(4), pp. 907–915 (cit. on pp. 8, 129).

Curtis, R. A., Ulrich, J., Montaser, A., Prausnitz, J. M., and Blanch, H. W. (2002). 'Protein-protein interactions in concentrated electrolyte solutions.' *Biotechnol. Bioeng.* Vol. 79(4), pp. 367–80 (cit. on pp. 2, 9, 11, 47, 59, 129).

Dong, A., Kendrick, B., Kreilgârd, L., Matsuura, J., Manning, M. C., and Carpenter, J. F. (1997). 'Spectroscopic study of secondary structure and thermal denaturation of recombinant human factor XIII in aqueous solution.' *Arch. Biochem. Biophys.* Vol. 347(2), pp. 213–220 (cit. on p. 123).

Du, W. and Klibanov, A. M. (2011). 'Hydrophobic salts markedly diminish viscosity of concentrated protein solutions'. *Biotechnol. Bioeng.* Vol. 108(3), pp. 632–636 (cit. on pp. 121, 124).

Galm, L. and Hubbuch, J. (2015). 'Manipulation of lysozyme phase behavior by additives as function of conformational stability'. *Int. J. Pharm. (Amsterdam, Neth.).* Vol. 494, pp. 370–380 (cit. on pp. 121, 124, 129–133).

Garidel, P. and Schott, H. (2006). 'Fourier-Transform Midinfrared Spectroscopy for Analysis and Screening of Liquid Protein Formulations Part 2: Details Analysis and Applications'. *Bioprocess Int.* Vol. 1, pp. 48–55 (cit. on p. 146).

Gonnelli, M. and Strambini, G. B. (1993). 'Glycerol effects on protein flexibility: a tryptophan phosphorescence study.' *Biophys. J.* Vol. 65(1), pp. 131–137 (cit. on p. 132).

Goto, Y. and Fink, A. L. (1989). 'Conformational states of beta-lactamase: molten-globule states at acidic and alkaline pH with high salt.' *Biochemistry.* Vol. 28(3), pp. 945–952 (cit. on p. 130).

Guo, Z., Chen, A., Nassar, R. A., Helk, B., Mueller, C., Tang, Y., Gupta, K., and Klibanov, A. M. (2012). 'Structure-activity relationship for hydrophobic salts as viscosity-lowering excipients for concentrated solutions of monoclonal antibodies'. *Pharm. Res.* Vol. 29(11), pp. 3102–3109 (cit. on pp. 120, 124, 133).

Hall, C. G. and Abraham, G. N. (1984). 'Reversible self-association of a human myeloma protein. Thermodynamics and relevance to viscosity effects and solubility.' *Biochemistry.* Vol. 23(22), pp. 5123–9 (cit. on p. 60).

Hamada, H., Arakawa, T., and Shiraki, K. (2009). 'Effect of additives on protein aggregation.' *Curr. Pharm. Biotechnol.* Vol. 10(4), pp. 400–407 (cit. on p. 121).

He, F., Woods, C. E., Litowski, J. R., Roschen, L. A., Gadgil, H. S., Razinkov, V. I., and Kerwin, B. A. (2011). 'Effect of sugar molecules on the viscosity of high concentration monoclonal antibody solutions.' *Pharm. Res.* Vol. 28(7), pp. 1552–60 (cit. on p. 132).

Ikeda, S. and Zhong, Q. (2012). 'Polymer and Colloidal Models Describing Structure-Function Relationships'. *Annu. Rev. Food Sci. Technol.* Vol. 3, pp. 405–424 (cit. on p. 8).

Inoue, N., Takai, E., Arakawa, T., and Shiraki, K. (2014a). 'Arginine and lysine reduce the high viscosity of serum albumin solutions for pharmaceutical injection.' *J. Biosci. Bioeng.* Vol. 117(5), pp. 539–43 (cit. on pp. 60, 121, 132, 133).

– (2014b). 'Specific decrease in solution viscosity of antibodies by arginine for therapeutic formulations'. *Mol. Pharm.* Vol. 11, pp. 1889–1896 (cit. on p. 133).

Jezek, J., Rides, M., Derham, B., Moore, J., Cerasoli, E., Simler, R., and Perez-Ramirez, B. (2011). 'Viscosity of concentrated therapeutic protein compositions'. *Adv. Drug Delivery Rev.* Vol. 63(13), pp. 1107–1117 (cit. on pp. 5, 7–9, 12–15, 24, 120, 131, 152).

Kim, A. J., Manoharan, V. N., and Crocker, J. C. (2005). 'Swelling-based method for preparing stable, functionalized polymer colloids.' *J. Am. Chem. Soc.* Vol. 127(6), pp. 1592–3 (cit. on pp. 26, 123).

Kohn, W. D., Kay, C. M., and Hodges, R. S. (1997). 'Salt effects on protein stability: two-stranded alpha-helical coiled-coils containing inter- or intrahelical ion pairs.' *J. Mol. Biol.* Vol. 267(4), pp. 1039–1052 (cit. on pp. 8, 9, 121).

Komaromy, A. Z., Kulsing, C., Boysen, R. I., and Hearn, M. T. W. (2015). 'Salts employed in hydrophobic interaction chromatography can change protein structure - insights from protein-ligand interaction thermodynamics, circular dichroism spectroscopy and small angle X-ray scattering'. *Biotechnol. J.* Vol. 10(3), pp. 417–426 (cit. on p. 129).

Kong, J. and Yu, S. (2007). 'Fourier transform infrared spectroscopic analysis of protein secondary structures'. *Acta Biochim. Biophys. Sin. (Shanghai).* Vol. 39(8), pp. 549–559 (cit. on p. 10).

Kozer, N., Kuttner, Y. Y., Haran, G., and Schreiber, G. (2007). 'Protein-protein association in polymer solutions: from dilute to semidilute to concentrated.' *Biophys. J.* Vol. 92(6), pp. 2139–2149 (cit. on pp. 121, 132).

Lefebvre, J. (1982). 'Viscosity of concentrated protein solutions'. *Rheol. Acta.* Vol. 21(4-5), pp. 620–625 (cit. on pp. 12, 13, 60, 131).

Liang, Y., Hilal, N., Langston, P., and Starov, V. (2007). 'Interaction forces between colloidal particles in liquid: Theory and experiment'. *Adv. Colloid Interface Sci.* Vol. 134-135, pp. 151–166 (cit. on pp. 2, 8, 75, 86, 90, 131).

Liu, J., Nguyen, M. D., Andya, J. D., and Shire, S. J. (2005). 'Reversible Self-Association Increases the Viscosity of a Concentrated Monoclonal Antibody in Aqueous Solution'. *J. Pharm. Sci.* Vol. 94(9), pp. 1928–1940 (cit. on pp. 5, 7, 13, 15, 18, 47, 60, 62, 120, 121, 129, 131, 143).

Mahler, H.-C., Friess, W., Grauschopf, U., and Kiese, S. (2009). 'Protein aggregation: Pathways, induction factors and analysis'. *J. Pharm. Sci.* Vol. 98(9), pp. 2909–2934 (cit. on pp. 1, 4, 5, 7, 9–11, 47, 120, 131, 143).

Meyer, T. E., Tollin, G., Hazzard, J. H., and Cusanovich, M. A. (1989). 'Photoactive yellow protein from the purple phototrophic bacterium, Ectothiorhodospira halophila. Quantum

yield of photobleaching and effects of temperature, alcohols, glycerol, and sucrose on kinetics of photobleaching and recovery.' *Biophys. J.* Vol. 56(3), pp. 559–564 (cit. on p. 132).

Minton, A. P. (2000). 'Implications of macromolecular crowding for protein assembly.' *Curr. Opin. Struct. Biol.* Vol. 10(1), pp. 34–9 (cit. on pp. 2, 5, 47, 58, 61, 63, 131).

– (2005). 'Influence of macromolecular crowding upon the stability and state of association of proteins: predictions and observations.' *J. Pharm. Sci.* Vol. 94(8), pp. 1668–75 (cit. on pp. 2, 5, 131).

Pace, C. N., Treviño, S., Prabhakaran, E., and Scholtz, J. M. (2004). 'Protein structure, stability and solubility in water and other solvents.' *Philos. Trans. R. Soc. Lond. B. Biol. Sci.* Vol. 359, 1225–1234, discussion 1234–1235 (cit. on pp. 2, 3).

Parmar, A. S. and Muschol, M. (2009). 'Hydration and Hydrodynamic Interactions of Lysozyme: Effects of Chaotropic versus Kosmotropic Ions'. *Biophys. J.* Vol. 97(2), pp. 590–598 (cit. on p. 87).

Patro, S. and Przybycien, T. (1996). 'Simulations of reversible protein aggregate and crystal structure'. *Biophys. J.* Vol. 70(6), pp. 2888–2902 (cit. on pp. 4, 121).

Pazur, J. H. and Kleppe, K. (1964). 'The Oxidation of glucose and related compounds by glucose oxidase from Aspergillus niger'. *Biochemistry.* Vol. 3, pp. 578–583 (cit. on p. 59).

Remmele Jr., R. L., Nightlinger, N. S., Srinivasan, S., and Gombotz, W. R. (1998). 'Interleukin-1 receptor (IL-1R) liquid formulation development using differential scanning calorimetry'. *Pharm. Res.* Vol. 15(2), pp. 200–208 (cit. on pp. 129, 132).

Salinas, B. A., Sathish, H. A., Bishop, S. M., Harn, N., Carpenter, J. F., and Randolph, T. W. (2010). 'Understanding and modulating opalescence and viscosity in a monoclonal antibody formulation'. *J. Pharm. Sci.* Vol. 99(1), pp. 82–93 (cit. on p. 60).

Schermeyer, M.-T., Sigloch, H., Bauer, K. C., Oelschlaeger, C., and Hubbuch, J. (2016). 'Squeeze flow rheometry as a novel tool for the characterization of highly concentrated protein solutions'. *Biotechnol. Bioeng.* Vol. 113(3), pp. 576–587 (cit. on pp. 12, 25, 26, 33, 48, 52).

Schmit, J. D., He, F., Mishra, S., Ketchem, R. R., Woods, C. E., and Kerwin, B. A. (2014). 'Entanglement model of antibody viscosity'. *J. Phys. Chem. B.* Vol. 118, pp. 5044–5049 (cit. on pp. 12, 131).

Scopes, R. K. (2013). *Protein Purification: Principles and Practice.* Springer Advanced Texts in Chemistry. Springer New York (cit. on pp. 129, 132).

Shih, Y. C., Prausnitz, J. M., and Blanch, H. W. (1992). 'Some characteristics of protein precipitation by salts'. *Biotechnol. Bioeng.* Vol. 40, pp. 1155–1164 (cit. on pp. 9, 38, 133).

Shire, S. J. (2009). 'Formulation and manufacturability of biologics'. *Curr. Opin. Biotechnol.* Vol. 20, pp. 708–714 (cit. on pp. 9, 13–15, 46, 121, 143, 149).

Shire, S. J., Shahrokh, Z., and Liu, J. (2004). 'Challenges in the development of high protein concentration formulations.' *J. Pharm. Sci.* Vol. 93(6), pp. 1390–402 (cit. on pp. 7, 10, 15, 18, 24, 46, 74, 120, 121, 129, 133, 142, 143, 149).

Singh, V. and Singh, D. (2014). 'Glucose oxidase immobilization on guar gum-gelatin dual-templated silica hybrid xerogel'. *Ind. Eng. Chem. Res.* Vol. 53(10), pp. 3854–3860 (cit. on p. 59).

Timasheff, S. N. (2002). 'Protein-solvent preferential interactions, protein hydration, and the modulation of biochemical reactions by solvent components.' *Proc. Natl. Acad. Sci. U. S. A.* Vol. 99(15), pp. 9721–6 (cit. on p. 132).

Tsuge, H. J., Natsuaki, O., and Ohashi, K. (1975). 'Purification, properties, and molecular features of glucose oxidase from Aspergillus niger.' *J. Biochem.* Vol. 78, pp. 835–843 (cit. on p. 49).

Uribe, S. and Sampedro, J. G. (2003). 'Measuring Solution Viscosity and its Effect on Enzyme Activity'. *Biol. Proced. Online.* Vol. 5(1), pp. 108–115 (cit. on pp. 8, 132).

Vagenende, V., Yap, M. G. S., and Trout, B. L. (2009). 'Mechanisms of protein stabilization and prevention of protein aggregation by glycerol'. *Biochemistry.* Vol. 48(46), pp. 11084–11096 (cit. on p. 121).

Wang, W. (1999). 'Instability, stabilization, and formulation of liquid protein pharmaceuticals'. *Int. J. Pharm. (Amsterdam, Neth.).* Vol. 185(2), pp. 129–188 (cit. on pp. 1, 2, 4, 9, 10, 14, 47, 62, 120, 129, 131, 133, 143, 149).

– (2005). 'Protein aggregation and its inhibition in biopharmaceutics.' *Int. J. Pharm. (Amsterdam, Neth.).* Vol. 289(1-2), pp. 1–30 (cit. on pp. 5, 7–10, 14, 132).

Wang, W., Nema, S., and Teagarden, D. (2010). 'Protein aggregation-Pathways and influencing factors'. *Int. J. Pharm. (Amsterdam, Neth.).* Vol. 390(2), pp. 89–99 (cit. on pp. 4, 5, 7–10, 12, 14, 18, 121, 130).

Yadav, S., Laue, T. M., Kalonia, D. S., Singh, S. N., and Shire, S. J. (2012). 'The influence of charge distribution on self-association and viscosity behavior of monoclonal antibody solutions'. *Mol. Pharm.* Vol. 9, pp. 791–802 (cit. on pp. 2, 7, 13).

Yadav, S., Shire, S. J., and Kalonia, D. S. (2011). 'Viscosity analysis of high concentration bovine serum albumin aqueous solutions.' *Pharm. Res.* Vol. 28(8), pp. 1973–83 (cit. on pp. 12, 60, 131).

3.6 Changes in aggregation tendency of protein solutions by concentration via tangential flow filtration - A study evaluating the impact of process-related effects and solution conditions by comparison to centrifugal concentrators

Katharina Christin Bauer, Nora Abigail Martínez Pérez, Jürgen Hubbuch

Institute of Engineering in Life Sciences, Section IV: Biomolecular Separation Science, Karlsruhe Institute of Technology (KIT), 76131 Karlsruhe, Germany

Abstract

Protein aggregation during concentration via tangential flow filtration is claimed to be affected by process-related effects, such as concentration polarization, shear or interfacial effects, and the respective solution condition. Yet, most publications evaluating strategies to avoid product loss and ensure stable processing during this process step focused on the impact of these effects and omitted the aggregation tendency of the respective protein solution. This study investigates the synergy of process-related effects and solution conditions on the aggregation tendency during concentration via tangential flow filtration of the model proteins lysozyme, α-lactalbumin apo, and glucose oxidase at different pH values. Protein aggregates were determined by dynamic light scattering. The phase behavior of the protein solutions was evaluated by comparison to samples concentrated with centrifugal concentrators. These samples were also used as a standard to examine changes in protein conformation by Fourier-transform-infrared spectroscopy. The results of this study revealed that process-related concentration polarization caused a decrease in yield due to the formation of a dense protein layer on the membrane. Solution conditions influenced this effect, as stable protein solutions resulted in lower gel formation and higher yields. Contrary to other publications, process-related stresses were shown to have minor impact. Changes in protein conformation for the proteins investigated in this study could only be detected for the shear-sensitive apo form of α-lactalbumin. Besides optimization of concentration processes, the identification of stable solution conditions for concentrated protein solutions could, therefore, be another essential factor to avoid protein aggregation and guarantee smooth processing during concentration via tangential flow filtration.

Keywords: *concentrated protein solutions, viscosity, phase behavior, shear*

Introduction

In biopharmaceutical production, the most common process unit for buffer exchange and concentration of protein solutions is tangential flow filtration (TFF). During this unit operation, the protein solution is circulated by pumping through a series of hollow fiber tubes or membranes. Across the membrane, a pressure differential is maintained, which retains large macromolecules but allows the passage of water and small molecules (Shire et al., 2004).

With the trend towards highly concentrated formulations, TFF is required to cope with the processing of increasing protein concentrations. From an economic point of view, these concentrated protein solutions provide quicker processing, savings in production material as well as storage space, and facilitate drug delivery to the patient (E. Rosenberg et al., 2009; Burckbuchler et al., 2010). However, attainment of concentrated formulations can be challenging because high protein concentrations tend to aggregate. Aggravating this situation for TFF processes, higher protein concentrations at the membrane boundary due

to filtration flux and process-related stresses, such as shear or interfacial effects, could have an impact on the aggregation tendency of the proteins. The potentially resulting concentration-dependent aggregation mechanisms, which could either evolve from changes in the proteins' colloidal or conformational stability, can be reversible or irreversible, visible or invisible as well as soluble or insoluble. At high concentrations, they not only tend to the formation of dense protein aggregates but also to the formation of spacious networks with elevated viscosity (W. Wang, 1999; J. Liu et al., 2005; Mahler et al., 2009). During concentration via TFF, both of these phenomena are undesired as they affect the regular operation of this process step. Whereas protein aggregates may provoke membrane blockage and product loss, high viscosity may complicate pumping and product removal at the end of the concentration process. Thus, to guarantee stable processing and save formulations, key parameters influencing protein aggregation during the concentration of protein solutions are of interest (E. Rosenberg et al., 2009; Shire, 2009).

Optimizing TFF concentration processes, publications already extensively evaluated the impact of various process-related effects (K. J. Kim et al., 1993). Besides concentration polarization close to the membrane (Bowen et al., 1995; Reis, Goodrich, et al., 1997), they reported changes in protein conformation due to adsorption to the membrane (Salgin et al., 2006; Rohani et al., 2010), stirring (Colombié et al., 2000), as well as shear and cavitation due to pumping (Ashton et al., 2009; Bekard et al., 2011; Bee et al., 2009) to increase the protein aggregation tendency of the protein molecules. E. Rosenberg et al., 2009 reported protein aggregation to correlate directly to the shear stress applied during TFF. Contrary, other publications (K. J. Kim et al., 1993; Bee et al., 2009) presumed a synergistic effect of shear and additional mechanical stresses to cause protein aggregation. However, by using analytical techniques simulating mechanical stresses during TFF, most of these observations were potentially made by exposing the protein solutions to different conditions than during the actual concentration process (Bee et al., 2009).

Furthermore, parameters influencing the solution condition, such as ionic strength, pH and additives, are relevant for the aggregation tendency and rheological properties of a protein solution (Shire et al., 2004; Ashton et al., 2009). Investigating viscosity and diffusion coefficients, Richard Bowen et al., 2001 could show that both parameters depending on solution condition have a significant impact on the TFF process and should, therefore, be taken into account. Other publications found ionic strength to have an impact on aggregate formation and filtration flux. Whereas Ahrer et al., 2006 found weak buffer solutions to suppress the formation of protein aggregates and increase filtration flux, Salgin, 2007 observed increased filtration flux for increasing ionic strength. However, yet, no article evaluating the influence of processing as well as solution conditions during concentration via TFF was published.

This work aims to assess the impact of both, process-related effects and solution conditions, on the aggregation tendency to evaluate essential key factors for the colloidal stability of protein solutions during concentration. For this purpose, three model proteins already investigated for their concentration-dependent aggregation tendency were concentrated via TFF at different pH values. Protein aggregation was investigated by dynamic light scattering measurements. The phase behavior of these protein solutions was compared to the phase behavior of samples concentrated by centrifugal concentrators. These samples

were also used as a standard to evaluate the impact of process-related stresses on the conformational stability by Fourier-transformed-infrared (FT-IR) spectroscopy.

Materials and Methods

Buffers and protein solutions

All buffers had an ionic strength of 100 mM. The respective buffer components were citric acid (Merck KGaA, Darmstadt, Germany) and sodium citrate (Sigma-Aldrich, St. Louis, MO, USA) for pH 3, acetic acid (Merck KGaA) and sodium acetate (Sigma-Aldrich) for pH 5, 3-Morpholino-2-hydroxypropanesulfonic acid (MOPSO) (AppliChem GmbH, Darmstadt, Germany) for pH 7, and BisTris propane (Molekula Limited, Newcastle upon Tyne, UK) for pH 9. The pH of the buffer solutions was determined with a five-point calibrated pH meter (HI-3220, Hanna® Instruments, Woonsocket, RI, USA) equipped with a SenTix® 62 pH electrode (Xylem Inc., White Plains, NY, USA) and corrected by titration with NaOH or HCl (Merck KGaA) with an accuracy of +/- 0.5 pH units. After titration, the buffers were filtered with a 0.2 µm membrane consisting of Supor® Polyethersulfone (PES) (Pall Corporation, Port Washington, NY, USA) for pH 9 or cellulose acetate (Sartorius AG, Göttingen, Germany) for all other pH values. Each solution was first used 24 hours after preparation. They were stored at room temperature and regularly checked for constant pH. Lyophilized lysozyme (Hampton Research, Aliso Viejo, CA, USA), α-lactalbumin from bovine milk, the calcium-depleted apo form, as well as glucose oxidase (Sigma-Aldrich) were weight in and dissolved in the respective buffer. Each protein solution was filtered with a 0.2 µm syringe filter (PES for pH 9, cellulose acetate for all other pH values (VWR, Radnor, PA, USA)). Production-related additives were removed by size exclusion chromatography, which was performed at an ÄKTAprime™ plus chromatography system using a Sephadex resin (GE Healthcare, Uppsala, Sweden). The concentration was determined by a NanoDrop™ 2000c UV-Vis spectrophotometer (Thermo Fisher Scientific, Waltham, MA, USA). The respective extinction coefficients were $E^{1\%}(280 \text{ nm}) = 16.81 \text{ L g}^{-1} \text{ cm}^{-1}$ for α-lactalbumin, $E^{1\%}(280 \text{ nm}) = 22.00 \text{ L g}^{-1} \text{ cm}^{-1}$ for lysozyme, and $E^{1\%}(280 \text{ nm}) = 12.00 \text{ L g}^{-1} \text{ cm}^{-1}$ for glucose oxidase.

Tangential flow filtration

Optimization and concentration experiments were conducted using a KrosFlo® Research II*i* TFF system with hollow fiber filter membranes consisting of modified Polyethersulfone (mPES) (Spectrum Laboratories, Los Angeles, CA, USA) and a minimal working volume of 4 mL. Before each run the system was tested for leakage and membrane integrity. Therefore, the pressure-dependent Normal Water Permeability (NWP) was determined. Only membranes with a value between 75 % < NWP < 125 % of the original NWP were used in this study (Shukla et al., 2006). During processing, system data was collected by the KF Comm Software (Spectrum Laboratories, Los Angeles, CA, USA). Cleaning of the filter membranes was conducted with 0.5 M NaOH and Ethanol 80 (v/v)% (VWR). The membranes were stored in an aqueous solution of 20 (v/v)% isopropyl alcohol (Merck KGaA).

Optimization Optimization experiments were conducted to determine the changes in normalized filtration flux for lysozyme solutions depending on the controllable process parameters shear rate and transmembrane pressure (TMP) as well as the solution characteristics pH and protein concentration. Covering the parameter range of the filtration system, shear rate varied from 4,000 to 10,000 s^{-1} and TMP from 0.6 to 1.8 bar within these experiments. The investigated pH values were pH 3, 5, and 9 and protein concentrations of 10, 50, and 125 mg/mL. For each condition, the protein concentration was kept constant by leading back the filtrate line to the retentate line. System data was collected when filtrate flux reached steady state. The impact of TMP was screened by increasing its value.

Concentration Within the concentration experiments, lysozyme, α-lactalbumin, and glucose oxidase solutions were concentrated using the filtration conditions of 1.5 bar and 10,000 s^{-1} determined by the optimization experiments. For lysozyme, pH 3, 5, and 9, for α-lactalbumin, pH 7 and 9, and for glucose oxidase, pH 5 and 9 were investigated. Each initial protein solution had a volume of about 100 mL and a concentration of about 10 mg/mL. During the experiment, samples from the filtrate reservoir were taken to determine the protein concentration. The theoretical protein concentration in the retenate, displayed in Figure 3.31, was determined by evaluating the mass balance of the respective filtration sample and the initial protein mass. Each protein solution was concentrated until the minimal volume of the tangential flow system was reached or filtrate flux was minimal due to membrane blockage. After evacuation of the concentrated protein solution, the final protein concentration was determined experimentally and its value was used to calculate the mass-dependent yield. Furthermore, the concentration-dependent overall retention

$$R = 1 - \frac{c_{filtrate}}{c_{initial}} \tag{3.10}$$

of each concentration experiment was calculated with the final protein concentration in the filtrate $c_{filtrate}$ and the initial protein concentration in the feed $c_{initial}$ (Millipore, 2003). The data for each sample is shown in Table 3.7.

Dynamic light scattering

Soluble protein aggregates before and after concentration of the protein solutions were determined by dynamic light scattering. These measurements were conducted with the ZetaSizer Nano ZSP (Malvern Instruments, Worcestershire, UK). Therefore, 45 μL of the respective protein sample were transferred in a ZEN2112 quartz cuvette (Hellma® GmbH & Co. KG, Müllheim, Germany). Each sample was determined in triplicate with the Non-Invasive Back Scatter (NIBS®) optics at 25 °C. The size measurement consisted of three replicates with automatic duration. The distribution result of the protein analysis model was used for further interpretation.

Phase behavior experiments

Changes in the aggregation tendency between protein samples concentrated via TFF and centrifugal concentrators as a reference were investigated by phase behavior experiments. Therefore, 24 μL of each sample were pipetted on a MRC Under Oil 96 Well Crystallization

Plate (SWISSCI AG, Neuheim, Switzerland) and sealed with Duck® Brand HD Clear sealing tape (ShurTech® brands, Avon, OH, USA) to avoid evaporation. The plates were incubation in the automated chrystallographer RockImager 54 (Formulatrix, Bedford, MA, USA) for 40 days at 20 °C. After this time, a photograph of each sample was taken to evaluate optical phase transitions.

FT-IR spectroscopy

Changes in conformational stability of the proteins concentrated by TFF and by centrifugal concentrators as reference were determined by FT-IR spectroscopy. This measurement was performed with a Nicolet™ iS5 and an iD7 ATR detector (Thermo Fisher Scientific). The absorbance of each sample was scanned 150 times with a spectral resolution of 2 cm^{-1} from 3500 to 1000 cm^{-1}. Background spectra at the respective additive concentration and pH were recorded with 256 scans. All measurements were conducted in duplicate with a sample volume of 5 μL. The OMNIC software (Thermo Fisher Scientific) was used for recording and processing of the FT-IR spectra. Processing steps were atmospheric suppression to delete the impact of water vapor bands and the calculation of the second derivative to investigate the protein conformation. For the formation of the second derivative Savitsky-Golay with 25 points and third polynomial order was applied. The wavenumber bands relevant for the conformational stability of a protein lie within a range of 1,700 - 1,600 cm^{-1} and can be assigned to α-helix (1,658 - 1,650 cm^{-1}), β-sheet (1,695 - 1,670 cm^{-1} and 1,640 - 1,620 cm^{-1}) and random coil (1,650 - 1,640 cm^{-1}) (Garidel et al., 2006).

Results

To determine changes in the aggregation tendency of protein solutions during the concentration via TFF, model proteins with known aggregation tendency were investigated. These proteins solutions were lysozyme at pH 3, 5, and 9, α-lactalbumin at pH 7 and 9, and glucose oxidase at pH 5 and 9. The conditions were chosen due to clear differences in aggregation tendency determined by concentration with centrifugal concentrators in previous investigations (Bauer, Göbel, et al., 2016). Within this study, lysozyme at pH 3 was found to form crystals with increasing protein concentration and stay stable at pH 5 and 9. Increasing concentrations of α-lactalbumin promoted light precipitate at pH 7 and strong precipitate as well as gelation at pH 9. Glucose oxidase at pH 5 stayed clear, whereas it precipitated and gelated at pH 9.

In the present work, the concentration of these protein solutions via TFF was investigated. Changes in aggregation tendency were evaluated by dynamic light scattering measurements and phase behavior experiments. Potential differences in protein conformation were examined by FT-IR spectroscopy. The respective results for the optimization and concentration experiments as well as the analytical methods for changes in the proteins' aggregation tendency are presented in the following section.

Optimization and concentration experiments

To determine optimal parameters for the concentration of the model proteins via TFF, the normalized filtration flux of lysozyme solutions varying in pH and protein concentration was determined at different shear rates and TMPs. Depending on the filtration system, these shear rates varied from 6,000 to 10,000 s^{-1} and TMPs from 0.6 to 1.8 bar. The
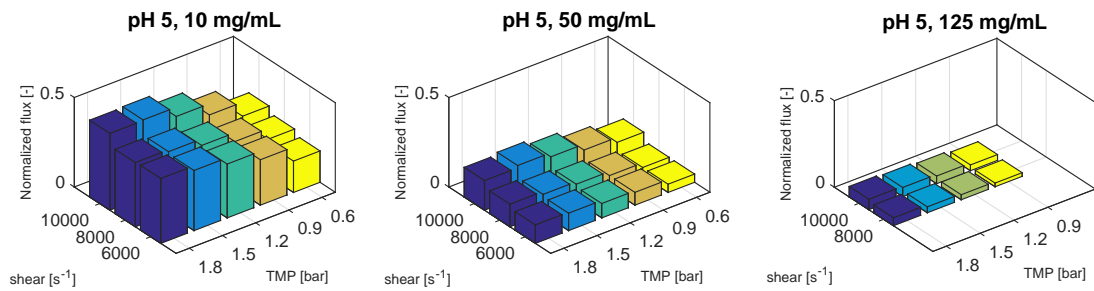
Figure 3.30: Changes in normalized filtration flux for lysozyme solutions of 10, 50, and 125 mg/mL at pH 5 depending on different shear rates and TMPs.
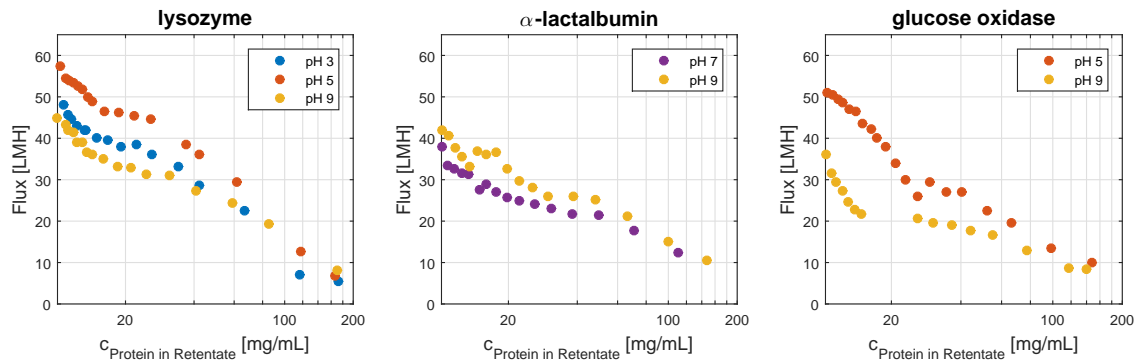
Figure 3.31: Filtration flux during concentration of lysozyme, α-lactalbumin and glucose oxidase depending on pH and the theoretical protein concentration in the retentate.

investigated lysozyme concentrations were 10, 50 and 125 mg/mL. Figure 3.30 displays the results of these optimization experiments exemplary for pH 5. For the pH values 3 and 9 also investigated in this study, the same trend depending on protein concentration, shear rate, and TMP could be determined. For all lysozyme solutions, a decrease in filtration flux with increasing protein concentration was determined. Whereas for lysozyme concentrations of 10 and 50 mg/mL a clear increase in filtration flux with increasing TMP and shear rate was determined, only small changes following this trend could be observed at a lysozyme concentration of 125 mg/mL.

Due to these optimization experiments and for an easier comparability, all protein solutions investigated in this study were concentrated at a shear rate of 10,000 s^{-1} and a TMP of 1.5 bar. Figure 3.31 displays the filtration flux for lysozyme, α-lactalbumin and glucose oxidase at different pH values depending on the protein concentration in the retentate. Analogous to the optimization experiments, filtration flux during concentration of the protein solutions decreased with increasing protein concentration. Contrary to optimization, changes in filtration flux depending on pH could be observed. These could be determined at protein concentrations below 60 mg/mL. For lysozyme, filtration flux decreased from pH 5, over 3, to 9. For α-lactalbumin, filtration flux was higher at pH 9 than at 7. For glucose

Table 3.7: Data of the concentration experiments with lysozyme, α-lactalbumin apo, and glucose oxidase at differing pH values.

Protein	pH [-]	$c_{initial}$ [mg/mL]	c_{final} [mg/mL]	yield [%]	retention [-]
Lysozyme	3	11.0	155.3	77.8	0.99
Lysozyme	5	11.6	152.9	83.4	0.99
Lysozyme	9	10.1	121.6	78.5	0.98
α-Lactalbumin apo	7	10.2	98.5	86.1	0.96
α-Lactalbumin apo	9	10.3	146.6	86.3	1.00
Glucose oxidase	5	10.6	148.5	95.9	0.98
Glucose oxidase	9	10.4	139.5	80.8	0.95

oxidase, flux decreased from pH 9 to 5. However, with increasing protein concentration, the pH-dependent variance of filtrate flux decreased and, finally, corresponded at high protein concentrations. For all proteins and conditions, filtration flux was close to 10 LMH at protein concentrations above 100 mg/mL. At this flux, the TFF process was stopped and the concentrated protein solution was pumped out of the filtration system. Besides for α-lactalbumin at pH 7, a protein concentration above 120 mg/mL could be reached. The yield for all protein samples concentrated was above 77 %, with the highest yield of 95 % for glucose oxidase at pH 5. Retentions were above 0.96. More details about each concentration experiment are displayed in Table 3.7.

Changes in aggregation tendency of model protein solutions after TFF

In this study, changes in the aggregation tendency due to differences in colloidal or conformational stability of concentrated protein solutions after TFF were evaluated. To investigate changes in colloidal stability, dynamic light scattering measurements and phase behavior experiments were conducted. Changes in conformational stability were determined by FT-IR spectroscopy.

To detect an increase in the amount of protein aggregates in the solutions investigated, dynamic light scattering was utilized directly before and after the concentration process. The results for the scattering intensity and mass proportions of the protein aggregates in solution are displayed in Figure 3.32. Regarding the intensity proportions, an increase in multimeric species for all protein solutions investigated could be determined after TFF. However, according to the idealized mass proportion of these species evaluated by the Zetasizer software, the propensity of these protein aggregates in solution was below 1 %. Changes in the long term stability of the protein solutions concentrated via TFF were determined by phase behavior experiments. The phase states of these samples and samples concentrated by centrifugal concentrators as a reference are displayed in Figure 3.33. These samples concentrated with centrifugal concentrators in a previous study (Bauer, Göbel, et al., 2016) had the same pH and protein concentrations with a deviation of +/-

10 mg/mL to the protein sample concentrated via TFF. By this comparison, changes in the aggregation tendency for the samples after TFF could be determined for lysozyme at pH 3 and 9, α-lactalbumin at pH 7 and 9, and glucose oxidase at pH 5 and 9. For lysozyme at pH 3 and 9 as well as glucose oxidase at pH 5 light aggregation could be determined. For the concentration with centrifugal concentrators, these samples stayed stable. For all other samples, a slight increase in the amount of aggregates in comparison to the samples concentrated with centrifugal concentrators was detected.

Changes in the secondary structure of the protein solutions due to concentration via TFF were investigated by FT-IR spectroscopy. Each sample after TFF was compared to a sample concentrated with centrifugal concentrators at the respective pH value and protein concentration. Figure 3.34 displays the difference Δ between the second derivative of these two FT-IR spectra for the proteins lysozyme, α-lactalbumin and glucose oxidase at the respective condition. A distinct deviation from the reference spectra was determined for α-lactalbumin at pH 7. For all other samples investigated, only slight differences to the reference spectra could be detected.
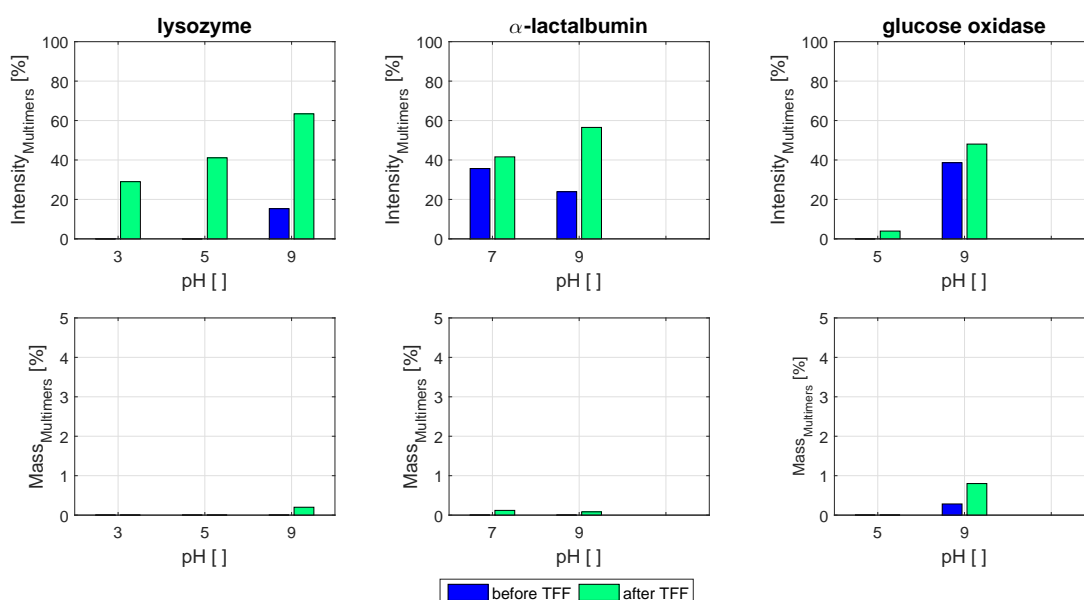
Figure 3.32: Changes in intensity and mass of multimers determined by dynamic light scattering measurements before and after concentration via TFF.

Discussion

Protein aggregation during concentration of protein solutions could either result from process-related effects or the respective solution condition (W. Wang, 1999; Shire et al., 2004; Shire, 2009). For the most common concentration unit during the biopharmaceutical production process, TFF, publications primarily investigated the impact of process-related effects omitting the respective aggregation tendency of the protein solutions. This work examines the synergy of process-related effects and different protein solution conditions on the aggregation tendency during concentration via TFF. For this purpose, lysozyme,
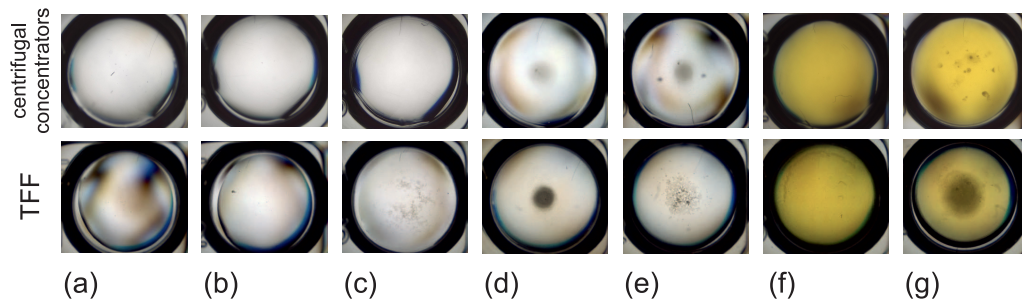
Figure 3.33: Long term stability of the protein samples concentrated by TFF (pictures lower row) and centrifugal concentrators (pictures upper row) (Bauer, Göbel, et al., 2016). Displayed are samples of lysozyme at pH 3 and 150 mg/mL (a), pH 5 and 150 mg/mL (b), and pH 9 and 125 mg/mL (c), α-lactalbumin at pH 7 and 100 mg/mL (d) and pH 9 and 150 mg/mL (e), and glucose oxidase at pH 5 and 150 mg/mL (f) and pH 9 and 130 (g).
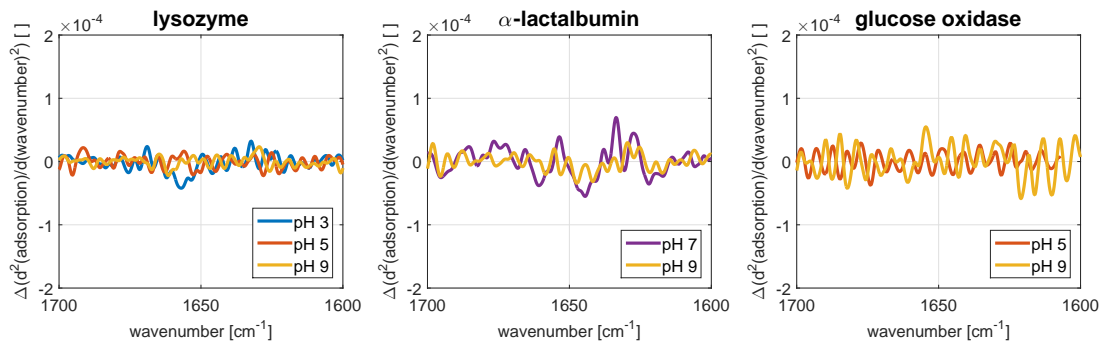
Figure 3.34: Difference of second derivative FT-IR spectra $\Delta(d^2(adsorption)/d(wavenumber)^2)$ between samples concentrated via TFF and centrifugal concentrators dependent on protein type and pH.

α-lactalbumin, and glucose oxidase solutions at different pH values, which were already determined to differ in aggregation tendency in an earlier study with centrifugal concentrators (Bauer, Göbel, et al., 2016), were examined. Within this previous study, lysozyme at pH 3 was found to be prone to crystallization for protein concentrations above 160 mg/mL, lysozyme solutions at pH 5 and 9 stayed stable. At these protein concentrations, α-lactalbumin at pH 7 and 9 precipitated, glucose oxidase was found to stay stable at pH 5 and precipitated at pH 9.

Impact of process-related effects and solution conditions on the concentration via TFF

In this study, a TFF system in lab scale with adjustable shear rate and TMP was used to evaluate the impact of process-related effects, like concentration polarization and shear, as well as different solution conditions on the aggregation tendency of protein solutions during concentration. Reducing adsorption of proteins to the membrane, hollow fiber filter membranes consisting of mPES were used to exclude an impact of the membrane surface on the filtration experiments. This modification could be similar to the one published by Zhao et al., 2011.

The optimization of process parameters for this system showed increasing shear rate and TMP to increase the filtration flux during TFF. Whereas TMP forces solute molecules through the membrane, shear inhibits the formation of a dense protein layer on the filtration membrane, which could evolve due to the TMP and the resulting protein concentration polarization (K. J. Kim et al., 1993).

For this study, the impact of concentration polarization and, thus, protein concentration was the most dominant parameter during optimization and concentration experiments. By means of optimization experiments, the permeability of a purified protein membrane was tested by filtrating protein solutions of a constant protein concentration until the filtration flux reached its equilibrium. Already for this experimental setup, at which the membrane was only required to retain proteins over short time, increased protein concentrations decreased the filtration flux significantly implying a direct deposition of protein molecules onto and into the porous membrane. This scenario is likely to occur when permeation flux is very high relative to the various backtransport mechanisms. It could also be determined for the concentration experiments displayed in Figure 3.31 where temporary the filtration flux deviated from linear dependence of logarithmic protein concentration and decreased more strongly in relation to the increase in protein concentration (Reis and Zydney, 2007). This sign for gel formation could be attributed to exceeding the solubility limit at the membrane (Bowen et al., 1995). It reflects the decrease in yield but good retention above 95 % of all concentrated protein samples during the concentration process, displayed in Table 3.7. For all samples investigated, filtration flux reached 20 % of the inital value at protein concentrations above 100 mg/mL. A dense layer evolved on the membrane pores decreased the impact of shear rate and TMP (Belfort et al., 1994). As this strong formulation-independent decrease in filtration flux occurred for all protein solutions at about the same protein concentration, this issue seems to be system- and process-related. With other filtration procedures, which cause lower concentration polarization at the membrane, probably, a more slowly decreasing filtration flux due to lower gel formation might enable the attainment of higher protein concentrations and higher yields (Reis, Goodrich, et al., 1997; Reis and Zydney, 2007; E. Rosenberg et al., 2009).

Whereas no clear impact of pH could be determined for the optimization experiments, changes in filtration flux during concentration were observed. These differences could be found for moderate protein concentrations in the retentate between 15 and 90 mg/mL for lysozyme and α-lactalbumin, respectively 0 and 100 mg/mL for glucose oxidase. In this concentration range, the different diffusion coefficients at the respective conditions had an impact on backtransport mechanisms from the membrane (Belfort et al., 1994; Shukla et al., 2006; Zydney et al., 2011). According to the results for the diffusion coefficients determined in previous studies (Bauer, Göbel, et al., 2016), for lysozyme and glucose oxidase, filtration flux decreased with decreasing diffusion coefficients determined at the respective condition. For α-lactalbumin, however, another trend was found. Analogous to the study of K. J. Kim et al., 1993, this could be attributed to changes in the secondary structure of this protein due to shear at pH 7 displayed in Figure 3.34. Besides diffusivity also the pH dependent aggregation tendency of the protein solutions determined in this earlier work (Bauer, Göbel, et al., 2016), influenced the concentration process. Lysozyme and glucose oxidase at pH 5, which were both found to be stable over a wide range of solution conditions, resulted in

a higher yield in comparison to samples with higher aggregation tendency of the same protein type. For glucose oxidase, even a lower tendency to gel formation on the filtration membrane by a more linear decrease of filtration flux dependent on logarithmic protein concentration could be determined (Figure 3.31) (Chan et al., 2001).

An impact of dynamic viscosity could not be found in this study. Due to the shear-thinning properties of concentrated protein solutions (Jezek et al., 2011), removal of the final product from the TFF system could be achieved easily for the protein concentrations reached.

In summary, process-related concentration polarization lead to the formation of a dense protein layer on the filtration membrane for all protein solutions in this study. Dependent on the aggregation tendency at the respective solution condition, this layer caused different filtration fluxes and yields for the concentration via TFF. Solutions with lower aggregation tendency like lysozyme and glucose oxidase at pH 5 achieved higher fluxes and yields in comparison to other conditions with higher aggregation tendency.

Impact of process-related effects and solution conditions on the aggregation tendency of concentrated protein solutions via TFF

Process-related effects during TFF and solution conditions are claimed to have an impact on the aggregation tendency of protein solutions (K. J. Kim et al., 1993; E. Rosenberg et al., 2009; Bee et al., 2009). This work investigated the changes in the colloidal and conformational stability of lysozyme, α-lactalbumin and glucose oxidase solutions at different pH values after concentration via TFF. Their aggregation tendency was already investigated in an earlier study, where concentration was conducted with centrifugal concentrators. This technique is used for the concentration of samples in lab scale and was, until now, not reported to promote protein aggregation due to mechanical stress or adsorption. The concentrated protein solutions with this method were, therefore, used as a reference.

Whereas Eppler et al., 2011 found the aggregation tendency during concentration with TFF and centrifugal concentrators to be similar, changes between these two techniques were determined in this study. For the samples concentrated via TFF, depicted in Figure 3.33, an increase in protein aggregates could be determined for lysozyme at pH 3 and 9, for α-lactalbumin at pH 7 and 9, and glucose oxidase at pH 5 and 9. Due to the high protein concentrations, these changes were rather minimal. Analogous to these findings and E. Rosenberg et al., 2009, an increase in intensity of scattering multimers was detected by dynamic light scattering measurements after TFF. However, by consideration of their mass propensity, as for the phase behavior experiments, this scattering intensity represented a rather negligible amount of less than 1 % of aggregates in the samples. Although correlation between the shift in scattered intensity and the difference in mass for idealized spheres within this approach is certainly not a calculation of high accuracy (Malvern, 2014), it should still give a valuable estimation and underline the minor impact of process-related stresses during TFF on protein aggregation.

Also changes in protein secondary structure due to shear or the interplay of different mechanical stresses during TFF, as reported by other publications (E. Rosenberg et al., 2009; Bee et al., 2009), could not be determined in this study. Only for α-lactalbumin, a protein known to be shear-sensitive, a distinct impact of the concentration process by TFF

was detected (Meireles et al., 1991; K. J. Kim et al., 1993).

In summary, changes in aggregation tendency due to process-related stresses, such as shear or caviation, during TFF were rather negligible. Changes in protein conformation could only be determined for the shear-sensitive α-lactalbumin. Analgous to Bee et al., 2009 we find publications, which reported process related stresses, such as shear or cavitation, to cause protein aggregation, to have exposed the protein solutions to different conditions than during the actual concentration process.

Conclusion

Protein aggregation is claimed to be affected by process-related effects as well as the respective solution condition during TFF. This study investigated the aggregation tendency of the model proteins lysozyme, α-lactalbumin and glucose oxidase during concentration via TFF. It showed process-related concentration polarization to cause product loss due to the formation of a dense protein layer close to the filtration membrane for all protein solutions investigated in this study. Solution conditions influenced the formation of this dense layer and yield, as solutions, which were identified as stable during concentration with centrifugal concentrators, achieved lower gel formation and higher yields than solutions with an elevated aggregation tendency. Contrary to other publications, an impact of process-related stresses, such as shear or caviation, on the aggregation tendency was rather negligible for the protein solutions studied. A distinct change in protein conformation could only be detected for the shear-sensitive α-lactalbumin. Consequently, besides optimization of TFF processes, the identification of stable solution condition for concentrated protein solutions could be another essential factor to avoid protein aggregation and guarantee stable processing during concentration via TFF.

Acknowledgments

References

Ahrer, K., Buchacher, A., Iberer, G., and Jungbauer, A. (2006). 'Effects of ultra-/diafiltration conditions on present aggregates in human immunoglobulin G preparations'. *J. Membr. Sci.* Vol. 274(1-2), pp. 108–115 (cit. on p. 143).

Ashton, L., Dusting, J., Imomoh, E., Balabani, S., and Blanch, E. W. (2009). 'Shear-Induced Unfolding of Lysozyme Monitored In Situ'. *Biophys. J.* Vol. 96(10), pp. 4231–4236 (cit. on pp. 9, 14, 143).

Bauer, K. C., Göbel, M., Schwab, M.-L., Schermeyer, M.-T., and Hubbuch, J. (2016). 'Concentration-dependent changes in apparent diffusion coefficients as indicator for colloidal stability of protein solutions'. *Int. J. Pharm. (Amsterdam, Neth.).* Vol. 511(1), pp. 276–287 (cit. on pp. 75, 84, 129, 146, 148, 150, 151).

Bee, J. S., Stevenson, J. L., Mehta, B., Svitel, J., Pollastrini, J., Platz, R., Freund, E., Carpenter, J. F., and Randolph, T. W. (2009). 'Response of a concentrated monoclonal antibody formulation to high shear'. *Biotechnol. Bioeng.* Vol. 103(5), pp. 936–943 (cit. on pp. 9, 14, 143, 152, 153).

Bekard, I. B., Asimakis, P., Bertolini, J., and Dunstan, D. E. (2011). 'The effects of shear flow on protein structure and function'. *Biopolymers.* Vol. 95(11), pp. 733–745 (cit. on pp. 2, 9, 14, 143).

Belfort, G., Davis, R. H., and Zydney, A. L. (1994). 'The behavior of suspensions and macromolecular solutions in crossflow microfiltration'. *J. Membr. Sci.* Vol. 96(1-2), pp. 1–58 (cit. on p. 151).

Bowen, W. and Jenner, F. (1995). 'Theoretical descriptions of membrane filtration of colloids and fine particles: An assessment and review'. *Adv. Colloid Interface Sci.* Vol. 56, pp. 141–200 (cit. on pp. 143, 151).

Burckbuchler, V., Mekhloufi, G., Giteau, A. P., Grossiord, J., Huille, S., and Agnely, F. (2010). 'Rheological and syringeability properties of highly concentrated human polyclonal immunoglobulin solutions'. *Eur. J. Pharm. Biopharm.* Vol. 76(3), pp. 351–356 (cit. on pp. 12, 15, 24, 47, 60, 61, 142).

Chan, R. and Chen, V. (2001). 'The effects of electrolyte concentration and pH on protein aggregation and deposition: critical flux and constant flux membrane filtration'. *J. Membr. Sci.* Vol. 185(2), pp. 177–192 (cit. on p. 152).

Colombié, S., Gaunand, A., Rinaudo, M., and Lindet, B. (2000). 'Irreversible lysozyme inactivation and aggregation induced by stirring: kinetic study and aggregates characterisation'. *Biotechnol. Lett.* Vol. 22(4), pp. 277–283 (cit. on p. 143).

Eppler, A., Weigandt, M., Schulze, S., Hanefeld, A., and Bunjes, H. (2011). 'Comparison of different protein concentration techniques within preformulation development'. *Int. J. Pharm. (Amsterdam, Neth.).* Vol. 421(1), pp. 120–129 (cit. on p. 152).

Garidel, P. and Schott, H. (2006). 'Fourier-Transform Midinfrared Spectroscopy for Analysis and Screening of Liquid Protein Formulations Part 2: Details Analysis and Applications'. *Bioprocess Int.* Vol. 1, pp. 48–55 (cit. on p. 146).

Jezek, J., Rides, M., Derham, B., Moore, J., Cerasoli, E., Simler, R., and Perez-Ramirez, B. (2011). 'Viscosity of concentrated therapeutic protein compositions'. *Adv. Drug Delivery Rev.* Vol. 63(13), pp. 1107–1117 (cit. on pp. 5, 7–9, 12–15, 24, 120, 131, 152).

Kim, K. J., Chen, V., and Fane, A. G. (1993). 'Some factors determining protein aggregation during ultrafiltration'. *Biotechnol. Bioeng.* Vol. 42(2), pp. 260–265 (cit. on pp. 143, 151–153).

Liu, J., Nguyen, M. D., Andya, J. D., and Shire, S. J. (2005). 'Reversible Self-Association Increases the Viscosity of a Concentrated Monoclonal Antibody in Aqueous Solution'. *J.*

Pharm. Sci. Vol. 94(9), pp. 1928–1940 (cit. on pp. 5, 7, 13, 15, 18, 47, 60, 62, 120, 121, 129, 131, 143).

Mahler, H.-C., Friess, W., Grauschopf, U., and Kiese, S. (2009). 'Protein aggregation: Pathways, induction factors and analysis'. *J. Pharm. Sci.* Vol. 98(9), pp. 2909–2934 (cit. on pp. 1, 4, 5, 7, 9–11, 47, 120, 131, 143).

Malvern (2014). *How accurate is the DLS volume distribution?* (Cit. on p. 152).

Meireles, M., Aimar, P., and Sanchez, V. (1991). 'Albumin denaturation during ultrafiltration: Effects of operating conditions and consequences on membrane fouling'. *Biotechnol. Bioeng.* Vol. 38(5), pp. 528–534 (cit. on p. 153).

Millipore (2003). *Protein Concentration and Diafiltration by Tangential Flow Filtration.* Tech. rep. Millipore (cit. on p. 145).

Reis, R. van, Goodrich, E., Yson, C., Frautschy, L., Whiteley, R., and Zydney, A. (1997). 'Constant Cwall ultrafiltration process control'. *J. Membr. Sci.* Vol. 130(1-2), pp. 123–140 (cit. on pp. 143, 151).

Reis, R. van and Zydney, A. (2007). 'Bioprocess membrane technology'. *J. Membr. Sci.* Vol. 297(1-2), pp. 16–50 (cit. on p. 151).

Richard Bowen, W. and Williams, P. M. (2001). 'Prediction of the rate of cross-flow ultrafiltration of colloids with concentration-dependent diffusion coefficient and viscosity - theory and experiment'. *Chem. Eng. Sci.* Vol. 56(10), pp. 3083–3099 (cit. on p. 143).

Rohani, M. M. and Zydney, A. L. (2010). 'Role of electrostatic interactions during protein ultrafiltration'. *Adv. Colloid Interface Sci.* Vol. 160(1-2), pp. 40–48 (cit. on p. 143).

Rosenberg, E., Hepbildikler, S., Kuhne, W., and Winter, G. (2009). 'Ultrafiltration concentration of monoclonal antibody solutions: Development of an optimized method minimizing aggregation'. *J. Membr. Sci.* Vol. 342(1-2), pp. 50–59 (cit. on pp. 15, 24, 142, 143, 151, 152).

Salgin, S. (2007). 'Effects of Ionic Environments on Bovine Serum Albumin Fouling in a Cross-Flow Ultrafiltration System'. *Chem. Eng. Technol.* Vol. 30(2), pp. 255–260 (cit. on p. 143).

Salgin, S., Takaç, S., and Özdamar, T. H. (2006). 'Adsorption of bovine serum albumin on polyether sulfone ultrafiltration membranes: Determination of interfacial interaction energy and effective diffusion coefficient'. *J. Membr. Sci.* Vol. 278(1-2), pp. 251–260 (cit. on p. 143).

Schermeyer, M.-T., Sigloch, H., Bauer, K. C., Oelschlaeger, C., and Hubbuch, J. (2016). 'Squeeze flow rheometry as a novel tool for the characterization of highly concentrated protein solutions'. *Biotechnol. Bioeng.* Vol. 113(3), pp. 576–587 (cit. on pp. 12, 25, 26, 33, 48, 52).

Shire, S. J. (2009). 'Formulation and manufacturability of biologics'. *Curr. Opin. Biotechnol.* Vol. 20, pp. 708–714 (cit. on pp. 9, 13–15, 46, 121, 143, 149).

Shire, S. J., Shahrokh, Z., and Liu, J. (2004). 'Challenges in the development of high protein concentration formulations.' *J. Pharm. Sci.* Vol. 93(6), pp. 1390–402 (cit. on pp. 7, 10, 15, 18, 24, 46, 74, 120, 121, 129, 133, 142, 143, 149).

Shukla, A. A. and Yigzaw, Y. (2006). *Process Scale Bioseparations for the Biopharmaceutical Industry.* Ed. by Shukla, A., Etzel, M., and Gadam, S. Vol. 31. Biotechnology and Bioprocessing. CRC Press, pp. 179–225 (cit. on pp. 144, 151).

Wang, W. (1999). 'Instability, stabilization, and formulation of liquid protein pharmaceuticals'. *Int. J. Pharm. (Amsterdam, Neth.).* Vol. 185(2), pp. 129–188 (cit. on pp. 1, 2, 4, 9, 10, 14, 47, 62, 120, 129, 131, 133, 143, 149).

Zhao, W., He, C., Wang, H., Su, B., Sun, S., and Zhao, C. (2011). 'Improved Antifouling Property of Polyethersulfone Hollow Fiber Membranes Using Additive of Poly(ethylene glycol) Methyl Ether-*b*-Poly(styrene) Copolymers'. *Ind. Eng. Chem. Res.* Vol. 50(6), pp. 3295–3303 (cit. on p. 150).

Zydney, A. and Reis, R. van (2011). 'Bioseparations'. *Compr. Biotechnol.* Second Edi. Vol. 1. Elsevier, pp. 499–520 (cit. on p. 151).

CHAPTER 4

Conclusion & Outlook

This work presented strategies to characterize and stabilize concentrated protein solutions to guarantee stable processing and safe formulations.

To accurately determine the dynamic viscosity or other rheological properties with microrheological measurements, the surface characteristics of the selected tracer particles were found to be an important issue. The results of the tracer particle screening suggested that the hydrophobicity of the tracer particle is the crucial surface property that needs to be considered to achieve high measurement accuracy. Of the tracer particles investigated, only PEG-PS resulted in good agreement for the dynamic viscosity determined with a standard measurement method and provided first promising results for the complex moduli G' and G''. The key factors were its hydrophilic character and uncharged surface.

Protein interactions in concentrated protein solutions could be characterized by changes in the apparent diffusion coefficient. Their impact on protein aggregation and viscosity correlated with deviations of the apparent diffusion coefficient from its concentration-dependent linearity. Samples with almost linear dependence for the apparent diffusion coefficient correlated to stable protein solutions, whereas deviations from linearity implied aggregation, like precipitation or crystallization. Stronger deviations resulted in high viscosity after preparation. For this study, the deviation of the apparent diffusion coefficient from concentration-dependent linearity was independent of protein type and solution properties. Thus, this single parameter showed the potential to act as a prognostic tool for the colloidal stability of protein solutions.

Its predictablity from protein structure properties determined *in silico* was shown by QSAR modeling. The QSAR model based on a trainingsset with apparent diffusion coefficients and three-dimensional structure properties was able to determine and predict other apparent diffusion coefficients of these proteins with a coefficient of determination R^2 of 0.9 and a predictability Q^2 of 0.88. This model did only enable a better understanding of the underlying interactions but also revealed the predictive capacity of this method in the field of protein phase behavior.

As hydrophobic interactions have an important impact on protein aggregation and high viscosity of concentrated protein solutions, a non-invasive stalagmometric method was developed. This method allowed the characterization of protein surface hydrophobicity by changes in surface tension. In the study conducted, differences in the hydrophobic character of lysozyme, human lysozyme, BSA, and α-lactalbumin depending on pH could be resolved. Whereas lysozyme was found to be hydrophilic, α-lactalbumin turned out to be the most hydrophobic at pH 3. The derived ranking was in good agreement with

literature and theoretical considerations regarding pH depending charge distributions. In comparison to an orthogonal and established spectrophotometric method for estimating protein hydrophobicity, the results of the stalagmometric method were not restricted by pH and protein size.

In order to maintain the colloidal stability while decreasing the dynamic viscosity of a concentrated protein solution, glycine was found to be a suitable additive for conformationally stable proteins. Low concentrations of NaCl also showed promising results, but high concentrations, analogous to ArgHCl, resulted in visible protein aggregation. Those additives proven to stabilize the protein conformation, PEG 300, PEG 1000, and glycerol, increased the dynamic viscosity of the concentrated protein solutions investigated due to their own viscosity. Thus, for the selection of an appropriate additive stabilizing the colloidal stability of concentrated protein solutions with respect to the formation of protein aggregates and high dynamic viscosity, the conformational stability of the protein, the impact of the additive on the colloidal stability and the additive's solution viscosity itself have to be considered.

The impact of process-related concentration polarization during TFF was found to cause product loss due to the formation of a dense protein layer close to the filtration membrane for all protein solutions investigated in this study. Solution conditions influenced the formation of this dense layer and the yield, as stable solutions achieved lower gel formation and higher yields. Contrary to other publications, an impact of process-related stresses, such as shear, was rather negligble. Besides optimization of TFF processes, the identification of stable solution conditions for concentrated protein solutions could, therefore, be another essential factor to avoid protein aggregation and guarantee stable processing during concentration.

By consideration of protein interactions, protein aggregation and dynamic viscosity of concentrated protein solutions, the presented strategies will provide valuable information to achieve safe processes and stable protein formulations. Due to reproducablity and availability, model proteins were investigated in this study. However, the strategies evaluated in this work could easily be applied to any other biomolecule of interest. With respect to the biopharmaceutical industry, experimental strategies that require low sample consumption and allow the integration into high throughput work flow were considered.

Bibliography

Absolom, D. R., Zingg, W., and Neumann, A. W. (1987). 'Protein adsorption to polymer particles: role of surface properties.' *J. Biomed. Mater. Res.* Vol. 21(2), pp. 161–171 (cit. on p. 99).

Ahamed, T., Esteban, B. N. A., Ottens, M., Dedem, G. W. K. van, Wielen, L. A. M. van der, Bisschops, M. A. T., Lee, A., Pham, C., and Thömmes, J. (2007). 'Phase behavior of an intact monoclonal antibody.' *Biophys. J.* Vol. 93(2), pp. 610–9 (cit. on pp. 11, 47, 75).

Ahrer, K., Buchacher, A., Iberer, G., and Jungbauer, A. (2006). 'Effects of ultra-/diafiltration conditions on present aggregates in human immunoglobulin G preparations'. *J. Membr. Sci.* Vol. 274(1-2), pp. 108–115 (cit. on p. 143).

Alizadeh-Pasdar, N. and Li-Chan, E. C. Y. (2000). 'Comparison of Protein Surface Hydrophobicity Measured at Various pH Values Using Three Different Fluorescent Probes'. *J. Agric. Food Chem.* Vol. 48(2), pp. 328–334 (cit. on p. 113).

Alvarez, P. A., Ramaswamy, H. S., and Ismail, A. A. (2008). 'High pressure gelation of soy proteins: Effect of concentration, pH and additives'. *J. Food Eng.* Vol. 88(3), pp. 331–340 (cit. on p. 121).

Amin, S., Barnett, G. V., Pathak, J. A., Roberts, C. J., and Sarangapani, P. S. (2014). 'Protein aggregation, particle formation, characterization & rheology'. *Curr. Opin. Colloid Interface Sci.* Vol. 19(5), pp. 438–449 (cit. on pp. 9–13, 15, 47, 58).

Amin, S., Rega, C. A., and Jankevics, H. (2011). 'Detection of viscoelasticity in aggregating dilute protein solutions through dynamic light scattering-based optical microrheology'. *Rheol. Acta.* Vol. 51(4), pp. 329–342 (cit. on pp. 12–14, 25, 26, 58).

Amrhein, S., Bauer, K. C., Galm, L., and Hubbuch, J. (2015). 'Non-invasive high throughput approach for protein hydrophobicity determination based on surface tension'. *Biotechnol. Bioeng.* Vol. 112(12), pp. 2485–2494 (cit. on p. 59).

Amrhein, S., Oelmeier, S. A., Dismer, F., and Hubbuch, J. (2014). 'Molecular dynamics simulations approach for the characterization of peptides with respect to hydrophobicity.' *J. Phys. Chem. B.* Vol. 118(7), pp. 1707–1714 (cit. on p. 99).

Amrhein, S., Schwab, M.-L., Hoffmann, M., and Hubbuch, J. (2014). 'Characterization of aqueous two phase systems by combining lab-on-a-chip technology with robotic liquid handling stations'. *J. Chromatogr. A.* Vol. 1367(0), pp. 68–77 (cit. on pp. 101, 105).

Anandakrishnan, R., Aguilar, B., and Onufriev, A. V. (2012). 'H++ 3.0: automating pK prediction and the preparation of biomolecular structures for atomistic molecular modeling and simulations'. *Nucleic Acids Res.* Vol. 40(W1), W537–W541 (cit. on p. 78).

Andrews, B. A., Schmidt, A. S., and Asenjo, J. A. (2005). 'Correlation for the partition behavior of proteins in aqueous two-phase systems: Effect of surface hydrophobicity and charge'. *Biotechnol. Bioeng.* Vol. 90(3), pp. 380–390 (cit. on p. 98).

Ansari, A., Jones, C. M., Henry, E. R., Hofrichter, J., and Eaton, W. A. (1992). 'The role of solvent viscosity in the dynamics of protein conformational changes.' *Science.* Vol. 256, pp. 1796–1798 (cit. on p. 8).

Arakawa, T., Ejima, D., Tsumoto, K., Obeyama, N., Tanaka, Y., Kita, Y., and Timasheff, S. N. (2007). 'Suppression of protein interactions by arginine: A proposed mechanism of the arginine effects'. *Biophys. Chem.* Vol. 127, pp. 1–8 (cit. on pp. 121, 133).

Arakawa, T. and Timasheff, S. N. (1982). 'Stabilization of protein structure by sugars.' *Biochemistry.* Vol. 21(25), pp. 6536–44 (cit. on pp. 8, 121).

– (1985). 'The stabilization of proteins by osmolytes.' *Biophys. J.* Vol. 47(3), pp. 411–4 (cit. on pp. 121, 129, 132).

– (1987). 'Abnormal solubility behavior of β-lactoglobulin: salting-in by glycine and sodium chloride'. *Biochemistry.* Vol. 26(16), pp. 5147–5153 (cit. on p. 133).

Arakawa, T. and Tsumoto, K. (2003). 'The effects of arginine on refolding of aggregated proteins: Not facilitate refolding, but suppress aggregation'. *Biochem. Biophys. Res. Commun.* Vol. 304(1), pp. 148–152 (cit. on p. 133).

Arzenšek, D., Kuzman, D., and Podgornik, R. (2012). 'Colloidal interactions between monoclonal antibodies in aqueous solutions'. *J. Colloid Interface Sci.* Vol. 384(1), pp. 207–216 (cit. on pp. 4, 5, 11, 47).

Asenjo, J. A. and Andrews, B. A. (2011). 'Aqueous two-phase systems for protein separation: A perspective'. *J. Chromatogr. A.* Vol. 1218(49), pp. 8826–8835 (cit. on p. 98).

Ashton, L., Dusting, J., Imomoh, E., Balabani, S., and Blanch, E. W. (2009). 'Shear-Induced Unfolding of Lysozyme Monitored In Situ'. *Biophys. J.* Vol. 96(10), pp. 4231–4236 (cit. on pp. 9, 14, 143).

Babu, K. R. and Bhakuni, V. (1997). 'Ionic-strength-dependent transition of hen egg-white lysozyme at low pH to a compact state and its aggregation on thermal denaturation.' *Eur. J. Biochem.* Vol. 245(3), pp. 781–789 (cit. on p. 7).

Baptista, R. P., Santos, A. M., Fedorov, A., Martinho, J. M. G., Pichot, C., Elaïssari, A., Cabral, J. M. S., and Taipa, M. A. (2003). 'Activity, conformation and dynamics of cutinase adsorbed on poly(methyl methacrylate) latex particles'. *J. Biotechnol.* Vol. 102(3), pp. 241–249 (cit. on p. 35).

Basu, S. K., Govardhan, C. P., Jung, C. W., and Margolin, A. L. (2004). 'Protein crystals for the delivery of biopharmaceuticals'. *Expert Opin. Biol. Ther.* Vol. 4(3), pp. 301–317 (cit. on p. 15).

Bauer, K. C., Göbel, M., Schwab, M.-L., Schermeyer, M.-T., and Hubbuch, J. (2016). 'Concentration-dependent changes in apparent diffusion coefficients as indicator for colloidal stability of protein solutions'. *Int. J. Pharm. (Amsterdam, Neth.).* Vol. 511(1), pp. 276–287 (cit. on pp. 75, 84, 129, 146, 148, 150, 151).

Bauer, K. C., Schermeyer, M.-T., Seidel, J., and Hubbuch, J. (2016). 'Impact of polymer surface characteristics on the microrheological measurement quality of protein solutions - A tracer particle screening'. *Int. J. Pharm. (Amsterdam, Neth.).* Vol. 505(1-2), pp. 246–254 (cit. on pp. 51, 123).

Baumgartner, K., Galm, L., Nötzold, J., Sigloch, H., Morgenstern, J., Schleining, K., Suhm, S., Oelmeier, S. A., and Hubbuch, J. (2015). 'Determination of protein phase diagrams by microbatch experiments: Exploring the influence of precipitants and pH'. *Int. J. Pharm. (Amsterdam, Neth.).* Vol. 479(1), pp. 28–40 (cit. on pp. 10, 47, 49, 82, 132).

Bee, J. S., Stevenson, J. L., Mehta, B., Svitel, J., Pollastrini, J., Platz, R., Freund, E., Carpenter, J. F., and Randolph, T. W. (2009). 'Response of a concentrated monoclonal antibody formulation to high shear'. *Biotechnol. Bioeng.* Vol. 103(5), pp. 936–943 (cit. on pp. 9, 14, 143, 152, 153).

Bekard, I. B., Asimakis, P., Bertolini, J., and Dunstan, D. E. (2011). 'The effects of shear flow on protein structure and function'. *Biopolymers.* Vol. 95(11), pp. 733–745 (cit. on pp. 2, 9, 14, 143).

Belfort, G., Davis, R. H., and Zydney, A. L. (1994). 'The behavior of suspensions and macromolecular solutions in crossflow microfiltration'. *J. Membr. Sci.* Vol. 96(1-2), pp. 1–58 (cit. on p. 151).

Beretta, S., Chirico, G., and Baldini, G. (2000). 'Short-Range Interactions of Globular Proteins at High Ionic Strengths'. *Macromolecules.* Vol. 33(23), pp. 8663–8670 (cit. on p. 37).

Berman, H. M. (2000). 'The Protein Data Bank'. *Nucleic Acids Res.* Vol. 28(1), pp. 235–242 (cit. on p. 78).

Bertsch, M., Mayburd, A. L., and Kassner, R. J. (2003). 'The identification of hydrophobic sites on the surface of proteins using absorption difference spectroscopy of bromophenol blue.' *Anal. Biochem.* Vol. 313(2), pp. 187–195 (cit. on pp. 99, 104, 112).

Bhaskar, K. R., Gong, D. H., Bansil, R., Pajevic, S., Hamilton, J. A., Turner, B. S., and LaMont, J. T. (1991). 'Profound increase in viscosity and aggregation of pig gastric mucin at low pH.' *Am. J. Physiol.* Vol. 261(5 Pt 1), G827–32 (cit. on p. 62).

Biasini, M., Bienert, S., Waterhouse, A., Arnold, K., Studer, G., Schmidt, T., Kiefer, F., Cassarino, T. G., Bertoni, M., Bordoli, L., and Schwede, T. (2014). 'SWISS-MODEL:

modelling protein tertiary and quaternary structure using evolutionary information'. *Nucleic Acids Res.* Vol. 42(W1), W252–W258 (cit. on p. 78).

Bigelow, C. C. (1967). 'On the average hydrophobicity of proteins and the relation between it and protein structure.' *J. Theor. Biol.* Vol. 16(2), pp. 187–211 (cit. on p. 112).

Biswas, K. M., DeVido, D. R., and Dorsey, J. G. (2003). 'Evaluation of methods for measuring amino acid hydrophobicities and interactions'. *J. Chromatogr. A.* Vol. 1000, pp. 637–655 (cit. on pp. 2, 99).

Bjerrum, O. J. (1968). 'Interaction of Bromphenol Blue and Bilirubin with Bovine and Human Serum Albumin Determined by Gel Filtration'. *Scand. J. Clin. Lab. Investig.* Vol. 22(1), pp. 41–48 (cit. on p. 112).

Black, S. D. and Mould, D. R. (1991). 'Development of hydrophobicity parameters to analyze proteins which bear post- or cotranslational modifications.' *Anal. Biochem.* Vol. 193(1), pp. 72–82 (cit. on p. 99).

Blake, R. C., Shute, E. A., and Howard, G. T. (1994). 'Solubilization of minerals by bacteria: Electrophoretic mobility of Thiobacillus ferrooxidans in the presence of iron, pyrite, and sulfur'. *Appl. Environ. Microbiol.* Vol. 60(9), pp. 3349–3357 (cit. on p. 28).

Boistelle, R. and Astier, J. (1988). 'Crystallization mechanisms in solution'. *J. Cryst. Growth.* Vol. 90(1-3), pp. 14–30 (cit. on p. 4).

Bowen, W. and Jenner, F. (1995). 'Theoretical descriptions of membrane filtration of colloids and fine particles: An assessment and review'. *Adv. Colloid Interface Sci.* Vol. 56, pp. 141–200 (cit. on pp. 143, 151).

Bramaud, C., Aimar, P., and Daufin, G. (1997). 'Whey protein fractionation: Isoelectric precipitation of α-lactalbumin under gentle heat treatment'. *Biotechnol. Bioeng.* Vol. 56, pp. 391–397 (cit. on p. 49).

Breedveld, V. and Pine, D. J. (2003). 'Microrheology as a tool for high-throughput screening'. *J. Mater. Sci.* Vol. 38(22), pp. 4461–4470 (cit. on pp. 25, 51).

Brems, D. N., Plaisted, S. M., Havel, H. A., and Tomich, C. S. (1988). 'Stabilization of an associated folding intermediate of bovine growth hormone by site-directed mutagenesis.' *Proc. Natl. Acad. Sci. U. S. A.* Vol. 85(10), pp. 3367–3371 (cit. on pp. 18, 98).

Bright, H. J. and Appleby, M. (1969). 'The pH Dependence of the Individual Steps in the Glucose Oxidase Reaction The pH Dependence of the Individual Glucose Oxidase Reaction*'. *J. Biol. Chem.* Vol. 244(13), pp. 3625–3634 (cit. on p. 131).

Broide, M. L., Tominc, T. M., and Saxowsky, M. D. (1996). 'Using phase transitions to investigate the effect of salts on protein interactions'. *Phys. Rev. E: Stat., Nonlinear, Soft Matter Phys.* Vol. 53(6), pp. 6325–6335 (cit. on p. 36).

Bryant, C. and McClements, D. (2000). 'Influence of NaCl and CaCl2 on Cold-Set Gelation of Heat-denatured Whey Protein'. *J. Food Sci.* Vol. 65(5), pp. 801–804 (cit. on p. 60).

Bull, H. B. and Breese, K. (1974). 'Surface tension of amino acid solutions: A hydrophobicity scale of the amino acid residues'. *Arch. Biochem. Biophys.* Vol. 161(2), pp. 665–670 (cit. on pp. 3, 99).

Burckbuchler, V., Mekhloufi, G., Giteau, A. P., Grossiord, J., Huille, S., and Agnely, F. (2010). 'Rheological and syringeability properties of highly concentrated human polyclonal immunoglobulin solutions'. *Eur. J. Pharm. Biopharm.* Vol. 76(3), pp. 351–356 (cit. on pp. 12, 15, 24, 47, 60, 61, 142).

Buyel, J., Woo, J., Cramer, S., and Fischer, R. (2013). 'The use of quantitative structure-activity relationship models to develop optimized processes for the removal of tobacco host cell proteins during biopharmaceutical production'. *J. Chromatogr. A.* Vol. 1322, pp. 18–28 (cit. on pp. 18, 75).

Byler, D. M. and Susi, H. (1986). 'Examination of the secondary structure of proteins by deconvolved FTIR spectra.' *Biopolymers.* Vol. 25(3), pp. 469–487 (cit. on p. 123).

Cao, W. G., Jiao, Q. C., Fu, Y., Chen, L., and Liu, Q. (2003). 'Mechanism of the Interaction Between Bromophenol Blue and Bovine Serum Albumin'. *Spectrosc. Lett.* Vol. 36(3), pp. 197–209 (cit. on p. 112).

Cardamone, M. and Puri, N. K. (1992). 'Spectrofluorimetric assessment of the surface hydrophobicity of proteins.' *Biochem. J.* Vol. 282, pp. 589–593 (cit. on p. 99).

Cassidy, O. E., Rowley, G., Fletcher, I. W., Davies, S. F., and Briggs, D. (1999). 'Surface modification and electrostatic charge of polystyrene particles'. *Int. J. Pharm. (Amsterdam, Neth.).* Vol. 182(2), pp. 199–211 (cit. on p. 25).

Chan, R. and Chen, V. (2001). 'The effects of electrolyte concentration and pH on protein aggregation and deposition: critical flux and constant flux membrane filtration'. *J. Membr. Sci.* Vol. 185(2), pp. 177–192 (cit. on p. 152).

Chari, R., Jerath, K., Badkar, A. V., and Kalonia, D. S. (2009). 'Long- and short-range electrostatic interactions affect the rheology of highly concentrated antibody solutions.' *Pharm. Res.* Vol. 26(12), pp. 2607–18 (cit. on pp. 2, 5, 8, 12, 15, 48, 58, 61, 120).

Chen, J., Yang, T., Luo, Q., Breneman, C. M., and Cramer, S. M. (2007). 'Investigation of protein retention in hydrophobic interaction chromatographic (HIC) systems using the preferential interaction theory and quantitative structure property relationship models'. *React. Funct. Polym.* Vol. 67(12), pp. 1561–1569 (cit. on p. 99).

Cheng, Y.-C., Bianco, C. L., Sandler, S. I., and Lenhoff, A. M. (2008). 'Salting-Out of Lysozyme and Ovalbumin from Mixtures: Predicting Precipitation Performance from Protein-Protein Interactions'. *Ind. Eng. Chem. Res.* Vol. 47(15), pp. 5203–5213 (cit. on p. 75).

Cheng, W., Joshi, S. B., Jain, N. K., He, F., Kerwin, B. A., Volkin, D. B., and Middaugh, C. R. (2013). 'Linking the solution viscosity of an IgG2 monoclonal antibody to its

structure as a function of pH and temperature'. *J. Pharm. Sci.* Vol. 102, pp. 4291–4304 (cit. on pp. 13, 60).

Chennamsetty, N., Helk, B., Voynov, V., Kayser, V., and Trout, B. L. (2009). 'Aggregation-prone motifs in human immunoglobulin G.' *J. Mol. Biol.* Vol. 391(2), pp. 404–413 (cit. on p. 99).

Chi, E. Y., Krishnan, S., Randolph, T. W., and Carpenter, J. F. (2003). 'Physical stability of proteins in aqueous solution: mechanism and driving forces in nonnative protein aggregation.' *Pharm. Res.* Vol. 20(9), pp. 1325–36 (cit. on pp. 1–5, 7–9, 90, 129).

Chon, J. H. and Zarbis-Papastoitsis, G. (2011). 'Advances in the production and downstream processing of antibodies'. *N. Biotechnol.* Vol. 28(5), pp. 458–463 (cit. on p. 120).

Chung, W. K., Hou, Y., Holstein, M., Freed, A., Makhatadze, G. I., and Cramer, S. M. (2010). 'Investigation of protein binding affinity in multimodal chromatographic systems using a homologous protein library'. *J. Chromatogr. A.* Vol. 1217(2), pp. 191–198 (cit. on pp. 18, 75).

Cohen, Y., Avram, L., and Frish, L. (2005). 'Diffusion NMR spectroscopy in supramolecular and combinatorial chemistry: an old parameter–new insights.' *Angew. Chem. Int. Ed. Engl.* Vol. 44(4), pp. 520–54 (cit. on pp. 12, 48).

Colombié, S., Gaunand, A., Rinaudo, M., and Lindet, B. (2000). 'Irreversible lysozyme inactivation and aggregation induced by stirring: kinetic study and aggregates characterisation'. *Biotechnol. Lett.* Vol. 22(4), pp. 277–283 (cit. on p. 143).

Connolly, B. D., Petry, C., Yadav, S., Demeule, B., Ciaccio, N., Moore, J. M. R., Shire, S. J., and Gokarn, Y. R. (2012). 'Weak interactions govern the viscosity of concentrated antibody solutions: high-throughput analysis using the diffusion interaction parameter.' *Biophys. J.* Vol. 103(1), pp. 69–78 (cit. on pp. 11, 12, 47, 51, 53, 60, 61, 75).

Corbett, J. C. W., Connah, M. T., and Mattison, K. (2011). 'Advances in the measurement of protein mobility using laser Doppler electrophoresis - the diffusion barrier technique.' *Electrophoresis.* Vol. 32(14), pp. 1787–94 (cit. on p. 28).

Crassous, J. J., Régisser, R., Ballauff, M., and Willenbacher, N. (2005). 'Characterization of the viscoelastic behavior of complex fluids using the piezoelastic axial vibrator'. *J. Rheol. (Melville, NY, U. S.).* Vol. 49(4), p. 851 (cit. on p. 28).

Crevenna, A. H., Naredi-Rainer, N., Lamb, D. C., Wedlich-Söldner, R., and Dzubiella, J. (2012). 'Effects of hofmeister ions on the α-helical structure of proteins'. *Biophys. J.* Vol. 102(4), pp. 907–915 (cit. on pp. 8, 129).

Crommelin, D. J. A., Sindelar, R. D., and Meibohm, B. (2013). *Pharmaceutical Biotechnology: Fundamentals and Applications.* SpringerLink : Bücher. Springer New York (cit. on pp. 2, 47, 75, 86).

Cromwell, M. E. M., Hilario, E., and Jacobson, F. (2006). 'Protein aggregation and bioprocessing.' *AAPS J.* Vol. 8(3), E572–9 (cit. on pp. 4, 5, 14, 47, 59).

Curtis, R. A., Steinbrecher, C., Heinemann, M., Blanch, H. W., and Prausnitz, J. M. (2002). 'Hydrophobic forces between protein molecules in aqueous solutions of concentrated electrolyte.' *Biophys. Chem.* Vol. 98(3), pp. 249–65 (cit. on pp. 9, 86, 90).

Curtis, R. A., Ulrich, J., Montaser, A., Prausnitz, J. M., and Blanch, H. W. (2002). 'Protein-protein interactions in concentrated electrolyte solutions.' *Biotechnol. Bioeng.* Vol. 79(4), pp. 367–80 (cit. on pp. 2, 9, 11, 47, 59, 129).

Dasgupta, B. R., Tee, S.-Y., Crocker, J. C., Frisken, B. J., and Weitz, D. A. (2002). 'Microrheology of polyethylene oxide using diffusing wave spectroscopy and single scattering'. *Phys. Rev. E: Stat., Nonlinear, Soft Matter Phys.* Vol. 65(5), p. 051505 (cit. on p. 29).

Dehmer, M., Varmuza, K., and Bonchev, D. (2012). *Statistical Modelling of Molecular Descriptors in QSAR/QSPR.* Ed. by Dehmer, M., Varmuza, K., and Bonchev, D. Weinheim, Germany: Wiley-VCH Verlag GmbH & Co. KGaA (cit. on p. 75).

Derewenda, Z. S. (2004). 'Rational Protein Crystallization by Mutational Surface Engineering'. *Structure.* Vol. 12(4), pp. 529–535 (cit. on p. 63).

Deryło-Marczewska, A., Goworek, J., Pikus, S., Kobylas, E., and Zgrajka, W. (2002). 'Characterization of Melamine-Formaldehyde Resins by XPS, SAXS, and Sorption Techniques'. *Langmuir.* Vol. 18(20), pp. 7538–7543 (cit. on p. 35).

Desbrières, J. (2000). 'Thermogelation of methylcellulose: rheological considerations'. *Polymer (Guildf).* Vol. 41(7), pp. 2451–2461 (cit. on pp. 59, 60).

Diederich, P., Amrhein, S., Hämmerling, F., and Hubbuch, J. (2013). 'Evaluation of PEG/phosphate aqueous two-phase systems for the purification of the chicken egg white protein avidin by using high-throughput techniques'. *Chem. Eng. Sci.* Vol. 104(0), pp. 945–956 (cit. on p. 98).

Dill, K. A. (1990). 'Dominant forces in protein folding'. *Biochemistry.* Vol. 29(31), pp. 7133–7155 (cit. on p. 98).

Dismer, F. and Hubbuch, J. (2010). '3D structure-based protein retention prediction for ion-exchange chromatography'. *J. Chromatogr. A.* Vol. 1217(8), pp. 1343–1353 (cit. on p. 79).

Donev, R. (2011). *Advances in Protein Chemistry and Structural Biology.* Academic Press. Academic Press (cit. on p. 49).

Dong, A., Kendrick, B., Kreilgârd, L., Matsuura, J., Manning, M. C., and Carpenter, J. F. (1997). 'Spectroscopic study of secondary structure and thermal denaturation of recombinant human factor XIII in aqueous solution.' *Arch. Biochem. Biophys.* Vol. 347(2), pp. 213–220 (cit. on p. 123).

Dooley, K. H. and Castellino, F. J. (1972). 'Solubility of amino acids in aqueous guanidinium thiocyanate solutions.' *Biochemistry.* Vol. 11(10), pp. 1870–1874 (cit. on p. 99).

Du, W. and Klibanov, A. M. (2011). 'Hydrophobic salts markedly diminish viscosity of concentrated protein solutions'. *Biotechnol. Bioeng.* Vol. 108(3), pp. 632–636 (cit. on pp. 121, 124).

Duan, Y., Wu, C., Chowdhury, S. S., Lee, M. C., Xiong, G., Zhang, W., Yang, R., Cieplak, P., Luo, R., Lee, T., Caldwell, J., Wang, J., and Kollman, P. (2003). 'A point-charge force field for molecular mechanics simulations of proteins based on condensed-phase quantum mechanical calculations.' *J. Comput. Chem.* Vol. 24(16), pp. 1999–2012 (cit. on p. 78).

Dumetz, A. C. (2007). *Protein Interactions and Phase Behavior in Aqueous Solutions: Effects of Salt, Polymer, and Organic Additives.* University of Delaware, p. 284 (cit. on pp. 58, 87).

Dumetz, A. C., Chockla, A. M., Kaler, E. W., and Lenhoff, A. M. (2008). 'Protein phase behavior in aqueous solutions: crystallization, liquid-liquid phase separation, gels, and aggregates.' *Biophys. J.* Vol. 94(2), pp. 570–83 (cit. on pp. 11, 47).

Duong-Ly, K. C. and Gabelli, S. B. (2014). 'Salting out of proteins using ammonium sulfate precipitation'. *Methods Enzymol.* Vol. 541, pp. 85–94 (cit. on p. 38).

Eisenberg, D. (1984). 'Three-dimensional structure of membrane and surface proteins'. *Annu. Rev. Biochem. Biochem.* Vol. 53, pp. 595–623 (cit. on p. 99).

Ellis, R. J. (2001). 'Macromolecular crowding: obvious but underappreciated.' *Trends Biochem. Sci.* Vol. 26(10), pp. 597–604 (cit. on p. 37).

Eppler, A., Weigandt, M., Schulze, S., Hanefeld, A., and Bunjes, H. (2011). 'Comparison of different protein concentration techniques within preformulation development'. *Int. J. Pharm. (Amsterdam, Neth.).* Vol. 421(1), pp. 120–129 (cit. on p. 152).

Eriksson, L., Byrne, T., Johansson, E., Trygg, J., and Wikström, C. (2013). *Multi- and Megavariate Data Analysis: Part I: Basic Principles and Applications.* MKS Umetrics AB, p. 425 (cit. on pp. 79, 82, 89).

Eriksson, L., Jaworska, J., Worth, A. P., Cronin, M. T., McDowell, R. M., and Gramatica, P. (2003). 'Methods for Reliability and Uncertainty Assessment and for Applicability Evaluations of Classification- and Regression-Based QSARs'. *Environ. Health Perspect.* Vol. 111(10), pp. 1361–1375 (cit. on p. 80).

Falahati, H., Wong, L., Davarpanah, L., Garg, A., Schmitz, P., and Barz, D. P. J. (2014). 'The zeta potential of PMMA in contact with electrolytes of various conditions: Theoretical and experimental investigation'. *Electrophoresis.* Vol. 35, pp. 870–882 (cit. on p. 35).

Felderhof, B. U. (1978). 'Diffusion of interacting Brownian particles'. *J. Phys. A. Math. Gen.* Vol. 11(5), pp. 929–937 (cit. on p. 85).

Feldman, K., Tervoort, T., Smith, P., and Spencer, N. D. (1998). 'Toward a Force Spectroscopy of Polymer Surfaces'. *Langmuir.* Vol. 14(2), pp. 372–378 (cit. on p. 38).

Fendler, J. H., Nome, F., and Nagyvary, J. (1975). 'Compartmentalization of Amino Acids in Surfactant Aggregates'. *J. Mol. Evol.* Vol. 6, pp. 215–232 (cit. on p. 99).

Feng, Y. W., Ooishi, A., and Honda, S. (2012). 'Aggregation factor analysis for protein formulation by a systematic approach using FTIR, SEC and design of experiments techniques.' *J. Pharm. Biomed. Anal.* Vol. 57, pp. 143–52 (cit. on pp. 8, 10).

Fink, A. L. (1998). 'Protein aggregation: folding aggregates, inclusion bodies and amyloid'. *Fold. Des.* Vol. 3(1), R9–R23 (cit. on p. 5).

Fiorucci, S. and Zacharias, M. (2010). 'Prediction of Protein-Protein Interaction Sites Using Electrostatic Desolvation Profiles'. *Biophys. J.* Vol. 98(9), pp. 1921–1930 (cit. on p. 4).

Flores, R. (1978). 'A Rapid and Reproducible Assay for Quantitative Estimation of Proteins using Bromophenol Blue'. *Anal. Biochem.* Vol. 88, pp. 605–611 (cit. on p. 112).

Fritz, G., Maranzano, B., Wagner, N., and Willenbacher, N. (2002). 'High frequency rheology of hard sphere colloidal dispersions measured with a torsional resonator'. *J. Nonnewton. Fluid Mech.* Vol. 102(2), pp. 149–156 (cit. on pp. 14, 25, 26).

Fritz, G., Pechhold, W., Willenbacher, N., and Wagner, N. J. (2003). 'Characterizing complex fluids with high frequency rheology using torsional resonators at multiple frequencies'. *J. Rheol. (Melville, NY, U. S.).* Vol. 47(2), p. 303 (cit. on pp. 25–27).

Gaigalas, A., Reipa, V., Hubbard, J., Edwards, J., and Douglas, J. (1995). 'A non-perturbative relation between the mutual diffusion coefficient, suspension viscosity, and osmotic compressibility: Application to concentrated protein solutions'. *Chem. Eng. Sci.* Vol. 50(7), pp. 1107–1114 (cit. on pp. 11, 12, 47, 48, 61).

Galm, L. and Hubbuch, J. (2015). 'Manipulation of lysozyme phase behavior by additives as function of conformational stability'. *Int. J. Pharm. (Amsterdam, Neth.).* Vol. 494, pp. 370–380 (cit. on pp. 121, 124, 129–133).

Garidel, P. and Schott, H. (2006). 'Fourier-Transform Midinfrared Spectroscopy for Analysis and Screening of Liquid Protein Formulations Part 2: Details Analysis and Applications'. *Bioprocess Int.* Vol. 1, pp. 48–55 (cit. on p. 146).

Genest, S., Schwarz, S., Petzold-Welcke, K., Heinze, T., and Voit, B. (2013). 'Characterization of highly substituted, cationic amphiphilic starch derivatives: Dynamic surface tension and intrinsic viscosity'. *Starch/Stärke.* Vol. 65, pp. 999–1010 (cit. on pp. 100, 109).

George, A. and Wilson, W. W. (1994). 'Predicting protein crystallization from a dilute solution property'. *Acta Crystallogr. Sect. D Biol. Crystallogr.* Vol. 50(4), pp. 361–365 (cit. on pp. 12, 47, 75).

Giannopoulou, A., Aletras, A. J., Pharmakakis, N., Papatheodorou, G. N., and Yannopoulos, S. N. (2007). 'Dynamics of proteins: Light scattering study of dilute and dense colloidal

suspensions of eye lens homogenates'. *J. Chem. Phys.* Vol. 127(20), pp. 1–24 (cit. on p. 61).

Gilroy, E. L., Hicks, M. R., Smith, D. J., and Rodger, A. (2011). 'Viscosity of aqueous DNA solutions determined using dynamic light scattering'. *Analyst (Cambridge, U. K.).* Vol. 136(20), p. 4159 (cit. on p. 25).

Gisler, T. and Weitz, D. A. (1998). 'Tracer microrheology in complex fluids'. *Curr. Opin. Colloid Interface Sci.* Vol. 3(6), pp. 586–592 (cit. on p. 25).

Gonnelli, M. and Strambini, G. B. (1993). 'Glycerol effects on protein flexibility: a tryptophan phosphorescence study.' *Biophys. J.* Vol. 65(1), pp. 131–137 (cit. on p. 132).

Goto, Y. and Fink, A. L. (1989). 'Conformational states of beta-lactamase: molten-globule states at acidic and alkaline pH with high salt.' *Biochemistry.* Vol. 28(3), pp. 945–952 (cit. on p. 130).

Grigsby, J. J., Blanch, H. W., and Prausnitz, J. M. (2000). 'Diffusivities of Lysozyme in Aqueous MgCl 2 Solutions from Dynamic Light-Scattering Data: Effect of Protein and Salt Concentrations'. *J. Phys. Chem. B.* Vol. 104(15), pp. 3645–3650 (cit. on p. 61).

Gronemeyer, P., Ditz, R., and Strube, J. (2014). 'Trends in Upstream and Downstream Process Development for Antibody Manufacturing'. *Bioengineering.* Vol. 1(4), pp. 188–212 (cit. on p. 46).

Guo, D., Mant, C. T., Taneja, A. K., Parker, J., and Rodges, R. S. (1986). 'Prediction of peptide retention times in reversed-phase high-performance liquid chromatography I. Determination of retention coefficients of amino acid residues of model synthetic peptides'. *J. Chromatogr. A.* Vol. 359(8), pp. 499–518 (cit. on pp. 59, 86, 111).

Guo, Z., Chen, A., Nassar, R. A., Helk, B., Mueller, C., Tang, Y., Gupta, K., and Klibanov, A. M. (2012). 'Structure-activity relationship for hydrophobic salts as viscosity-lowering excipients for concentrated solutions of monoclonal antibodies'. *Pharm. Res.* Vol. 29(11), pp. 3102–3109 (cit. on pp. 120, 124, 133).

Hall, C. G. and Abraham, G. N. (1984). 'Reversible self-association of a human myeloma protein. Thermodynamics and relevance to viscosity effects and solubility.' *Biochemistry.* Vol. 23(22), pp. 5123–9 (cit. on p. 60).

Halle, B. (2004). 'Protein hydration dynamics in solution: a critical survey'. *Philos. Trans. R. Soc. B Biol. Sci.* Vol. 359(1448), pp. 1207–1224 (cit. on p. 61).

Hamada, H., Arakawa, T., and Shiraki, K. (2009). 'Effect of additives on protein aggregation.' *Curr. Pharm. Biotechnol.* Vol. 10(4), pp. 400–407 (cit. on p. 121).

Harris, J. M. (1992). *Poly(Ethylene Glycol) Chemistry: Biotechnical and Biomedical Applications.* Ethylene Glycol Chemistry: Biotechnical and Biomedical Applications. Springer (cit. on pp. 103, 109).

Harris, P. (2012). *Food Gels.* Elsevier Applied Food Science Series. Springer Netherlands (cit. on p. 59).

Hawe, A., Sutter, M., and Jiskoot, W. (2008). 'Extrinsic fluorescent dyes as tools for protein characterization.' *Pharm. Res.* Vol. 25(7), pp. 1487–1499 (cit. on p. 99).

He, F., Becker, G. W., Litowski, J. R., Narhi, L. O., Brems, D. N., and Razinkov, V. I. (2010). 'High-throughput dynamic light scattering method for measuring viscosity of concentrated protein solutions.' *Anal. Biochem.* Vol. 399(1), pp. 141–3 (cit. on p. 25).

He, F., Woods, C. E., Litowski, J. R., Roschen, L. A., Gadgil, H. S., Razinkov, V. I., and Kerwin, B. A. (2011). 'Effect of sugar molecules on the viscosity of high concentration monoclonal antibody solutions.' *Pharm. Res.* Vol. 28(7), pp. 1552–60 (cit. on p. 132).

Heinen, M., Zanini, F., Roosen-Runge, F., Fedunová, D., Zhang, F., Hennig, M., Seydel, T., Schweins, R., Sztucki, M., Antalík, M., Schreiber, F., and Nägele, G. (2012). 'Viscosity and diffusion: crowding and salt effects in protein solutions'. *Soft Matter.* Vol. 8(5), pp. 1404–1419 (cit. on pp. 11, 47).

Hendriks, J., Gensch, T., Hviid, L., Horst, M. A. van der, Hellingwerf, K. J., and Thor, J. J. van (2002). 'Transient exposure of hydrophobic surface in the photoactive yellow protein monitored with Nile Red.' *Biophys. J.* Vol. 82(3), pp. 1632–1643 (cit. on p. 99).

Ikeda, S. and Nishinari, K. (2001). 'On solid-like rheological behaviors of globular protein solutions'. *Food Hydrocoll.* Vol. 15(4-6), pp. 401–406 (cit. on p. 13).

Ikeda, S. and Zhong, Q. (2012). 'Polymer and Colloidal Models Describing Structure-Function Relationships'. *Annu. Rev. Food Sci. Technol.* Vol. 3, pp. 405–424 (cit. on p. 8).

Inoue, H. and Matsumoto, T. (1996). 'Viscoelastic characterization of solid-like structure in aqueous colloids of globular proteins'. *Colloids Surf. A. Physicochem. Eng. Asp.* Vol. 109, pp. 89–96 (cit. on p. 13).

Inoue, N., Takai, E., Arakawa, T., and Shiraki, K. (2014a). 'Arginine and lysine reduce the high viscosity of serum albumin solutions for pharmaceutical injection.' *J. Biosci. Bioeng.* Vol. 117(5), pp. 539–43 (cit. on pp. 60, 121, 132, 133).

– (2014b). 'Specific decrease in solution viscosity of antibodies by arginine for therapeutic formulations'. *Mol. Pharm.* Vol. 11, pp. 1889–1896 (cit. on p. 133).

Jackson, M. B. (2006). *Molecular and Cellular Biophysics.* Cambridge University Press (cit. on p. 89).

Jańczuk, B., Białopiotrowicz, T., and Wójcik, W. (1989). 'The components of surface tension of liquids and their usefulness in determinations of surface free energy of solids'. *J. Colloid Interface Sci.* Vol. 127(1), pp. 59–66 (cit. on pp. 105, 106).

Janin, J. (1979). 'Surface and inside volumes in globular proteins'. *Nature.* Vol. 277, pp. 491–492 (cit. on p. 99).

Janson, J.-C. (2012). *Protein purification: principles, high resolution methods, and applications.* Vol. 151. John Wiley & Sons (cit. on p. 98).

Jezek, J., Rides, M., Derham, B., Moore, J., Cerasoli, E., Simler, R., and Perez-Ramirez, B. (2011). 'Viscosity of concentrated therapeutic protein compositions'. *Adv. Drug Delivery Rev.* Vol. 63(13), pp. 1107–1117 (cit. on pp. 5, 7–9, 12–15, 24, 120, 131, 152).

Jiao, M., Li, H. T., Chen, J., Minton, A. P., and Liang, Y. (2010). 'Attractive protein-polymer interactions markedly alter the effect of macromolecular crowding on protein association equilibria'. *Biophys. J.* Vol. 99(3), pp. 914–923 (cit. on p. 7).

Kamerzell, T. J., Pace, A. L., Li, M., Danilenko, D. M., McDowell, M., Gokarn, Y. R., and Wang, Y. J. (2013). 'Polar solvents decrease the viscosity of high concentration IgG1 solutions through hydrophobic solvation and interaction: Formulation and biocompatibility considerations'. *J. Pharm. Sci.* Vol. 102(4), pp. 1182–1193 (cit. on p. 60).

Kanai, S., Liu, J. U. N., Patapoff, T. W., and Shire, S. J. (2008). 'Reversible Self-Association of a Concentrated Monoclonal Antibody Solution Mediated by Fab-Fab Interaction That Impacts Solution Viscosity'. *J. Pharm. Sci.* Vol. 97(10), pp. 4219–4227 (cit. on pp. 13, 60).

Kato, A. and Nakai, S. (1980). 'Hydrophobicity determined by a fluorescence probe method and its correlation with surface properties of proteins'. *Biochim. Biophys. Acta.* Vol. 624, pp. 13–20 (cit. on p. 99).

Keshavarz, E. and Nakai, S. (1979). 'The relationship between hydrophobicity and interfacial tension of proteins.' *Biochim. Biophys. Acta.* Vol. 576(2), pp. 269–279 (cit. on p. 99).

Kessler, W. (2007). *Multivariate Datenanalyse.* Weinheim, Germany: Wiley-VCH Verlag GmbH & Co. KGaA, p. 340 (cit. on pp. 82, 89).

Kim, A. J., Manoharan, V. N., and Crocker, J. C. (2005). 'Swelling-based method for preparing stable, functionalized polymer colloids.' *J. Am. Chem. Soc.* Vol. 127(6), pp. 1592–3 (cit. on pp. 26, 123).

Kim, K. J., Chen, V., and Fane, A. G. (1993). 'Some factors determining protein aggregation during ultrafiltration'. *Biotechnol. Bioeng.* Vol. 42(2), pp. 260–265 (cit. on pp. 143, 151–153).

Kirby, B. J. and Hasselbrink, E. F. (2004). 'Zeta potential of microfluidic substrates: 2. Data for polymers'. *Electrophoresis.* Vol. 25(2), pp. 203–213 (cit. on p. 35).

Kirschenmann, L. (2003). 'Aufbau zweier piezoelektrischer Sonden (PRV / PAV) zur Messung der viskoelastischen Eigenschaften weicher Substanzen im Frequenzbereich 0.5 Hz-2 kHz bzw. 0.5 Hz- 7 kHz'. PhD Thesis. Universität Ulm (cit. on p. 29).

Kohn, W. D., Kay, C. M., and Hodges, R. S. (1997). 'Salt effects on protein stability: two-stranded alpha-helical coiled-coils containing inter- or intrahelical ion pairs.' *J. Mol. Biol.* Vol. 267(4), pp. 1039–1052 (cit. on pp. 8, 9, 121).

Komaromy, A. Z., Kulsing, C., Boysen, R. I., and Hearn, M. T. W. (2015). 'Salts employed in hydrophobic interaction chromatography can change protein structure - insights from protein-ligand interaction thermodynamics, circular dichroism spectroscopy and small angle X-ray scattering'. *Biotechnol. J.* Vol. 10(3), pp. 417–426 (cit. on p. 129).

Kondo, A., Murakami, F., and Higashitani, K. (1992). 'Circular dichroism studies on conformational changes in protein molecules upon adsorption on ultrafine polystyrene particles.' *Biotechnol. Bioeng.* Vol. 40, pp. 889–894 (cit. on p. 10).

Kong, J. and Yu, S. (2007). 'Fourier transform infrared spectroscopic analysis of protein secondary structures'. *Acta Biochim. Biophys. Sin. (Shanghai).* Vol. 39(8), pp. 549–559 (cit. on p. 10).

Kozer, N., Kuttner, Y. Y., Haran, G., and Schreiber, G. (2007). 'Protein-protein association in polymer solutions: from dilute to semidilute to concentrated.' *Biophys. J.* Vol. 92(6), pp. 2139–2149 (cit. on pp. 121, 132).

Kragh-Hansen, U., Møller, J. V., and Lind, K. E. (1974). 'Relation between binding of phenolsulfophtalein dyes and other ligands with a high affinity for human serum albumin'. *Biochim. Biophys. Acta.* Vol. 365, pp. 360–371 (cit. on p. 112).

Krieger, E., Koraimann, G., and Vriend, G. (2002). 'Increasing the precision of comparative models with YASARA NOVA-a self-parameterizing force field'. *Proteins Struct. Funct. Bioinforma.* Vol. 47(3), pp. 393–402 (cit. on pp. 3, 78).

Kuehner, D. E., Heyer, C., Rämsch, C., Fornefeld, U. M., Blanch, H. W., and Prausnitz, J. M. (1997). 'Interactions of lysozyme in concentrated electrolyte solutions from dynamic light-scattering measurements.' *Biophys. J.* Vol. 73(6), pp. 3211–24 (cit. on pp. 61, 77).

Kuehner, D. E., Engmann, J., Fergg, F., Wernick, M., Blanch, H. W., and Prausnitz, J. M. (1999). 'Lysozyme Net Charge and Ion Binding in Concentrated Aqueous Electrolyte Solutions'. *J. Phys. Chem. B.* Vol. 103(8), pp. 1368–1374 (cit. on p. 59).

Kulicke, W.-M. and Porter, R. S. (1980). 'Relation between steady shear flow and dynamic rheology'. *Rheol. Acta.* Vol. 19(5), pp. 601–605 (cit. on p. 29).

Kumar, N., Parajuli, O., Gupta, A., and Hahm, J. I. (2008). 'Elucidation of protein adsorption behavior on polymeric surfaces: Toward high-density, high-payload protein templates'. *Langmuir.* Vol. 24(6), pp. 2688–2694 (cit. on p. 36).

Kumar, V., Dixit, N., Zhou, L., and Fraunhofer, W. (2011). 'Impact of short range hydrophobic interactions and long range electrostatic forces on the aggregation kinetics of a monoclonal antibody and a dual-variable domain immunoglobulin at low and high concentrations'. *Int. J. Pharm. (Amsterdam, Neth.).* Vol. 421(1), pp. 82–93 (cit. on pp. 5, 7, 8, 11, 12, 14, 47, 51, 60, 61, 90).

Kyte, J. and Doolittle, R. F. (1982). 'A simple method for displaying the hydropathic character of a protein'. *J. Mol. Biol.* Vol. 157(1), pp. 105–132 (cit. on pp. 78, 99).

Ladiwala, A., Xia, F., Luo, Q., Breneman, C. M., and Cramer, S. M. (2006). 'Investigation of protein retention and selectivity in HIC systems using quantitative structure retention relationship models.' *Biotechnol. Bioeng.* Vol. 93(5), pp. 836–50 (cit. on pp. 18, 75).

Lang, K. M. H., Kittelmann, J., Dürr, C., Osberghaus, A., and Hubbuch, J. (2015). 'A comprehensive molecular dynamics approach to protein retention modeling in ion exchange chromatography'. *J. Chromatogr. A.* Vol. 1381, pp. 184–193 (cit. on p. 79).

Lazzari, S., Moscatelli, D., Codari, F., Salmona, M., Morbidelli, M., and Diomede, L. (2012). 'Colloidal stability of polymeric nanoparticles in biological fluids'. *J. Nanopart. Res.* Vol. 14(6), p. 920 (cit. on p. 25).

Leckband, D. and Israelachvili, J. (2001). *Intermolecular forces in biology.* Vol. 34. 2. Quarterly reviews of biophysics, pp. 105–267 (cit. on p. 2).

Lefebvre, J. (1982). 'Viscosity of concentrated protein solutions'. *Rheol. Acta.* Vol. 21(4-5), pp. 620–625 (cit. on pp. 12, 13, 60, 131).

Lehermayr, C., Mahler, H.-C., Mäder, K., and Fischer, S. (2011). 'Assessment of Net Charge and Protein-Protein Interactions of Different Monoclonal Antibodies'. *J. Pharm. Sci.* Vol. 100(7), pp. 2551–2562 (cit. on pp. 11, 15, 77, 85).

Lewus, R. A., Darcy, P. A., Lenhoff, A. M., and Sandler, S. I. (2011). 'Interactions and phase behavior of a monoclonal antibody'. *Biotechnol. Prog.* Vol. 27(1), pp. 280–289 (cit. on pp. 5, 12, 47, 74).

Lewus, R. A., Levy, N. E., Lenhoff, A. M., and Sandler, S. I. (2015). 'A comparative study of monoclonal antibodies. 1. phase behavior and protein-protein interactions'. *Biotechnol. Prog.* Vol. 31(1), pp. 268–276 (cit. on p. 12).

Liang, Y., Hilal, N., Langston, P., and Starov, V. (2007). 'Interaction forces between colloidal particles in liquid: Theory and experiment'. *Adv. Colloid Interface Sci.* Vol. 134-135, pp. 151–166 (cit. on pp. 2, 8, 75, 86, 90, 131).

Lijnzaad, P., Berendsen, H. J. C., and Argos, P. (1996). 'A method for detecting hydrophobic patches on protein surfaces.' *Proteins.* Vol. 26(2), pp. 192–203 (cit. on p. 99).

Lindman, S., Xue, W.-F., Szczepankiewicz, O., Bauer, M. C., Nilsson, H., and Linse, S. (2006). 'Salting the Charged Surface: pH and Salt Dependence of Protein G B1 Stability'. *Biophys. J.* Vol. 90(8), pp. 2911–2921 (cit. on pp. 59, 62).

Liu, J., Nguyen, M. D., Andya, J. D., and Shire, S. J. (2005). 'Reversible Self-Association Increases the Viscosity of a Concentrated Monoclonal Antibody in Aqueous Solution'. *J. Pharm. Sci.* Vol. 94(9), pp. 1928–1940 (cit. on pp. 5, 7, 13, 15, 18, 47, 60, 62, 120, 121, 129, 131, 143).

Liu, W., Cellmer, T., Keerl, D., Prausnitz, J. M., and Blanch, H. W. (2005). 'Interactions of lysozyme in guanidinium chloride solutions from static and dynamic light-scattering measurements.' *Biotechnol. Bioeng.* Vol. 90(4), pp. 482–90 (cit. on p. 11).

Lounnas, V., Pettitt, B. M., and Phillips, G. N. (1994). 'A global model of the protein-solvent interface.' *Biophys. J.* Vol. 66(3 Pt 1), pp. 601–14 (cit. on p. 63).

Maa, Y. F. and Hsu, C. C. (1996). 'Effect of high shear on proteins'. *Biotechnol. Bioeng.* Vol. 51(4), pp. 458–465 (cit. on pp. 9, 14).

Mahler, H.-C., Friess, W., Grauschopf, U., and Kiese, S. (2009). 'Protein aggregation: Pathways, induction factors and analysis'. *J. Pharm. Sci.* Vol. 98(9), pp. 2909–2934 (cit. on pp. 1, 4, 5, 7, 9–11, 47, 120, 131, 143).

Mahn, A., Lienqueo, M. E., and Asenjo, J. A. (2004). 'Effect of surface hydrophobicity distribution on retention of ribonucleases in hydrophobic interaction chromatography'. *J. Chromatogr. A.* Vol. 1043(1), pp. 47–55 (cit. on p. 99).

Malvern (2014). *How accurate is the DLS volume distribution?* (Cit. on p. 152).

Manuel García-Ruiz, J. (2003). 'Nucleation of protein crystals'. *J. Struct. Biol.* Vol. 142(1), pp. 22–31 (cit. on p. 4).

Mayburd, A. L., Tan, Y., and Kassner, R. J. (2000). 'Complex formation between Chromatium vinosum ferric cytochrome c' and bromophenol blue.' *Arch. Biochem. Biophys.* Vol. 378(1), pp. 40–44 (cit. on p. 112).

Mazza, C. B., Sukumar, N., Breneman, C. M., and Cramer, S. M. (2001). 'Prediction of protein retention in ion-exchange systems using molecular descriptors obtained from crystal structure.' *Anal. Chem.* Vol. 73(22), pp. 5457–61 (cit. on p. 75).

Mazza, C. B., Whitehead, C. E., Breneman, C. M., and Cramer, S. M. (2002). 'Predictive quantitative structure retention relationship models for ion-exchange chromatography'. *Chromatographia.* Vol. 56(3-4), pp. 147–152 (cit. on pp. 18, 75).

Meireles, M., Aimar, P., and Sanchez, V. (1991). 'Albumin denaturation during ultrafiltration: Effects of operating conditions and consequences on membrane fouling'. *Biotechnol. Bioeng.* Vol. 38(5), pp. 528–534 (cit. on p. 153).

Melinder, Å. (2007). 'Thermophysical properties of aqueous solutions used as secondary working fluids'. PhD thesis. School of Industrial Engineering and Management, Royal Institute of Technology, KTH Stockholm (cit. on pp. 105, 106).

Metzger, T. G. (2012). *The Rheology Handbook.* 4th ed. Hannover: Vincentz Network, pp. 51–56 (cit. on p. 29).

Meyer, T. E., Tollin, G., Hazzard, J. H., and Cusanovich, M. A. (1989). 'Photoactive yellow protein from the purple phototrophic bacterium, Ectothiorhodospira halophila. Quantum yield of photobleaching and effects of temperature, alcohols, glycerol, and sucrose on kinetics of photobleaching and recovery.' *Biophys. J.* Vol. 56(3), pp. 559–564 (cit. on p. 132).

Militello, V., Casarino, C., Emanuele, A., Giostra, A., Pullara, F., and Leone, M. (2004). 'Aggregation kinetics of bovine serum albumin studied by FTIR spectroscopy and light scattering.' *Biophys. Chem.* Vol. 107(2), pp. 175–87 (cit. on p. 7).

Miller, S., Janin, J., Lesk, A. M., and Chothia, C. (1987). 'Interior and surface of monomeric proteins.' *J. Mol. Biol.* Vol. 196, pp. 641–656 (cit. on p. 99).

Millipore (2003). *Protein Concentration and Diafiltration by Tangential Flow Filtration.* Tech. rep. Millipore (cit. on p. 145).

Minton, A. P. (1983). 'The effect of volume occupancy upon the thermodynamic activity of proteins: some biochemical consequences'. *Mol. Cell. Biochem.* Vol. 55(2), pp. 119–140 (cit. on pp. 8, 61).

Minton, A. P. (1997). 'Influence of excluded volume upon macromolecular structure and associations in 'crowded' media'. *Curr. Opin. Biotechnol.* Vol. 8(1), pp. 65–69 (cit. on pp. 47, 58, 61).

Minton, A. P. (2000). 'Implications of macromolecular crowding for protein assembly.' *Curr. Opin. Struct. Biol.* Vol. 10(1), pp. 34–9 (cit. on pp. 2, 5, 47, 58, 61, 63, 131).

– (2005). 'Influence of macromolecular crowding upon the stability and state of association of proteins: predictions and observations.' *J. Pharm. Sci.* Vol. 94(8), pp. 1668–75 (cit. on pp. 2, 5, 131).

Miriani, M., Eberini, I., Iametti, S., Ferranti, P., Sensi, C., and Bonomi, F. (2014). 'Unfolding of beta-lactoglobulin on the surface of polystyrene nanoparticles: Experimental and computational approaches'. *Proteins: Struct., Funct., Bioinf.* Vol. 82(7), pp. 1272–1282 (cit. on p. 38).

Moon, Y., Anderson, C., Blanch, H., and Prausnitz, J. (2000). 'Osmotic pressures and second virial coefficients for aqueous saline solutions of lysozyme'. *Fluid Phase Equilib.* Vol. 168(2), pp. 229–239 (cit. on pp. 11, 47).

Mosbæk, C. R., Konarev, P. V., Svergun, D. I., Rischel, C., and Vestergaard, B. (2012). 'High concentration formulation studies of an IgG2 antibody using small angle X-ray scattering.' *Pharm. Res.* Vol. 29(8), pp. 2225–35 (cit. on pp. 5, 7).

Murakami, K., Sano, T., and Yasunaga, T. (1981). 'Kinetic Studies of the Interaction of Bromophenol Blue with Bovine Serum Albumin by Pressure-jump Method'. *Bull. Chem. Soc. Jpn.* Vol. 54(3), pp. 862–868 (cit. on p. 112).

Muschol, M. and Rosenberger, F. (1995). 'Interactions in undersaturated and supersaturated lysozyme solutions: Static and dynamic light scattering results'. *J. Chem. Phys.* Vol. 103(24), p. 10424 (cit. on pp. 11, 12, 47, 48, 61, 75, 77, 84).

Myers, J. and Pace, C. (1996). 'Hydrogen bonding stabilizes globular proteins'. *Biophys. J.* Vol. 71(4), pp. 2033–2039 (cit. on p. 2).

Naidu, A. S. (2000). *Natural Food Antimicrobial Systems.* Ed. by Naidu, A. CRC Press, p. 382 (cit. on p. 26).

Nance, E. A., Woodworth, G. F., Sailor, K. A., Shih, T.-Y., Swaminathan, G., Xiang, D., and Eberhart, C. (2013). 'A Dense Poly(Ethylene Glycol) Coating Improves Penetration of Large Polymeric Nanoparticles Within Brain Tissue'. *Sci. Transl. Med.* Vol. 4(149), 149ra119 (cit. on p. 26).

Neal, B. L., Asthagiri, D., and Lenhoff, A. M. (1998). 'Molecular origins of osmotic second virial coefficients of proteins.' *Biophys. J.* Vol. 75(5), pp. 2469–77 (cit. on pp. 11, 47).

Neergaard, M. S., Kalonia, D. S., Parshad, H., Nielsen, A. D., Møller, E. H., and Weert, M. van de (2013). 'Viscosity of high concentration protein formulations of monoclonal antibodies of the IgG1 and IgG4 subclass - prediction of viscosity through protein-protein interaction measurements.' *Eur. J. Pharm. Sci.* Vol. 49(3), pp. 400–10 (cit. on pp. 12, 47, 53).

Nieba, L., Honegger, A., Krebber, C., and Plückthun, A. (1997). 'Disrupting the hydrophobic patches at the antibody variable/constant domain interface: improved in vivo folding and physical characterization of an engineered scFv fragment.' *Protein Eng.* Vol. 10(4), pp. 435–444 (cit. on pp. 18, 98).

Nozaki, Y. and Tanford, C. (1971). 'The solubility of amino acids and two glycine peptides in aqueous ethanol and dioxane solutions'. *J. Biol. Chem.* Vol. 246(7), pp. 2211–2217 (cit. on p. 99).

Nozaki, Y. and Tanford, C. (1963). 'The Solubility of Amino Acids and Related Compounds in Aqueous Urea Solutions'. *J. Biol. Chem.* Vol. 238, pp. 4074–4081 (cit. on p. 99).

– (1965). 'The solubility of amino acids and related compounds in equeous ethylene glycol solutions'. *J. Biol. Chem.* Vol. 240, pp. 3568–3573 (cit. on p. 99).

– (1970). 'The solubility of amino acids, diglycine, and triglycine in aqueous guanidine hydrochloride solutions'. *J. Biol. Chem.* Vol. 245, pp. 1648–1652 (cit. on p. 99).

Ochoa, N. (2003). 'Effect of hydrophilicity on fouling of an emulsified oil wastewater with PVDF/PMMA membranes'. *J. Membr. Sci.* Vol. 226(1-2), pp. 203–211 (cit. on p. 38).

Ohsawa, K., Murata, M., and Ohshima, H. (2005). 'Zeta potential and surface charge density of polystyrene-latex; comparison with synaptic vesicle and brush border membrane vesicle'. *Colloid Polym. Sci.* Vol. 264, pp. 1005–1009 (cit. on p. 36).

Olmsted, J. and Williams, G. (1997). *Chemistry: The Molecular Science.* Jones & Bartlett Learning, p. 1189 (cit. on p. 35).

O'Malley, J. J. and Weaver, J. L. (1972). 'Subunit structure of glucose oxidase from Aspergillus niger'. *Biochemistry.* Vol. 11(19), pp. 3527–3532 (cit. on p. 3).

Onwu, F. K. and Ogah, S. (2011). 'Adsorption of lysozyme unto silica and polystyrene surfaces in aqueous medium'. *Afr. J. Biotechnol.* Vol. 10(15), pp. 3014–3021 (cit. on p. 37).

Oss, C. J. van (2003). 'Long-range and short-range mechanisms of hydrophobic attraction and hydrophilic repulsion in specific and aspecific interactions'. *J. Mol. Recognit.* Vol. 16(4), pp. 177–190 (cit. on pp. 2, 47, 75).

Pace, C. N., Shirley, B. A., McNutt, M., and Gajiwala, K. (1996). 'Forces contributing to the conformational stability of proteins.' *FASEB J.* Vol. 10(1), pp. 75–83 (cit. on p. 2).

Pace, C. N., Treviño, S., Prabhakaran, E., and Scholtz, J. M. (2004). 'Protein structure, stability and solubility in water and other solvents.' *Philos. Trans. R. Soc. Lond. B. Biol. Sci.* Vol. 359, 1225–1234, discussion 1234–1235 (cit. on pp. 2, 3).

Palmer, K. J., Ballantyne, M., and Galvin, J. A. (1948). 'The molecular weight of lysozyme determined by the X-ray diffraction method.' *J. Am. Chem. Soc.* Vol. 70(3), pp. 906–908 (cit. on pp. 3, 49).

Papadopoulos, K. N. (2008). *Food Chemistry Research Developments.* Nova Science Publishers (cit. on pp. 58, 59).

Parmar, A. S. and Muschol, M. (2009). 'Hydration and Hydrodynamic Interactions of Lysozyme: Effects of Chaotropic versus Kosmotropic Ions'. *Biophys. J.* Vol. 97(2), pp. 590–598 (cit. on p. 87).

Patro, S. and Przybycien, T. (1996). 'Simulations of reversible protein aggregate and crystal structure'. *Biophys. J.* Vol. 70(6), pp. 2888–2902 (cit. on pp. 4, 121).

Pawelzyk, P., Herrmann, H., and Willenbacher, N. (2013). 'Mechanics of intermediate filament networks assembled from keratins K8 and K18'. *Soft Matter.* Vol. 9(37), p. 8871 (cit. on p. 28).

Pazur, J. H. and Kleppe, K. (1964). 'The Oxidation of glucose and related compounds by glucose oxidase from Aspergillus niger'. *Biochemistry.* Vol. 3, pp. 578–583 (cit. on p. 59).

Pegram, L. M. and Record, M. T. (2007). 'Hofmeister Salt Effects on Surface Tension Arise from Partitioning of Anions and Cations between Bulk Water and the Air-Water Interface'. *J. Phys. Chem. B.* Vol. 111(19), pp. 5411–5417 (cit. on p. 108).

Permyakov, E. A. and Berliner, L. J. (2000). 'α-Lactalbumin: structure and function'. *FEBS Lett.* Vol. 473(3), pp. 269–274 (cit. on pp. 3, 7, 49, 59, 80, 111).

Philo, J. S. and Arakawa, T. (2009). 'Mechanisms of protein aggregation.' *Curr. Pharm. Biotechnol.* Vol. 10(4), pp. 348–51 (cit. on pp. 5, 46, 47).

Prausnitz, J. M. (2003). 'Molecular thermodynamics for some applications in biotechnology'. *J. Chem. Thermodyn.* Vol. 35(1), pp. 21–39 (cit. on p. 47).

Radzicka, A. and Wolfenden, R. (1988). 'Comparing the polarities of the amino acids: side-chain distribution coefficients between the vapor phase, cyclohexane, 1-octanol, and neutral aqueous solution'. *Biochemistry.* Vol. 27(5), pp. 1664–1670 (cit. on p. 99).

Rakel, N., Bauer, K. C., Galm, L., and Hubbuch, J. (2015). 'From osmotic second virial coefficient (B 22) to phase behavior of a monoclonal antibody'. *Biotechnol. Prog.* Vol. 31(2), pp. 438–451 (cit. on pp. 12, 47).

Rakel, N., Galm, L., Bauer, K. C., and Hubbuch, J. (2015). 'Influence of macromolecular precipitants on phase behavior of monoclonal antibodies'. *Biotechnol. Prog.* Vol. 31(1), pp. 145–153 (cit. on pp. 12, 47).

Rallison, J. M. and Hinch, E. J. (1986). 'The effect of particle interactions on dynamic light scattering from a dilute suspension'. *J. Fluid Mech.* Vol. 167, p. 131 (cit. on p. 61).

Reis, R. van, Goodrich, E., Yson, C., Frautschy, L., Whiteley, R., and Zydney, A. (1997). 'Constant Cwall ultrafiltration process control'. *J. Membr. Sci.* Vol. 130(1-2), pp. 123–140 (cit. on pp. 143, 151).

Reis, R. van and Zydney, A. (2007). 'Bioprocess membrane technology'. *J. Membr. Sci.* Vol. 297(1-2), pp. 16–50 (cit. on p. 151).

Reißer, S., Strandberg, E., Steinbrecher, T., and Ulrich, A. S. (2014). '3D Hydrophobic Moment Vectors as a Tool to Characterize the Surface Polarity of Amphiphilic Peptides'. *Biophys. J.* Vol. 106(11), pp. 2385–2394 (cit. on p. 99).

Remmele Jr., R. L., Nightlinger, N. S., Srinivasan, S., and Gombotz, W. R. (1998). 'Interleukin-1 receptor (IL-1R) liquid formulation development using differential scanning calorimetry'. *Pharm. Res.* Vol. 15(2), pp. 200–208 (cit. on pp. 129, 132).

Richard Bowen, W. and Williams, P. M. (2001). 'Prediction of the rate of cross-flow ultrafiltration of colloids with concentration-dependent diffusion coefficient and viscosity - theory and experiment'. *Chem. Eng. Sci.* Vol. 56(10), pp. 3083–3099 (cit. on p. 143).

Roberts, C. J. (2007). 'Non-native protein aggregation kinetics'. *Biotechnol. Bioeng.* Vol. 98(5), pp. 927–938 (cit. on p. 60).

Rohani, M. M. and Zydney, A. L. (2010). 'Role of electrostatic interactions during protein ultrafiltration'. *Adv. Colloid Interface Sci.* Vol. 160(1-2), pp. 40–48 (cit. on p. 143).

Rose, G. D. and Wolfenden, R. (1993). 'Hydrogen bonding, hydrophobicity, packing, and protein folding'. *Annu. Rev. Biophys. Biomol. Struct.* Vol. 22, pp. 381–415 (cit. on p. 99).

Rosenberg, E., Hepbildikler, S., Kuhne, W., and Winter, G. (2009). 'Ultrafiltration concentration of monoclonal antibody solutions: Development of an optimized method minimizing aggregation'. *J. Membr. Sci.* Vol. 342(1-2), pp. 50–59 (cit. on pp. 15, 24, 142, 143, 151, 152).

Rosenberg, M. (1981). 'Bacterial adherence to polystyrene: a replica method of screening for bacterial hydrophobicity.' *Appl. Envir. Microbiol.* Vol. 42(2), pp. 375–377 (cit. on p. 37).

Saito, S., Hasegawa, J., Kobayashi, N., Kishi, N., Uchiyama, S., and Fukui, K. (2012). 'Behavior of monoclonal antibodies: relation between the second virial coefficient (B (2)) at low concentrations and aggregation propensity and viscosity at high concentrations.' *Pharm. Res.* Vol. 29(2), pp. 397–410 (cit. on pp. 7, 8, 10–13, 15, 47, 60).

Salgado, J. C., Rapaport, I., and Asenjo, J. A. (2005). 'Is it possible to predict the average surface hydrophobicity of a protein using only its amino acid composition?' *J. Chromatogr. A.* Vol. 1075(1), pp. 133–143 (cit. on p. 99).

– (2006a). 'Predicting the behaviour of proteins in hydrophobic interaction chromatography: 1: Using the hydrophobic imbalance (HI) to describe their surface amino acid distribution'. *J. Chromatogr. A.* Vol. 1107(1), pp. 110–119 (cit. on p. 99).

– (2006b). 'Predicting the behaviour of proteins in hydrophobic interaction chromatography 2. Using a statistical description of their surface amino acid distribution'. *J. Chromatogr. A.* Vol. 1107(1), pp. 120–129 (cit. on p. 99).

Salgin, S. (2007). 'Effects of Ionic Environments on Bovine Serum Albumin Fouling in a Cross-Flow Ultrafiltration System'. *Chem. Eng. Technol.* Vol. 30(2), pp. 255–260 (cit. on p. 143).

Salgin, S., Takaç, S., and Özdamar, T. H. (2006). 'Adsorption of bovine serum albumin on polyether sulfone ultrafiltration membranes: Determination of interfacial interaction energy and effective diffusion coefficient'. *J. Membr. Sci.* Vol. 278(1-2), pp. 251–260 (cit. on p. 143).

Salinas, B. A., Sathish, H. A., Bishop, S. M., Harn, N., Carpenter, J. F., and Randolph, T. W. (2010). 'Understanding and modulating opalescence and viscosity in a monoclonal antibody formulation'. *J. Pharm. Sci.* Vol. 99(1), pp. 82–93 (cit. on p. 60).

Saluja, A., Badkar, A. V., Zeng, D. L., Nema, S., and Kalonia, D. S. (2006). 'Application of high-frequency rheology measurements for analyzing protein-protein interactions in high protein concentration solutions using a model monoclonal antibody (IgG2)'. *J. Pharm. Sci.* Vol. 95(9), pp. 1967–1983 (cit. on pp. 25, 26).

– (2007). 'Ultrasonic storage modulus as a novel parameter for analyzing protein-protein interactions in high protein concentration solutions: correlation with static and dynamic light scattering measurements.' *Biophys. J.* Vol. 92(1), pp. 234–44 (cit. on pp. 11–15, 24, 25, 48, 51, 75, 77, 86).

Saluja, A. and Kalonia, D. S. (2008). 'Nature and consequences of protein-protein interactions in high protein concentration solutions.' *Int. J. Pharm. (Amsterdam, Neth.).* Vol. 358(1-2), pp. 1–15 (cit. on pp. 2, 5, 7, 10–13, 15, 36, 46–48, 58, 59, 61, 62, 75).

Scherer, T. M., Liu, J., Shire, S. J., and Minton, A. P. (2010). 'Intermolecular interactions of IgG1 monoclonal antibodies at high concentrations characterized by light scattering.' *J. Phys. Chem. B.* Vol. 114(40), pp. 12948–57 (cit. on pp. 12, 47, 62).

Schermeyer, M.-T., Sigloch, H., Bauer, K. C., Oelschlaeger, C., and Hubbuch, J. (2016). 'Squeeze flow rheometry as a novel tool for the characterization of highly concentrated protein solutions'. *Biotechnol. Bioeng.* Vol. 113(3), pp. 576–587 (cit. on pp. 12, 25, 26, 33, 48, 52).

Schmit, J. D., He, F., Mishra, S., Ketchem, R. R., Woods, C. E., and Kerwin, B. A. (2014). 'Entanglement model of antibody viscosity'. *J. Phys. Chem. B.* Vol. 118, pp. 5044–5049 (cit. on pp. 12, 131).

Scopes, R. K. (2013). *Protein Purification: Principles and Practice.* Springer Advanced Texts in Chemistry. Springer New York (cit. on pp. 129, 132).

Shanbhag, V. P. and Axelsson, C.-G. (1975). 'Hydrophobic interaction determined by partition in aqueous two-phase systems'. *Eur. J. Biochem.* Vol. 60, pp. 17–22 (cit. on p. 99).

Shaw, K. L., Grimsley, G. R., Yakovlev, G. I., Makarov, A. A., and Pace, C. N. (2001). 'The effect of net charge on the solubility, activity, and stability of ribonuclease Sa'. *Protein Sci.* Vol. 10(6), pp. 1206–1215 (cit. on pp. 7, 59).

Sheinerman, F. B., Norel, R., and Honig, B. (2000). 'Electrostatic aspects of protein-protein interactions'. *Curr. Opin. Struct. Biol.* Vol. 10(2), pp. 153–159 (cit. on p. 60).

Shih, Y. C., Prausnitz, J. M., and Blanch, H. W. (1992). 'Some characteristics of protein precipitation by salts'. *Biotechnol. Bioeng.* Vol. 40, pp. 1155–1164 (cit. on pp. 9, 38, 133).

Shire, S. J. (2009). 'Formulation and manufacturability of biologics'. *Curr. Opin. Biotechnol.* Vol. 20, pp. 708–714 (cit. on pp. 9, 13–15, 46, 121, 143, 149).

Shire, S. J., Shahrokh, Z., and Liu, J. (2004). 'Challenges in the development of high protein concentration formulations.' *J. Pharm. Sci.* Vol. 93(6), pp. 1390–402 (cit. on pp. 7, 10, 15, 18, 24, 46, 74, 120, 121, 129, 133, 142, 143, 149).

Shukla, A. A. and Yigzaw, Y. (2006). *Process Scale Bioseparations for the Biopharmaceutical Industry.* Ed. by Shukla, A., Etzel, M., and Gadam, S. Vol. 31. Biotechnology and Bioprocessing. CRC Press, pp. 179–225 (cit. on pp. 144, 151).

Singh, V. and Singh, D. (2014). 'Glucose oxidase immobilization on guar gum-gelatin dual-templated silica hybrid xerogel'. *Ind. Eng. Chem. Res.* Vol. 53(10), pp. 3854–3860 (cit. on p. 59).

Stradner, A., Cardinaux, F., and Schurtenberger, P. (2006). 'A Small-Angle Scattering Study on Equilibrium Clusters in Lysozyme Solutions'. *J. Phys. Chem. B.* Vol. 110(42), pp. 21222–21231 (cit. on p. 26).

Tanford, C. (1962). 'Contribution of hydrophobic interactions to the stability of the globular conformation of proteins'. *J. Am. Chem. Soc.* Vol. 84(22), pp. 4240–4247 (cit. on p. 98).

Tardieu, A., Bonneté, F., Finet, S., and Vivarès, D. (2002). 'Understanding salt or PEG induced attractive interactions to crystallize biological macromolecules'. *Acta Crystallogr. Sect. D Biol. Crystallogr.* Vol. 58, pp. 1549–1553 (cit. on p. 59).

Tate, T. (1864). 'On the magnitude of a drop of liquid formed under different circumstances'. *London, Edinburgh, Dublin Philos. Mag. J. Sci.* Vol. 27(181), pp. 176–180 (cit. on p. 100).

Tatsumi, E. and Hirose, M. (1997). 'Highly ordered molten globule-like state of ovalbumin at acidic pH: native-like fragmentation by protease and selective modification of Cys367 with dithiodipyridine.' *J. Biochem.* Vol. 122, pp. 300–308 (cit. on p. 80).

Tayyab, S. and Qasim, M. (1990). 'Binding of bromophenol blue to bovine serum albumin and its succinylated forms'. *Int. J. Biol. Macromol.* Vol. 12(1), pp. 55–58 (cit. on p. 112).

Ter Veen, R., Fromell, K., and Caldwell, K. D. (2005). 'Shifts in polystyrene particle surface charge upon adsorption of the Pluronic F108 surfactant'. *J. Colloid Interface Sci.* Vol. 288(1), pp. 124–128 (cit. on p. 25).

Thakkar, S. V., Allegre, K. M., Joshi, S. B., Volkin, D. B., and Middaugh, C. R. (2012). 'An application of ultraviolet spectroscopy to study interactions in proteins solutions at high concentrations.' *J. Pharm. Sci.* Vol. 101(9), pp. 3051–61 (cit. on p. 15).

The Uniprot Consortium (2015). 'UniProt: a hub for protein information'. *Nucleic Acids Res.* Vol. 43(D1), pp. D204–D212 (cit. on p. 78).

Timasheff, S. N. (2002). 'Protein-solvent preferential interactions, protein hydration, and the modulation of biochemical reactions by solvent components.' *Proc. Natl. Acad. Sci. U. S. A.* Vol. 99(15), pp. 9721–6 (cit. on p. 132).

Trinquier, G. and Sanejouand, Y.-H. (1998). 'Which effective property of amino acids is best preserved by the genetic code?' *Protein Eng.* Vol. 11(3), pp. 153–169 (cit. on p. 99).

Tropsha, A., Gramatica, P., and Gombar, V. (2003). 'The Importance of Being Earnest: Validation is the Absolute Essential for Successful Application and Interpretation of QSPR Models'. *QSAR Comb. Sci.* Vol. 22(1), pp. 69–77 (cit. on p. 80).

Tsierkezos, N. G. and Molinou, I. E. (1998). 'Thermodynamic Properties of Water + Ethylene Glycol at 283.15, 293.15, 303.15, and 313.15 K'. *J. Chem. Eng. Data.* Vol. 43(6), pp. 989–993 (cit. on pp. 105, 106).

Tsuge, H. J., Natsuaki, O., and Ohashi, K. (1975). 'Purification, properties, and molecular features of glucose oxidase from Aspergillus niger.' *J. Biochem.* Vol. 78, pp. 835–843 (cit. on p. 49).

Uribe, S. and Sampedro, J. G. (2003). 'Measuring Solution Viscosity and its Effect on Enzyme Activity'. *Biol. Proced. Online.* Vol. 5(1), pp. 108–115 (cit. on pp. 8, 132).

Vadillo, D. C., Tuladhar, T. R., Mulji, A. C., and Mackley, M. R. (2010). 'The rheological characterization of linear viscoelasticity for ink jet fluids using piezo axial vibrator and torsion resonator rheometers'. *J. Rheol. (Melville, NY, U. S.).* Vol. 54(4), p. 781 (cit. on p. 28).

Vagenende, V., Yap, M. G. S., and Trout, B. L. (2009). 'Mechanisms of protein stabilization and prevention of protein aggregation by glycerol'. *Biochemistry.* Vol. 48(46), pp. 11084–11096 (cit. on p. 121).

Valentine, M., Perlman, Z., Gardel, M., Shin, J., Matsudaira, P., Mitchison, T., and Weitz, D. (2004). 'Colloid Surface Chemistry Critically Affects Multiple Particle Tracking Measurements of Biomaterials'. *Biophys. J.* Vol. 86(6), pp. 4004–4014 (cit. on pp. 14, 17, 25).

Veerman, C., Rajagopal, K., Palla, C. S., Pochan, D. J., Schneider, J. P., and Furst, E. M. (2006). 'Gelation kinetics of β-hairpin peptide hydrogel networks'. *Macromolecules.* Vol. 39(19), pp. 6608–6614 (cit. on pp. 5, 13, 60).

Velev, O. D., Kaler, E. W., and Lenhoff, A. M. (1998). 'Protein interactions in solution characterized by light and neutron scattering: comparison of lysozyme and chymotrypsinogen.' *Biophys. J.* Vol. 75(6), pp. 2682–97 (cit. on p. 84).

Vieille, C., Burdette, D. S., and Zeikus, J. G. (1996). 'Thermozymes.' *Biotechnol. Annu. Rev.* Vol. 2, pp. 1–83 (cit. on p. 2).

Waigh, T. A. (2005). 'Microrheology of complex fluids'. *Rep. Prog. Phys.* Vol. 68(3), pp. 685–742 (cit. on pp. 14, 17, 25, 26, 51).

Waldmann-Meyer, H. and Schilling, K. (1956). 'The Interaction of Bromophenol Blue with Serum Albumin and γ-Globulin in Acid Medium'. *Arch. Biochem. Biophys.* Vol. 64, pp. 291–301 (cit. on p. 112).

Wang, N., Hu, B., Lonescu, R., Mac, H. H., Sweeney, J., Hamm, C., Kirchmeier, M. J., and Meyer, B. K. (2009). 'Opalescence of an IgGi monoclonal antibody formulation is mediated by ionic strength and excipients'. *BioPharm Int.* Vol. 22(4), pp. 36–47 (cit. on p. 60).

Wang, W. (1999). 'Instability, stabilization, and formulation of liquid protein pharmaceuticals'. *Int. J. Pharm. (Amsterdam, Neth.).* Vol. 185(2), pp. 129–188 (cit. on pp. 1, 2, 4, 9, 10, 14, 47, 62, 120, 129, 131, 133, 143, 149).

– (2005). 'Protein aggregation and its inhibition in biopharmaceutics.' *Int. J. Pharm. (Amsterdam, Neth.).* Vol. 289(1-2), pp. 1–30 (cit. on pp. 5, 7–10, 14, 132).

Wang, W., Nema, S., and Teagarden, D. (2010). 'Protein aggregation-Pathways and influencing factors'. *Int. J. Pharm. (Amsterdam, Neth.).* Vol. 390(2), pp. 89–99 (cit. on pp. 4, 5, 7–10, 12, 14, 18, 121, 130).

Wei, Y.-J., Li, K.-A., and Tong, S.-Y. (1996). 'The interaction of Bromophenol Blue with proteins in acidic solution'. *Talanta.* Vol. 43(1), pp. 1–10 (cit. on p. 112).

Whitney, P. L., Tanford, C., W, P. L., and Tanford, C. (1962). 'Solubility of amino acids in aqueous urea solutions and its implications for the denaturation of proteins by urea'. *J. Biol. Chem.* Vol. 237, pp. 1735–1737 (cit. on p. 99).

Willenbacher, N. and Oelschlaeger, C. (2007). 'Dynamics and structure of complex fluids from high frequency mechanical and optical rheometry'. *Curr. Opin. Colloid Interface Sci.* Vol. 12(1), pp. 43–49 (cit. on pp. 14, 25).

Wilson, R. and Turner, A. (1992). 'Glucose oxidase: an ideal enzyme'. *Biosens. Bioelectron.* Vol. 7(3), pp. 165–185 (cit. on pp. 3, 49).

Winzor, D. J. (2004). 'Determination of the net charge (valence) of a protein: a fundamental but elusive parameter'. *Anal. Biochem.* Vol. 325(1), pp. 1–20 (cit. on p. 28).

Wisz, M. S. and Hellinga, H. W. (2003). 'An empirical model for electrostatic interactions in proteins incorporating multiple geometry-dependent dielectric constants'. *Proteins Struct. Funct. Genet.* Vol. 51(3), pp. 360–377 (cit. on p. 90).

Yadav, S., Laue, T. M., Kalonia, D. S., Singh, S. N., and Shire, S. J. (2012). 'The influence of charge distribution on self-association and viscosity behavior of monoclonal antibody solutions'. *Mol. Pharm.* Vol. 9, pp. 791–802 (cit. on pp. 2, 7, 13).

Yadav, S., Shire, S. J., and Kalonia, D. S. (2011). 'Viscosity analysis of high concentration bovine serum albumin aqueous solutions.' *Pharm. Res.* Vol. 28(8), pp. 1973–83 (cit. on pp. 12, 60, 131).

Yang, M. X., Shenoy, B., Disttler, M., Patel, R., McGrath, M., Pechenov, S., and Margolin, A. L. (2003). 'Crystalline monoclonal antibodies for subcutaneous delivery'. *Proc. Natl. Acad. Sci.* Vol. 100(12), pp. 6934–6939 (cit. on p. 15).

Yang, T., Breneman, C. M., and Cramer, S. M. (2007). 'Investigation of multi-modal high-salt binding ion-exchange chromatography using quantitative structure-property relationship modeling'. *J. Chromatogr. A*. Vol. 1175(1), pp. 96–105 (cit. on p. 75).

Young, M. E., Carroad, P. A., and Bell, R. L. (1980). 'Estimation of diffusion coefficients of proteins'. *Biotechnol. Bioeng.* Vol. 22(5), pp. 947–955 (cit. on pp. 61, 77).

Zhang, J. and Liu, X. Y. (2003). 'Effect of protein-protein interactions on protein aggregation kinetics'. *J. Chem. Phys.* Vol. 119(20), p. 10972 (cit. on pp. 12, 48, 75).

Zhao, W., He, C., Wang, H., Su, B., Sun, S., and Zhao, C. (2011). 'Improved Antifouling Property of Polyethersulfone Hollow Fiber Membranes Using Additive of Poly(ethylene glycol) Methyl Ether-*b*-Poly(styrene) Copolymers'. *Ind. Eng. Chem. Res.* Vol. 50(6), pp. 3295–3303 (cit. on p. 150).

Zimmerman, S. B. and Minton, A. P. (1993). 'Macromolecular crowding: biochemical, biophysical, and physiological consequences.' *Annu. Rev. Biophys. Biomol. Struct.* Vol. 22, pp. 27–65 (cit. on pp. 47, 58, 61).

Zydney, A. and Reis, R. van (2011). 'Bioseparations'. *Compr. Biotechnol.* Second Edi. Vol. 1. Elsevier, pp. 499–520 (cit. on p. 151).

List of Figures

List of Tables

Curriculum Vitae

Katharina Christin Bauer

Place of birth	Ludwigsburg, Germany
Email	katharina.bauer@kit.edu

Education

12/2012–11/2016	PhD student
	Institute of Process Engineering in Life Sciences, Section IV: Biomolecular Separation Engineering, Karlsruhe Institute of Technology (KIT), Germany
01/2012–07/2012	Diploma thesis: *'Characterization of protein interactions for protein crystallization using static light scattering'*
	Institute of Process Engineering in Life Sciences, Section IV: Biomolecular Separation Engineering, Karlsruhe Institute of Technology (KIT), Germany
02/2011–07/2011	Studies of Chemical Engineering
	Ecole supérieure de chimie physique électronique de Lyon (CPE Lyon), France
10/2010–05/2011	Student Research Project: *'Studies on the reaction of N-heterocyclic carbenes from ionic liquids with benzaldehyde in supercritical CO_2'*
	Institute for Technical Thermodynamics and Refrigeration & Institute of Organic Chemistry, Karlsruhe Institute for Technology (KIT), Germany
10/2006–08/2012	Studies of Bioengineering at Karlsruhe Institute of Technology (KIT), Germany

Working experience

12/2012–11/2016	Scientific Associate
	Institute of Process Engineering in Life Sciences, Section IV: Biomolecular Separation Engineering, Karlsruhe Institute of Technology (KIT), Germany
08/2012–09/2012	Scientific Assistant
	Institute of Process Engineering in Life Sciences, Section IV: Biomolecular Separation Engineering, Karlsruhe Institute of Technology (KIT), Germany
08/2011–11/2011	Scientific Assistant
	Institute for Technical Thermodynamics and Refrigeration, Karlsruhe Institute for Technology (KIT), Germany

10/2009–03/2010   Intern

Cognis GmbH, Düsseldorf, Germany

12/2008–05/2009   Scientific Assistant

Institute of Process Engineering in Life Sciences, Section III: Bioprocess Engineering, Karlsruhe Institute of Technology (KIT), Germany

Publications

Paper

Katharina Christin Bauer, Susanna Suhm, Anna Katharina Wöll, Jürgen Hubbuch (2017). 'Impact of additives on the formation of protein aggregates and viscosity in concentrated protein solutions'. *International Journal of Pharmaceutics*. Vol. 516(1-2), pp. 82–90.

Katharina Christin Bauer, Mathias Göbel, Marie-Luise Schwab, Marie-Therese Schermeyer, Jürgen Hubbuch (2016). 'Concentration-dependent Changes in Apparent Diffusion Coefficients as Indicator for Colloidal Stability of Protein Solutions'. *International Journal of Pharmaceutics*. Vol. 511(1), pp. 276-287.

Katharina Christin Bauer, Marie-Therese Schermeyer, Jonathan Seidel, Jürgen Hubbuch (2016). 'Impact of polymer surface characteristics on the microrheological measurement quality of protein solutions - a tracer particle screening'. *International Journal of Pharmaceutics*. Vol. 505(1-2), pp. 246-254.

Marie-Therese Schermeyer, Heike Sigloch, Katharina Christin Bauer, Claude Oelschlaeger, Jürgen Hubbuch (2016). 'Squeeze flow rheometry as a novel tool for the characterization of highly concentrated protein solutions'. *Biotechnology and Bioengineering*. Vol. 113(3), pp. 576-587.

Sven Amrhein, Katharina Christin Bauer, Lara Galm, Jürgen Hubbuch (2015). 'Non-invasive high throughput approach for protein hydrophobicity determination based on surface tension'. *Biotechnology and Bioengineering*. Vol. 112(12), pp. 2485-2494.

Natalie Rakel, Katharina Christin Bauer, Lara Galm, Jürgen Hubbuch (2015). 'From Osmotic Second Virial Coefficient (B_{22}) to Phase Behavior of a Monoclonal Antibody'. *Biotechnology Process*. Vol. 31(2), pp. 438-451.

Natalie Rakel, Lara Galm, Katharina Christin Bauer, Jürgen Hubbuch (2015). 'Influence of macromolecular precipitants on phase behavior of monoclonal antibodies'. *Biotechnology Process*. Vol. 31(1), pp. 145-153.

Talks

Marie-Therese Schermeyer, Katharina Christin Bauer, Jonathan Seidel, Jürgen Hubbuch (2016). 'Impact of polymer surface characteristics on the microrheological measurement quality of protein solutions - a tracer particle screening'. *International Congress on Particle Technology*, Nürnberg, Germany.

Katharina Christin Bauer, Marie-Therese Schermeyer, Mathias Göbel, Marie-Luise Schwab, Jürgen Hubbuch (2015). 'Concentration dependent changes in protein diffusion as an approach to characterize the stability and viscosity of concentrated protein solutions'. *3rd European Congress of Applied Biotechnology*, Nice, France.

Katharina Christin Bauer, Marie-Therese Schermeyer, Mathias Göbel, Marie-Luise Schwab, Jürgen Hubbuch (2014). 'Characterizing phase behavior of highly concentrated protein solutions by dynamic light scattering'. *Biological and Pharmaceutical Complex Fluids II: Novel Trends in Characterizing Interactions, Microstructure and Rheology*, Durham, NC, USA.

Sven Amrhein, Katharina Christin Bauer, Lara Galm, Marie-Therese Schermeyer, Jürgen Hubbuch (2014). 'Predictive Approaches for Protein Phase Behavior'. *Recovery of Biological Products Conference XVI*, Rostock, Germany.